Ancient Greek harbours used as geo-archives for palaeotsunami research

-

Case studies from Krane (Cefalonia), Lechaion (Gulf of Corinth) and Kyllini (Peloponnese)

Dissertation

zur Erlangung des Grades

„Doktor der Naturwissenschaften“

im Promotionsfach Geographie

am Fachbereich Chemie, Pharmazie und Geowissenschaften

der Johannes Gutenberg-Universität

in Mainz

vorgelegt von

Hanna Hadler

geb. in Stade

Mainz, den 19. Dezember 2013

Berichterstatter

(1. Berichterstatter)

(2. Berichterstatter)

(3. Berichterstatter)

Tag der mündlichen Prüfung:

19. Februar 2014

„About the same time, the sea came in [...] on the part which then was land and, being impetuous withal, overflowed most part of the city, whereof part it covered and part it washed down and made lower in the return so that it is now sea which before was land.“

(Thukydides 3.89.2)

Abstract

Since historical times, coastal areas throughout the eastern Mediterranean are exposed to tsunami hazard. For many decades the knowledge about palaeotsunamis was solely based on historical accounts. However, results from timeline analyses reveal different characteristics affecting the quality of the dataset (i.e. distribution of data, temporal thinning backward of events, local periodization phenomena) that emphasize the fragmentary character of the historical data. As an increasing number of geo-scientific studies give convincing examples of well dated tsunami signatures not reported in catalogues, the non-existing record is a major problem to palaeotsunami research. While the compilation of historical data allows a first approach in the identification of areas vulnerable to tsunamis, it must not be regarded as reliable for hazard assessment.

Considering the increasing economic significance of coastal regions (e.g. for mass tourism) and the constantly growing coastal population, our knowledge on the local, regional and supraregional tsunami hazard along Mediterranean coasts has to be improved. For setting up a reliable tsunami risk assessment and developing risk mitigation strategies, it is of major importance (i) to identify areas under risk and (ii) to estimate the intensity and frequency of potential events. This approach is most promising when based on the analysis of palaeotsunami research seeking to detect areas of high palaeotsunami hazard, to calculate recurrence intervals and to document palaeotsunami destructiveness in terms of wave run-up, inundation and long-term coastal change.

Within the past few years, geo-scientific studies on palaeotsunami events provided convincing evidence that throughout the Mediterranean ancient harbours were subject to strong tsunami-related disturbance or destruction. Constructed to protect ships from storm and wave activity, harbours provide especially sheltered and quiescent environments and thus turned out to be valuable geo-archives for tsunamigenic high-energy impacts on coastal areas.

Directly exposed to the Hellenic Trench and extensive local fault systems, coastal areas in the Ionian Sea and the Gulf of Corinth hold a considerably high risk for tsunami events, respectively. Geo-scientific and geoarcheaological studies carried out in the environs of the ancient harbours of Krane (Cefalonia Island), Lechaion (Corinth, Gulf of Corinth) and Kyllini (western Peloponnese) comprised on-shore and near-shore vibracoring and subsequent sedimentological, geochemical and microfossil analyses of the recovered sediments. Geophysical methods like electrical resistivity tomography and ground penetrating radar were applied in order to detect subsurface structures and to verify stratigraphical patterns derived from vibracores over long distances. The overall geochronological framework of each study area is based on radiocarbon dating of biogenic material and age determination of diagnostic ceramic fragments.

Results presented within this study provide distinct evidence of multiple palaeotsunami landfalls for the investigated areas. Tsunami signatures encountered in the environs of Krane, Lechaion and Kyllini include (i) coarse-grained allochthonous marine sediments intersecting silt-dominated quiescent harbour deposits and/or shallow marine environments, (ii) disturbed microfaunal assemblages and/or (iii) distinct geochemical fingerprints as well as (iv) geo-archaeological destruction layers and (v) extensive units of beachrock-type calcarenitic tsunamites.

Abstract

For Krane, geochronological data yielded *termini ad* or *post quem* (maximum ages) for tsunami event generations dated to 4150 ± 60 cal BC, ~ 3200 ± 110 cal BC, ~ 650 ± 110 cal BC, and ~ 930 ± 40 cal AD, respectively. Results for Lechaion suggest that the harbour was hit by strong tsunami impacts in the 8th-6th century BC, the 1st-2nd century AD and in the 6th century AD. At Kyllini, the harbour site was affected by tsunami impact in between the late 7th and early 4th cent. BC and between the 4th and 6th cent. AD. In case of Lechaion and Kyllini, the final destruction of the harbour facilities also seems to be related to the tsunami impact. Comparing the tsunami signals obtained for each study areas with geo-scientific data from palaeotsunami events from other sites indicates that the investigated harbour sites represent excellent geo-archives for supra-regional mega-tsunamis.

Kurzzusammenfassung

Bereits seit historischer Zeit sind die Küstengebiete im östlichen Mittelmeerraum der Gefährdung durch Tsunamis ausgesetzt. Viele Jahrzehnte basierte das Wissen über Paläotsunamis ausschließlich auf historischen Berichten. Die Analyse von Zeitreihen zeigt jedoch, dass verfügbare Daten verschiedenen Faktoren unterliegen (z.B. raumzeitliche Verteilung, Periodisierungseffekte), die die Qualität deutlich beeinflussen und den lückenhafte Charakter der Aufzeichnungen hervorheben. Durch eine steigende Anzahl geowissenschaftlich belegter und datierter, historisch aber nicht überlieferter Tsunami-Ereignisse, wird die nicht existente Überlieferung als ein großer Problem in der Paläotsunami-Forschung erkannt. Zwar bieten historische Daten einen ersten Ansatz zur Identifikation tsunamigefährdeter Küstenregionen, die historische Berichterstattung stellt jedoch keine belastbare Basis für eine verlässliche Risikoprävention dar.

Vor dem Hintergrund einer zunehmenden wirtschaftlichen Bedeutung (z.B. Massentourismus) sowie der stetig wachsenden Bevölkerung von Küstenregionen, muss unser Wissen über die lokale wie auch (über-)regionale Tsunami-Gefährdung mediterraner Küsten verbessert werden.

Um eine verlässliche Einschätzung des Tsunamirisikos geben und Strategien für eine Risikominderung entwickeln zu können, ist es von größter Bedeutung (i) gefährdete Regionen zu identifizieren sowie (ii) die Intensität und Frequenz möglicher Ereignisse abzuschätzen. Ein solcher Ansatz ist insbesondere vielversprechend, wenn auf Basis einer Analyse von Paläotsunami-Ereignissen Regionen hoher Gefährdung erkannt, Wiederkehrintervalle berechnet und Auswirkungen in Bezug auf Überflutungshöhe und -reichweite abgeschätzt werden können.

In den letzten Jahren haben geowissenschaftliche Studien wiederholt Belege dafür geliefert, dass antike Häfen im Mittelmeerraum von Tsunami-Ereignissen getroffen oder sogar zerstört wurden. Als Schutz vor Sturm- und Wellenwirkung konstruiert, weisen Häfen ruhige Sedimentationsbedingungen auf und bieten daher ein optimales Geoarchiv für tsunamigene Hochenergie-Ereignisse in Küstenregionen.

Bedingt durch die Nähe des Hellenischen Bogens sowie ausgedehnte lokale Störungszonen, besitzen die Küstenregionen des Ionischen Meeres wie auch des Golfs von Korinth ein hohes Tsunami-Risiko. Geowissenschaftliche und geoarchäologische Untersuchungen der antiken Hafenanlagen von Krane (Kefalonia), Lechaion (Korinth, Golf von Korinth) und Kyllini (westl. Peloponnes) umfassen terrestrische und küstennahe Rammkernsondierungen sowie anschließende sedimentologische, geochemische und mikrofaunistische Untersuchungen von Sedimentproben. Ebenfalls wurden geophysikalische Methoden (Geoelektrische Tomographie, Georadar) angewandt, um Strukturen des oberflächennahen Untergrunds zu erkennen und stratigraphische Abfolgen über weite Strecken nachzuverfolgen. Die zeitliche Einordnung von Ereignissen basiert auf Radiokohlenstoffdatierung sowie der Altersbestimmung diagnostischer Keramikfragmente.

Die in der vorliegenden Arbeit dargestellten Untersuchungen liefern deutliche Belege für Paläotsunami-Ereignisse in den jeweiligen Untersuchungsgebieten. Befunde für den tsunamigenen Einfluss auf Krane, Lechaion und Kyllini umfassen (i) Einschaltungen grobkörniger allochthoner mariner Sedimente in schluff-dominierte ruhige Hafensedimente und/oder flachmarine Fazies, (ii) gestörte Zusammensetzungen der Mikrofauna und/oder (iii) deutliche geochemische Signale

sowie (iv) geoarchäologische Zerstörungslagen und (v) ausgedehnte Vorkommen beachrockartig verfestigter Tsunamite.

Für Krane liefert die Datierung der Ereignislagen jeweils Maximalalter, die die unterschiedlichen Tsunamigenerationen auf 4150 ± 60 cal v. Chr., ~ 3200 ± 110 cal v. Chr., ~ 650 ± 110 cal v. Chr. und ~ 930 ± 40 cal n. Chr. datieren. Datierungsergebnisse für Lechaion zeigen, dass der Hafen im 8. - 6. Jhd. v. Chr., im 1. - 2. Jhd. n. Chr. sowie im 6. Jhd. n. Chr. von starken Tsunami-Ereignissen betroffen war, während der antike Hafen von Kyllini zwischen dem späten 7. und frühen 4. Jhd. v. Chr. sowie zwischen dem 4. und 6. Jhd. n. Chr. von Tsunamis getroffen wurde. In beiden Fällen scheint die endgültige Zerstörung der Hafenanlagen die direkte Folge eines Paläotsunami-Ereignissen zu sein.

Ein Vergleich der Tsunami-Signale eines jeden Untersuchungsgebiets mit geowisschenschaftlichen Befunden anderer Regionen ergibt, dass die untersuchten Hafenanlagen ausgezeichnete Geoarchive für überregionale Mega-Tsunamis darstellen.

Table of Contents

List of Figures

List of Tables

1 Introduction

1.1 Tsunamis as coastal hazard in the eastern Mediterranean – implications for palaeotsunami research

Coastal areas all over the world are hot spots for human settlement and trading activity since ancient times, as they represent a transition zone between terrestrial and marine environs. Although coastal areas merely constitute 20% of all land area, about half of the world's population lives in a maximum distance of about 100 km from the coastline (Burke et al. 2001, Mee 2012). At present, two out of three cities with more than 10 million inhabitants are also located within the coastal zone. Furthermore, industrial facilities and economic investments are especially concentrated in coastal regions (Crossland 2005).

Worldwide, coastlines are subject to a broad variety of natural hazards like tropical storms, tsunamis, storm surges, landslides, constant coastal erosion or sea-level rise (Gornitz 2005). The intense agglomeration of human population and infrastructure thus inevitably increases the vulnerability of coastal areas in terms of natural hazards (Burke et al. 2001). Floods, storm surges or major tropical storms like the 2005 hurricane Katrina or 2008 cyclone Nargis are recognized as hazards that are capable to cause many fatalities and major devastation of coastal areas (Münchener Rück 2013).

However, it is only since the December 26th, 2004 Indian Ocean Tsunami (IOT) that tsunami events suddenly became another worldwide focus of public and also scientific awareness regarding coastal hazards. The succeeding Tohoku-Oki event, that hit the Japanese coast on March 11th, 2011 revealed even more the destructive potential of such seismically induced extreme wave events.

As Japanese risk mitigation strategies and prevention measures like early warning systems are well adapted to the frequent occurrence of tsunamis (Hoshiba & Ozaki 2014), the 2011 Tohoku-Oki event particularly emphasizes the vulnerability even of such coastal areas that are generally considered as "well prepared" for natural disasters. The severe and devastating consequences of major tsunami impact on coastal regions that are unaware of and unprepared for tsunami events already became dramatically evident during the 2004 IOT. Future (geo-) scientific research priorities must therefore especially concentrate on the identifications coastal areas that are highly prone to tsunami landfall but are not yet in the focus of tsunami risk mitigation.

Throughout the eastern Mediterranean, the occurrence of tsunami events is already known since historical times. As most tsunamis are seismic sea waves or induced by seismically triggered underwater mass movements, their occurrence is mainly bound to the major plate boundary between Africa and Europe. Along the Hellenic Arc, the African Plate is being subducted under the Aegean Microplate (Fig. 1.1). Rapid plate movements up to 50 mm/a result in considerable crustal deformation and seismic activity. Thus, the eastern Mediterranean is characterized by the highest rate of seismicity throughout Europe (Cocard et al. 1999, Sachpazi et al. 2000, Hollenstein et al. 2008a).

Strong offshore earthquakes originating along the Hellenic Arc or other major faults such as the North Anatolian Fault are frequent and often accompanied by co-seismic displacements of the

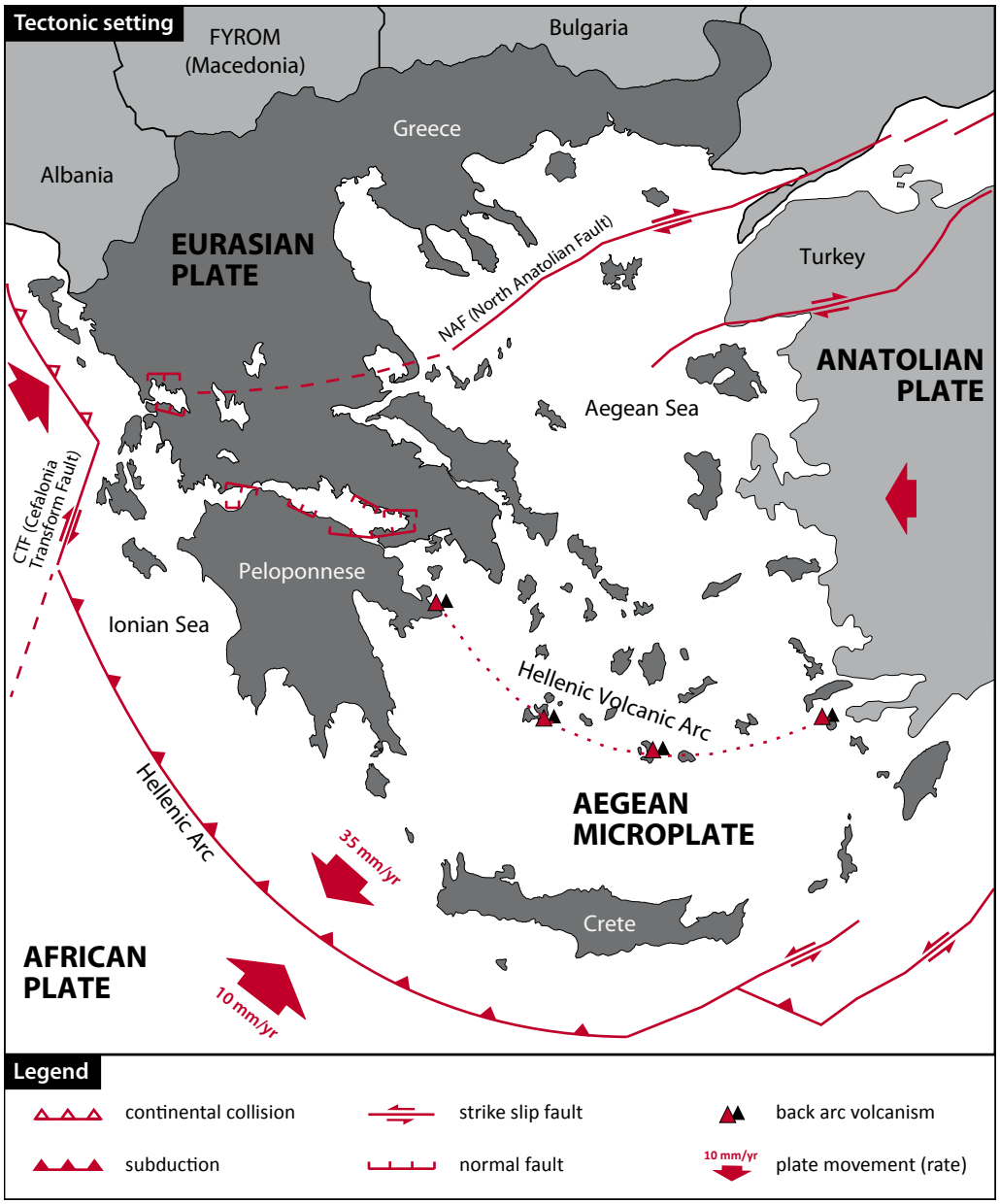

Fig. 1.1: Tectonic setting of the eastern Mediterranean (map modified after DOUTSOS & KOKKALAS 2001).

sea floor and/or submarine slides. These earthquakes therefore hold a particularly high risk of tsunami generation (SOLOVIEV 1990, PAPAZACHOS & DIMITRIU 1991). Large water depths up to 5 km, highly variable geomorphologies of continental slope and shelf regions and short shore-to-shore distances further enhance the risk of strong tsunami events along eastern Mediterranean coasts.

Nevertheless, systematic scientific research on their occurrence and distribution has only begun during the last decades and it is not until the 2004 IOT that tsunami research in the Mediterranean region has been strongly intensified.

First estimations of tsunami hazard started in the 1960s and were merely based on the collection of local historical records compiled in tsunami catalogues for different coastal regions. For Greece, such data were published by Galanopoulos (1960), Ambrasey (1962), and, later, by Antonopoulos (1980). In the 1990s, with regard to the tectonic background and historical data, Soloviev (1990) and Papazachos & Dimitriu (1991) classified those areas capable of triggering future tsunamis as so-called "tsunamigenic zones". Regarding western Greece, most coastal areas along the Peloponnese, the Ionian Islands and the Gulf of Corinth show a high risk of tsunami impact. At the same time, these areas possess a high vulnerability because major settlements such as Corinth, Aegio, Patras, Pyrgos, Kalamata (Peloponnese), Zakynthos, Argostoli and Lefkada (Ionian Islands), as well as economic infrastructure concerning mass tourism are located at the immediate coastline.

Due to long recurrence intervals of several hundreds of years between major events, tsunamis in the eastern Mediterranean are scarcely embedded into social memory and have not yet been considered in regional disaster plans (Papathoma & Dominey-Howes 2003). Consequently, only a minor awareness for tsunami hazard has evolved since historical times. Today, highly destructive earthquakes and tsunamis that occurred, for instance, offshore western Crete (Greece) in 365 AD, offshore the Peloponnese Peninsula (Greece) in 1303 AD and in the Strait of Messina (southern Italy) in 1908 AD are well known to the scientific community (Antonopoulos 1980, Soloviev 1990, Papadopoulos & Fokaefs 2005, Guidoboni & Ebel 2009) and helped to recognize the considerable tsunami risk. At the same time, these deadly events are scarcely remembered by the local administration and population.

Considering the increasing economic significance of coastal regions (e.g. for mass tourism) and the constantly growing coastal population, our knowledge on the local, regional and supraregional tsunami hazard along Mediterranean coasts has to be improved (Tselentis et al. 2010). For setting up a reliable tsunami risk assessment and developing risk mitigation strategies, it is of major importance (i) to identify areas under risk and (ii) to estimate the intensity and frequency of potential events. This approach is most promising when based on the analysis of palaeotsunami research seeking to detect areas of high palaeotsunami hazard, to calculate recurrence intervals and to document palaeotsunami destructiveness in terms of wave run-up, inundation and long-term coastal change. Coastal areas which turned out to have been repeatedly affected by tsunami impact in the past are best-fit candidates for future tsunami landfalls. This had to be bitterly learned from the Japan 2011 tsunami where preceding deadly events such as 869 AD had occurred in the past were known but neglected or at least underestimated (Minoura et al. 2001, Satake et al. 2007). Palaeotsunami research is thus a key to better assess present and future tsunami risk all over the world and to improve the protection of the coastal population.

1.2 The role of ancient Mediterranean harbours in palaeotsunami research

Literary sources like the well-known historical account by Ammianus Marcellinus, who reports on the 365 AD tsunami, repeatedly describe tsunami impact along eastern Mediterranean shores (Amm. Mar. 26.10.15-19 after Rolfe 1940). Nevertheless, the historical record of tsunami events is generally sparse and does merely comprise younger events and/or those that had more or less devastating effects on larger areas (Hadler et al. 2012). In order to better assess the hazard potential of an area and to prepare for future events, it is however inevitable, to gather

sufficient data on the frequency and effects of palaeotsunami events. To better understand the historically known tsunami risk for an area, it is absolutely necessary to further fill in the gaps in the historical record by geo-scientific studies. However, to detect palaeotsunami impact by geo-scientific methods, there is certainly a need for suitable geo-archives that preserve sedimentary evidence of previous events.

During the past two decades, interdisciplinary research on ancient harbours in the eastern Mediterranean has been strongly intensified on the part of archaeological and geographical sciences. Nowadays, ancient harbours are mostly landlocked and may even lie many kilometers inland because coastlines have shifted dramatically since ancient times (Vött & Brückner 2006, Marriner & Morhange 2007, Marriner et al. 2010). An example for considerable coastline changes is Piraeus, site of the present-day harbour of Athens, which was an island until the midst of the 2nd millennium BC (Goiran et al. 2011) and is now part of the Attic mainland. The main objectives of geoarchaeological research in ancient harbour areas are to locate harbour basins as such and to clarify how they were connected to the sea. At Miletus, Priene and Myous (western Turkey), for example, Müllenhoff (2005) and Brückner et al. (2006) reconstructed the local palaeogeographical settings and identified several landing sites. In western Greece, the shipsheds of ancient Oiniadai were found to have been part of a lagoonal harbour whereas, on the other side of the former island, a potential river harbour was detected (Vött 2007, Vött et al. 2007). For Pella, northern Greece, Fouache et al. (2008) and Ghilardi et al. (2008) showed that at the time of Alexander the Great the site of Pella did not lie at the coast but at the shore of a large lake that was connected to the sea via a man-made channel. Complex geoarchaeological harbour studies were also conducted at Claudius and Trajan's marine harbours on the Tiber delta (Italy) with respect to access channels to the sea (Giraudi 2009, Goiran 2010). Further key questions of harbour geoarchaeology are to reconstruct the time interval during which harbour facilities were in use and when and why they were abandoned. The palaeogeographical and palaeoenvironmental settings of harbours were strongly altered in the course of time due to different factors such as sediment transport from the hinterland, changing coastal dynamics, sea level fluctuations and man-made impact. In many cases, it is by these gradual changes that delta progradation and coastal aggradation were triggered and harbour installations experienced partial or complete siltation.

In the context of geo-scientific research, ancient harbours do not only provide information on gradual coastal changes but also turned out to be valuable geo-archives for tsunamigenic high-energy impacts on coastal areas. As reflected by the Japanese origin of the word "tsunami" meaning "harbour wave", tsunami events do often manifest first and strongest in harbours (Sugawara et al. 2008). Where long-period waves like tsunamis approach coastal areas, an amplification of the wave already takes place as the wavelength decreases and amplitude increases. Depending on the harbour basin geometry, the structure of the entrance channel or the deposition of moles and quays, tsunami waves become "trapped" inside the harbour by wave reflection. The subsequent superposition of waves induces strong oscillations, generally known as "harbour resonance" that may cause severe damage to the harbour infrastructure (Lee & Raichlen 1971, Zelt 1986, Martinez & Naverac 1988). Thus, even minor waves may develop a considerably destructive potential in basin-like structures, so that harbours are highly prone to be affected by tsunami impacts. The devastating consequences known from recent tsunami impacts (e.g. Chile 2010, Japan 2011) are not limited to modern harbours but must have had similar effects on ancient harbours as well.

Constructed to protect ships from storm and wave activity, ancient harbour basins provide especially sheltered quiescent environments. Storm deposits are therefore not expected to play a major role in the sedimentary record, while at the same time harbour basins act as perfect sediment traps for tsunami deposits. The comparison of geo-stratigraphical data from coastal areas outside and inside ancient harbour settings allows distinguishing between the influence of tsunamis and storms on the coastal evolution – a question which is vividly debated in coastal geosciences all over the world (e.g. Dawson & Shi 2000, Kortekaas & Dawson 2007, Morton et al. 2007). Given that the stratigraphical record was not seriously disturbed or deleted by dredging activities, which were carried out to prevent the harbour basin from siltation, ancient harbour basins thus provide excellent man-made geo-archives to reconstruct palaeotsunami impact.

Within the past few years, convincing evidence was found that ancient harbours throughout the Mediterranean were subject to strong tsunami-related disturbance or destruction (Morhange & Marriner 2010). Outstanding sedimentary and geoarchaeological palaeotsunami evidence was, for example, found for the 6th century AD at Yenikapı in Istanbul (Bony et al. 2012) underlining the considerable tsunami risk associated to the large seismic event expected for this region in the near future. By underwater geoarchaeological studies, Reinhardt et al. (2006) and Goodman-Tchernov et al. (2009) identified shallow shelf deposits of tsunamigenic origin associated to the destruction of the harbour at Caesarea Maritima in 115 AD and detected that the site had already been affected by older tsunami impacts. For the harbour at Alexandria (Egypt), both sedimentological and microfaunal indicators of tsunami-related impact and destruction during the 365 AD earthquake and tsunami are well known (Stanley & Bernasconi 2006, Bernasconi et al. 2006). For Crete, distinct geo-scientific studies evidence of the 365 AD tsunami is preserved at the harbour site of Phalasarna (Pirazzoli et al. 1992). Along the North African shore, sedimentary traces of tsunami impact were additionally found for the ancient harbour sites of and Leptis Magna (Pantosti et al. 2011, Pucci et al. 2011).

Concerning central and western Greece, manifold geo-scientific evidence of tsunami impact was found for harbour sites such as ancient Lefkada (Vött et al. 2009a, May et al. 2011) or Palairos-Pogonia (Vött et al. 2011a). In the western Peloponnese, Olympia's harbour site Pheia was found to have been completely destroyed by co-seismic subsidence and coincidental tsunami rollover in the 6th century AD (Vött et al. 2011b). In the Gulf of Corinth, the ancient city of Helike seems to have also been erased by an earthquake and tsunami inundation in 373 BC (Soter 1999, Soter & Katsonopoulou 2011).

1.3 Aims of the study

Although during the past decades geo-scientific studies have largely increased the public awareness of the tsunami risk in the eastern Mediterranean, many coastal areas still remain a blank spot on the map concerning the possibility of tsunami impact and hence call for further palaeotsunami research. Today, different approaches are applied for evaluating the tsunami hazard along Mediterranean coasts including (i) the analysis of historical accounts (e.g. Gerardi et al. 2008), (ii) geo-scientific analyses of palaeotsunami traces (e.g. Kortekaas 2011, Vött et al. 2010, 2011a, 2011b, 2012) and (iii) modelling tsunami events (e.g. Salamon 2007, Tselentis et al. 2010).

Identifying tsunami sediments, so called tsunamites, by geo-scientific analyses of ancient harbours is an emerging field in modern geoarchaeological research as it combines aspects

of man-environment interaction with the cultural and socio-economic background of harbour development and the geo-scientific quest to identify destructive tsunami events and their recurrence interval. Palaeotsunami research that focuses on different harbour sites at the same at provides both, an identification of locally restricted events as well as a basis for the reconstruction of supra-regional tsunami impacts.

Based on the geo-scientific study of selected ancient harbour basins, the present work intends to extend and to complement the knowledge about palaeotsunami events affecting western Greece in order to better assess the future hazard potential. Therefore, the main objectives are

(i) to analyse the availability and reliability of data on historical tsunami events for selected study areas in the Ionian Sea and (north-)western Greece and to evaluate their applicability for tsunami risk assessment,

(ii) to identify traces of palaeo-tsunami impact from the stratigraphical record of selected ancient harbour sites by sedimentary, geochemical, microfaunal, geophysical and geoarchaeological evidence,

(iii) to correlate historical accounts of the selected harbour sites with geo-scientific evidence to estimate the influence of tsunami events on ancient infrastructure, and

(iv) to establish a local as well as supra-regional geochronostratigraphy of tsunami events to calculate recurrence intervals.

In order to assess the suitability as well as reliability of single harbour sites as geo-archive, further key questions have to be answered. For each study area, the following aspects must be considered as relevant.

(i) To which extend does the geographical situation of the selected harbour site support or prohibit the preservation of tsunami events?

(ii) Do historical accounts on the harbour foundation, usage and abandonment correlate with geo-scientific evidence and is there any written evidence of tsunami events that hit the harbour?

(iii) Is there any indication, that traces of tsunami impact have been deleted by anthropogenic activity, i.e. initial excavation work during the construction of the harbour basin or subsequent dredging activity?

(iv) Is the history of a harbour (foundation, renovation or destruction) somehow related to palaeo-tsunami impact?

1.4 The study areas

Exposed to the tectonically most active zones in the Eastern Mediterranean – the subduction zone of the Hellenic Arc and the half-graben system of the Gulf of Corinth – coastal areas along the western Peloponnese and the Ionian Islands are especially prone to tsunami hazard. Ancient harbour sites located along these coastlines where most likely affected by tsunami events during their history and are thus expected to provide evidence of palaeotsunami impact. Highly prone to be repeatedly affected by local as well as supra-regional events, the ancient harbour sites of Krane (Cefalonia, Ionian Islands), Lechaion (Corinth, Gulf of Corinth) and Kyllini (western Peloponnese) have been selected as promising geo-archives to identify palaeotsunami traces.

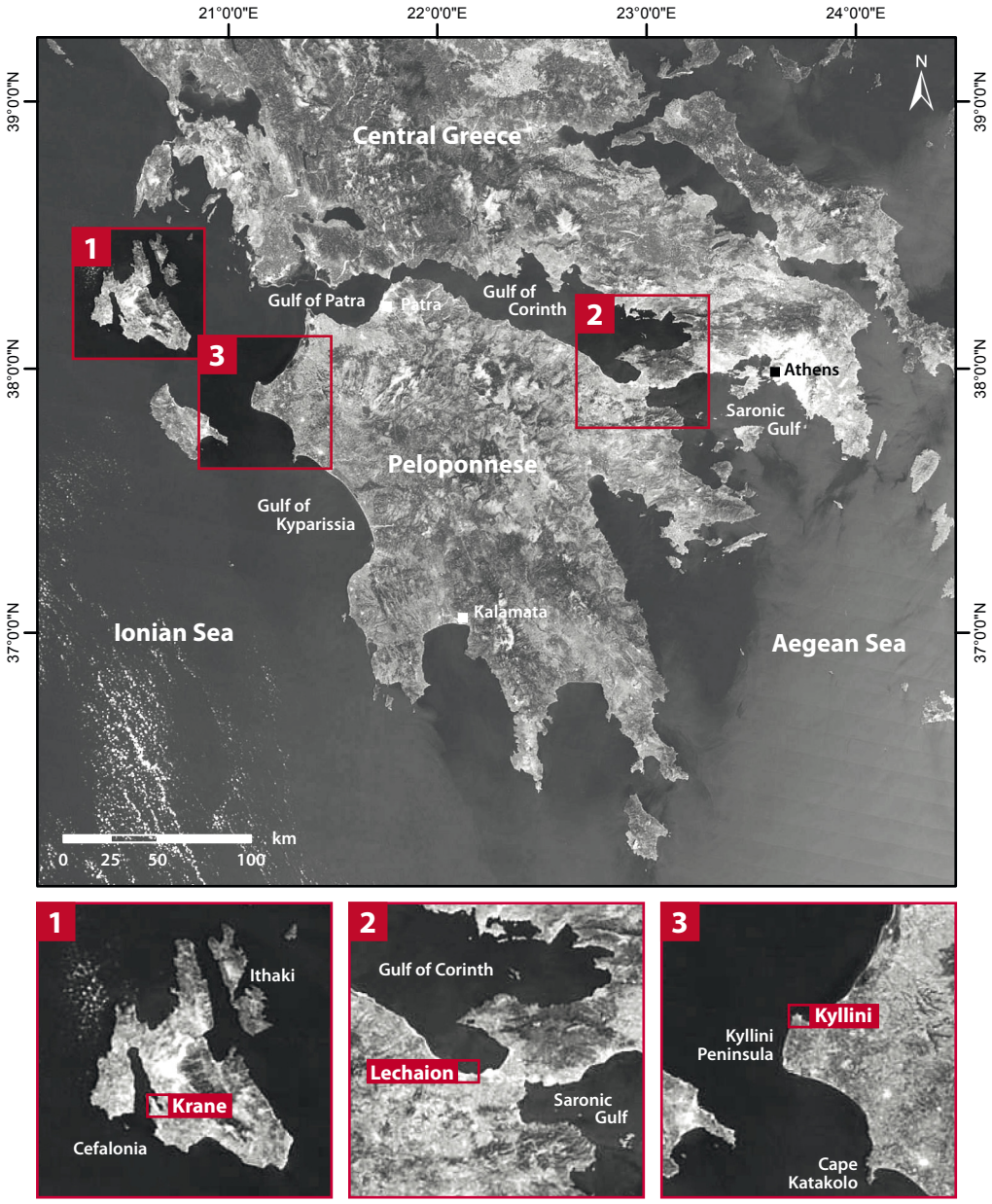

Fig. 1.2: Location of study areas (overview map) and detailed map of the harbour sites at Krane (a), Lechaion (b) and Kyllini (c). Map modified after Bing Aerial Images 2012.

The ancient harbour site of Krane, Cefalonia

Seismic activity throughout the eastern and northern Ionian Sea is controlled by two major tectonic structures – the Hellenic Arc and the Cefalonia Transform Fault (Cocard et al. 1999, Louvari et al. 1999). According to Tselentis et al. (2010), the Ionian Islands of Lefkada, Cefalonia and Zakynthos are frequently affected by potential tsunamigenic earthquakes (M > 6). On Cefalonia, the harbour of ancient Krane is situated in a cul-de-sac-type embayment that branches off the Gulf of Argostoli (Fig. 1.2). The natural harbour site is characterized by quiescent lagoonal conditions with extremely low water depth. As the bay is sheltered from storm influence, wave action decreases to a minimum while strong refraction effects may amplify the impact of tsunami waves.

Lechaion, the harbour of ancient Corinth

Located between the Greek mainland and the Peloponnese, the Gulf of Corinth represents one of the seismically most active regions in the world. Due to ongoing continental rifting, extension rates reach up to 16 mm/yr. The half-graben structure is characterized by numerous active on-shore and submarine faults (Papazachos & Dimitriu 1991, Sachpazi et al. 2003, Avallone et al. 2004). Frequent strong earthquakes often induce submarine slides, a major factor for tsunami generation within the gulf. Water depths of maximum 900 m, steep submarine slopes and a narrow shelf additionally enhance the potential of strong tsunami events (Hasiotis et al. 2002, Stefatos et al. 2006). Solely for the 20th century, six tsunamis have been recorded; the most destructive occurred near Aegio in 1963 (Papadopoulos 2003). Lechaion, the ancient harbour of Corinth, is situated in the south-easternmost part of the gulf (Fig. 1.2). The artificial harbour basin has been connected to the city of Corinth by massive walls and was thus well protected from storm influence. As one of the major ports for Corinth, the history of Lechaion spans about one millennium and makes the harbour a promising long-term geo-archive especially for local tsunami events that goes back to Archaic times.

The ancient harbour site of Kyllini, western Peloponnese

Directly exposed to the Hellenic Arc, the western Peloponnese is known to be threatened by major offshore earthquakes (Koukouvelas et al. 1996). Low-lying areas such as the coastal plains between Cape Araxos and Kyllini and between Pyrgos and Kyparissia must be considered as especially prone to tsunami inundation. Nevertheless, the elongated coastline offers few natural embayments that are suitable geo-archives for palaeotsunami research. Situated at the northern fringe of Cape Kyllini, the eponymous ancient harbour site lies in a natural embayment, sheltered from storm influence or wave action and fortified by men. Like Lechaion, strong fortification walls create a quiescent environment inside the harbour basin that provides optimal preservation conditions for traces of palaeotsunami impact.

1.5 Outline of research

Regarding the tectonic constellation of the Mediterranean Sea (Chapter [Section] 1), the past as well as future hazard of major tsunami impacts is evident for the ancient harbour sites presented within this study. In order to assess the present state of knowledge of the site-specific tsunami histories, an analysis of historical records on tsunamis, especially for the Ionian Sea and the Gulf of Corinth as documented in modern earthquake and tsunami catalogues is given in Chapter 2. Available data about earthquake and tsunami events has been summarized and studied according their spatial and temporal distribution in order to evaluate their potential for tsunami risk assessment.

In the following, detailed results from geo-scientific investigations are presented for the harbour sites of Krane (Chapter 3), Lechaion (Chapter 4) and Kyllini (Chapter 5). Comprehensive sedimentary, geochemical and microfossil analyses aimed at the detection of high-energy event layers that intersect the stratigraphical record of the harbour basins and are potential candidates for tsunami impact. Geophysical studies carried out at all harbour sites intend to decipher the spatial distribution, maximum extend and internal structure of high-energy deposits. Additionally, geophysical methods were applied to detect subsurface archaeological remains that may be correlated to harbour facilities. Were possible, geomorphological and archaeological finds are considered in terms of high-energy wave impact. For each site a local event-geochronology is

presented and discussed in terms of dating inaccuracies, comparability to historical records on tsunami impact and anthropogenic activities like dredging. Finally, all evidence of high-energy wave impact is reviewed regarding the transport mechanism of the associate sediments, also discussing the possibility of storm influence.

In a synthesis (Chapter 6), all obtained results are compared for accordances between study areas and all investigated harbour sites are evaluated regarding their potential as geo-archive for palaeo-tsunami research. The outline of the study is presented in Tab. 1.1.

Tab. 1.1: Study design

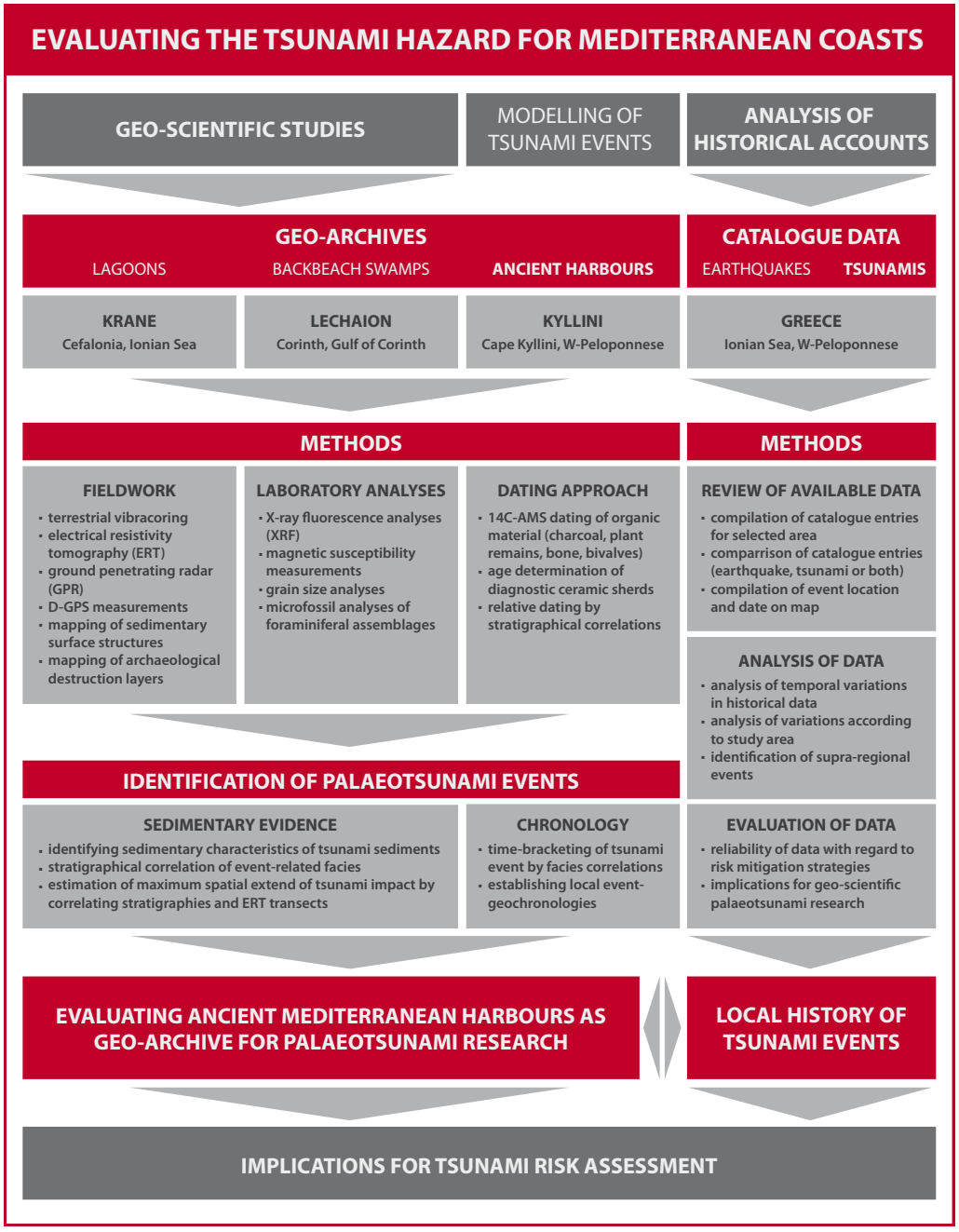

2 Catalogue entries and non-entries of earthquake and tsunami events in the Ionian Sea and the Gulf of Corinth (eastern Mediterranean, Greece) and their interpretation with regard to palaeotsunami research*

Abstract Since historical times coastal areas throughout the eastern Mediterranean are exposed to tsunami hazard. While the detailed geo-scientific investigation of palaeotsunami events is still a young approach, for many decades the knowledge about palaeotsunamis was solely based on historical accounts. This chapter focuses on the analysis of historical data compiled from tsunami and earthquake catalogues for western Greece and its potential for recent tsunami risk assessment. For the Ionian Islands, the western Peloponnese and the Gulf of Corinth a record comprising 284 earthquakes and 51 tsunami events was assembled covering a timespan of almost 3500 years. Results from timeline analyses reveal different characteristics affecting the quality of the dataset, though. Concerning the distribution of data different trends are obvious, such as a temporal thinning backward of events or local periodization phenomena. The fragmentary character of the historical data must also be emphasized. As an increasing number of geo-scientific studies give convincing examples of well dated tsunami signatures not reported in catalogues, the non-existing record is perceived as a major problem to palaeotsunami research. The non-entry of a tsunami event in a catalogue may be due to a number of reasons and does not mean at all that the event did not take place. While the compilation of historical data allows a first approach in the identification of areas vulnerable to tsunamis, it must not be regarded as reliable for hazard assessment.

2.1 Significance of historical records for palaeotsunami research

While detailed geo-scientific investigation and geochronological age determination of palaeotsunami events is still a young approach, for many decades palaeotsunami data was analysed solely on the base of historical accounts known from epigraphic studies or literary sources (Papadopoulos & Fokaefs 2005, Ambrasey 2009). These records show that tsunamis are a long known phenomenon in the Mediterranean.

One of the earliest known references directly related to tsunami impact in Greece is that of Thucydides. He gives a detailed account on earthquakes and a following tsunami in the summer of 426 BC during the 6th year of the Peloponnesian War:

> *"About the same time that these earthquakes were so common, the sea at Orobiae, in Euboea, retiring from the then line of coast, returned in a huge wave and invaded a great part of the town, and retreated leaving some of it still under water; so that what was once land is now sea; such of the inhabitants perishing as could not run up to the higher ground in time. A similar inundation also occurred at Atalanta, the island off the Opuntian Locrian coast, carrying away part of the Athenian fort and wrecking one of two ships which were drawn up on the beach. [...]*

*This chapter is based on:
Hadler, H., Willershäuser, T., Ntageretzis, K., Henning, P. & Vött, A. (2012): Catalogue entries and non-entries of earthquake and tsunami events in the Ionian Sea and the Gulf of Corinth (eastern Mediterranean, Greece) and their interpretation with regard to palaeotsunami research. – Bremer Beiträge zur Geographie und Raumplanung 44: 1-15.

> *The cause, in my opinion, of this phenomenon must be sought in the earthquake. At the point where its shock has been the most violent, the sea is driven back and, suddenly recoiling with redoubled force, causes the inundation. Without an earthquake I do not see how such an accident could happen."*
>
> (Thuc. III.XI after Crawley 2009)

The record gives distinct evidence for a tsunami affecting eastern central Greece. Thucydides even recognizes the tsunami as related to the earthquake. It is therefore a good example of detailed information provided by historical records.

Quite frequently though, descriptions of tsunamis are only a secondary aspect mentioned along with detailed information on earthquakes primarily focusing on the extent of damage caused by ground shaking. Therefore, historical data do not always comprise information on the exact time and location or destructiveness of associated tsunami events. In many cases, tsunami descriptions are vague, because, according to Guidoboni & Ebel (2009), many ancient writers basically focus on the most evident characteristics of a tsunami, such as the exposed sea floor due to receding water followed by a sudden influx of seawater. Ambrasey & Synolakis (2010) emphasize that observational and historical data do not necessarily reflect the maximum geographical extent of a tsunami. Contemporaneous accounts from different coastal sites that report on individual tsunami events were often thought to be of local dimension, but, in fact, they might even be related to each other and represent one and the same supraregional tsunami impact. This is an important aspect regarding tsunami catalogues – the more reliable historical records are available, the more reliable are the reconstructions of tsunami events. An excellent example is the tsunami generated by the 365 AD earthquake that is reported for many areas of the eastern Mediterranean such as Crete, the southern Peloponnese, Alexandria or Sicily by different ancient writers (Antonopoulos 1980a, Papazachos & Dimitriu 1991, Guidoboni & Ebel 2009).

Against the background of powerful, high-resolution present-day technical capabilities for recording earthquakes and tsunamis the question may arise how – probably incomplete – historical catalogues contribute to modern palaeotsunami research. Even in seismically active regions like the eastern Mediterranean, major earthquakes and/or tsunamis remain high magnitude – low frequency events. They may occur once in a few hundreds of years (Papazachos & Papazachou 1997, Papadopoulos et al. 2007), a fact which has dramatically been documented by the 2011 Japan earthquake and tsunami, the youngest predecessor of comparable dimension was found for the 9th century AD (Goto et al. 2011). As a matter of fact, we have to be aware that the modern instrumental record does not cover a time span long enough to cover major tsunami events. As a consequence, tsunami risk assessment which is merely based on seismographic records and tidal monitoring remains incomplete. Even an incomplete compilation of historical records may allow a better estimation of recurrence intervals and thus a more reliable extrapolation for future events (Ambrasey 2009, Guidoboni & Ebel 2009).

This chapter concentrates on the analysis of historical records on tsunamis, especially for the Ionian Sea and the Gulf of Corinth as documented in modern earthquake and tsunami catalogues. The main objectives are (i) to summarize the available data about earthquake and tsunami events, (ii) to study their spatial and temporal distribution, and (ii) to evaluate their potential for tsunami risk assessment.

2.2 Catalogues on earthquakes and tsunamis

Catalogues on earthquake and tsunami events may be defined as

> *"a chronological listing of the occurrences of past earthquakes and tsunamis for an area, where the list normally includes such parameters as the date, time, location and strength of each earthquake and/or tsunami, as well as other parameters deemed important by the compiler of the catalogue (e.g. wave height, inundation distance, damages)."*
>
> (GUIDOBONI & EBEL 2009)

Written reports on earthquakes and tsunamis affecting the Mediterranean region start as early as in the 1st millennium BC. At the present state of knowledge, the first reliable record including the location and date of an earthquake originates from the 8th century BC describing an earthquake in Jerusalem (GUIDOBONI & EBEL 2009). The earliest reliable record of a tsunami refers to the year 479 BC when, according to Herodotus, the Persian fleet at Potidaea (Chalkidiki Peninsula, northern Aegean Sea, Greece) was destroyed by tsunami impact (PAPAZACHOS & DIMITRIU 1991, SOLOVIEV 2000). Information for the Classical and Roman periods is still scattered and mainly based on inscriptions or ancient accounts. From medieval to modern times, written sources mainly comprise chronicles and annals that – in a best-case-scenario – already provide a compilation of local data (AMBRASEY 2009). However, considerable gaps in historical data are well known to exist for the Dark Ages in the 1st third of the 1st millennium BC and between early and late medieval times.

Catalogues in terms of chronological listings of past events first appeared in the mid-15th century AD listing earthquake events. From the 16th century AD onwards their number increased steadily. Today, a large variety of earthquake and tsunami catalogues have been published, while those catalogues unique to tsunami events are still few in numbers and often subject to uncertainties resulting from differences in translation, interpretation and classification of texts depending on the respective author (GUIDOBONI & EBEL 2009).

For the eastern Mediterranean, the data assembled in tsunami catalogues either covers a large area (for the eastern Mediterranean see ANTONOPOULOS 1980a-f, GUIDOBONI 1994, SOLOVIEV et al. 2000, AMBRASEY 2009, GUIDOBONI & EBEL 2009) or has a regional focus (for Greece see PAPADOPOULOS & CHALKIS 1984, PAPADOPOULOS 2003, for Italy see TINTI et al. 2004). Regarding their reliability, two different types of catalogues have to be considered. The first type comprises catalogues based on original data (e.g. GUIDOBONI 1994, GUIDOBONI & COMASTRI 2005, AMBRASEY 2009). These catalogues seem to be the most reliable sources; however, they may still include mistakes or misinterpretations made by the ancient writer or by the compiling author. The second type consists of catalogues with few or no reference to the original data. These alleged new catalogues are merely based on already existing catalogues, thus adopting or amplifying possible errors or misinterpretation (e.g. PAPADOPOULOS & FOKAEFS 2005, VÖTT et al. 2006).

For the first time, data on earthquake and tsunami events is presented, compiled for the Ionian Sea and the Gulf of Corinth based on the analysis of different contemporary tsunami catalogues (Tab. 2.1 and Tab. 2.3, references therein). As many catalogues are based on cross-references and not on original data, information on the reliability of the individual events remains uncertain. Nevertheless, Tab. 2.1 offers the largest database available for the Ionian Sea and the Gulf of Corinth tsunami events known so far.

Tab. 2.1: Historical tsunami events for the Ionian Sea and the Gulf of Corinth compiled after contemporary tsunami catalogues (Galanopouls 1960, Antonopoulos 1979, Antonopoulos 1980a-f, Papadopoulos & Chalkis 1984, Guidoboni 1994, Papazachos & Papazachou 1997, Soloviev et al. 2000, Papadopoulos 2003, Guidoboni & Comatri 2005, Papadopoulos & Fokaefs 2005, Vött et al. 2006, Ambrasey 2009, Ambrasey & Synolakis 2010, Tselentis et al. 2010, NOAA 2011).

No	Date	Region	Area affected by tsunami	References
1	1380 BC	EM, AS, HA	Eastern Mediterranean	c
2	1300 BC	IS, AS	Ionian Sea, Aegean Sea	(z), i
3	373 BC	GC	Helike	a, b, c, e, f, i, k, x, y, z
4	365, July 21	HA, P	Peloponnese, Methoni	a, b, c ,h, i, x, y, z
5	521/22	GC	northern Gulf of Corinth	c, i
6	1169, Feb 11	IS	Ionian Sea	z, c, g, i
7	1270, March	IS	North Ionian Sea	e
8	1303	EM, HA, P	(Eastern) Peloponnese	a, c, h, x, y, z
9	1402, < Aug 30	GC	Gulf of Corinth, Aegio, Xylokastro, Vitrinitsa	a, d, e, f, k, x, y, z
10	1622, May 5	II	Zakynthos	b, c, g, h, i, k, z
11	1629, Feb	HA, II	Zakynthos	x
12	1633, Nov 5	II	Zakynthos	b, c, d, g, h, i, k, x, z
13	1636, Sept 30	II	Cefalonia	g, k, y, z
14	1723, Feb 18	II	Cefalonia	x
15	1723, Feb 21/22	II	Cefalonia (Lixouri), Lefkada	c, g, h, i, k, y, z
16	1723, Feb 29	II	Cefalonia (Argostoli)	x
17	1732, Nov	II	Kerkyra	c, g, h, i, k, y, (z)
18	1742, Feb 21	GC	Corinth, Aegio	d ,e, f
19	1742, Feb 25	II, IS, GC	Aegio	x
20	1748, May 25	GC	Aegio	b, c, d, e, f, h, i, k, x, y, z
21	1769	GC	Rio, Antirio, Nafpaktos, Desfina	d, e, f, x
22	1791, Nov 2	II, P	Zakynthos, Peloponnese	c, d, e, g, h, i, k, (z)
23	1794, June 11	GC	Galaxidi	d, e, f, k, y
24	1804, June 8	II, IS, GC	Patra	b, c, g, h, i, k, y, z
25	1805, Jan 8	P, GC, IS	Patra	g, k
26	1817, Aug	GC	Aegio	c, d, e, f, h, i, k, x, y, z
27	1820, March 17	II	Lefkada	g, k, (z)
28	1820, Dec 29	II, P	Zakynthos	g, k, y
29	1821, Jan 6	II, P	Patras	b, h, i, k, z
30	1821, Jan 9	GC	Gulf of Corinth, Alcyonic Sea, Patra, Zakynthos	c, g, x
31	1825, Jan 19	II	Ionian Sea, Lefkas	c, g, i, k, x, z
32	1835, July 12	II	Ionian Sea, Zakynthos	g, h, i, z
33	1861, Dec 26	GC	Galaxidi, Itea, Valimitika, Temeni, Diakofto, Vitrinitsa	b, c, d, e, f, h, i, k, x, y, z
34	1862, Jan 1	P, GC, IS	Galaxidi, Itea	k, z
35	1867, Feb 4	II	Cefalonia (Lixouri), Lefkada	d, e, g, k, y, z
36	1867, April 10	II	Cefalonia (Lixouri)	g, z
37	1867, Sept 20	II, P	Peloponnese, Zakynthos, Lefkada, Cefalonia (Lixouri, Argostoli)	c, h, i, z
38	1869, Dec 28	II	Lefkada	b, g, k, y
39	1870, Aug 1	GC	Chalkida	k, z
40	1871, Oct 5	GC	Gulf of Corinth	z
41	1881, Dec	P, GC, IS	Patra, Etoliko	c, k, z
42	1883, June 27	II	Ionian Sea, Kerkyra	b, d, e, g, h, i, k, z
43	1886, Aug 27	P	Peloponnese, Gialova, Agrilos, Filiatra	x, z, b, c, d, e, g, h, i, k
44	1887, Oct 3	GC	Galaxidi, Xylokastro, Sykia	x, y, z, b, c, d, e, f, h, i, k
45	1888, Sept 9	GC	Aegio, Galaxidi	(x), z, d, e, f, k
46	1893, April 17	II	Ionian Sea, Zakynthos	e, g, k
47	1894, April 27	P	Kyparissia	(y)
48	1897, Dec	IS	Ionian Sea, Zakynthos	g, h, i
49	1898, June 2	GC	Gulf of Corinth	x, d, e, f, k
50	1898, Dec 3	II	Ionian Sea, Zakynthos	z, c, g, i
51	1899, Jan 22	P	Kyparissia, Marathoupole, Marathon	x, y, z, d, e, g, h, i, k

2.3 Historical records on tsunami events – written or non-written?

2.3.1 Problems concerning written records

Based on the afore mentioned tsunami and earthquake catalogues (Tab. 2.1), a record comprising 284 earthquakes and 51 tsunami events was assembled for the Ionian Islands, the western Peloponnese and the Gulf of Corinth covering a timespan of almost 3500 years (Figs. 2.1a and 2.2a).

The data collection allows several observations regarding main differences in the temporal distribution of tsunami and earthquake events. While there are almost no entries in the studied catalogues for the 2nd and 1st millennia BC, an increased number of historical sources reporting on such events can be found for the time period between the 1st and the 6th century AD (Fig. 2.1b). However, up to the 15th century AD the written record mainly comprises major extreme events of a supraregional nature such as the 365 AD or 1303 AD earthquake and tsunami events. It is not until the mid-15th century that the catalogues show a rapid increase in records, especially concerning earthquakes (Fig. 2.1c). The data clearly documents that, from 1500 AD onwards, the total number of earthquakes reported for western Greece has in fact doubled every century (Fig. 2.2). A similar trend has been found by GUIDOBONI & EBEL (2009) for the Italian earthquake record. Regarding the number of tsunamis reported for the time period covered by the studied catalogues, the record is much more fragmented and irregular over the centuries. A strong

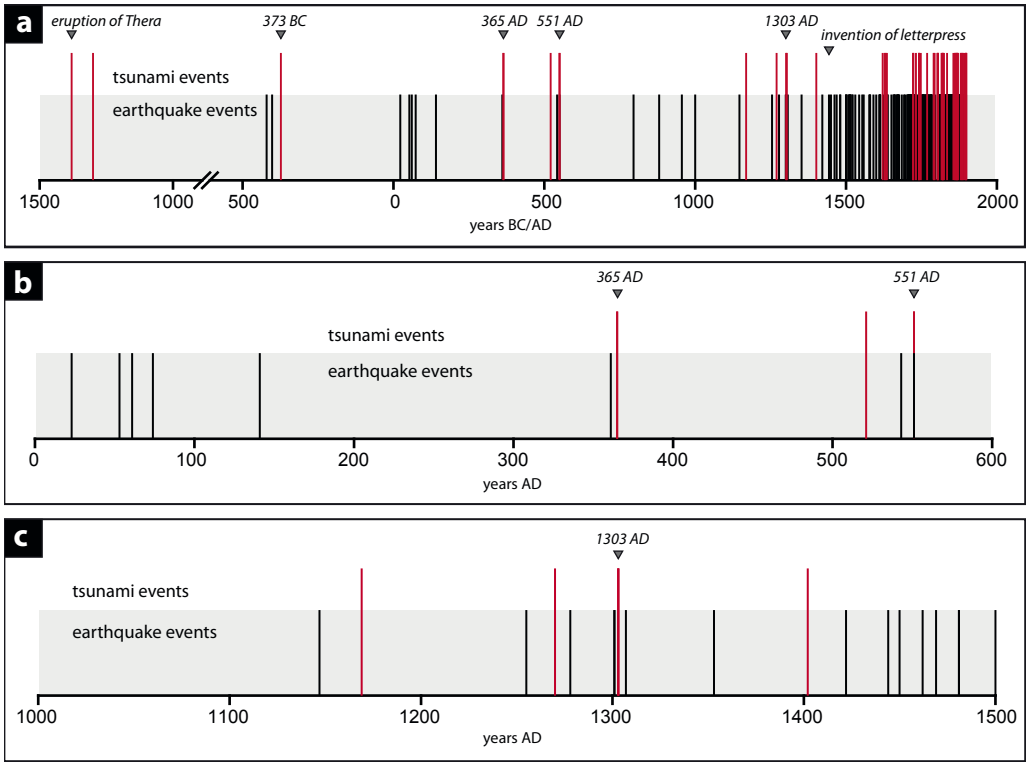

Fig. 2.1: Earthquakes and tsunamis as registered in modern catalogues for the Ionian Islands, the western Peloponnese and the Gulf of Corinth. Timeline for earthquake and tsunami events between the 2nd millennium BC and modern times. Major events are labelled (a). Detailed view of event timeline between 1 and 600 AD (b). Detailed view of event timeline between 1000 AD and 1500 AD (c). For references see Table 3.

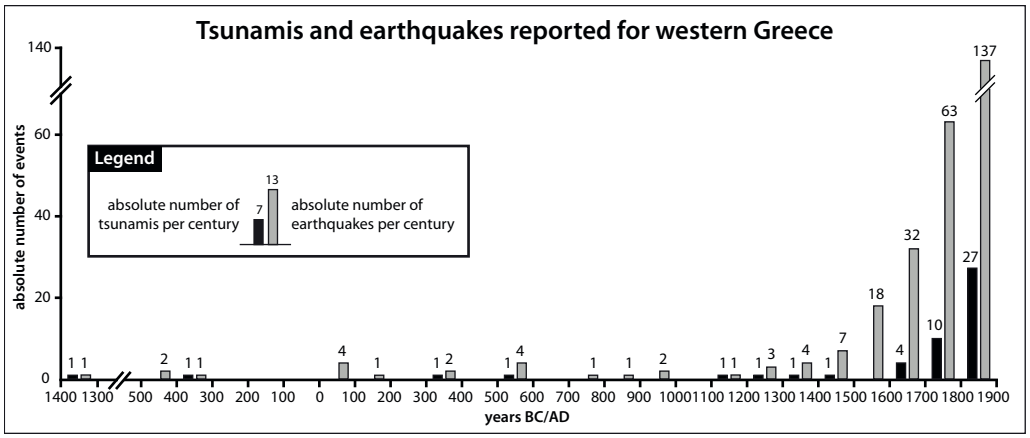

Fig. 2.2: Absolute number of earthquake and tsunami events per century for the Ionian Sea and the Gulf of Corinth (for references see Tab. 2.3).

increase in the tsunami record can only be observed from the late 17th century onwards. As will be discussed below, this might be due to the local historical context.

From the temporal distribution of earthquake and tsunami data (Fig. 2.1), it can thus be concluded that (i) only few records of tsunami events exist compared to the number of recorded earthquakes for the same time period, (ii) both earthquake and tsunami data show a thinning backward tendency through time, and (iii) the older the tsunami event recorded in the catalogue, the wider was the area reported to have been affected by the event.

While the predominance of the number of earthquake records over the number of tsunami records is obvious – not every earthquake has triggered a tsunami event –, several reasons seem to be responsible for the temporal thinning backward of the number of event records. Going further back in time the preservation potential of written records is smaller. Moreover, the absolute number of written records is a direct function of the size of the observed area; this means that the smaller the area of interest, the smaller is the number of entries in the studied catalogues. Thus, it is plausible that the catalogues rather comprise major events chronicled for various places all over the eastern Mediterranean whereas smaller events of more local dimensions are clearly underrepresented. Small events consequently appear more fragmented and incompletely documented.

The abrupt increase in as well as the subsequently strongly growing number of written records during recent centuries can be explained by the comparatively short time that has passed since the events took place. Moreover, revolutionary technical innovations have to be taken into account. With Johannes Gutenberg's (1400-1468 AD) invention of printing in the midst of the 15th century AD the preservation potential for written records suddenly increased due to the rapidly increasing reproducibility and accessibility of printed sources. Originally handwritten chronicles, annals, letters and other documents could now be easily duplicated and spread over larger regions. Additionally, printing allowed the gradual development of newspapers. Newspapers are excellent historical archives for their reports usually comprise precise information on location and date of tsunami and earthquake events (Guidoboni & Ebel 2009, Ambrasey 2009). Explaining a sudden increase of earthquake and tsunami records within the course of a few decades by increased seismicity is highly questionable (Ambrasey & Synolakis 2010).

Tab. 2.2: Overview of possible explanations for tsunami events that are not documented in the historical record.

OVERVIEW OF POSSIBLE EXPLANATIONS FOR TSUNAMI EVENTS MISSING IN THE HISTORICAL RECORD

There is no documentation of a tsunami in the historical record.

The tsunami **did not occur** - no written record exists.

The tsunami **did occur** - no written record exists, because...

- ...the record was lost. The probability of a lost record is all the higher the more time has elapsed since the event.
- ...the event affected an uninhabited or only sparsely populated area and was thus not reported over time.
- ...the event did not cause noticeable destruction or fatalities and was too small to attract attention. Based on this scenario, a fragmentary record must be assumed for minor events. The assumption is supported for older events.
- ...the tsunami affected a populated area, but no one survived to write or pass a record.
- ...the triggering earthquake overshadowed the following tsunami.
- ...the chronicler did not understand what he saw and therefore recorded only the "known" phenomena such as the effects of the earthquake.
- ...the affected area suffered from political instability, wars or invasions, crop failures or diseases generally leading to a decreased production of written records.
- ...the tsunami occurred at night and was thus not observed. While even weak earthquakes are felt over wide areas independent from daytime the account on weak tsunami events might especially depend on whether they have been observed at all.

The tsunami did occur - a written record exists, but...

- ...the record itself has not yet been discovered.
- ...the description of the event has not been correctly translated or understood, for instance due to metaphorical issues.
- ...the record was misinterpreted as storm or other flood catastrophe, often in conjunction with religious interpretations.

Conclusion: Many events must be missing from the historical record.

2.3.2 The problem of non-existing tsunami records

In palaeotsunami research, it is frequently argued that geo-scientifically dated earthquakes or tsunami events are not likely to have really taken place as long as there is no contemporaneous historical record which can be considered as final proof. However, an increasing number of geo-scientific studies have given convincing examples of well dated tsunami signatures for areas where no written records exist. Evidence of locally non-reported tsunami impact was found, for instance, for northwestern Greece (Vött et al. 2009b, 2011a, May et al. 2012), the Ionian Islands (Vött et al. 2012), the Peloponnese (Vött et al. 2010, 2012, Willershäuser et al., 2012), the Gulf of Corinth (Hadler et al. 2011b, Kortekaas et al. 2011), Sicily (De Martini et al. 2010) and southern mainland Italy (Mastronuzzi & Sanso 2012).

Both the timeline analysis of earthquake and tsunami records (Fig. 2.2) and geomorphological and sedimentological evidence from geo-scientific studies document the fragmentary character of the historical tsunami record for western Greece. As a matter of fact, palaeotsunami research has shown that there are traces of much more strong tsunami events than registered in the catalogues. The decision tree (Tab. 2.2) presents an overview of possible explanations for tsunami events missing in the historical record. In a summary view, a variety of reasons may be responsible for the non-existence of written historical records. It thus has to be strongly emphasized that a missing record of a tsunami event must not be used as prove that the event did not take place.

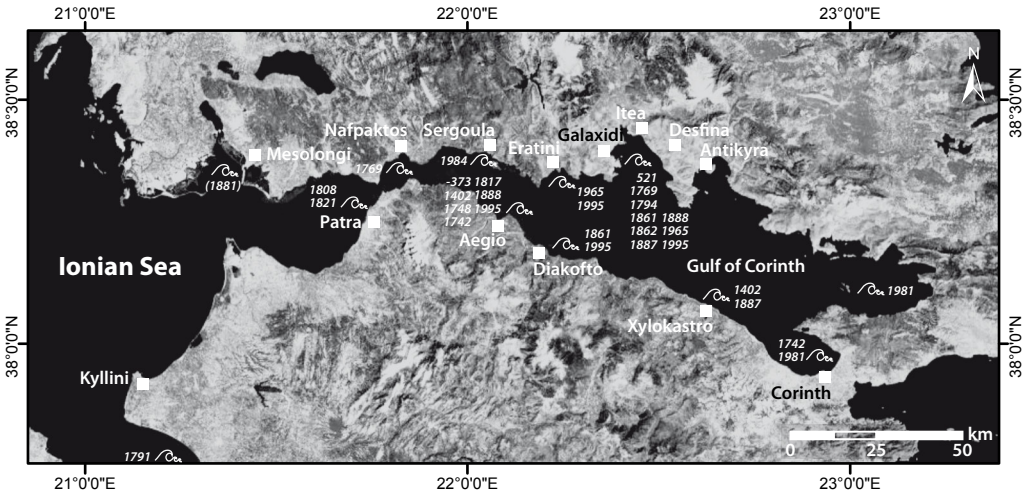

Fig. 2.3: Distribution of tsunami events for the Gulf of Corinth as compiled from modern catalogues (for references see Tab. 2.3). Map modified after Bing Aerial Images 2012.

2.4 Evaluating the historical record of tsunami events

2.4.1 Historical and modern tsunami events in the Gulf of Corinth

As shown above, numerous tsunami catalogues for the Mediterranean and especially for Greece report on historical tsunami events that occurred within the Gulf of Corinth (Soloviev et al., 2000; Papadopoulos, 2003; Ambraseys & Synolakis, 2010). An overall number of 73 earthquakes and 12 tsunamis was compiled from catalogues for the period from 500 BC to 1900 AD (Fig. 2.3, for references see Tab. 2.3). Events that took place between 1900 and 2000 AD are derived from instrumentally recorded data.

Throughout the last decades, the Gulf of Corinth has been recognized as an outstanding natural laboratory for geo-scientific earthquake and tsunami research and is frequently monitored by numerous research groups (e.g. SACHPAZI et al. 2003, AVALLONE et al. 2004, BOUROUIS & CORNET 2009). Additionally, the instrumental record of seismic activity covers about the last century (AMBRASEY & JACKSON 1997). Thus, the area offers good conditions to compare the validity of historical data with detailed data available from recent instrumental records.

Time line analysis (Fig. 2.4a) allows to detect different trends regarding the earthquake and tsunami record over the past centuries. While the absolute number of reliable tsunami events shows only a slightly increasing trend for the past three centuries, a strong increase can be observed for earthquakes. The number of events recorded for the second half of the 20th century exceeds the 19th century record by a factor of 24. Since a rapid increase of seismic activity over a couple of centuries has to be regarded as implausible, the increasing numbers of catalogue entries is related to considerable progress in modern instrumental recording. So, the high-resolution scientific data available today forms a strong contrast to the historical data available from the 19th century backwards both for earthquake and tsunami events. Implying a more or less constant seismic activity for past historical periods, this contrast in data once again clearly demonstrates the fragmented character of ancient accounts, especially concerning minor earthquake events.

The absolute number of tsunamis recorded for the Gulf of Corinth since the 1800 AD is only slightly increasing through time with a calculated average number of five tsunamis per century. This trend allows the conclusion that the tsunami record for the Gulf of Corinth is more or less reliable for the last three centuries. In contrast, for earlier times, the catalogues show only three records for a period spanning more than a millennium. We can thus suggest that this gap reflects a considerable decrease in the reliability of catalogue entries towards older time periods.

2.4.2 Tsunami events in the Ionian Sea and the western Peloponnese

The compilation of catalogue entries for earthquake and tsunami events that affected Cefalonia Island revealed historical records only from the late 17th century AD until our days (Fig. 2.4b). While for adjacent islands earlier reports on earthquakes do exist, no events are known to have affected Cefalonia before the 17th century AD (Tab. 2.3). From a geophysical point of view, the complete absence of earthquakes and tsunamis over many centuries is unrealistic. This is all the more true as Cefalonia is a hot spot in terms of seismic and tsunami events.

Regarding the tsunami timeline of Cefalonia, the island may represent a so-called silent area. A silent area is characterized by an extraordinarily long return period for extreme events, so that the hazard has not been recognized so far (GUIDOBONI & EBEL 2009). In case only few major tsunami events have affected the island during history, there might eventually be no record about it. As a consequence, the area seems to be silent as if it was not endangered by tsunamis at all. However, the frequent appearance of tsunamis all around the Ionian Islands which is reflected in the tsunami record since the 17th century (Fig. 2.5) and also the various geo-scientific tsunami traces found for Cefalonia and Lefkada Island in recent years (HADLER et al. 2011a, WILLERSHÄUSER et al. 2011, VÖTT et al. 2012) rather indicate a lack of historical records than a missing of events.

Another aspect that has to be considered is the periodization phenomenon of events which is explained by a greater availability of historical documents for certain periods (GUIDOBONI & EBEL 2009). For instance, only very little is known about medieval Cefalonia (PARTSCH 1890). Due

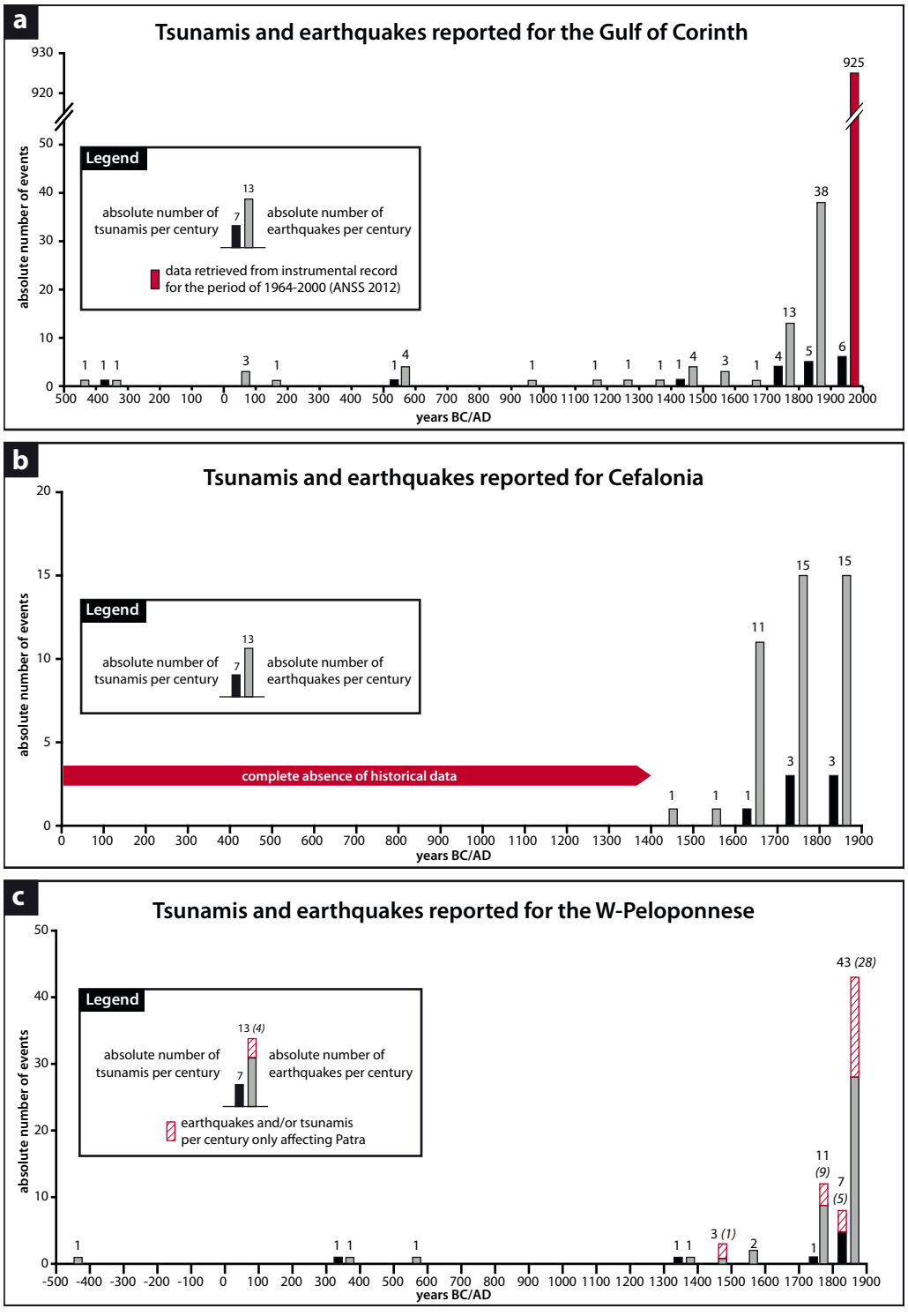

Fig. 2.4: Absolute number of earthquake and tsunami events per century from 500 BC to 2000 AD for the Gulf of Corinth (a), from 1 AD to 1900 AD for Cefalonia Island (b) and from 500 BC to 1900 AD for the western Peloponnese (c). For the 20th century, the absolute number of earthquakes in the Gulf of Corinth refers to the period from 1964 to 2000 (ANSS 2012), tsunami events from 1900 to 2000 are compiled after Papadopoulos 2003. For references see Tab. 2.3.

to political reasons, documents might have been lost during times of instability or occupation by a foreign power or the initial production of documents might as well have been reduced (GUIDOBONI & EBEL 2009). Indeed, until the early 19th century AD, Cefalonia Island was frequently affected by acts of war or civil disturbances with negative effects on written historical records (PARTSCH 1890). This might explain why the data compilation for Cefalonia is only fragmented. However, from the 19th century onwards, political disturbances calmed down under British governance. Subsequently, the historical perception may have focused more intensively on non-political events, e.g. earthquakes or tsunamis. Additionally, it has to be taken into account that, during the 17th century AD, Cefalonia served as a centre of Venetian print production which might have contributed to a greater number of historical records for this period (STEINHART & WIRBELAUER 2002).

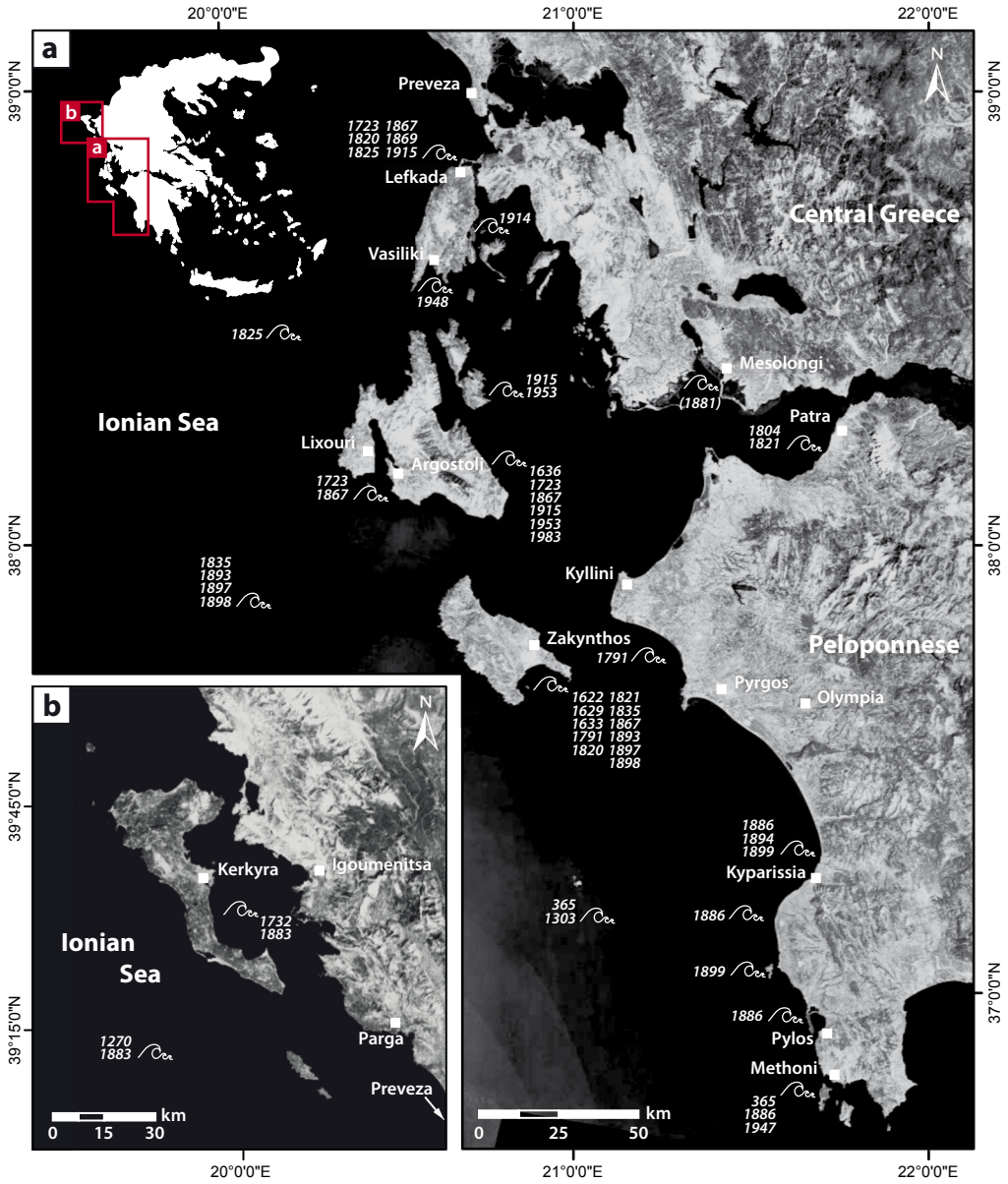

Fig. 2.5: Distribution of tsunami events for the Ionian Sea and western Peloponnese as compiled from modern catalogues. For references see Tab. 2.3. Map modified after Bing Aerial Images 2012.

In a summary view, the historical timeline for tsunami and earthquake events that are reported for Cefalonia Islands is not a reliable base for palaeotsunami research. Concerning the time period until the 17th century AD, it is a good example for the phenomenon that the absence of historical evidence does not at all mean that tsunami and earthquake events had not taken place at all.

In comparison to the tsunami timelines presented above, the compilation of catalogue entries for earthquake and tsunami events for the western Peloponnese (Fig. 2.4c) reveals an equally scarce level of historical records until the 15th century AD. For nearly two millennia the timeline only documents some major events like the 365 AD earthquake and tsunami or the 1303 AD earthquake. A wide gap in the historical record must thus be assumed for the western Peloponnese from 500 BC to 1400 AD.

A slight increase in the number of catalogue entries can be observed for the 15th and 16th century AD, again, most probably due to the invention of printing technology by Gutenberg in the mid-15th century AD. A strong increase in catalogue entries is documented only for the 18th century AD onwards, due to further progress in and increased spread of printing technologies or due to political reasons or even due to the distribution and density of settlements. While most areas along the western Peloponnesian coastline are characterized by rather small rural settlements, Patra represents the only major urban settlement of the Peloponnese. Over the last three centuries, a considerable proportion of catalogue entries especially for earthquake events accounts for Patra. Regarding the city's geographical location, Patra probably bears an increased earthquake and tsunami risk, for it may be affected by events occurring in the Ionian Sea and in the Gulf of Corinth. Additionally, the preservation potential of historical records held by a major urban settlement seems to exceed rural areas by far. The gap in the historical records concerning the 17th century backwards is most probably due to the destruction of Patra in 1822 during the war of independence (Brockhaus 1827). The time line for tsunami and earthquake events compiled for the western Peloponnese thus clearly documents the influence of political and socio-economic factors on historical records.

2.5 Conclusions

The presented compilation and analysis of historical data on tsunami and earthquake events for western Greece is based on a set of comprehensive modern catalogues (for references see Tab. 2.3). It documents a high risk of coastal areas with regard to earthquake and especially tsunami events. At the same time, the vulnerability of the studied area has been considerably increasing during the past decades. Historical records are valuable tools for palaeotsunami research although a combination with geo-scientific studies is much more reliable. The analysis of local to regional catalogue-based timelines for earthquake and tsunami events brought to light several major conclusions:

(i) Timelines of earthquake and tsunami events compiled are very fragmented especially regarding older events documenting a thinning backward tendency through space and time.

(ii) The compilation of data is often influenced by the (local) historical and political context.

(iii) Only scarce information is available especially for areas of minor population density.

(iv) Three different phases in the timelines of earthquake and tsunami entries in the studied catalogues were recognized. A first phase of rare and fragmented entries starting in the 1st millennium BC until the 15th century AD is followed by a second phase of significantly increased records obviously bound to the innovation and rapid spread of printing technologies initiated by Johannes Gutenberg and others. The third phase starts in the 17th/18th century AD showing exponentially increasing records in the catalogues due to systematic improvements in newspaper printing and instrumental documentation of the events.

Summarizing, the analysis of historical data allows the preliminary identification of areas prone to tsunami events. Hazard assessment based only on the analysis of historical records, however, must not be regarded as reliable, though. Gaps in the record are due to periodization effects or long return rates for major events. Palaeotsunami research has thus to focus on both recorded and non-recorded events. Finally, it is stated that a non-entry of a tsunami event in a catalogue for which geo-scientific traces have been found does not mean at all that the event did not take place. Geo-scientific analyses of sedimentological and geomorphological palaeotsunami traces as well as modelling of event scenarios are essential approaches to improve our knowledge on areas vulnerable to future tsunami events and to enhance reliable risk assessment and development of mitigation strategies.

Tab. 2.3: Compilation of earthquake and tsunami events from 1400 BC to 1900 AD after modern catalogues. Regions: AS - Aegean Sea, BO - Boeotia, CA - Calabria, EM - Eastern Mediterranean, G - Greece, GC - Gulf of Corinth, HA - Hellenic Arc, II - Ionian Islands, IS - Ionian Sea, P - Peloponnese; Data compiled after: a - Guidoboni 1994, Guidoboni & Ebel (2009), b - Galanopoulos 1960, c - Papadopoulos & Chalkis 1984, d - Ambrasey & Synolakis (2010), e - Papadopoulos & Fokaefs (2005), f - Papadopoulos 2003, g - Tselentis et al. 2010, h - Antonopoulos 1980, i - Antonopoulos 1980a-f, k - NDGC-NOAA, x - Ambrasey 2009, y - Papazachos & Papazachou 1997, z - Soloviev et al. 2000.

No.	Date	Region	Area affected by... ...earthquake	Ref.	...earthquake & tsunami	Ref.	...tsunami	Ref.
1	1380 BC	EM, AS, HA	Island of Thira	z		c		
2	1300 BC	IS, AS						(z),i
3	420 BC	GC	Corinth	a, x				
4	403-400 BC	P	Elis, Olympia	a, x				
5	373 BC	GC	Bura	a, x	Helike	a, b, c, e, f, i, k, x, y, z		
6	c.23	GC	Aighio	a, x				
7	53	HA	Crete, Rhodes	x				
8	61	GC	Achaia	a, x				
9	69-79, June 20	GC	Corinth	a, x				
10	141-142	GC	Sycione	x				
11	361, June	GC	Corinth, Nafpaktos?, Delfi?	a, (x)				
12	365, July 21	HA, P			Peloponnese, Methoni	a, b, c ,h, i, x, y, z		
13	521/22	GC	Corinth	a, b, x	northern Gulf of Corinth	c, i		
14	543	GC	Corinth	a, (x)				
15	551	GC, BO	Schisma, Corinth	x	Boeotia/Thessalia	x		
16	551	GC, P	Nafpaktos, Patra, Olympia	a, x, z				
17	796, April	HA		x				
18	881	HA		x				
19	956, Jan 5	EM		x				
20	976-1025	GC	Galaxidi	x				
21	1147	GC	Galaxidi	(x)				
22	1169, Feb 11	IS					Ionian Sea	z

No.	Date	Region	Area affected by... ...earthquake	Ref.	...earthquake & tsunami	Ref.	...tsunami	Ref.
23	1255	GC	Galaxidi	x				
24	1270, March	IS			North Ionian Sea	e		
25	1278, Feb 25	II	Kerkyra	a				
26	1301	G, GC	Corinth	a, x				
27	1303	EM, HA, P			(Eastern) Peloponnese	a, c, h, x, y, z		
28	1307	G		x				
29	1353, Oct 16	HA		x				
30	1402, < Aug 30	GC	Patra, Corinth, Diakofto	a	Gulf of Corinth, Aighio (Vostiza), Xylokastro, Vitrinitsa	a, d, e, f, k, x, y, z		
31	1422, April 13	P		a, x				
32	<1444	GC	Nafpaktos	x				
33	1450	GC, IS	Patra, Nafpaktos	x				
34	1462	GC	Nafpaktos	a				
35	1469	II	Cephalonia, Lefkas, Zakynthos	a, x				
36	1481, March 18	EM, HA		x				
37	1500, July 24	HA, P		x				
38	1502, Aug 25	II	Navarino, near Lefkas (St. Maura)	x				
39	1508, May 29	HA		x				
40	1510, <May 24	GC	Nafpaktos	x				
41	1513, April 16	II	Zakynthos	x				
42	1513, Sept 18	II	Zakynthos	x				
43	1515, April 6	II	Lefkas (St. Maura)	(x)				
44	1515, July 31			x				
45	1521, Aug 16	II	Zakynthos	x				
46	1522, Jan	II	Zakynthos	x				
47	1531, Sept 13	II	Kerkyra	x				
48	1544, April 24	GC	Nafpaktos, Zituni	x				
49	1554	II	Zakynthos	x				
50	1559, Sept 12	II	Cefalonia	x				
51	<1577	II	Lefkas	x				
52	1580	GC	Galaxidi, Nafpaktos	x				
53	1580	II	Zakynthos	x				
54	1591, May 28	II	Zakynthos	x				
55	1600, Sept	II	Zakynthos	x				
56	1611, May 16	II	Lefkas	x				
57	1611, Oct 2	II	Lefkas (St. Maura)	x				
58	1613, > Jan 12	II	Zakynthos	x				
59	1613, March	HA		x				
60	1613, Oct 2	II	Lefkas (St. Maura)	x				
61	1622, May 5	II	Zakynthos	(x)	Zakynthos	b, c, g, h, i, k, z		
62	1625, June 18	II	Lefkas (St. Maura)	x				
63	1629, Feb	HA, II	Crete	x			Zakynthos	x
64	1630, July 4	II	Lefkas (St. Maura), Ithaka, Cefalonia	x				
65	1630, Sept	II	Zakynthos	x				
66	1633, Nov 5	II			Zakynthos	b, c, d, g, h, i, k, x, z		
67	1636, Sept 30	II	Cefalonia (Argostoli), Zakynthos	x	Kefalonia	g, k, y, z		
68	1636, Oct 1	II	Zakynthos, Kefalonia	x				
69	1636, Oct 2	II	Zakynthos	x				
70	1638, March 27	II, CA	Cefalonia, Zakynthos	(x)				
71	1638, July 16	II	Cefalonia (Argostoli)	x				
72	1651	II	Kerkyra	x				
73	1658, Aug 12	II	Cefalonia (Paliki, Lixouri)	x				
74	1660, April 22	GC	Galaxidi	x				
75	1661	II	Cephalonia	x				
76	1662, March 16	II	Zakynthos	x				
77	1668?	II	Cefalonia	x				
78	1669, Aug 5	II	Lefkas	x				
79	1672, Nov	II	Zakynthos	x				
80	1673	II	Zakynthos, Cefalonia	x				
81	1674, Jan 16	II	Kerkyra	x				

No.	Date	Region	Area affected by... ...earthquake	Ref.	...earthquake & tsunami	Ref.	...tsunami	Ref.
82	1674, March 27	II	Kerkyra	x				
83	1676, > April 23	II	Zakynthos	x				
84	1685, Dec 20	II	Zakynthos	x				
85	1693, Jan 11	II	Cefalonia	x				
86	1696, Sept 4	II	Zakynthos	x				
87	1703, Jan 19	GC	Nafpaktos	x				
88	1704, Nov 22	II	Lefkas,Cefalonia, Kastro	x				
89	1707, June 6	II	Zakynthos	x				
90	1707, July 22	II	Zakynthos	x				
91	1708, Jan 25	II	Kerkyra	x				
92	1709, March 13	IS	Vonitsa	x				
93	1710, May 17	II	Zakynthos	x				
94	1714, July 29	GC, IS	Patra, Nafpaktos	x				
95	1714, Aug 28	II	Cefalonia, Argostoli	x				
96	1714, Sept 3	GC, P	Patra, Morea	x				
97	1714, Sept 8	II	Kefalonia	x				
98	1716, May 10	II	Zakynthos	x				
99	1720, Sept 12	II		(x)				
100	1722, June 5	II	Lefkas (St. Maura)	x				
101	1723, Feb 18	II			Kefalonia	x		
102	1723, Feb 20	II	Kefalonia (Argostoli, Lixouri), Lefkas, Zakynthos	x				
103	1723, Feb 21/22	II	Lefkas	x	Kefalonia (Lixouri), Lefkas	c, g, h, i, k, y, z		
104	1723, Feb 29	II			Kefalonia (Argostoli)	x		
105	1725, Feb 8	II	Zakynthos	x				
106	<1727, Feb 21	GC	Corinth	x				
107	1727	II	Zakynthos	(x)				
108	1729, Feb 2	II	Kefalonia	x				
109	1729, July 8	II	Zakynthos	x				
110	1732, < March	II	Kerkyra	x				
111	1732, Nov	II			Kerkyra	c, g, h, i, k, y, (z)		
112	1736	II	Kefalonia	x				
113	1741, June 23	II	Kefalonia (Argostoli, Lixouri), Lefkas, Zakynthos	x				
114	1742, Feb 21	GC	Corinthia	x	Corinth, Vostiza	d ,e, f		
115	1742, Feb 25	II, IS, GC	Zakynthos, Nafpaktos, Patra	x	Aighio	x		
116	1743, Feb 20	II, P, GC	Corinth, Kefalonia, Lefkas, Nafpakto, Preveza, Zakynthos	x				
117	1745	II	Kerkyra	x				
118	1748, May 25	GC	Corinth	x	Aighio, Vostiza	b, c, d, e, f, h, i, k, x, y, z		
119	1750, June	P	(Kythira), Navarino	x				
120	1752, June 1	II	Zakynthos	x				
121	1754, June 15	GC, P	Nafpaktos, Morea	x				
122	1756, Feb 13	EM	Eastern Mediterranean	x				
123	1756, Oct 20	GC, P	Nafpaktos, Fokis	x				
124	1759, June 13	II	Kefalonia	x				
125	1759, June 14	II	Kefalonia (Argostoli, Lixouri), Zakynthos	x				
126	1762, April 9	II	Lefkas	x				
127	1765, July 11	II	Kefalonia	x				
128	1766, July 22	II	Kefalonia (Argostoli, Lixouri, Paliki), Zakynthos	x				
129	1767, July 22	II	Kefalonia (Argostoli, Lixouri, Paliki), Lefkas, Zakynthos	x				
130	1767, Oct 3	II	Lefkas (St. Maura)	x				
131	1769, Oct 12	II	Lefkas, Kefalonia	x				
132	1769, Dec	HA, P	Methoni	x				
133	1769	GC			Rio, Antirio, Nafpaktos, Desfina	d, e, f, x		
134	1770, Jan	II	Lefkas (St. Maura)	x				
135	1773, < May 23	II	Kerkyra	x				
136	1775, April 16	II	Zakynthos	x				
137	1775, April 18	GC	Corinth	x				

No.	Date	Region	Area affected by... ...earthquake	Ref.	...earthquake & tsunami	Ref.	...tsunami	Ref.
138	1778, Dec 20	II	Zakynthos	x				
139	1780, June 10	II	Zakynthos	x				
140	1783, Feb 5	II, CA	Lefkas (St. Maura)	x				
141	1783, March 20	II	Lefkas (St. Maura), Kefalonia	x				
142	1783, March 22	II	Lefkas	x				
143	1783, March 23	II	Lefkas	x				
144	1783, March 26	II	Lefkas (St. Maura)	(x)				
145	1783, June 7	II	Lefkas	x				
146	1791, Nov 2	II, P	Zakynthos, Gastuni	x	Zakynthos, Peloponnese	c, d, e, g, h, i, k, (z)		
147	1791, Nov 8	II	Zakynthos	x				
148	1794, June 11	GC			Galaxidi	d, e, f, k, y		
149	1796, Aug		Navarino	x				
150	1804, June 8	II, IS, GC	Patra, Lefkas (St. Maura), Zakynthos	x, z	Patra	b, c, g, h, i, k, y, z		
151	1805, Jan 8	P, GC, IS					Patra	g,k
152	1805, May 30	P, GC, IS	Patra	x				
153	1805, July 3	HA, P		x				
154	1806, Jan 24		Elis	x				
155	1809, May 4	II	Kerkyra	x				
156	1809, June 14	II	Zakynthos	x				
157	1809, Dec	P, GC, IS	Patra	x				
158	1810, Feb 16	HA, P		x				
159	1810, May 4	II	Kerkyra					
160	1810, June 22	II	Zakynthos	x				
161	1810, Nov 11	HA, P		x				
162	1811	II	Zakynthos	x				
163	1811, Dec 18	P, GC, IS	Patra	x				
164	1814, April 1	II	Kerkyra	x				
165	1814	GC	Corinthia	x				
166	1815	II	Lefkas	x				
167	1817, Jan 1			x				
168	1817, Aug	GC	Aighio	b	Aighio	c, d, e, f, h, i, k, x, y, z		
169	1817, Sept 4	II	Kerkyra					
170	1818	II	Kefalonia	x				
171	1819, Sept 4	II	Kerkyra	x				
172	1820, Jan 31	II	Lefkas (St. Maura)	x				
173	1820, Feb 21	II	Lefkas (St. Maura)	x				
174	1820, March 17	II	Lefkas (St. Maura)	x, z			Lefkas	g, k, (z)
175	1820, Dec 29	II, P	Zakynthos, Kefalonia, Pyrgos, Elis	x	Zakynthos	g, k, y		
176	1821, Jan 6	II, P	Zakynthos	b, x, z	Patras	b, h, i, k, z		
177	1821, Jan 9	GC			Gulf of Corinth, Patra, Zakynthos	c, g	Alcyonic Sea	x
178	1821, April 7	P, GC, IS	Patra	x				
179	1821, April 15	P, GC, IS	Patra	x				
180	1821	II	Kerkyra	x				
181	1822	II	Kerkyra	x				
182	1825, Jan 19	II	Preveza (x,z), Kerkyra, Lefkas, Kefalonia, Zakynthos (z)	x, z	Ionian Sea, Lefkas	c, g, i, k, x, z		
183	1825, Jan 20	II	Lefkas (St. Maura)	x				
184	1825, Sept 25	II	Ithaka	x				
185	1825, Oct 15	II	Zakynthos	x				
186	1826, Jan 26	IS	Preveza	x				
187	1829, Feb 8	P, GC, IS	Patra	x				
188	1832, June 25	P	Methoni	x				
189	1832, Dec	P	Kerkyra	x				
190	1834, Jan 1	P	Olympia	x				
191	1834, June	II	Kefalonia (Argostoli, Lixouri)	x				
192	1835, July 12	II	Zakynthos	x	Ionian Sea, Zakynthos	g, h, i	Zakynthos	z
193	1837, Aug 15		Pyrgos	x				
194	1839, June 5	II	Kefalonia	x				

No.	Date	Region	Area affected by... ...earthquake	Ref.	...earthquake & tsunami	Ref.	...tsunami	Ref.
195	1840, Oct 30	II	Zakynthos	x				
196	1840, Dec 30	P	Pyrgos	x				
197	1841, Feb 26	II	Zakynthos	x				
198	1841, Dec 31	P	Pyrgos	x				
199	1842, Feb 3	II, P	Zakynthos, Pyrgos	x				
200	1842, April 18	P	Methoni	x				
201	1842, April 25	P, GC, IS	Patra	x				
202	1842, July 12	P	Kalamata	x				
203	1842, Sept 12	P, GC, IS	Patra	x				
204	1844, June 23	P, GC, IS	Patra	x				
205	1844, Aug 30	II	Kerkyra	x				
206	1846, March 28	HA/II	Ionian Islands	x				
207	1846, June 10	P	Peloponnese, Ionian Islands	x				
208	1846, June 10	P	Peloponnese, Ionian Islands	x				
209	1848, Feb 13	II	Kerkyra	x				
210	1849	P	Pyrgos	x				
211	1850, Jan 13	GC	Corinth	x				
212	1852, March 6	P, GC, IS	Patra	x				
213	1852, July 14	GC	Gravia, Fokis	x				
214	1853, Dec 10	P, GC, IS	Patra	x				
215	1854, July 29	II	Zakynthos	x				
216	1855, Dec 10	GC	Corinth, Isthmus of Corinth, Kalamaki	x				
217	1856, Oct 12	EM, HA	Hellenic Arc	x	Malta	(x)		
218	1858, Feb 21	GC	Corinth	x				
219	1859, March 13	II	Kerkyra	x				
220	1860, Sept 23	IS	Preveza	x				
221	1860, Oct 21	IS	Preveza	x				
222	1861, Dec 26	GC	Aighio	x, z	Galaxidi, Itea, Valimitika, Temeni, Diakofto, Vitrinitsa	b, c, d, e, f, h, i, k, x, y, z		
223	1862, Jan 1	P, GC, IS	Patra, Aighio	z	Galaxidi, Itea	k, z		
224	1862, Feb 19	II	Kerkyra	x				
225	1862, Feb 22	II	Kerkyra	x				
226	1862, June 21	HA, P	Hellenic Arc, Peloponnese	x				
227	1865, March 5	II	Kerkyra	x				
228	1865, March 14	II	Kerkyra	x				
229	1865, March 27	II	Kerkyra	x				
230	1865, April 2	II	Kerkyra	x				
231	1865, Aug 29	II	Kerkyra	x				
232	1866, Feb 6	P, GC, IS	Patra	z				
233	1866, Nov 9	II	Kerkyra	x				
234	1867, Feb 1	II	Kerkyra	x				
235	1867, Feb 3	II	Kefalonia	x				
236	1867, Feb 4	II	Kefalonia (Lixouri, Paliki, Argostoli), Zakynthos	x	Kefalonia (Lixouri), Kalamata	d, e, g, y	Kefalonia, Levkas	k, z
237	1867, March 19	II	Kerkyra	x				
238	1867, March 23	II	Kerkyra	x				
239	1867, April 10	II					Kefalonia (Lixouri)	g, z
240	1867, Sept 19	P	Peloponnese	x				
241	1867, Sept 20	II, P	Kefalonia, Lefkas, Patra	x, z	Peloponnese, Zakynthos, Lefkas, Kefalonia (Lixouri, Argostoli)	c, h, i, z		
242	1868, Feb 14	II	Kefalonia	x				
243	1868, Feb 20	II	Kerkyra	x				
244	1869, Dec 28	II	Lefkas	x, z	Lefkas	b, g, k, y		
245	1870, Aug 1	GC	Fokis, Itea, Kira	x, z	Chalkida	k, z		
246	1870, Aug 1	GC	Fokis, Itea	x				
247	1870, Aug 1	GC	Fokis, Itea, Galaxidi	x				
248	1870, Aug 6	GC	Fokis	x				
249	1870, Oct 25	GC	Fokis	x				
250	1870, Oct 27	GC	Fokis	x				
251	1870, Oct 10	II	Kerkyra	x				
252	1870, Nov 30	GC	Fokis	x				
253	1870, Dec 28	IS	Preveza	x				
254	1871, April 9	II	Kerkyra	x				

No.	Date	Region	Area affected by... ...earthquake	Ref.	...earthquake & tsunami	Ref.	...tsunami	Ref.
255	1871, Oct 5	GC						z
256	1873, Oct 22	II	Zakynthos	x				
257	1873, Oct 25	II, P	Killini, Patra, Pyrgos, Zakynthos, Kerkyra	z				
258	1873, Nov 15	II	Kerkyra	x				
259	1874, Sept 17	II	Kerkyra	x				
260	1875, April 24	P	Kyparissia	x				
261	1875, Aug 15	II	Kerkyra	x				
262	1875, Sept 7	II	Kerkyra	x				
263	1875, Dec 10	II	Kerkyra	x				
264	1876, June 26	GC	Corinthia	x				
265	1879, Nov 20	II	Kerkyra	x				
266	1880, June 18	II	Kerkyra	x				
267	1881, Dec	P, GC, IS					Patra, Etoliko	z, c, k
268	1882, Oct 31	II	Kerkyra	x				
269	1883, April 16	GC	Corinth	x				
270	1883, June 27	II	Kerkyra	x	Ionian Sea, Kerkyra	b, d, e, g, h, i, k	Kerkyra	z
271	1886, Aug 27	P	Pyrgos to Methoni	x	Peloponnese, Gialova, Agrilos, Filiatra	x, z, b, c, d, e, g, h, i, k		
272	1887, July 17	HA	Hellenic Arc, Peloponnese	x				
273	1887, Oct 3	GC			Galaxidi, Xylokastro, Sykia	x, y, z, b, c, d, e, f, h, i, k		
274	1888, Sept 9	GC	Corinth, Aighio	x	Aighio, Galaxidi	(x), z, d, e, f, k		
275	1889, March 21	IS	Preveza	x				
276	1889, Aug 25	GC, IS	Aigio, Diakofto, Patra, Mesolongi	x				
277	1891, June 27	IS	Preveza	x				
278	1893, Jan 31	II	Zakynthos	x				
279	1893, April 17	II	Zakynthos	x	Ionian Sea, Zakynthos	e, g, k		
280	1894, March 26	GC	Xylokastro	x				
281	1894, April 27	P	Atalanti	x	Kyparissia	(y)		
282	1897, May 28	IS		x				
283	1897, June 30	IS		x				
284	1897, Nov 2	II	Lefkas	(x)				
285	1897, Dec	IS			Ionian Sea, Zakynthos	g, h, i		
286	1898, June 2	GC			Gulf of Corinth	x, d, e, f, k		
287	1898, Nov 9	P	Kyparissia	x				
288	1898, Dec 3	II			Ionian Sea, Zakynthos	z,c,g,i		
289	1899, Jan 22	P			Kyparissia, Marathoupole, Marathon	x, y, z, d, e, g, h, i, k		

3 Ancient harbours used as tsunami sediment traps - the case study of Krane (Cefalonia Island, Greece)*

Abtract Geoarchaeological studies in the environs of ancient Krane (Cefalonia Island) were conducted to reconstruct gradual as well as event-related palaeoenvironmental changes and to identify the location of the ancient harbour. At the (south-) eastern shores of the Bay of Koutavos and in the Koutavos coastal plain 9 vibracores were drilled and analysed by means of sedimentological, geomorphological and geochemical methods. A local geochronostratigraphy was achieved by means of radiocarbon AMS dating and archaeological age estimations of diagnostic ceramic fragments. Electrical resistivity tomography was carried out in order to detect subsurface structures and to verify stratigraphical patterns derived from vibracores over long distances. Results show that the local stratigraphical record comprises both the signal of an autochthonous gradual development of shallow water or distal alluvial plain environments, and of repeated interferences related to high-energy events. Altogether, four distinct interferences were detected. As the Bays of Argostoli and Koutavos represent an excellent natural harbour completely sheltered from storm influence and, at the same time, the wider region is well known to have experienced multiple tsunami impacts triggered by the adjacent Hellenic Arc, ex situ-marine depositional interferences in the stratigraphical record are interpreted to be caused by multiple tsunami landfall. Geochronological data yielded *termini ad* or *post quem* (maximum ages) for the tsunami event generations I to IV of 4150 ± 60 cal BC, ~ 3200 ± 110 cal BC, ~ 650 ± 110 cal BC, and ~ 930 ± 40 cal AD, respectively. Comparing the tsunami signal encountered near ancient Krane with geo-scientific data from palaeotsunami events from other sites indicate that the Bay of Koutavos, due to its cul-de-sac-type topography, represents an excellent archive for supra-regional mega-tsunamis. As historical and archaeological data from ancient Krane are sparse, it remains speculative to infer from the geoarchaeological reconstructions that the development of the polis was crucially affected by tsunami impact. As a conclusion, ancient harbours such as the one of Krane represent outstanding archives to detect the number, dimension, intensity and spatial extent of tsunamigenic impacts.

3.1 Introduction and natural settings

The ancient city of Krane is located on Cefalonia Island, western Greece, at the southeastern edge of the Bay of Koutavos on top of a hill out of Cretaceous limestone some 60 to 110 m above present sea level (m a.s.l.) (Fig. 3.1; IGME 1985). The Bay of Koutavos, approximately 1.5 km long and 900 m wide, is characterized by shallow water depths less than 1 m, its length axis trending in SE-NW direction (Fig. 3.2). The sedimentary conditions are those of a shallow water quiescent lagoonal environment. During hot summer months high evaporation rates may cause anoxic conditions associated to the formation of hydrogen sulfide. Apart from a narrow drainage channel that brings freshwater from karstic springs at the foot of the Krane hill to the lagoonal shore, there are no apparent geomorphological signs of present fluvial activity in the Koutavos coastal plain.

* This chapter is partly based on:
Hadler, H., Vött, A., Brückner, H., Bareth, G., Ntageretzis, K., Warnecke, H. & Willershäuser, T. (2011a): The harbour of ancient Krane, Kutavos Bay (Cefalonia, Greece) – an excellent geo-archive for palaeo-tsunami research. – Coastline Reports 17: 111-122.
This chapter is further accepted for publication in Byzas as „Ancient harbours used as tsunami sediment traps – the case study of Krane (Cefalonia Island, Greece)“ together with A. Vött, T. Willershäuser, K. Ntageretzis, H. Brückner, H. Warnecke, P.M. Grootes, F. Lang, O. Nelle and D. Sakellariou.

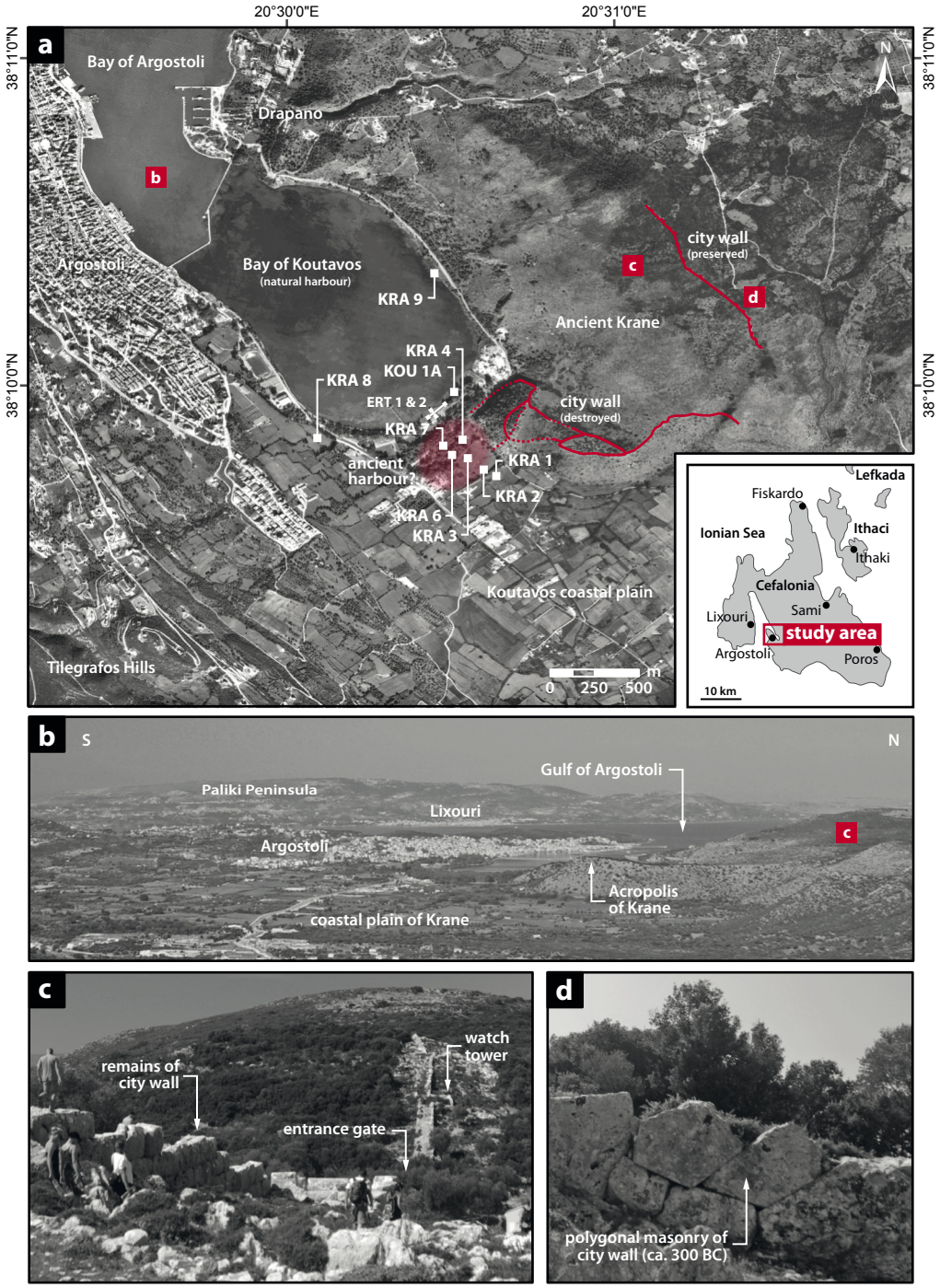

Fig. 3.1: Detail map (a) and panoramic view (b) of the Bay of Koutavos and the Koutavos coastal plain in the environs of ancient Krane. White squares mark vibracoring sites. Electrical resistivity measurements were carried out along the shore near site KOU 1A, marked by thin white lines. The ancient settlement is still marked by remains of a massive city wall (c) of polygonal masonry (d). Map based on Topographic Map 1:75.000 Cephalonia/Ithaka (ORAMA EDITIONS 2011) and Google Earth images (2005).

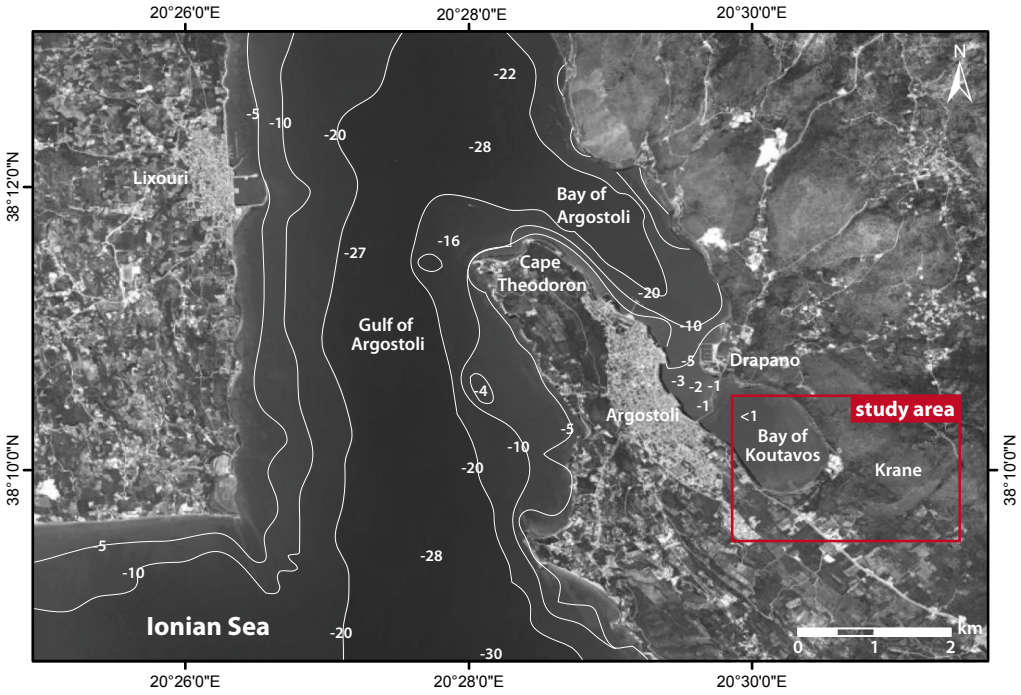

Fig. 3.2: Overview of the southern part of the Gulf of Argostoli showing the SE-NW trending cul-de-sac-type annex formed by the Bays of Argostoli and Koutavos. Note that water depths in the gulf are much deeper (> 20 m) than in the inner Bay of Argostoli (< 10 m) and in the Bay of Koutavos (< 1 m). The Bays of Argostoli and Koutavos represent an excellent natural harbour setting completely sheltered from storm influence. Bathymetric data after ORAMA EDITIONS (2011), map based on Google Earth images (2009).

High-resolution DGPS surveys conducted during the past two decades revealed that Cefalonia Island generally shows a net downward movement associated to the subduction of the African Plate underneath the Aegean Microplate along the Hellenic Arc which is located to the south of Cefalonia (Fig. 3.3; CLÉMENT et al. 2000). This movement, however, is episodically interrupted by relaxative co-seismic uplifts resulting in an overall yo-yo type movement of the crust (HOLLENSTEIN et al. 2008a, 2008b; see also LAGIOS et al. 2007). Straight offshore the western part of Cefalonia, the Hellenic Arc is represented by the Cefalonia Transform Fault (CTF) which leads over to a northerly adjacent zone of continent-continent collision (SACHPAZI et al. 2000).

The geotectonic constellation is known to provoke earthquakes like in 1953 when large parts of the island where destroyed and co-seismic uplift of up to 70 cm was observed at many coastal sites (M = 7.2, STIROS et al. 1994). The last major earthquakes occurred in 1983 on Cefalonia Island (M = 7.0, SCORDILIS et al. 1985) and in 2004 on the adjacent Lefkada Island (M = 6.3, Papadimitriou et al. 2006). Recent studies on Cefalonia have shown that both exposed coastal sections such as the Paliki Peninsula and inner parts of the Gulf of Argostoli experienced repeated tsunami landfall, most probably triggered by local to regional earthquakes (Fig. 3.3; VÖTT et al. 2010, WILLERSHÄUSER et al. 2011). Palaeo-tsunami signatures were also detected for the neighbouring Lefkada Island (VÖTT et al. 2009a) and coastal Akarnania (VÖTT et al. 2011a).

This chapter focuses on the significance of the harbour of ancient Krane as a tsunami sediment trap for deciphering the regional tsunami chronology. The main objectives of the geoarchaeological studies were (i) to detect the exact position of the ancient harbour in the environs of the Koutavos

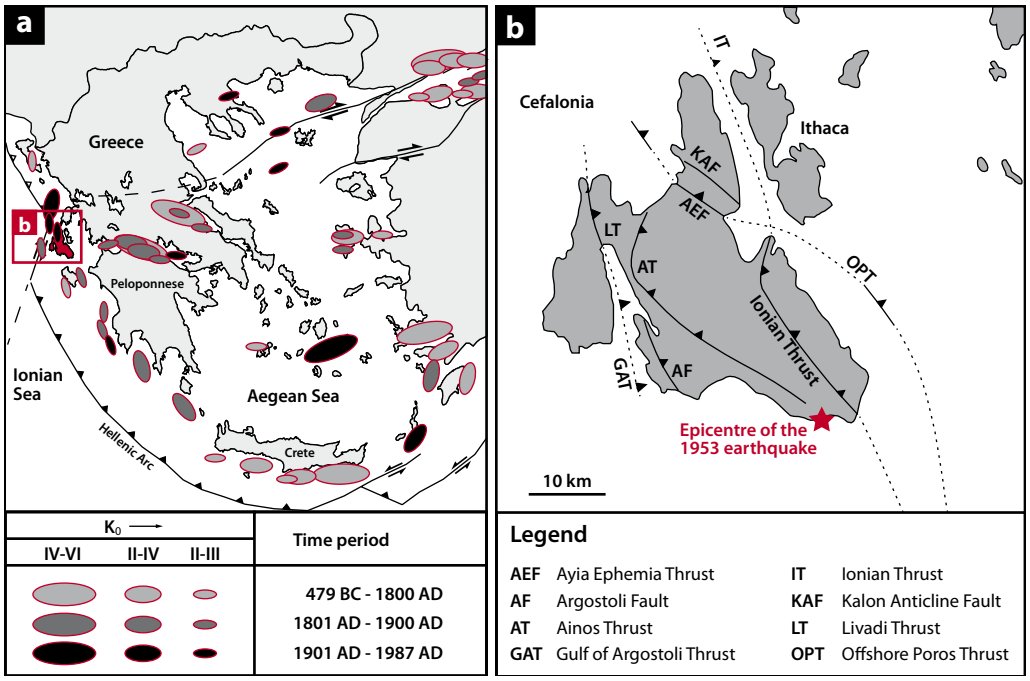

Fig. 3.3: Tectonic overview and tsunamigenic zones of the Ionian and Aegean Seas (a). Cefalonia Island is exposed to the seismically highly active Hellenic Arc where subduction, transform faulting and collision between different plates are taking place (after HASLINGER et al. 1999, DOUTSOS & KOKKALAS 2001). Tsunamigenic sources in Greece after PAPAZACHOS & DIMITRIU (1991), known and inferred from tsunami catalogues. Ellipse size is proportional to the (estimated) maximum tsunami intensity. (b) Local fault systems on Cefalonia Island after STIROS et al. (1994) and IGME (1985). Note the Argostoli Fault which is responsible for the fact that the Bay of Koutavos forms a cul-de-sac-type annex to the Gulf of Argostoli.

coastal plain, (ii) to reconstruct gradual palaeoenvironmental changes and their consequences for the site, and (iii) to find out the magnitude and frequency of tsunami impacts on the harbour since the mid-Holocene.

3.2 Historical and archaeological background

According to PARTSCH (1890), Mycenaean remains document early settlement activities along the shores of the Bay of Koutavos. WARNECKE (2008) hypothesizes that Krane was the home town of Bronze Age Odysseus and that modern Cefalonia therefore corresponds to Ithaka in Homer's Iliad. According to RANDSBORG (2002), the heavy fortification walls that protect the Acropolis of Krane were not constructed before the 5th cent. BC. The chronology of settlement activity at ancient Krane is however hard to decipher, as the site comprises many different archaeological remains where a reliable age determination is uncertain (RANDSBORG 2002).

During the Peloponnesian War, ancient Krane is already mentioned as polis by THUKYDIDES (after LANDMANN 2010) and seems to have fought aside the Athenian allies in the Corinthian aggression in 431/430 BC (BIEDERMANN 1887, GEHRKE & WIRBELAUER 2004). At that time, Krane was also part of the Tetrapolis, an alliance formed between the four major settlements on Cefalonia – Krane, Same, Pale and Pronnoi (THUKIDIDES 2.30.2 after Landmann 2010). While the city seems to flourish in Classical to Early Hellenistic times (RANDSBORG 2002), historic accounts do not give evidence of

the existence of the polis far beyond 370 BC. As suggested by PARTSCH (1890: 83f.), the city was abandoned due to an unknown catastrophe. According to RANDSBORG (2002), archaeological evidence such as the sudden termination of minting, an unfinished massive entrance gate and the well planned but never accomplished expansion of the city seem to support this theory. It is only in medieval times that parts of the ancient acropolis were reinforced and re-used for a short period.

In ancient times, the city and its acropolis were well fortified by polygonal and isodomic walls (Fig. 3.1c-d) parts of which were erected to connect the hill with the adjacent Koutavos coastal plain. PARTSCH (1890: Fig. 3.1a) postulates that the harbour of ancient Krane is situated at the northwestern tip of the coastal plain. However, this has not been verified so far.

3.3 Methods

First geoarchaeological investigations in the Koutavos coastal plain were conducted in 2003 under the auspices of the regional government (Nomarchia) of Cefalonia and the diocese of the island. Supplementary studies were carried out in 2010. Studies comprised vibracoring along the shores of the Koutavos coastal plain down to a maximum coring depth of 7 m below ground surface (m b.s.) using an engine-driven coring device type Cobra mk1 and core diameters ranging from 6 cm to 3.6 cm. Vibracores were cleaned, photographed and described in the field using geomorphological and sedimentological methods (AD-HOC-ARBEITSGRUPPE BODEN 2005). Macrofossil fragments were used to determine the sedimentary facies and to reconstruct palaeoenvironmental changes (POPPE & GOTO 1991, 2000).

Geochemical parameters analysed for selected sediment samples comprised pH-value, electrical conductivity, carbonate content, content of organic material (loss on ignition) and concentrations of (earth alkaline, alkaline and heavy) metals (BLUME et al. 2011). Vibracore KOU 1A was recovered from site KRA 5 using sediment-filled plastic inliners in 2010. In the laboratory, X-ray fluorescence measurements were conducted using a portable XRF spectrometer (type Niton XL3t 900s GOLDD) to obtain total concentrations of around 30 elements.

Electrical resistivity tomography was carried out along two transects by means of a multi-electrode geoelectrical instrument (Iris Instruments, type Syscal R1+ Switch 48) in order to screen subsurface conditions and to check for differences in the general stratigraphical sequence. Position and elevation of vibracoring sites and ERT transects were measured using a differential GPS (type Leica SR 530 and Topcon HiPer Pro). A geochronological frame was established by radiocarbon dating of selected organic samples or samples out of biogenically produced carbonate as well as by archaeological age determination of diagnostic ceramic fragments.

3.4 Geoarchaeological investigations in the Koutavos coastal plain

3.4.1 The stratigraphical record of the Koutavos coastal plain

Within the framework of geoarchaeological studies, 9 vibracores were drilled in environs of ancient Krane (Figs. 3.1 and 3.4). Vibracoring sites are located in the Koutavos coastal plain and at the southeastern (KRA 1 to 7), the southern (KRA 8) and the eastern shores of the Bay of Koutavos (KRA 9). Vibracoring sites KRA 1 to 7 were arranged in the form of two more or less parallel SE-NW running transects (KRA 1, 2, 4, 3, 5; KRA 1, 2, 6, 7, 5) perpendicular to the present lagoonal shoreline (Fig. 3.4).

Vibracoring site KRA 1 (N 38°09'43.8'', E 20°30'37.9'', ground surface at 1.12 m a.s.l.) is located some 450 m inland. The lower part of the core (0.15 m b.s.l. – 0.43 m a.s.l.) is made up of greyish brown, silty to clayey material enriched with grus and pebbles and including ceramic fragments, the grain size distribution being clearly bimodal and the sediment badly sorted. The upper part of the core is made up of brown clayey silt. At 1.27 m b.s. drilling was stopped by large blocks in the subground.

Vibracores KRA 2 to 7 (KRA 2: N 38°09'44.6'', E 20°30'36.2'', ground surface at 0.73 m a.s.l.; KRA 3: N 38°09'50.0'', E 20°30'31.9'', 0.58 m a.s.l.; KRA 4: N 38°9'47.2", E 20°30'32.6", 0.70 m a.s.l.; KRA 5/KOU 1A: N 38°09'56.9'', E 20°30'29.3'', 0.20 m a.s.l.; KRA 6: N 38°09'47.5", E 20°30' 30.9", 0.68 m a.s.l.; KRA 7: N 38°09'48.8", E 20°30' 28.4", 0.48 m a.s.l.) show an overall consistent stratigraphical pattern starting with reddish brown (bottom) to yellowish brown (top) clay-dominated deposits including only little carbonate or locally no carbonate at all. Due to the high iron content and the decalcified character, this facies is interpreted as a palaeosol, most probably late Pleistocene to early Holocene in age. On top, a homogeneous sequence of stiff grey deposits was found, reaching from silty clay to clayey silt. In core KRA 7, this unit is almost 2 m thick (Fig. 3.5; 5.68-3.79 m b.s.l.). Due to its moderate carbonate content and the fact that marine macrofaunal remains are missing, deposition of the material in a shallow water limnic environment can be assumed. However, at vibracoring site KRA 5 remains of a brackish fauna document a lagoonal character of this unit. Towards the flank of Krane hill, at coring site KRA 3, the corresponding facies is a transition between limnic and fluvial, the alluvial input remaining fine-grained but brownish in colour. Towards the top of the cores, fine-grained sediments still prevail but become rust-coloured. Most striking, however, is that these deposits are repeatedly intersected by layers of unsorted sand, shell debris, pebbles, stones and ceramic fragments.

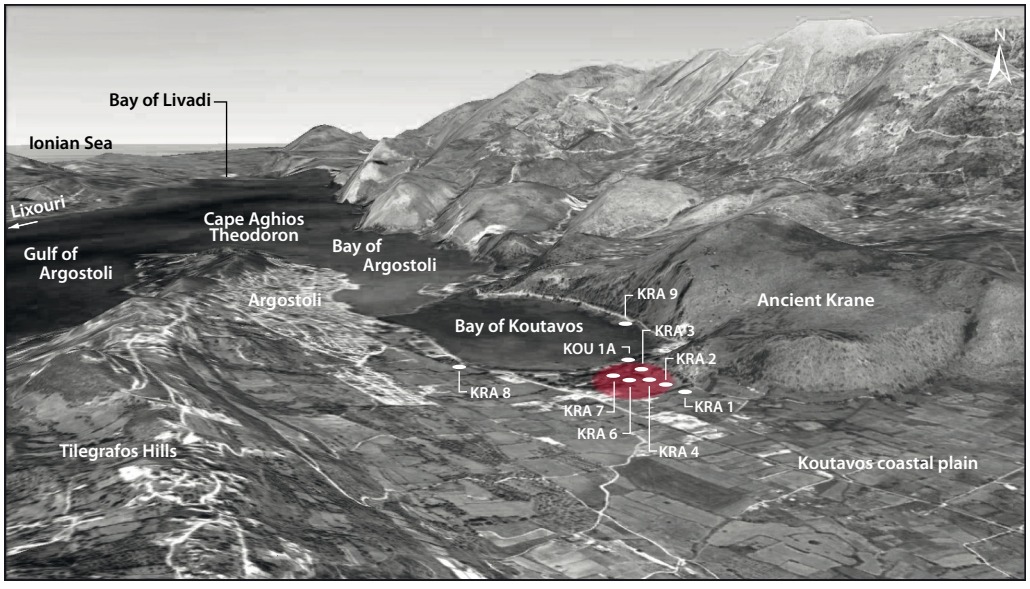

Fig. 3.4: Bird's eye view towards the NW of the Koutavos coastal plain, the Bays of Koutavos and Argostoli and the Gulf of Argostoli. In the background, the Bay of Livadi marks the northern end of the gulf. Vibracoring sites are marked with white ellipsoidal dots. Note the Argostoli Promontory with Cape Aghios Theodoron at its northwestern end which separates the Koutavos annex from the gulf. Figure based on Google Earth image (2009).

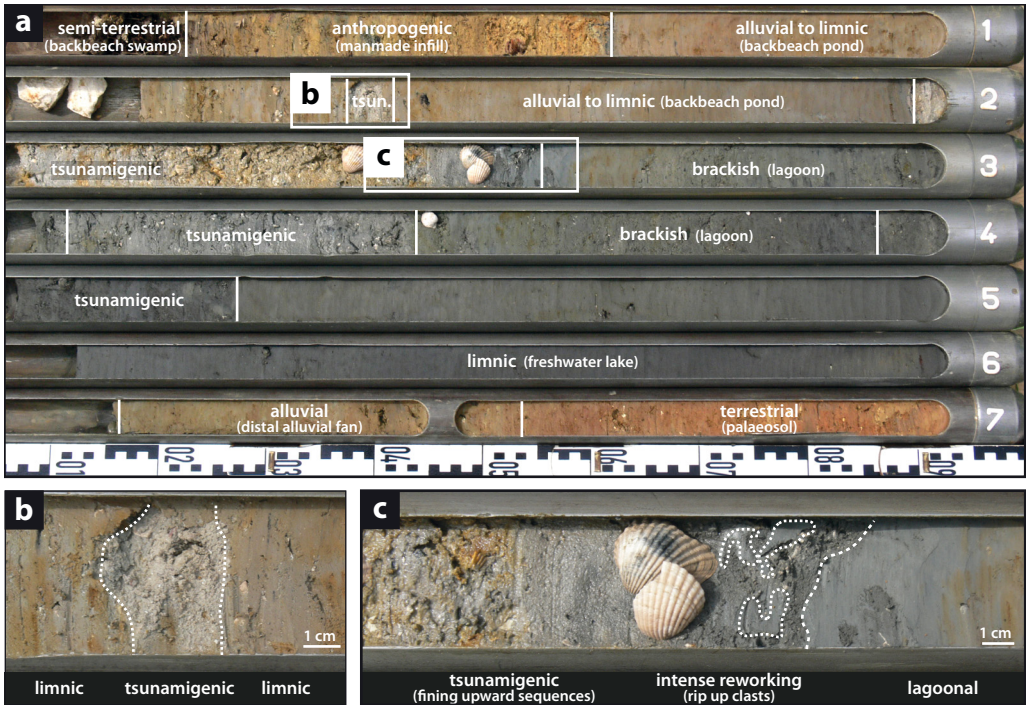

Fig. 3.5: Simplified facies distribution pattern for vibracore KRA 7 drilled in the central Koutavos coastal plain (a). Note the coarse-grained high-energy tsunami deposits out of allochthonous sand, gravel and shell debris intersecting autochthonous fine-grained silty sediments. Youngest tsunami layer out of sand and marine shell fragments with sharp erosional unconformity at the base (b). Youngest but one tsunamite encountered at site KRA 7 showing basal erosional unconformity, layering and clayey to silty rip-up clasts out of lagoonal deposits incorporated into the high-energy deposit (c).

Though the material of the intersecting layers appears coarse-grained and is mostly unsorted, it locally shows layering and includes rip-up clasts out of grey clay or silt originating from the underlying limnic deposits. In every case, the coarse-grained sediments follow on top of a sharp erosional unconformity. In several cores, their internal structure reveals multiple fining-upward sequences mostly starting with marine shell debris at the base, followed by a mixture of sand and ending with sandy silt at the top (Fig. 3.6). These features can be seen best in core KRA 7 which is illustrated in Fig. 3.5.

Grain size and sedimentary characteristics of the intersecting deposits document that they were associated to an energetic level way higher than the one required for accumulating the fine-grained limnic sediments encountered below. By the occurrence of macrofaunal remains of marine origin, it is clear that the high-energy influence must have come from the seaside triggering the deposition of allochthonous material in an originally low-energetic environment. Each time after a high-energy impulse occurred, low-energy conditions were re-established and allochthonous sediments were subsequently covered by fine-grained clayey to silty deposits. Post-depositional rust-coloured staining of both allochthonous and overlying autochthonous deposits must be associated to an abrupt lowering of the groundwater level so that oxidation could start. This abrupt change of the groundwater level is probably caused by co-seismic uplift of coastal sections, a phenomenon which is well-known to have happened during recent earthquakes at Cefalonia. Thus, cores KRA 2 to 7 do not only give sedimentary evidence of abrupt

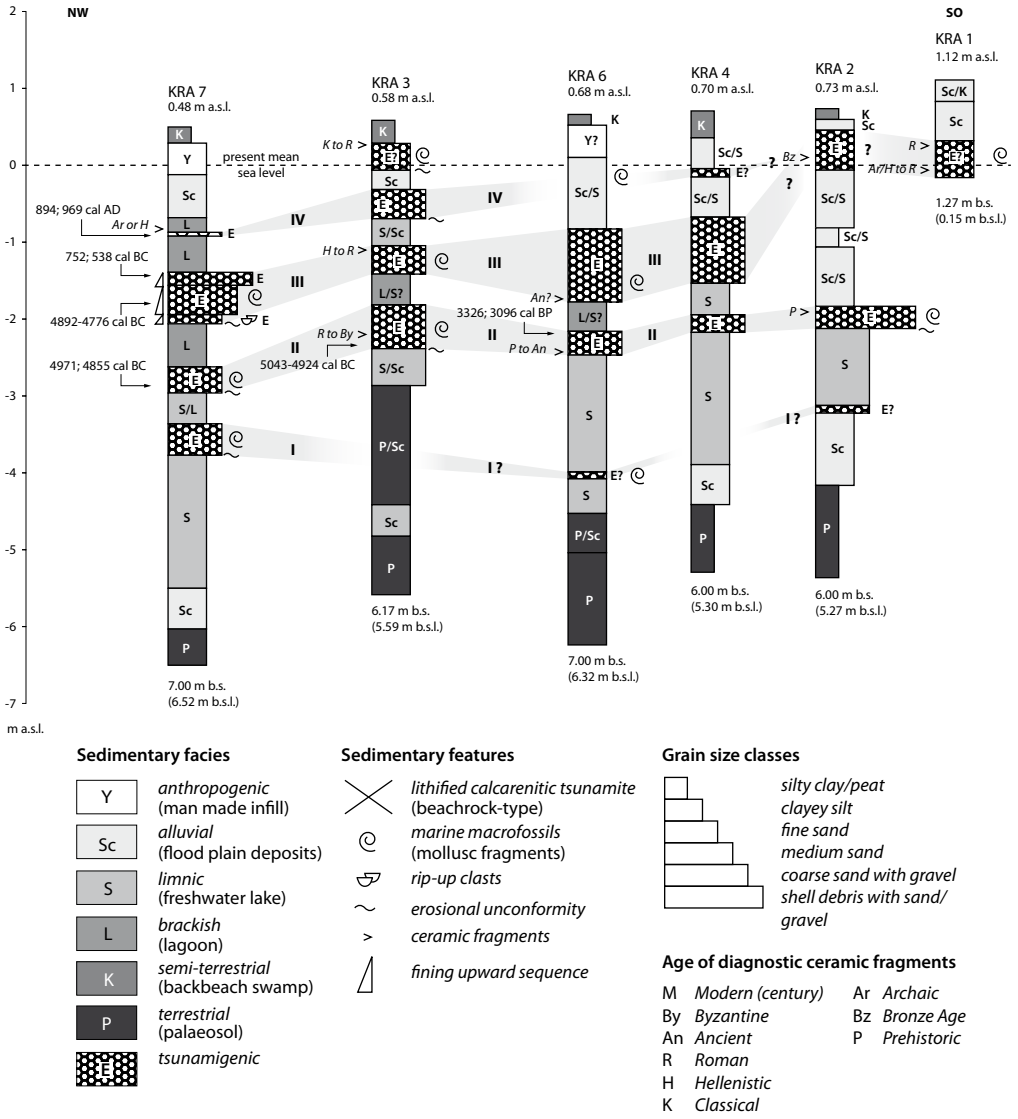

Fig. 3.6: Transect of vibracores KRA 1 to 4, 6 and 7 drilled in the Koutavos coastal plain. For location of vibracoring sites see Fig. 3.1.

high-energy wave impulses but also of earthquakes as potential causative triggers of these events. Fig. 3.6 shows that, altogether, four different high-energy layers were found between the present lagoonal shore (KRA 5/KOU 1A) and up to 220 m inland (KRA 3, 7) and three high-energy layers up to 420 m inland (KRA 2, 4, 6). The most landward core KRA 1, some 460 m distant from the recent shore, still revealed one generation of high-energy deposits. High-energy deposits at the different coring sites were encountered in stratigraphically consistent positions. Fig. 3.6 depicts a general thinning inland tendency of the allochthonous high-energy layers together with increasing elevations towards inland. With regard to thickness, composition and sedimentary characteristics, however, high-energy deposits revealed a considerable variability over short distances. The uppermost parts of the cores are made up of alluvial deposits, partly covered with rubble infill from the 1953 earthquake that destroyed the city of Argostoli almost completely (Moschopoulos & Marabegia-Kosta 2007).

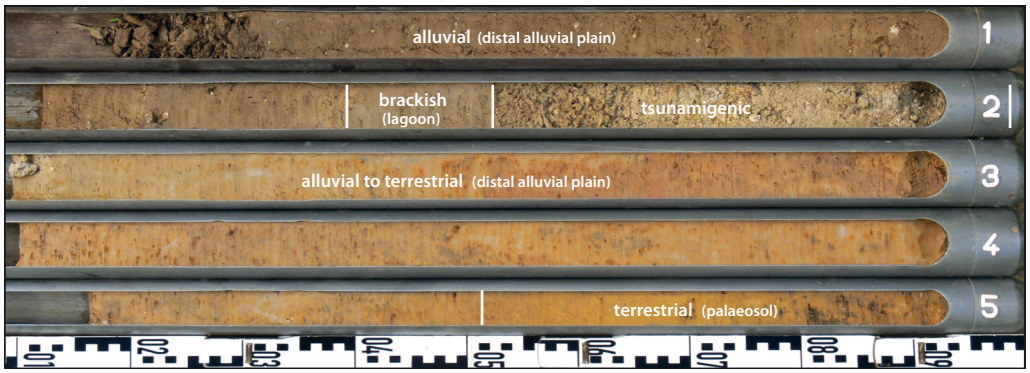

Fig. 3.7: Simplified facies distribution pattern for vibracore KRA 8 drilled at the southern shore of the Bay of Koutavos. The tsunamigenic interference between approximately 1.50-2.00 m b.s., made out of sand and shell debris, differs considerably from the autochthonous silt-dominated distal alluvial fan sediments.

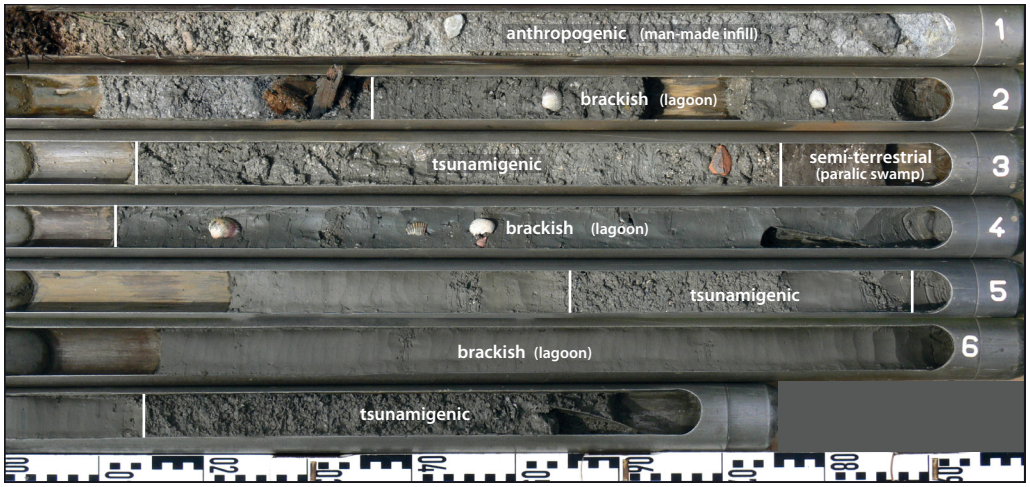

Fig. 3.8: Simplified facies distribution pattern for vibracore KRA 9 drilled at the eastern shore of the Bay of Koutavos. Tsunami influence is depicted in the form of multiple layers out of coarse-grained sediments and marine shell debris intersecting homogeneous lagoonal deposits. The uppermost part of the profile consists of building rubble dumped at the site after the catastrophic earthquake that destroyed large parts of Argostoli city in 1953.

In contrast to the stratigraphies found for the central shore and the Koutavos coastal plain, vibracore KRA 8 (N 38°09'51.7", E 20°30'05.5", ground surface at 1.45 m a.s.l.) – drilled some 65 m inland from the southern shore – revealed thick yellowish brown, clayey to silty alluvial deposits accumulated on top of the ubiquitous palaeosol unit (Fig. 3.7). However, the upper part of the core shows an intriguing intersecting layer (0.69-0.07 m b.s.l.) out of marine shell debris, sand and small pebbles with an erosional unconformity at the base and a sharp boundary towards the subsequently overlying fine-grained deposits. The material is partly cemented and resembles beachrock. From its sedimentary structure and composition and with regard to the clearly low-energetic in-situ conditions, this layer is a high-energy deposit par excellence (Figs. 3.7 and 3.9).

Vibracore KRA 9 (N 38°10' 20.2", E 20° 30' 27.3", ground surface at 0.09 m a.s.l.) was drilled some 700 m to the north of site KRA 5 at the eastern shore of the Bay of Koutavos. Here, the hill

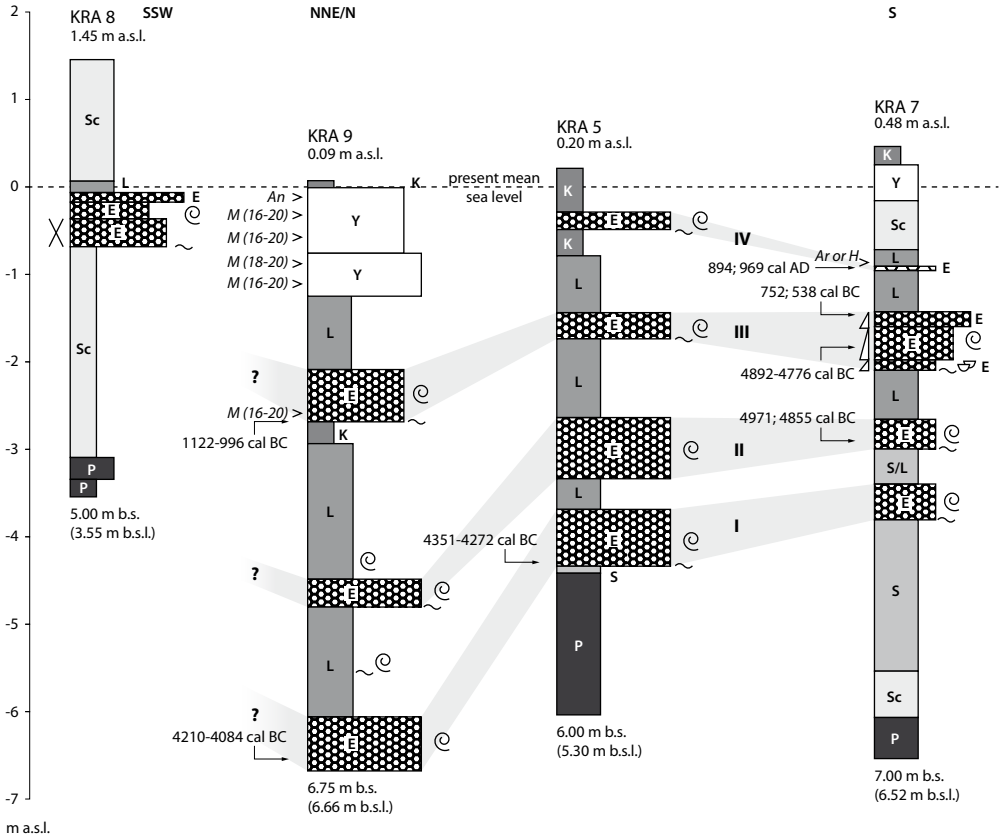

Fig. 3.9: Transect of vibracores KRA 5, 8 and 9 drilled along the shore of the Bay of Koutavos and vibracore KRA 7 from the western Koutavos coastal plain. For location of vibracoring sites see Fig. 3.1, for legend see Fig. 3.6.

slope is steep and obviously bound to a SE-NW running fault system (IGME 1985). The overall predominant material is homogeneously grey clayey silt including macrofaunal remains of a brackish fauna thus mirroring a typical lagoonal environment (Fig. 3.8). However, similar to vibracores KRA 2 to 7, three distinct intersecting layers (6.51-6.04, 4.78-4.36, 2.66-2.06 m b.s.l.) of mostly marine shell debris, sand and individual pebbles and stones were found (Fig. 3.9). Associated sedimentological features such as erosional unconformities, distinct layering and incorporated rip-up clasts of eroded lagoonal deposits were also encountered.

The uppermost coarse-grained layer (1.26 m b.s.l.-0.01 m a.s.l.) is reported to have been dumped by the inhabitants of Argostoli after the earthquake that shook the island in 1953. Vibracoring site KRA 9 clearly documents a threefold high-energy impact that hit the Bay of Koutavos during the Holocene. Stratigraphical position and composition of the KRA 9 high-energy deposits are consistent with those found in the central Koutavos coastal plain (Fig. 3.9).

3.4.2 Electrical resistivity tomography

Electrical resistivity tomography was carried out along two transects near vibracoring site KRA 5/KOU 1A. Transect KOU ERT 1 runs along, transect KOU ERT 2 perpendicular to the shore of the Bay of Koutavos (Fig. 3.10). The area is characterized by massive building rubble, up to 2 m thick, that was dumped in the original coastal swamp during the 1990s as a land reclamation measure. According to the inverse model resistivity section of transect KOU ERT 1 the subsurface

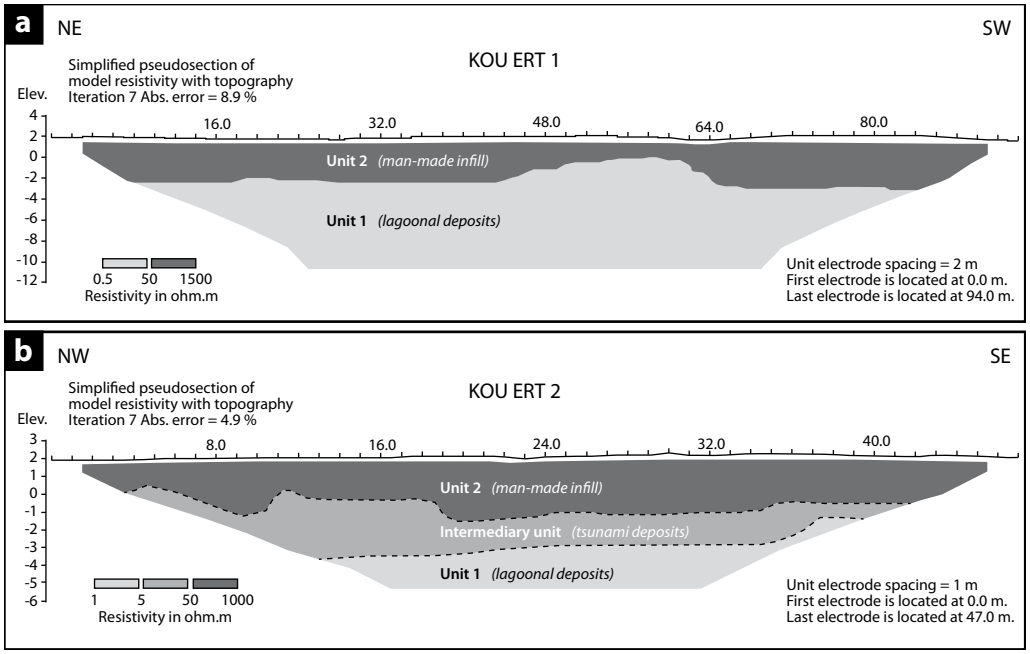

Fig. 3.10: Simplified results from electrical resistivity tomography along transects KOU ERT 1 and KOU ERT 2 conducted at the shore of the Bay of Koutavos near vibracoring site KOU 1A. For location of transects see Fig. 3.1, for further explanations see text.

can be subdivided into two main units. Unit 1 lies below approximately 3 m b.s.l. and shows comparatively low resistivity values (< 50 Ωm). On the contrary, unit 2 reaches resistivity values higher than 1000 Ωm. Compared to the stratigraphy of vibracore KRA 5, unit 1 corresponds to fine-grained autochthonous lagoonal deposits, whereas unit 2 clearly reflects overlying anthropogenic infill. Transect KOU ERT 2 has a higher vertical resolution which allows to better understand the transition between units 1 and 2. Fig. 3.10 illustrates that at the seaward end of the transect, units 1 and 2 are separated from each other by an intermediary unit with values between approximately 5 and 50 Ωm. This zone may correspond to the stratigraphical section of core KRA 5 that revealed multiple input of coarse-grained allochthonous material. Fig. 3.10 documents that the intermediary unit shows a landward decrease in thickness. Vibracoring site KRA 5 itself is not covered by building rubble as it is located at the mouth of a narrow drainage canal.

3.4.3 Geochemical analyses

In this paper, selected results of detailed geochemical analyses are presented, carried out for selected samples taken from vibracores KRA 1 to 9 and KOU 1A. Total concentrations of Ca and Ti, together with 28 other elements, were measured using a portable XRF analyser (Type Thermo Niton Xl3t 900s) yielding laboratory quality data consistent with standard or specific calibrations, with results from laboratory XRF instruments, and with elemental concentrations measured in acidic solutions (Zhu & Weindorf 2010). Measurements were conducted using the SOIL software mode of the instrument. Each sample was continuously measured for 30.5 seconds using three different filters to obtain mean relative concentrations per measured element. The limit of detection for Ti concentrations is given as 0.01 ppm. For standardization issues and in order to eliminate potential influences of grain size and moisture, elemental ratios are preferred

against absolute concentrations yielded per element. Elements were measured with a vertical resolution between several centimeters to decimeters per core depending on relevant changes in the stratigraphic record and sampling density.

With respect to the identification of allochthonous sediment layers in near-coast sedimentary archives, the Ca/Ti ratio of sediment samples is of special interest. Hereby, Ca is used as an indicator for marine influence as it is mainly brought into the elemental budget by carbonate shells of marine macro- and microfauna. On the contrary, Ti is produced through terrestrial weathering of minerals such as feldspar, quartz and mica and by residual accumulation in limestone areas. The Ca/Ti ratio is thus an indicator for the relation between marine and terrigenous processes and their influences on geo-ecosystems. On a longer term, a general geochemical equilibrium is to be expected for every ecosystem unit. In contrast, high-energy impacts affect coastal ecosystems abruptly and temporarily so that they should leave unusual geochemical signals of restricted duration beyond the normal background. A similar methodological approach has already been

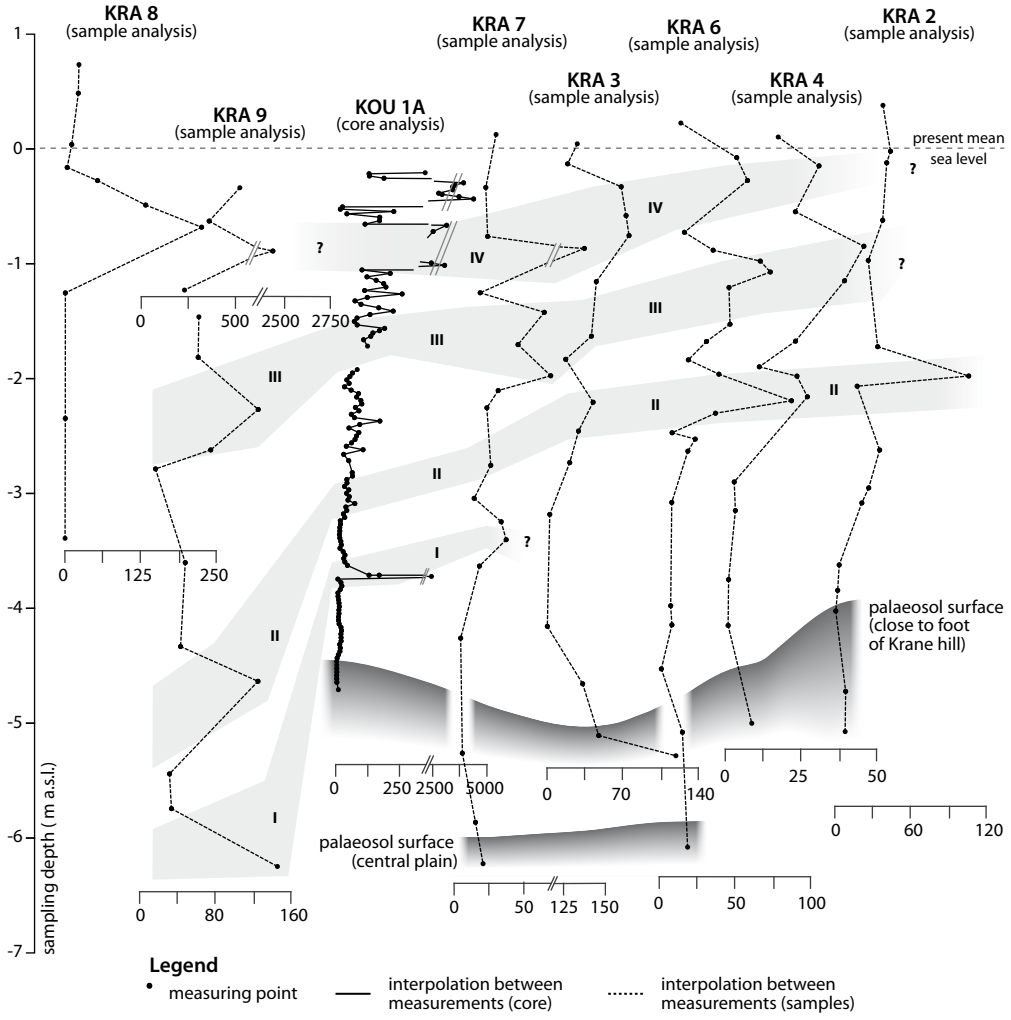

Fig. 3.11: Ca/Ti ratios for vibracores drilled in the Koutavos coastal plain and at the shores of the Bay of Koutavos based on XRF measurements. Ca/Ti peaks indicate non-equilibrium temporary interferences of the ecological system by high-energy impact from the sea side. For location of vibracoring sites see Fig. 3.1; for further explanation see text.

approved within the framework of other studies dealing with the detection of tsunamites in ancient Greek harbours (Vött et al. 2011a, 2011b). However, potential post-depositional alteration of the carbonate content by subaerial weathering has to be taken into consideration. In the case of Krane, allochthonous high-energy sediments were deposited in a wet environment, and local decalcification, for instance induced by co-seismic uplift, remains secondary.

Fig. 3.11 shows a compilation of vertical Ca/Ti ratios obtained for vibracores KRA 2 to 9 and KOU 1A. In a general view, the Ca/Ti ratio is continuously increasing from the base towards the top of each profile. However, there are significant peaks that exceed the usual background trend by far. A comparison of these Ca/Ti peaks with the overall stratigraphical pattern (Fig. 3.6, 3.9 and 3.11) shows that each peak corresponds with a layer of allochthonous coarse-grained high-energy sediments. For vibracore KOU 1A, for example, four and for vibracore KRA 9 three distinct peaks were found representing clear interferences of the autochthonous system and being consistent with the stratigraphical data. Regarding vibracore KRA 8, the abrupt and temporary input of marine deposits into a terrestrial environment (1.52-2.14 m b.s.) is reflected by an outstanding Ca/Ti peak. Relatively high Ca/Ti values at the base of core KRA 3 correspond to an older palaeosol section that is weathered to a slightly lesser extent. Increased Ca/Ti values right below ground surface were found in areas were building rubble, rich in carbonate, was dumped.

3.4.4 Geochronostratigraphy of environmental changes

Altogether 9 samples out of organic material or biogenically produced carbonate were selected for ^{14}C-AMS dating (Tab. 3.1). As the variability in space and time of the marine reservoir effect for samples out of marine carbonate is still unknown, a mean marine reservoir effect of 408 years was assumed (Reimer & McCormac 2002). Diagnostic ceramic fragments encountered in sediment cores were used for cross-checking radiometric ages. Both radiometric ages and archaeological age estimates were considered within the stratigraphical context in order to establish a geochronostratigraphy of high-energy events that struck the Bay of Koutavos (Figs. 3.6 and 3.9).

Dating high-energy events is a difficult task to fulfil due to several problems caused by complex erosional and depositional processes. This is especially true for processes associated to tsunami landfall. First, dating samples taken from the allochthonous high-energy deposit only yield maximum ages or *termini ad* or *post quos* for the event. The reason is that the event deposits might include reworked older deposits, which has been observed in many other case studies dealing with the reconstruction of palaeo-events (for example Vött et al. 2011b). Second, the deposition of event sediments may be preceded by considerable erosion of the youngest pre-event deposits as indicated by the presence of ripped up sediment clasts out of underlying older material within the event layer. The dimension of the erosional hiatus produced by the event is impossible to estimate using radiocarbon and/or ceramic age dating; determining sedimentary ages for allochthonous high-energy deposits using the Optically Stimulated Luminescence (OSL) technique is the best theoretical option but practically problematic due to the high contents of carbonate in Mediterranean deposits. Carbonate crystals, other than quartz or feldspar, are not datable by the OSL method. Moreover, bleaching processes during the deposition of event layers turned out to be incomplete in some cases (for example Vött et al. 2011a). Third, dating of post-event sediments overlying the high-energy deposit is difficult in cases when the event deposits were accumulated in terrestrial environments above sea level where subaerial weathering is dominating. *Termini ante quos* for the event derived from post-event deposits are much closer

Tab. 3.1: Radiocarbon dates of samples from vibracores drilled in the environs of ancient Krane (Cefalonia Island). Note: b.s. – below ground surface; b.s.l. – below sea level; 1σ max; min cal BP/BC (AD) – calibrated ages, 1σ-range; ";" – semicolon is used in case there are several possible age intervals due to multiple intersections with the calibration curve; Lab. No. – laboratory number, Leibniz-Laboratory for Radiometric Dating and Isotope Research, Christian-Albrechts-Universität zu Kiel (Kia); * – marine reservoir correction with assumed mean reservoir age of 408 years. Calibration based on Calib 6.0 software (Reimer et al. 2009).

Sample	Depth (m b.s.)	Depth (m b.s.l.)	Sample description	Lab. No. (KIA)	$\delta^{13}C$ (ppm)	^{14}C Age (BP)	1σ max; min (cal BP)	1σ max;min (cal BC/AD)
KRA 3/9 M	2.85	0.76	Scrobicularia sp., articulated specimen	39692	-0.40 ± 0.34	6445 ± 40	6992 – 6873	5043 – 4924 BC*
KRA 5/9+ M	4.16	3.96	Dosinia exoleta, articulated specimen	39693	1.80 ± 0.45	5850 ± 35	6300 – 6221	4351 – 4272 BC*
KRA 6/13 HK	2.86	2.18	charcoal	39694	-23.70 ± 0.34	4475 ± 25	5275; 5045	3326; 3096 BC
KRA 7/4 HK	1.41	0.93	charcoal	39695	-26.70 ± 0.13	1120 ± 25	1056; 981	894 AD; 969 AD
KRA 7/6 HK	1.90	1.42	charcoal	39696	-24.87 ± 0.15	2475 ± 25	2701; 2487	752; 538 BC
KRA 7/7 M	2.26	1.78	Cerastoderma glaucum, articulated specimen	39698	-5.38 ± 0.34	6320 ± 40	6841 – 6725	4892 – 4776 BC*
KRA 7/11+ M	3.25	2.77	Scrobicularia sp., articulated specimen	39699	-5.01 ± 0.36	6390 ± 35	6920; 6804	4971; 4855 BC*
KRA 9/8+ M	2.75	2.66	Dosinia exoleta, articulated specimen	39700	-4.86 ± 0.22	3205 ± 35	3071 – 2945	1122 – 996 BC*
KRA 9/15+ M	6.49	6.29	Loripes lacteus, single valve	39701	0.29 ± 0.15	5680 ± 35	6159 – 6033	4210 – 4084 BC*

to the date of the event if the deposits were brought into lagoonal or limnic environments where autochthonous sediment deposition is immediately re-established. At present, the so called sandwich dating approach is the most promising method to achieve a best-fit age interval for an event by dating both the underlying and the overlying deposits of an event layer. This kind of time bracketing yields a time window framed by a *terminus ad* or *post quem* below and *a terminus ante quem* above the event deposit. For example, radiocarbon sandwich dating helped to identify the first field evidence of the 365 AD Crete tsunamite in northwestern Greece in the Lake Voulkaria near Preveza (Vött et al. 2009b).

However, for the Krane case study, no datable material was found above or below the encountered event deposits. All ages given in Table 3.1 are thus mere maximum ages or *termini ad* or *post quos* for high-energy events that hit the Koutavos coastal plain. Samples KRA 7/7 M (4892-4776 cal BC) and KRA 7/6 HK (752-538 cal BC) originate from the same high-energy layer so that sample KRA 7/7 M has to be considered as reworked. The same is true for sample KRA 9/8+ M (1122-996 cal BC) which was found associated to a ceramic fragment dating to the 16th-20th centuries AD. Finally, sample KRA 3/9 M yielded an age of 5043-4924 cal BC which considerably differs from the age of a ceramic fragment encountered in the same event layer dated to Roman to Byzantine times. This radiocarbon age is thus not considered reliable.

3.5 Discussion

3.5.1 The Bay of Koutavos – a tsunami sediment trap par excellence

The Ionian Islands are characterized by prevailing wind and wind-generated waves from western and northwestern directions (Hofrichter 2002, Soukissian et al. 2008). Maximum observed

storm wave heights in the open Ionian Sea are not higher than 6-7 m (Scicchitano et al. 2007; Soukissian et al. 2007; De Martini et al. 2010). For areas some kilometers distant from the coast, the winter mean significant wave height is lower than 1.2 m and the probability of a significant wave event with a wave height of more than 4 m is almost nil (Medatlas Group 2004, Cavaleri 2005). On the base of gauge records, Tsimplis & Shaw (2010) show that seasonal sea level extremes are restricted to autumn and winter months and are less than 40 cm.

The shallow water lagoonal environment of the Bay of Koutavos together with the directly adjacent Bay of Argostoli follows the same SE-NW strike direction with water depths rapidly increasing from less than 1 m to 26 m below present sea level (m b.s.l.) towards the NW (Fig. 3.2). With regard to the local topography and coastline configuration, they represent a cul de sac-type annex of the N-S running Golf of Argostoli and are well protected from storms. The Bay of Argostoli and especially the Bay of Koutavos are completely sealed off from open sea wave dynamics. They represent one of the best storm-protected natural harbours in the Mediterranean. Today, Argostoli is one of the most important landing sites for large cargo, military and passenger ships on the Ionian Islands. The Gulf of Argostoli – more than 13.5 km long and 3.5 km wide – is, however, prone towards occasional storms from southern directions because of the comparatively long local fetch and channeling effects between the Cape of Aghios Theodoron and the coast at Lixouri (Fig. 3.2). Against this background, storms can definitely be excluded as being responsible for the deposition of high-energy event deposits encountered at the southeastern fringe of the Bay of Koutavos.

On the contrary, the Gulf of Argostoli is directly exposed towards the Hellenic Arc which is well-known to have triggered numerous tsunamigenic earthquakes in the past related to the subduction of the African Plate underneath the Aegean Microplate (see, for example, Papazachos & Dimitriu 1991; Fig. 3.3). In case of a tsunami generated in the eastern Ionian Sea travelling towards a northern direction, the funnel-shaped coastline configuration between Cefalonia airport and Cape Aghios Theodoron is supposed to enhance both tsunami wave height and tsunami velocity (Fig. 3.12a) and trigger the following tsunami landfall scenario. The narrow and long middle and northern parts of the Gulf of Argostoli are expected to add a further acceleration momentum to the tsunami by channeling effects. Reaching Cape Aghios Theodoron, parts of the tsunami water masses are diverted to the SE into the Bays of Argostoli and Koutavos by wave diffraction (Fig. 3.12b).

However, major parts continue travelling towards the northern end of the gulf (Fig. 3.12c) where the high mountain ridges flanking the Livadi coastal plain reflect tsunami waters back southward. On their way back south, the promontory between Cape Aghios Theodorou and Argostoli acts as separating funnel branching off considerable tsunami water masses into the Bays of Argostoli and Koutavos (Fig. 3.12d). There, by their high velocity and inertia and through the quasi-nonstop water inflow due to the long tsunami wave length, the tsunami waters reach the southeastern end of the cul-de-sac type embayment near Krane. Subsequently, the water is reflected and drains off towards the NW back into the Gulf of Argostoli and the Ionian Sea.

The stratigraphical record encountered around ancient Krane documents multiple high-energy impact associated to both erosion of pre-existing fine-grained autochthonous and deposition of allochthonous coarse-grained sediments (Figs. 3.6 and 3.9). According to the macrofossil content and geochemical fingerprints, the *ex situ*-material was transported to the Koutavos coastal plain from the seaside. As storms are not able to reach the study area let alone to leave significant

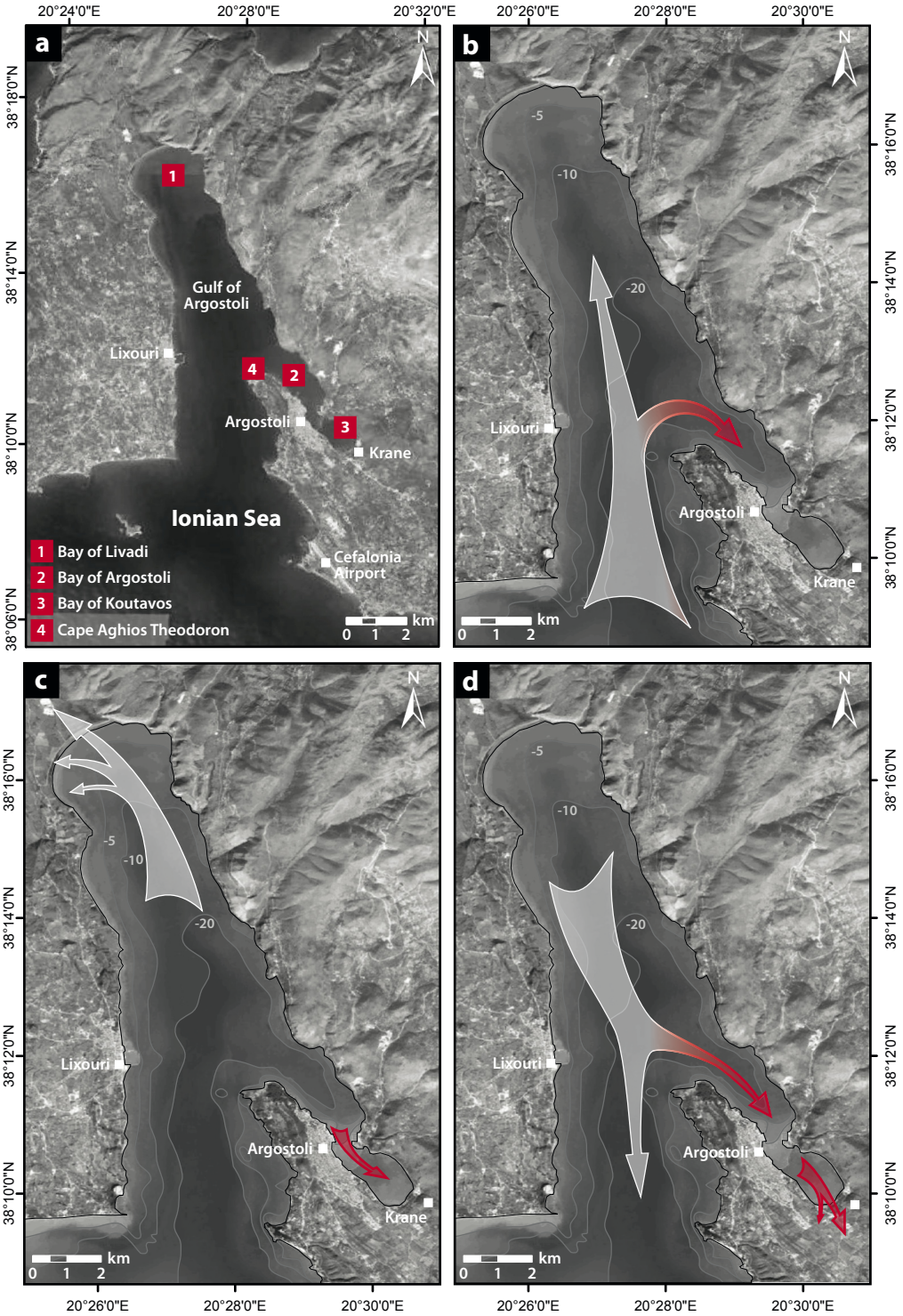

Fig. 3.12: Tsunami landfall scenario for the Gulf of Argostoli and the Bays of Argostoli and Koutavos based on a northward propagating tsunami event generated in the environs of the Hellenic Arc. The topographic overview shows the funnel-type coastal configuration at the entrance of the Gulf of Argostoli (a). Tsunami wave propagation and tsunami landfall in the Koutavos coastal plain due to wave amplification, acceleration, refraction, diffraction and reflection (b) to (d). Maps based on Topographic Map 1:75.000 (ORAMA EDITIONS 2011) and Google Earth images (2009). See text for further explanation.

imprints on the stratigraphical record, the tsunami scenario is the only plausible setting by which the occurrence, thickness, distribution and composition of allochthonous high-energy sediments can be explained. Based on the presented tsunami wave propagation scenario and field evidence by vibracoring, the Bay of Koutavos and the adjacent coastal plain are regarded as a (palaeo-) tsunami sediment trap par excellence.

3.5.2 Location of the harbour of ancient Krane

PARTSCH (1890), on the base of detailed field observations, supposed that the harbour of ancient Krane is located at the southwestern foot of Krane hill not far from the present shore of the Bay of Koutavos (Fig. 3.1a). Results from vibracoring, however, indicate that this area is not appropriate as a harbour site. Vibracores 3, 4, 6 and 7 mostly revealed thick sections of tsunami deposits while autochthonous lagoonal or limnic sediments hardly exceed 40-50 cm (Fig. 3.6). Even if parts of these deposits were eroded by tsunamigenic impact, the corresponding water depth was not sufficient to allow navigating with larger ships. At the southern fringe of the bay near coring site KRA 8, no deposits belonging to a quiescent water body were discovered at all. On the contrary, vibracoring sites KRA 5 and especially KRA 9 lying at the immediate waterfront revealed thick lagoonal sequences that offered perfect conditions for anchoring (Figs. 3.8 and 3.9). It is therefore suggested that the harbour installations of ancient Krane were most likely located right between sites KRA 5 and 9 where parts of the fortification system run towards the shore and nowadays lies an industrial area. This site would also be in favour of a short and rapid access to the western part of the ancient city.

3.5.3 Local event geochronostratigraphy

Results of ^{14}C-AMS dating and ages of diagnostic ceramic fragments are depicted in Fig. 6 and Fig. 9 within the stratigraphical context. Vibracoring sites KRA 5 and 7 are considered as key sites for the area showing traces of four different tsunami generations. The oldest tsunami generation I obviously hit a pre-existing shallow water limnic environment whereas conditions had already turned brackish (lagoon) when generations II and III affected the area. Sedimentary traces of the youngest tsunami generation IV were only found at sites KRA 5 and 7 intersecting coastal swamp deposits. Radiocarbon ages obtained for samples from cores KRA 3, 5, 6, 7 and 9 represent mere maximum ages.

Tsunami generation I

Samples KRA 5/9+ M and KRA 9/15+ M are *termini ad* or *post quos* for tsunami generation I of 4351-4272 cal BC and 4210-4084 cal BC, respectively (Table 3.1). As they belong to the same stratigraphical unit, the younger age of 4210-4084 cal BC from sample KRA 9/15+ M is considered more reliable so that the maximum age of tsunami generation I is assumed as approximately 4150 ± 60 cal BC.

Tsunami generation II

Stratigraphical comparisons between cores KRA 5, 7 and 9 show that sample KRA 7/11+ (4971-4855 cal BC) belongs to tsunami generation II; its age thus indicates strong reworking of older deposits. For tsunami generation II, only sample KRA 6/13 HK gives reliable age information. It yields a maximum age of 3326-3096 cal BC which is generally approved by a ceramic fragment from the same event layer that is probably as old as prehistoric times (Fig. 3.6).

Tsunami generation III and IV

Tsunami generation III is dated by sample KRA 7/6 HK to the time around 752-538 cal BC or later (Table 3.1). For tsunami generation IV, sample KRA 7/4 HK yielded an age of 894-969 cal AD or younger. Unfortunately, the ceramic fragments encountered in the vibracores were always related to high-energy event deposits. Thus, ages derived from diagnostic ceramic fragments are also to be regarded as mere maximum ages and do not allow to refine the geochronostratigraphy based on radiocarbon datings.

3.5.4 Regional tsunami signals

During the past years, palaeotsunami studies have been intensified along the coasts of western Greece. With regard to tsunami generation I encountered in the Koutavos coastal plain and dated to approximately 4150 ± 150 cal BC or younger (Figs. 3.6 and 3.9), there are potentially correlating tsunamites published for the Bays of Palairos-Pogonia (Akarnania) and Aghios Andreas (western Peloponnese). A tsunami layer found in the central Palairos coastal plain yielded maximum ages of 4449-4360 cal BC and 4461-4356 cal BC (Vött et al. 2011a). A tsunamite described from ancient Pheia, harbour of Olympia, was radiocarbon dated using the sandwich approach to 4300 ± 200 cal BC (Vött et al. 2011b). These ages are in good accordance with the results from Krane and suggest a potential supra-regional tsunami event that hit Cefalonia, the western Peloponnese and coastal Akarnania in the last third of the 5th millennium BC.

Tsunamite generation II from Krane shows a maximum age of 3326-3096 cal BC which corresponds to a tsunamite maximum age found for the Palairos coastal plain of 3584-3414 cal BC (Vött et al. 2011a). This event is possibly identical with a supra-regional mega-tsunami that was dated to approximately 2900 cal BC and traces of which were found in the Sound of Lefkada (Vött et al. 2009a) and the Gulf of Corinth (Kortekaas et al. 2011). High-energy sediments of the same age that are associated to sedimentary features and a foraminiferal content indicating strong tsunami influence are also known from the Messenian Gulf (core AKO 1, southwestern Peloponnese, Engel et al. 2009).

Tsunamite generation III encountered near ancient Krane shows a maximum age of 752-538 cal BC (Table 3.1). It remains speculative if this event induced the abandonment of the polis in the 4th century BC. Alternatively, it may be identical with or related to one of several events (E9, E8, E7) between 800-400 cal BC documented by tsunami deposits identified in the Augusta Bay (eastern Sicily, De Martini et al. 2010, Smedile et al. 2011). In this case, event II would also represent a tsunami of supra-regional nature.

Tsunami generation IV affected the Koutavos area at 894-969 cal AD or later. Smedile et al. (2011) identified tsunami impact for Augusta Bay (Sicily) for the time around 930-1170 cal AD (E3). Another potentially associated tsunami candidate from the 12th century AD found in Siracusa (Sicily) is described by Scicchitano et al. (2010). Vött et al. (2006) report on geomorphological and sedimentological traces of a tsunami that struck the Bay of Aghios Nikolaos near Preveza between 1000 and 1400 cal AD. Tsunamigenic inundation of the Sound of Lefkada is reconstructed for the time during or after 1244-1293 cal AD (Vött et al. 2009a). Based on field evidence, Kortekaas et al. (2011) suggest that the Gulf of Corinth was affected by the 1402 AD tsunami. There is further sedimentary evidence that the southern Peloponnese was hit by tsunami impact around 1300 cal AD (Scheffers et al. 2008). Hence, it cannot be excluded that Krane tsunamite IV also has a supra-regional background. The time period of tsunami generation IV, other than tsunami

generations I to III, is well known from catalogues to have experienced numerous catastrophic tsunami events (for example GUIDOBONI & COMASTRI 2005, AMBRASEYS 2009).

Although dating of the Krane tsunamites turned out to be difficult due the fact that only maximum ages are available (Figs. 3.6 and 3.9), all results document that the Koutavos coastal plain is an excellent tsunami sediment trap in which supra-regional tsunami signals seem to be widely recorded.

3.6 Conclusions

The Koutavos coastal plain and the shores of the Bay of Koutavos were subject to geoarchaeological and geomorphological investigations aiming to detect the location of the harbour of ancient Krane as well as to determine gradual and event-related coastal changes. Stratigraphical data based on vibracores and electrical resistivity tomography and geochemical data based on the analysis of sediment samples allowed to reconstruct palaeoenvironmental changes in space and time. ^{14}C-AMS dating helped to establish a geochronological time frame. Based on the present results, the following conclusions can be made.

(i) The stratigraphical record of the Koutavos area revealed two different types of sediment. Besides fine-grained silt-dominated deposits accumulated in a shallow water or distal alluvial fan environment of a low energetic level, intersecting layers were found that consist of coarse-grained, sandy to gravelly material of marine origin rich in marine shell debris. The latter is associated to sedimentary characteristics typical of high-energy impact such as fining upward sequences, incorporated rip-up clasts and sharp erosional unconformities at the base (Figs. 3.5 to 3.9) with an overall thinning landward tendency of tsunami layers (Fig. 3.10).

(ii) Due to their cul-de-sac-type configuration as annex of the long and narrow Gulf of Argostoli, the Bays of Argostoli and Koutavos represent an excellent natural harbour belonging to the best storm-protected landing sites all over the Mediterranean (Fig. 3.2).

(iii) The Gulf of Argostoli is directly exposed to the seismically highly active Hellenic Arc which is, by historic accounts and well documented geo-scientific evidence, known to have triggered numerous tsunami events during the past millennia (Fig. 3.3). A tsunami inundation scenario (Fig. 3.12) based on the northward propagation of a tsunami into the Gulf of Argostoli plausibly shows that, by refraction, diffraction and reflection, considerable parts of the tsunami wave would reach the Bays of Argostoli and Koutavos and affect the Koutavos coastal plain.

(iv) Against the background of the natural storm-protected setting and the high tsunamigenic potential of the Hellenic Arc, it is concluded that multiple allochthonous coarse-grained high-energy intersections encountered in the Koutavos coastal plain sedimentary archive were deposited by tsunami impact. The local stratigraphical record revealed four distinct tsunami layers related to four different tsunami generations (Figs. 3.6 and 3.9).

(v) Based on ^{14}C-AMS datings of organic samples and biogenically produced carbonate and archaeological age estimates of diagnostic ceramic fragments, maximum ages (*termini ad* or *post quos*) for the four encountered tsunami generations were found (I: ~ 4150 ± 60 cal BC; II: ~ 3200 ± 110 cal BC; III: ~ 650 ± 110 cal BC; IV: ~ 930 ± 40 cal AD; Figs. 3.6 and 3.9, Table 3.1). By comparison to palaeotsunami impacts known and dated for the wider

region, it is suggested that Krane tsunami generations I to IV reflect tsunami impacts that affected the Ionian Islands, the Peloponnese and the coasts of the western central Greek mainland. The Koutavos coastal area thus seems to be an excellent archive for tsunami events of a supra-regional nature.

(vi) The autochthonous palaeogeographical evolution of the Koutavos coastal plain starts with a late Pleistocene to early Holocene palaeosol which is subsequently covered by lacustrine deposits of a shallow freshwater lake. Initiated by tsunamigenic impact, the water body then became brackish but still remained shallow (Figs. 3.5 to 3.9). After having experience repeated tsunami landfalls the lagoon was finally silted up by alluvial and colluvial deposits. The present data shows that the Koutavos coastal plain was not an appropriate location for the harbour of ancient Krane (PARTSCH 1890). On the contrary, the central (south-)eastern shores of the Bay of Koutavos revealed excellent conditions for harbour installations such as a sufficient water depth and direct connection to the polis (Figs. 3.8 and 3.9). It is therefore conclude that the Koutavos lagoon as such was used as (natural) harbour during antiquity.

(vii) Geoarchaeological studies in the vicinity of ancient Krane revealed that ancient harbours represent outstanding archives to detect the number, dimension, intensity and spatial extent of tsunamigenic impacts. Using ancient harbours as palaeotsunami archives, a (supra-)regional tsunami chronology can be established. Palaeotsunami research in ancient harbours of Krane, Lefkada, Palairos-Pogonia, Pheia/Olympia and others revealed an approximate recurrence interval for mega-tsunamis of 500-1000 or so years.

4 Multiple late-Holocene tsunami landfall in the eastern Gulf of Corinth recorded in the palaeotsunami geo-archive at Lechaion, harbour of ancient Corinth (Peloponnese, Greece)*

Abstract This chapter presents geomorphological and geo-scientific evidence of repeated tsunami impact on Lechaion, the harbour of ancient Corinth (Peloponnese, Greece) and adjacent coastal zones of the Gulf of Corinth. Due to extensive fault systems, the seismic activity in the Gulf of Corinth is high and often related to landslides or submarine mass movements. Thus, the study area is strongly exposed to tsunami hazard. Geomorphological, sedimentological, geoarchaeological, geochemical and microfaunal studies as well as geophysical methods revealed evidence of multiple palaeotsunami landfall at the harbour site and surrounding coastal area. Tsunami signatures include coarse-grained, sandy to gravelly allochthonous marine sediments intersecting silt-dominated quiescent harbour deposits, geo-archaeological destruction layers as well as extensive units of beachrock-type calcarenitic tsunamites. A local event-geochronostratigraphy was established by radiocarbon dating and geoarchaeological findings. The present results suggest that Lechaion was hit by strong tsunami impacts in the 8th-6th century BC, the 1st-2nd century AD and in the 6th century AD. The youngest event obviously led to final destruction of harbour facilities and the early Christian harbour basilica.

4.1 Introduction

Throughout the Mediterranean, the Gulf of Corinth is one of the seismo-tectonic hot spots. On-going continental rifting with extension rates up to 16 mm/a has created a half-graben structure that is surrounded by numerous active onshore and submarine faults (Papazachos & Dimitriu 1991, Sachpazi et al. 2003, Avallone et al. 2004). Although it represents a rather small and enclosed basin, the Gulf of Corinth holds a comparably high potential for tsunami events, controlled by three major factors: seismicity, bathymetry and mass movements (Papathoma & Dominey-Howes 2003).

Along the faults bordering the gulf, co-seismic displacements of the seafloor often induce tsunamis (Tinti et al. 2007a), whereas the prevailing fault orientation parallel to the coastline further allows easy tsunami wave propagation in northern and southern direction. While the western gulf is rather characterized by high frequency/low intensity seismic activity (magnitudes below 4.5), earthquakes in the eastern part seem to be less frequent but of higher intensity (magnitudes up to 7, Bourouis & Cornet 2009). According to Papadopoulos (2003), the highest tsunami risk is associated to near-shore or offshore earthquakes with magnitudes of 5 or higher. For earthquakes with magnitudes of 6 or higher, the return rate is estimated to be 20 years only (Stefatos et al. 2006).

With water depths of maximum 900 m, steep submarine slopes and a narrow shelf, the bathymetry of the gulf strongly enhances the development of strong tsunami waves (Hasiotis et

*This chapter is based on:
Hadler, H., Vött, A., Koster, B., Mathes-Schmidt, M., Mattern, T., Ntageretzis, K., Reicherter, K. & Willershäsuser, T. (2013): Multiple late-Holocene tsunami landfall in the eastern Gulf of Corinth recorded in the palaeotsunami geo-archive at Lechaion, harbour of ancient Corinth (Peloponnese, Greece). – Zeitschrift für Geomorphologie N.F. Suppl. 57 (4): 139-180.

al. 2002, Papadopoulos 2003, Stefatos et al. 2002, 2006). Due to high sedimentation rates in the shelf zone and steep continental slopes, coastal landslides or submarine slides are often caused by seismic events (e.g. during the 1981 earthquake series, Jackson et al. 1982, Charalampakis et al. 2007a, Tinti et al. 2007b). According to Stefatos et al. (2006), tsunami waves generated by coastal landslides do even exceed the average tsunami wave height generated by seafloor displacements. Regarding that landslides or submarine slides do also occur during aseismic periods, they must be considered the most common source for tsunamis in the Gulf of Corinth (Papadopoulos et al. 2007a, 2007b, Tinti et al. 2007b) with overall return rates of 30-50 years (Lykousis et al. 2007, Charalampakis et al. 2007b).

In accordance to the major hazard potential, numerous tsunami catalogues report on historical events within the Gulf of Corinth (Soloviev et al. 2000, Papadopoulos 2003, Ambrasey & Synolakis 2010). For the period from 500 BC to 1900 AD an overall number of 12 tsunamis is listed, most of them have been documented since the 18th century AD (Hadler et al. 2012). For the 20th century AD, six events are known – the most destructive occurred near Aegio in 1963 with run-up heights of at least 5 m above present sea level (m a.s.l.) (Papadopoulos 2003, Papathoma & Dominey-Howes 2003).

In order to better assess the present and future tsunami hazard in the Gulf of Corinth, it is necessary to complement the historical record by geo-scientific palaeotsunami studies. The study thus focuses on Lechaion, the harbour of ancient Corinth, as a promising geo-archive to identify past tsunami events. The main objectives of the study were (i) to establish a stratigraphical record for the ancient harbour of Lechaion, (ii) to reconstruct the harbour evolution through space and time, (iii) to search for tsunami signatures in order to estimate the magnitude and frequency of major tsunami events and (iv) to use geomorphological and sedimentological traces to reconstruct palaeotsunami inflow and backflow dynamics.

4.2 Natural and archaeological setting

The ancient harbour of Lechaion is located at the southeastern branch of the Corinthian Gulf, the so-called Lechaion Gulf (Fig. 4.1a). The mouth of the gulf is controlled by major active offshore faults, the NE-SW trending Perachora fault and the E-W trending Xylokastro or Corinth fault, well known for triggering submarine slides (Stefatos 2002, Bell et al. 2009, Taylor et al. 2011). The Lechaion Gulf is a comparatively narrow but deep lateral basin of the Gulf of Corinth showing a width of 8 km only and water depths down to 250 m with an overall high potential of submarine mass movements. Opposite to Lechaion, the Perachora Peninsula is bound to the offshore segment of the Loutraki fault. Onshore faults like the Pisia or Skinos fault make the Perachora Peninsula a seismically very active region in the immediate environs of the study area (Stefatos 2006, Bell et al. 2009). The southern margin of the gulf is controlled by numerous active onshore faults, responsible for the present day topography (Vita-Finzi & King 1985, Hayward 2003).

The ancient harbour site is situated directly at the present coastline approximately 3.5 km west of modern Corinth. The recent beach mainly consists of sand and gravel. At various places, consolidated sediments form beachrock-type complexes. Alluvial deposits form a coastal plain that stretches about 4 km inland (IGME 1972, von Freyberg 1973). As a result of on-going faulting and considerable eustatic sea level changes during the Quaternary, the topography towards the southwest is dominated by uplifted marine terraces out of Pliocene to Pleistocene marls overlain by marine and near-shore conglomerates and sands. In the Corinthia, the terraces

reach up to 800 m a.s.l. and are separated by steep slopes that correspond to fault scarps. Where the conglomeratic cover is removed by erosion, strong incision of the terraces locally leads to gully erosion and badland formation (IGME 1972, KERAUDREN & SOREL 1987, GATSIS et al. 2001). Terrace altitudes increase from E to W, indicating only minor uplift rates in the Corinth area. Mid-Jurassic limestone builds up the promontory of Akrocorinth situated some 4 km south of the Lechaion harbour site. In the Corinthia, relief energy rapidly decreases towards the present coastline (IGME 1972, HIGGING & HIGGINS 1996).

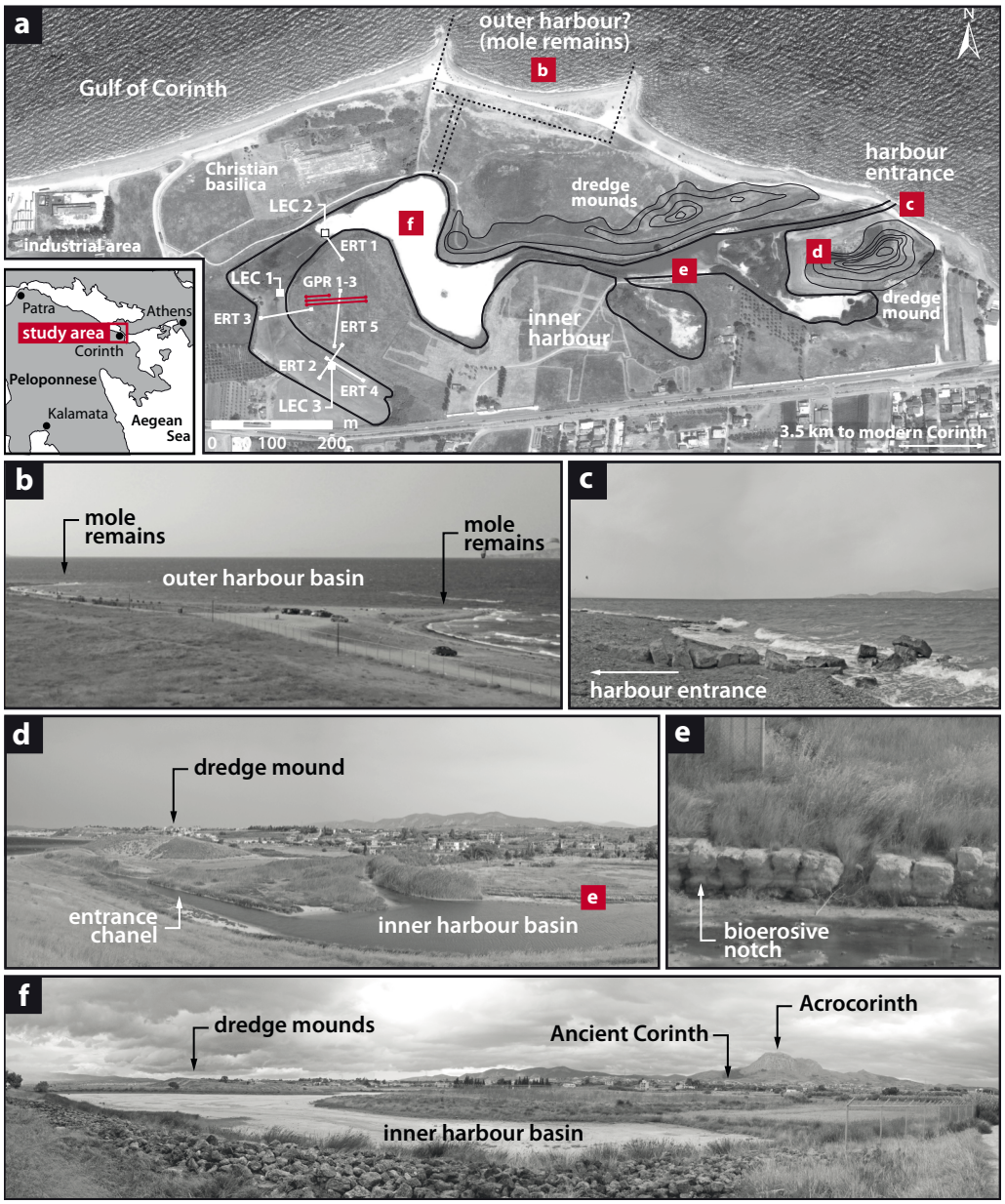

Fig. 4.1: Overview of the Lechaion harbour site including locations of field work (a). The harbour can be separated in an outer basin with moles (b), and an inner basin accessible through a narrow entrance channel (c, d). A quay wall with an uplifted bio-erosive notch is part of the inner basin (e). The latter is characterized today by a serpentine shape (f).

4.2.1 A brief history of the harbour

The city of ancient Corinth, located some 3 km south of Lechaion, was more or less continuously settled since 3000 BC (Blegen 1920, Keraudren & Sorel 1987). Starting around 900 BC, Corinth held a significant commercial as well as military power, mostly based on its naval strength and documented by the foundation of the Corinthian colony Corcyra (Corfu) during the 8th century BC. Also, Corinth was involved in the earliest recorded naval battle among Greek opponents carried out between the Corinthians and Corcyraeans in the mid-7th century BC (Graham 1964).

The foundation of Lechaion is associated with a further expansion of Corinthian military and trading activities in the late 7th to early 6th century BC and is generally ascribed to Periander, second tyrant of Corinth. Due to its favourable location at the Isthmus of Corinth, the harbour was in use for almost one millennium (Graham 1964, Sanders & Whitebread 1990, Rothaus 1995, Stiros et al. 1996). The polis of Corinth also possessed an eastern harbour at the shore of the Saronic Gulf, called Kenchreai, situated some 10 km to the east of the ancient city.

In the early 4th century BC, during the Corinthian War, Lechaion served as a naval base for the Corinthian and Spartan fleets. According to Xenophon, the harbour then held a complex infrastructure including dock houses and fortification walls. Since walls connected the harbour to the ancient city of Corinth, Lechaion belonged to the so-called *epineon*-type of harbour (Xen. Hell. 4.4.6-8 after Brownson 1918, Lehmann-Hartleben 1923, Blackman 1982). Around 200 BC, the harbour became the main base for the Macedonian fleet under Philipp V. As Polybius notes, six thousand Macedonian and Achaean soldiers and twelve hundred mercenaries set out from Lechaion, which allows the estimation of nearly 40 triremes assembled in the harbour area (Polyb. Hist. 5.2.11 after Paton 1923, Dahlheim 1997). With the Roman devastation of Corinth in 146 BC, Lechaion was abandoned for the term of a century. It is unknown, however, whether the harbour was also destroyed at that time. After the re-colonisation of Corinth under Julius Caesar in 44 BC, it regained its former importance (Paus. 2.1.1 after Frazer 1965).

During Roman times, repeated reconstruction of Lechaion was carried out, presumably in the 1st century AD (Rothaus 1995) and from 353-358 AD (Kent 1966). As indicated by contemporary descriptions, the harbour most likely served for economic rather than military purposes (Strab. Geogr. 8.6.23 after Hamilton & Falconer 1903). The final abandonment of Lechaion is generally associated with the destruction of Corinth by a series of strong earthquakes in 521 or 551 AD, whereas the area probably remained populated until the 7th century AD. Though occasionally re-used in medieval times, the harbour never regained its former importance (Rothaus 1995). Historic accounts from travellers in the 19th century AD still refer to Lechaion as a "cove" or "lagoon" close to modern Corinth but describe the site as "desolated" and "deserted" (Blaquiere 1825, Leake 1830).

4.2.2 Visible remains of harbour works

Until today, the archaeological site of Lechaion has remained mostly unexcavated. Nevertheless, certain harbour installations are still visible and allow a rough estimation of the former harbour structure (Fig. 4.1a). According to Paris (1915), Lechaion was most probably separated into an outer harbour and an inner harbour basin. The outer harbour is indicated by two large moles perpendicular to the present coastline (Fig. 4.1b). Further towards the east, wall remains outline the entrance to the inner harbour, a channel about 150 m long and 12 m wide (Fig. 4.1c, 4.1d, Stiros et al. 1996).

The inner harbour basin as visible today has a notably elongated, serpentine shape which was interpreted to reflect two main basins used for navigation and four adjacent basins for anchoring (Paris 1915, Lehmann-Hartleben 1923). In its eastern parts, ancient quay walls are well preserved (Fig. 4.1e). Remains of a harbour monument or small building most probably of Roman age are still visible in the central harbour basin (Shaw 1969, Rothaus 1995).

The present day topography of the harbour site is further characterized by large sediment mounds (Fig. 4.1d, 4.1f), generally associated to dredging activity or referred to as natural dunes (Frazer 1965, Rothaus 1995, Stiros et al. 1996). Up to 16 m high, these mounds are located in the eastern harbour area, situated to both sides of the entrance channel.

4.2.3 The Lechaion basilica

In the western part of the Lechaion harbour site, remains of an early Christian basilica were excavated by D. Pallas between 1955 and 1965 (Fig. 4.7, Pallas 1960, Krautheimer 1989). With a total length of 186 m this basilica represents the largest known sacred building from its period and is comparable to St. Peter in Rome (Fig. 4.7a). The basilica is situated on a narrow tongue-like piece of land between the inner harbour basin and the beach some 100 m distant from the present shore. It was thus clearly visible from both the land and the sea side (Krautheimer 1989, Rothaus 1995).

The exceptional location and dimensions of the building must be considered against the historical background of the development of Christianity in Greece. In Corinth, an early Christian congregation formed around 50 AD subsequent to the missionary work of Paul the Apostle (Becker 1998). However, it is only from the 5th century AD onwards that Greece experienced an increasing popularity of Christianity (Krautheimer 1989). Christian influence especially developed in coastal cities, where the new religion was imported and cultivated by sailors. Large churches were therefore often built in coastal cities such as Corinth. Here, at least five basilicas were constructed in or close to the ancient city, including the Lechaion basilica (Scranton 1960, Krautheimer 1989).

Columns encountered at Lechaion during excavation works indicate a 5th century AD age of the building (Fig. 4.7b). Finds of coins associated to the foundation and inner pavement document initial construction work for the mid-5th century AD that continued at least until the early 6th century AD (Pallas 1960, 1970, Krautheimer 1989, Rothaus 1995). As the building shows an overall good state of preservation (well-preserved plaster decoration, Fig. 4.7d inlay), Krautheimer (1989) assumes that the basilica has been in use for only a short time prior to its destruction.

4.2.4 The ancient diolkos

At the western entrance to the Corinth Canal, about 7 km to the northeast of Lechaion, remains of an ancient ship slipway have been excavated in the 1950s (Verdelis 1960). In historic times, ships travelling between the Ionian and the Aegean Seas had to circumnavigate the Peloponnese on a time-consuming and hazardous journey past Cape Malea (Werner 1997). Throughout history, various approaches failed to cut a channel through the Isthmus of Corinth in order to shorten the passage between the Gulf of Corinth and the Saronic Gulf. It was not until 1893 that a joint venture of French and Hungarian enterprises finally managed to realize the project (Lewis 2001). However, in antiquity a slipway across the narrowest part of the isthmus already

connected the Lechaion Gulf with the Saronic Gulf. First mentioned by Thucydides, the so called *diolkos* most probably dates to the late 7th or 6th century BC and is, like Lechaion, ascribed to Periander (Thuk. 3.15 after Landmann 2010). Ships were towed across the Isthmus at several occasions throughout history. It must be assumed, though, that the transport of ships was rather uncommon and limited to small and light (war-) ships (MacDonald 1986, Werner 1997). In general, the *diolkos* was used as "railway" to transport trading goods by carriages from ship to ship across the Isthmus (Lohmann 2013).

Based on literary evidence, the diolkos was active at least between the early 5th century BC and the mid-1st century AD. The term *diolkos* was no more mentioned after 67 AD, when it was most probably truncated by Nero's attempt to cut a channel across the isthmus. Later sources only referred to the isthmus itself (Werner 1997, Lewis 2001).

At the western entrance to the Corinth Canal, the pavement of the *diolkos* and adjacent docking site is covered by a beachrock-type, calcified layer of sand and gravel, obviously postdating the slipway (Fowler & Stillwell 1932, Mourtzas & Marinos 1994, Pirazzoli 2010).

4.3 Methods

A multidisciplinary approach was used to understand the sedimentary history of the Corinthian harbour Lechaion and to decipher its palaeotsunami record. In this study, detailed stratigraphic information from the inner harbour basin and its surroundings are presented.

Geo-scientific studies carried out at Lechaion comprised vibracoring using an Atlas Copco Cobra mk 1 coring device with core diameters of 3 cm, 5 cm and 6 cm and a maximum coring depth of 9 m below surface (m b.s.). Photo-documentation, description and sampling of the retrieved cores were realized in the field. Core description comprised grain size, sediment colour and content of calcium carbonate, fossil content, ceramic fragments and further sedimentological and pedological features (Ad-hoc-Arbeitsgruppe Boden 2005).

A handheld XRF spectrometer (type Thermo Niton XL3t 900s GOLDD, calibration mode SOIL) was applied to measure total amounts of about 30 elements. Samples were measured in situ for 30.5 sec with an average vertical resolution of 5 cm.

In the laboratory, further analyses of sediment samples comprised standard geochemical parameters such as pH-value, electrical conductivity, loss on ignition and contents of calcium carbonate. Microfaunal studies focused on the foraminiferal fingerprint of the encountered deposits.

On-site geophysical studies were carried out for a better understanding of subsurface stratigraphies, bedrock topography and to detect archaeological remains. They comprised electrical resistivity tomography (ERT) carried out by means of a multi-electrode geo-electrical unit (type Iris Instruments, Syscal R2 Plus Switch 48) and ground penetrating radar (GPR) using a 400 MHz antenna (type GSSI) with a survey wheel and a data recording unit (type GSSI SIR-3000). Position and elevation of vibracoring sites, ERT and GPR transects were measured using a DGPS unit (type TOPCON HiPer Pro FC-200).

A local geochronostratigraphy was established by ^{14}C-AMS dating of plant material and biogenic calcium carbonate as well as by archaeological age estimations of diagnostic ceramic fragments and architectural remains. The calibration software Calib 6.0 was used to calculate calendar ages (see Reimer et al. 2004). Data from existing local geochronologies (Morhange et al. 2012, Stiros

et al. 1996) was recalibrated as base for comparison. Radiocarbon dating was accomplished by the Keck Carbon Cycle AMS Facility at the Earth System Science Department of the University of California at Irvine (UCI).

4.4 Evidence of high energy impact from the inner Lechaion harbour basin

At Lechaion, three vibracores were drilled in the present day visible inner harbour basin (for coring locations see Fig. 4.1a). This study gives detailed information on the harbour basin stratigraphy as well as on the event stratigraphical record.

4.4.1 The sedimentary sequence of the harbour basin

Vibracore LEC 2 (-0.04 m a.s.l., N 37°55'58.6" E 22°53'03.5") was drilled in the central inner harbour basin of Lechaion. The coring site is approximately 240 meters distant from the shoreline. Fig. 4.2a gives a simplified facies profile of the vibracore.

The lower part of the profile is dominated by homogeneous, light grey sediments of marine origin (9.00-7.21 m b.s.). A gradual coarsening upward from silty clay to clayey silt seems to be due to decreasing water depths. Subsequently, the lower marine unit is overlain by grey clayey to sandy silt (7.21-4.74 m b.s.). Numerous remains of *Posidonia* and marine shells indicate shallow near-coast conditions dominated by seaweed meadows. On top of this unit, a sharp erosional contact marks a sudden environmental change (Fig. 4.1c). In strong contrast to the seaweed meadows, the subsequent layer is a thick deposit of homogeneous mean to fine grained sand (4.74-2.87 m b.s.), void of plant remains and macroscopic fauna. Delimited by alternating layers of sand and clayey silt (2.87-2.56 m b.s.) it reflects a temporary increase in transport energy and clearly represents a high energy deposit. The following greyish-brown, clayey to silty sediments document a change back towards more quiescent sedimentation conditions (2.56-1.83 m b.s.). Fragments of *Cerastoderma glaucum* as well as a high content of organic substance document a lagoonal environment, corresponding to harbour conditions.

The lagoonal system was later affected by the high energy input of marine shell debris and gravel (1.83-1.50 m b.s.) together with large limestone fragments. A basal erosion unconformity (Fig. 4.2b) as well as the rapid re-establishment of the lagoonal environment (1.50-0.95 m b.s.) document sudden and temporary sediment input. Following another sharp contact, the upper part of vibracore LEC 2 is dominated by deposits of a semi-terrestrial (0.95-0.90) and later limnic environment (0.90-0.00 m b.s.). The latter is characterized by a thick layer of calcium carbonate which reflects a longer period of epilimnic decalcification typical of a shallow lake that is highly saturated with $CaCO_3$.

In a summarizing view, the local stratigraphy of the harbour site as deduced from vibracore LEC 2 comprises (i) shallow marine pre-harbour deposits that are overlain by (ii) quiescent lagoonal sediments corresponding to typical harbour basin deposits and (iii) limnic to terrestrial deposits accumulated when the harbour was already out of use. This facies pattern reflects a general regression trend with the formation and subsequent siltation of a lagoonal system in a pre-existing open-shore environment. The overall dominating grain size reflecting this autochthonous development is silt.

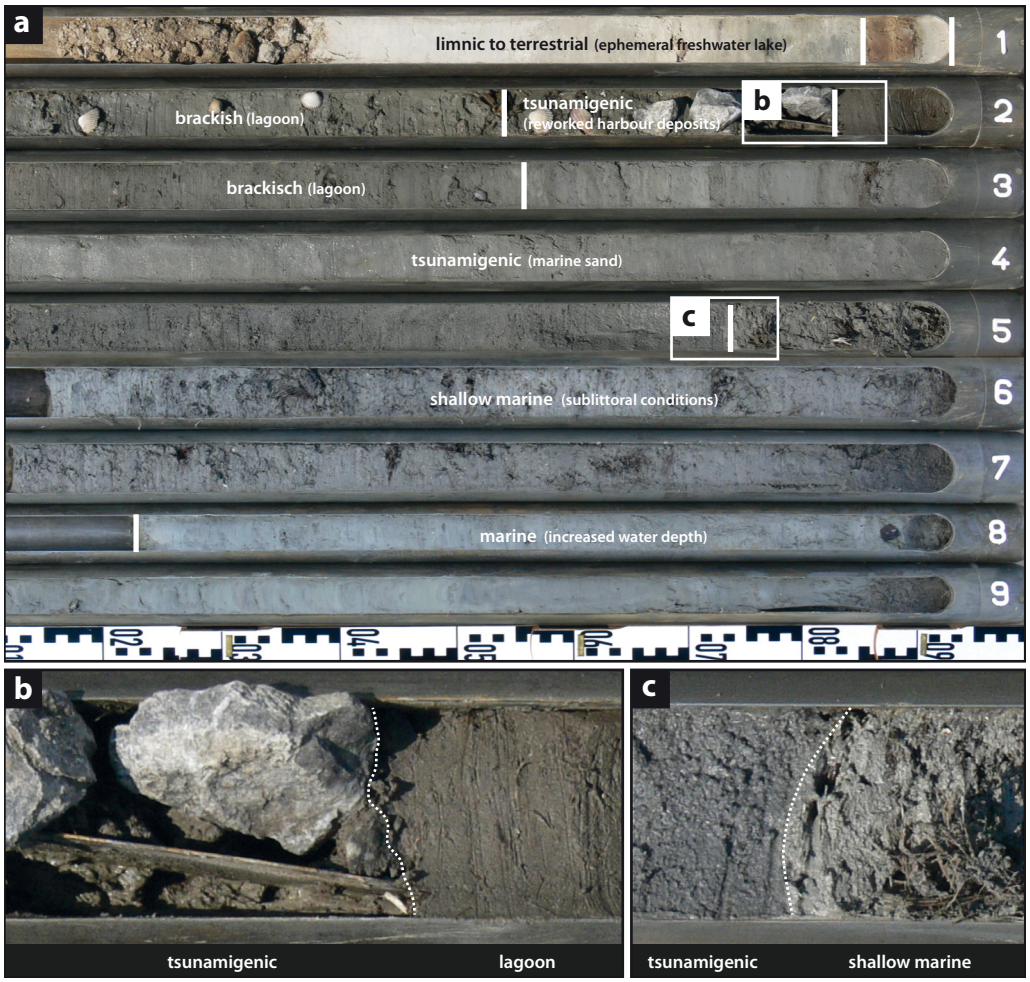

Fig. 4.2: Simplified facies profile of vibracore LEC 2 drilled in the inner harbour basin, north of cores LEC 1 and LEC 3 (a). Enlarged parts show abrupt onset of stratigraphical sections out of allochthonous high-energy deposits (b, c). See text for further explanation.

However, the LEC 2 stratigraphical record is repeatedly interrupted by layers of coarse-grained sediments and shell debris, clearly indicating short-term high-energy interference of the site (for comparable grain size analysis of core LEC 1 see Fig. 4.4).

4.4.2 The event-stratigraphic record of Lechaion

The vibracore transect begins in the western central harbour basin (LEC 2) that is seasonally still flooded due to rainfall and/or groundwater and trends in N-S direction. Vibracoring sites LEC 1 (0.37 m a.s.l., N 37°55'55.6'' E 22°52'00.9'') and LEC 3 (0.56 m a.s.l., N 37°55'51.7'' E 22°53'03.7'') are located in the more landward part of the harbour basin that is nowadays used for agricultural purposes. Regarding the transect, it has to be noted that the modern surface of the harbour basin almost equals sea level and that the ground surface of the surrounding area ranges from 2 m to 6 m a.s.l.. Thus, the vibracore transect only represents the sedimentary record from inside today's basin and does not reveal stratigraphical information about adjacent, more elevated parts where drilling was not possible for archaeological reasons. Detailed stratigraphical information about the transect is given in Fig. 4.3.

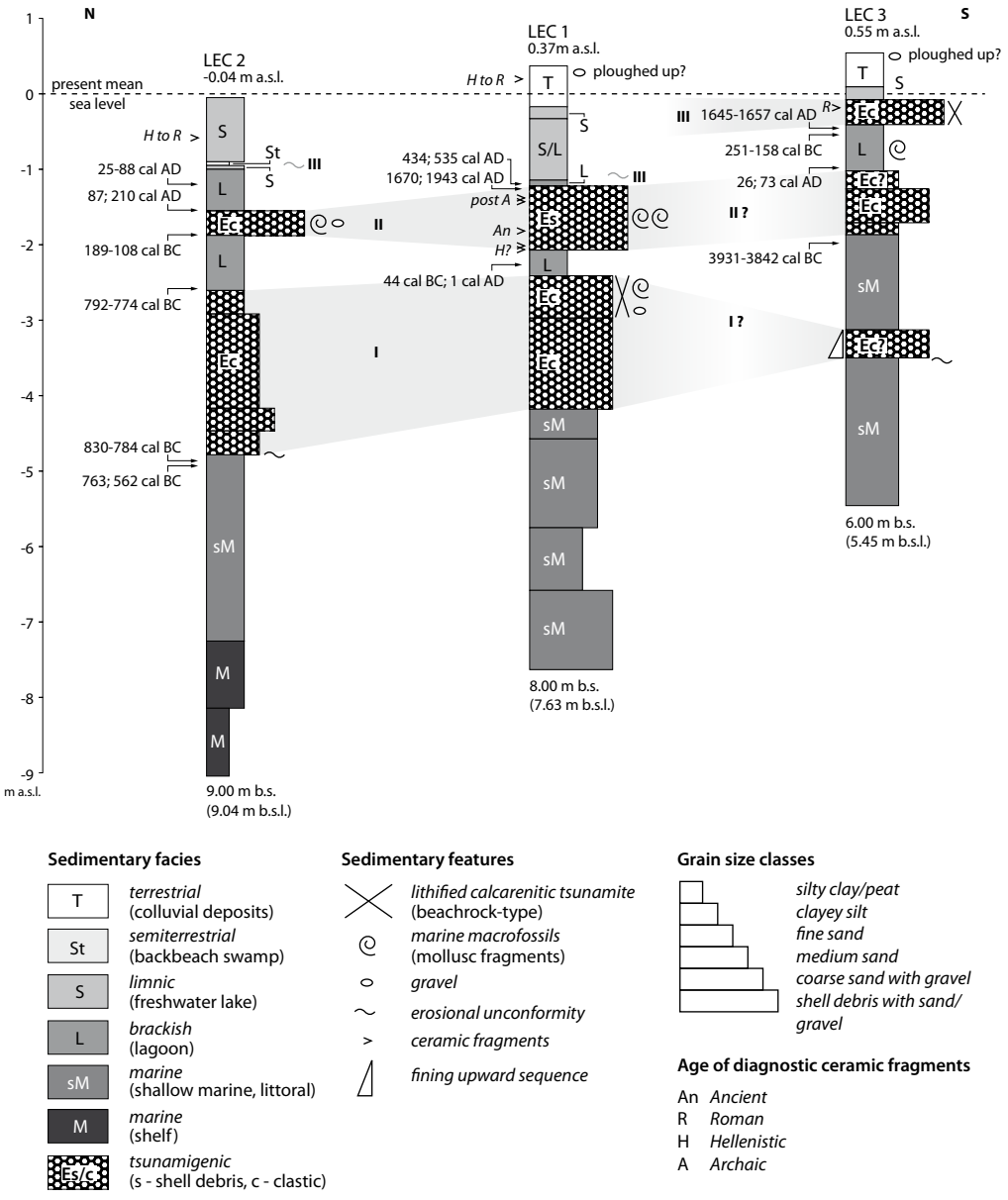

Fig. 4.3: Stratigraphies, facies distribution and geochronostratigraphy for the LEC 1-3 vibracore transect across the inner Lechaion harbour basin. For location of vibracores see Fig. 1a. Details on radiocarbon ages are presented in Tab. 1.

Stratigraphies recovered at coring sites LEC 1 and 3 strongly resemble the stratigraphy already described for coring site LEC 2. Interfering high-energy deposits were found in consistent stratigraphical positions over long distances. The findings support an event-stratigraphical approach for the Lechaion harbour site which is described as follows.

Event generation I affects a pre-harbour, shallow marine environment. At site LEC 1 the overflow of a sand bar obviously leads to decelerating velocities and major sediment deposition at the seaward site LEC 2. Possibly event-related geomorphological changes seem to have caused a more or less sheltered shallow marine depression in leeward position, dominated by seaweed

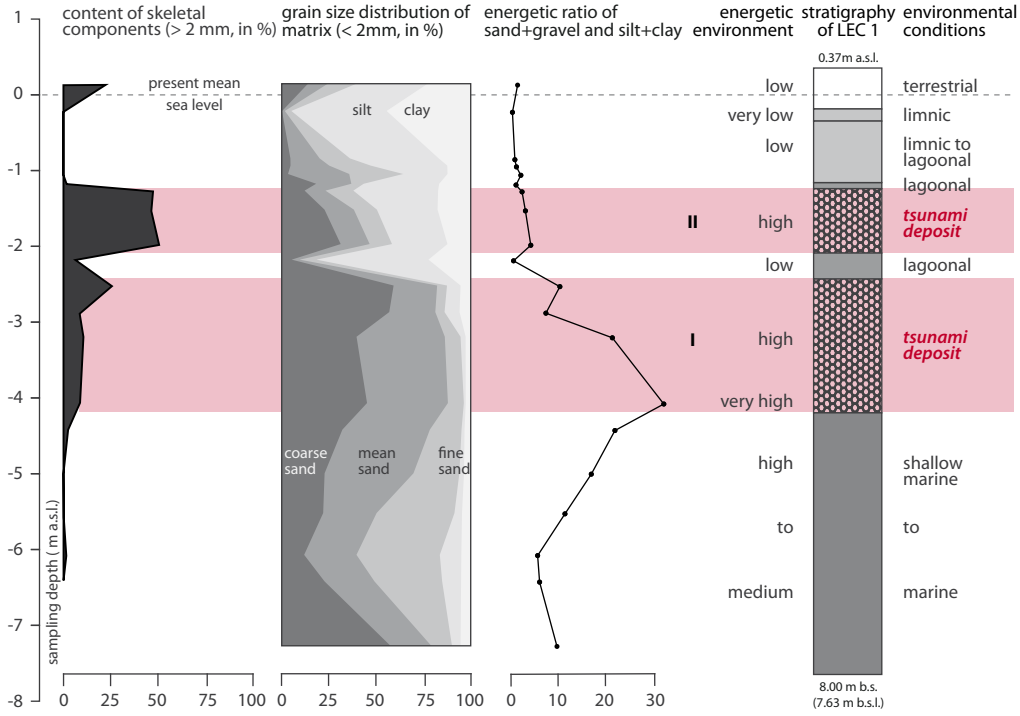

Fig. 4.4: Results from grain size analyses for vibracore LEC 1. Event deposits are characterized by a high content of skeletal components and noticeable coarsening of the matrix. The energetic ratio indicates increased transport energy for the lower event layer. The upper layer does not show high energetic ratios as the calculation does not include skeletal components.

meadows. It seems as if this was the place where the early harbour was installed. The mid-core stratigraphy of cores LEC 2 and LEC 1 reveal an initial phase of harbour sediments following the first high-energy impact that hit the coast.

The harbour facies encountered at coring sites LEC 2 and LEC 1 is repeatedly interrupted by a thick layer of shell debris and massive rubble fragments, respectively, together with a clear erosional unconformity at the base and followed by the sudden re-establishment of harbour conditions. With regard to the quiescent environment of the Lechaion harbour basin and to protective walls that have presumably surrounded the site at that time, the sedimentary features of the intercalating layers are interpreted as a second generation of short-term, high-energy impact to the harbour basin. It seems as if in-situ harbour deposits were considerably eroded possibly due to scouring effects by overflowing water masses.

Along the vibracore transect, the lagoonal-type harbour facies finally changes into limnic (LEC 2) and later terrestrial conditions (LEC 1, LEC 3). At site LEC 3, a third event generation is evident from a thick, partly calcified layer of sand, gravel, marine molluscs and ceramic fragments. However, this event deposit is only locally preserved and was not found at sites LEC 1 and 2. Nevertheless, the geomorphological consequences of this event were apparently severe, since the lagoonal system was not re-established after this impact.

4.4.3 XRF measurements

Vibracores retrieved from the ancient harbour area at Lechaion underwent X -ray fluorescence analyses (XRF). XRF values for vibracores LEC 1 and LEC 2 were measured directly at the original cores with an average depth interval of 5 cm. In case of core LEC 3, selected sediment samples from different stratigraphical units were analysed so that the vertical resolution is thinner. By XRF analyses, concentrations of altogether 33 elements were measured.

By calculating Ca-Fe ratios, the study attempts to differentiate between stratigraphical units deposited under predominantly terrestrial or marine conditions. High Ca-Fe ratios are supposed to reflect a dominating marine influence, since the production of calcium carbonate ($CaCO_3$) by marine organisms (e.g. foraminifera, ostracods, molluscs) leads to increased calcium concentrations in seawater and associated sediments. In contrast, low Ca-Fe ratios of sediments may correlate with an increased terrestrial influence by subaerial decalcification and formation of iron (hydro)oxides (Vött et al. 2011b).

As high-energy marine flooding events are capable of transporting marine sediments far inland into (semi-)terrestrial or limnic environments, they are expected to leave a geochemical fingerprint in the stratigraphy of the corresponding geoarchive. Using XRF analyses, Vött et al. (2011a) identified repeated tsunami landfall by unusual Ca-Fe ratios found in sediment cores from NW Greece.

Ca-Fe ratios achieved for vibracores LEC 1, 2 and 3 are illustrated in Fig. 4.5, all profiles are adjusted to the local topography. Taking into account the stratigraphical record at sites LEC 1 and 2, more or less constant Ca-Fe ratios dominate the pre-harbour marine units, whereas event generation I is characterized by significantly increased Ca-Fe values followed by constantly decreasing values. While the harbour deposits following on top show a constant but rather low ratio at site LEC 2, at site LEC 1 increased values are probably caused by the rich macrofossil content of the LEC 1 harbour facies. However, the geochemical fingerprint clearly marks the transition from marine to event related to lagoonal deposits.

Concerning event generation II, increased Ca-Fe ratios found at site LEC 2 document an abrupt and strong marine impact to the harbour basin. More or less constant values found at site LEC 1 may be explained by event deposits which are predominantly made out of reworked autochthonous harbour deposits; alternatively, this is due to a methodological problem, since vibracoring produced a gap in the sedimentary record of the event deposit (Fig. 4.5, dotted line). For the subsequent limnic unit, corresponding to post-harbour conditions, the strongly increased Ca-Fe ratio is related to marine influence in so far as post-depositional decalcification of event generation III deposits obviously resulted in the formation of a carbonate gyttja in the present day harbour basin.

Sediment cores LEC 1, 2 and 3 were also analysed for lead (Pb) concentrations. In Greece, increased exploitation of lead deposits started in the mid-1st millennium BC, when lead was won mainly as by-product from smelting silver and caused initial environmental pollution (Hong et al. 1994, Åberg et al. 2001). A major mining site was, for example, at Laurion, close to Athens and only some 100 km distant from Corinth (Gowland 1901). During Roman times, lead mining reached a maximum around the 1st century AD, as did the environmental contamination; sediments from those periods show highly increased lead concentrations, comparable to the 19th century AD industrial revolution (Gowland 1901, Labonne et al. 1998, Le Roux et al. 2005).

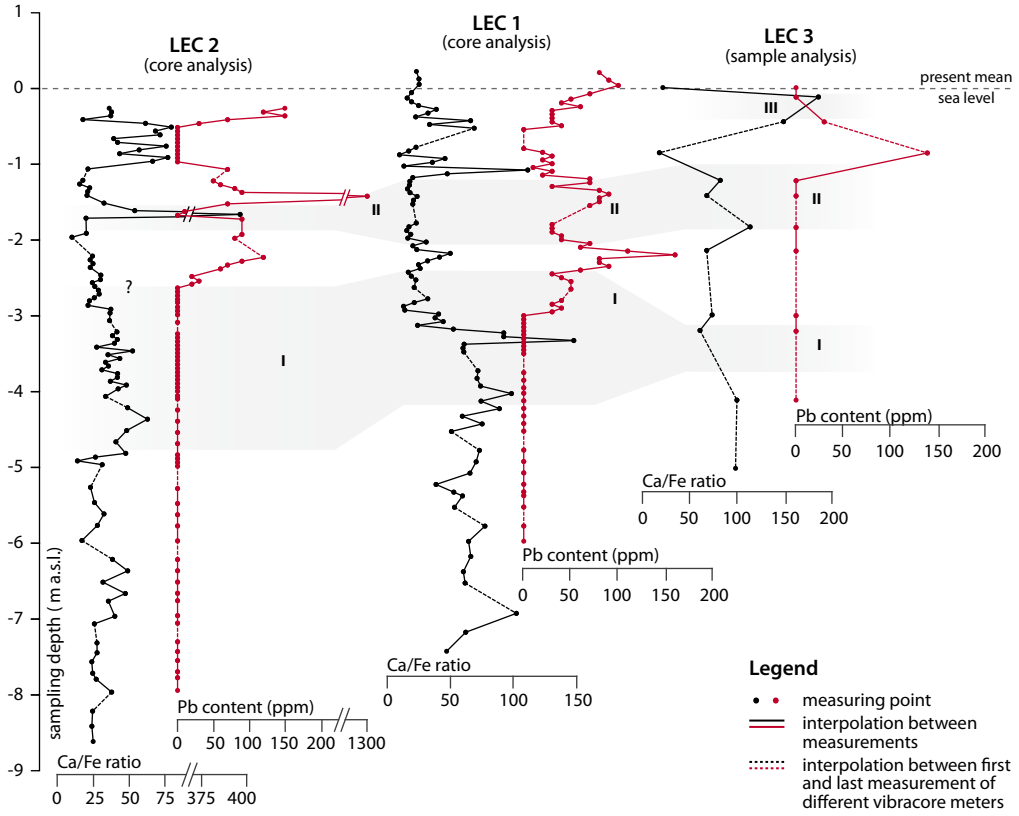

Fig. 4.5: Ca-Fe ratios and Pb content (ppm) for the LEC 1-3 vibracore transect derived from XRF measurements. Interferences of the predominant environmental conditions are represented by sudden changes in the Ca/Fe ratio. Harbour deposits are characterized by increased Pb values due to anthropogenic influences on the ecosystem.

With the decline of the Roman Empire, the production of lead decelerated until medieval times (Hong et al. 1994).

From sediment samples of the ancient harbour of Marseilles, Le Roux et al. (2005) verified strong anthropogenic lead contamination for Greek and especially Roman times. For the Lechaion harbour site, results of XRF measurements of lead are depicted in Fig. 4.5. Pre-harbour marine sediments at Lechaion show to be void of lead, so that the natural lead background is presumably nil. Sediments associated to the Greek harbour foundation (8th to 6th century BC), however, show a sudden increase of the lead content (LEC 2) with maxima roughly corresponding to the Roman period (LEC 2, upper lagoonal unit; LEC 1, lower lagoonal deposits, Fig. 4.5). On the contrary, post-harbour limnic units are void of lead which correlates well with an overall assumed post-Roman decrease in Pb pollution. However, strongly increasing lead concentrations in near-surface sediments document considerable input of lead to the ecosystem by modern societies.

In contrast to the harbour deposit, strongly polluted with lead, event deposits of generation II and III are characterized by decreased lead concentrations, implying the input of allochthonous, non-polluted sediments. Where autochthonous material has been reworked, Pb values remain at a considerably high level (LEC 1, upper part of event generation II, Fig. 4.5). The fact that, at site LEC 1, pre-harbour deposits of event generation I also show considerable lead concentrations is probably due to a mixing of harbour sediments and event deposits by dredging activities.

Generally, high-energy impacts as well as the anthropogenic influence to the Lechaion environment also proved to be well assessable by analysing the lead concentration of the recovered sediments.

4.4.4 Microfossil analysis of vibracore LEC 2

Foraminifera are ubiquitous in coastal sedimentary environments where salt-water conditions are prevailing. Unlike ostracods, gastropods and bivalves, foraminifera do not appear in freshwater environments. Due to their common distribution and good preservation potential, foraminifera are frequently used as environmental indicators to reconstruct palaeoenvironmental conditions in offshore and near-shore areas (Gupta 2002). Changes of living conditions are excellently reflected in changing microfossil assemblages as long as the sediments are not influenced by oxidation (Fiorini 2004, Mamo et al. 2009).

Since many foraminifera tolerate a wide range of environmental factors, such as salinity, temperature or oxygen content, species may adapt to slowly changing environmental conditions (Murray 2006). A gradual shift in fossil assemblages must consequently be considered as equally gradual transition between environments whereas an abrupt alteration of species points to a sudden, possibly catastrophic change due to allochthonous factors.

In near-shore or coastal environments, high-energy events such as storm surges or tsunamis may trigger major changes, depending on their magnitude and impact, and lead to disturbed foraminiferal assemblages (Mamo et al. 2009). In the Gulf of Corinth, Alvarez-Zarikian et al. (2008) used foraminiferal assemblages as palaeoenvironmental proxies to identify high-energy impact at the ancient town of Helike while Kortekaas et al. (2011) detected multiple high-energy influence along the northern shore of the gulf by foraminiferal analyses.

For the Lechaion harbour site, detailed foraminiferal analyses were carried out for vibracore LEC 2. From a total number of 21 samples, 72 species of foraminifera from 35 genera were identified (Loeblich & Tappan 1988, Cimerman & Langer 1991). According to the microfossil content and with regard to the local stratigraphy, vibracore LEC 2 was divided into 6 specific units (Fig. 4.6). Foraminiferal assemblages were analysed in total in order to achieve an optimum environmental classification for each unit. Specific species that show similar abundances throughout all studied samples are not regarded as decisively indicative and were thus not included in the figure (for species names see Fig. 4.6 captions)

The foraminiferal assemblage encountered in *Unit 1* at the base of the profile LEC 2 (9.00-7.21 m b.s.) is characterized by a high diversity in species but low abundances. *Elphidium crispum* and miliolid species like *Triloculina* sp. or *Quinqueloculina* sp. are common and indicate fully marine conditions while *Nonionella* sp., *Spirillina vivapara* and *Polymorphina* sp. point to increased water depth and may indicate the deeper shelf zone as source area (Gupta 2002, Murray 1973, 1991, 2006). Occasional pyritization features point to post-sedimentary alterations of the fossils under anoxic conditions, while disintegrated foraminifera tests may document reworked older marine sediments.

Unit 2 (7.21-4.74 m b.s.) documents a gradual shift in the foraminiferal assemblage towards shallow water condition. While miliolid species disappear, the environment is increasingly dominated by *Cibicides lobatulus* and *C. refulgens*, *Rosalina* sp., *R. bradyi* and *R. globularis* as well as *Elphidium crispum*. The assemblage thus documents a clear decrease in water depth; in the Mediterranean, it is known to be typical of seaweed meadows in near-coast shallow waters (Murray 2006).

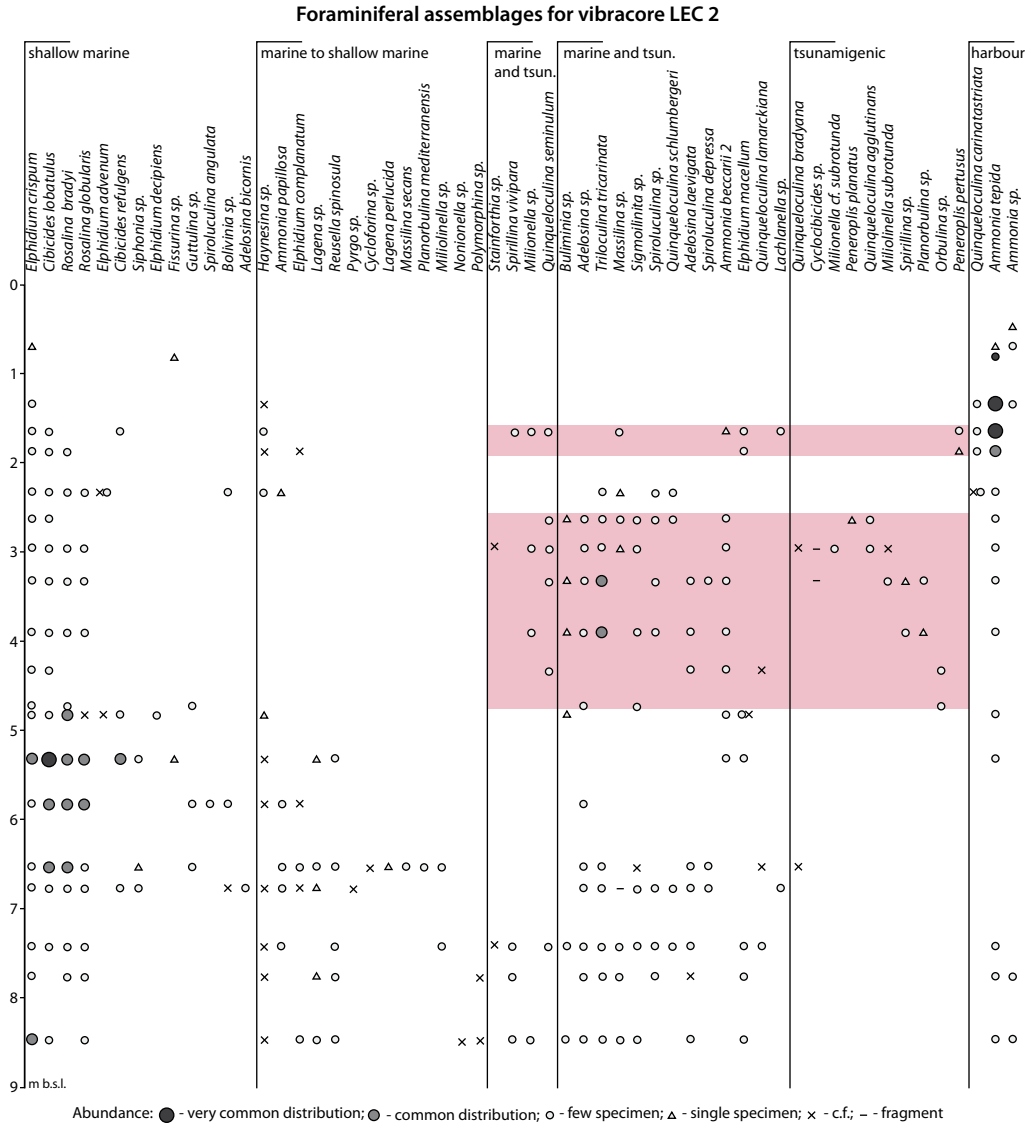

Fig. 4.6: Results of foraminiferal analyses of sediment samples from vibracore LEC 2. Species are sorted according to their sedimentary environment. Encountered specimens of the species *Ammonia beccarii, Asteriginata mamilla, Brazilina* sp., *Cibicides* sp., *Cribroelphidium* sp., *Cyclocibicides vermiculatus, Elphidium* sp., *Elphidium delicatum, Elphidium excavatum, Elphidium williamsoni, Nonion* sp., *Nonionella turgida, Quinqueloculina* sp., *Rosalina* sp., *Triloculina* sp. and *Triloculina trigonula* are not regarded as decisively indicative and are not included in the figure.

Unit 3 (4.74-2.56 m b.s.) follows on top of a sharp erosional contact; the overall fossil content is low but exotic. Miliolids like *Triloculina tricarinata*, characteristic of the local open marine environment (see *Unit 1*), suddenly reappear. Simultaneously, species atypical of the local environs appear in the assemblage: While *Miliolinella subrotunda* and *Spirillina* sp. are indicators for open marine, cold to temperate conditions, *Peneroplis* inhabits warm and shallow lagoonal environments (Murray 1973, 1991, 2006). The microfossil content of *Unit 3* thus clearly documents the mixing of foraminifera species from different marine environments. According to Mamo et al. (2009) a sudden trend towards open marine species or mixed species may be

characteristic for high-energy impact. Moreover, in the lower part of *Unit 3*, most foraminiferal tests and macrofossil remains are damaged or broken, indicating intense reworking due to high-energy dynamics. Hence, in accordance to the sedimentary evidence, *Unit 3* is considered to clearly reflect high-energy influence on the microfossil content.

The foraminiferal assemblage encountered in *Unit 4* (2.56-1.83 m b.s., 1.50-0.95 m b.s.) documents an essential environmental change subsequent to the high-energy influence. While marine foraminifera disappear, the unit is increasingly dominated by *Ammonia tepida* which is typical of muddy lagoonal environments and may tolerate highly fluctuating salinity and oxygen conditions (Murray 2006). Being adaptable to environmental stress, *A. tepida* is commonly found in ancient (Reinhardt et al. 1994, Marriner & Morhange 2007, Di Bella et al. 2011) as well as modern harbour basins (Howarth & Murray 1969). Thus, *Unit 4* neatly represents the onset of the Lechaion harbour facies.

Unit 5, intercalating the muddy *Unit 4* harbour deposits (1.83-1.50 m b.s.), comes along with coarse sediments and shell debris. Comparable to *Unit 3*, multiple foreshore open marine (e.g. *Spirillina vivipara*, *Massilina* sp.) as well as locally atypical species (*Peneroplis pertusus)* suddenly appear, whereas *A. tepida* remains still dominant. This distribution thus mirrors a significant marine influence on the autochthonous harbour basin deposits. With regard to the sedimentary characteristics, *Unit 5* corresponds to a second marine-borne, high-energy impact to the harbour site.

Unit 6 comprises the uppermost part of vibracore LEC 2 (0.95-0.00 m b.s.). Apart from few individuals of the *Ammonia* sp. group, no foraminifera were found in the samples.

4.5 Geoarchaeological traces of high-energy impact from the Lechaion harbour area

4.5.1 The early Christian basilica

So far, the destruction and sedimentary burial of the 5th century AD Christian basilica have been associated to earthquake influence in the 6th century AD (521 AD or 551 AD, Krautheimer 1989). Detailed geoarchaeological observations in the immediate environs of the building, however, rather suggest tremendous high-energy impact from the sea-side as decisive cause of the destruction. Collapsed arch fragments along the northeastern section (Fig. 4.7c) as well as impact marks visible at the inner ground floor caused by fallen parts of the ceiling clearly indicate earthquake damage. At the same time, though, the entire building appears embedded in a conspicuous sediment layer, up to 2 m thick, which consists of a silty to sandy matrix, abundant well rounded gravel, numerous marine molluscs and angular ceramic fragments (Fig. 4.7d-g).

Archaeological excavations along the northern side of the building, directly exposed to the Gulf of Lechaion, revealed that the foundation level of the church walls lies up to 2 m below present day ground surface (Fig. 4.7d, 4.7h). Taking into account that the foundation level was identical with the original ground surface, as shown by decorative plaster at the outer wall now covered by sediments (Fig. 4.7d inlay), the massive character of the sedimentary burial becomes clear. To the landward side of the building, the sediment cover thins to approximately 0.5 m indicating that the sedimentary burial was most intense on the seaward side. Regarding the excavation reports (Pallas 1960), the encountered sedimentary characteristics and stratigraphic pattern as

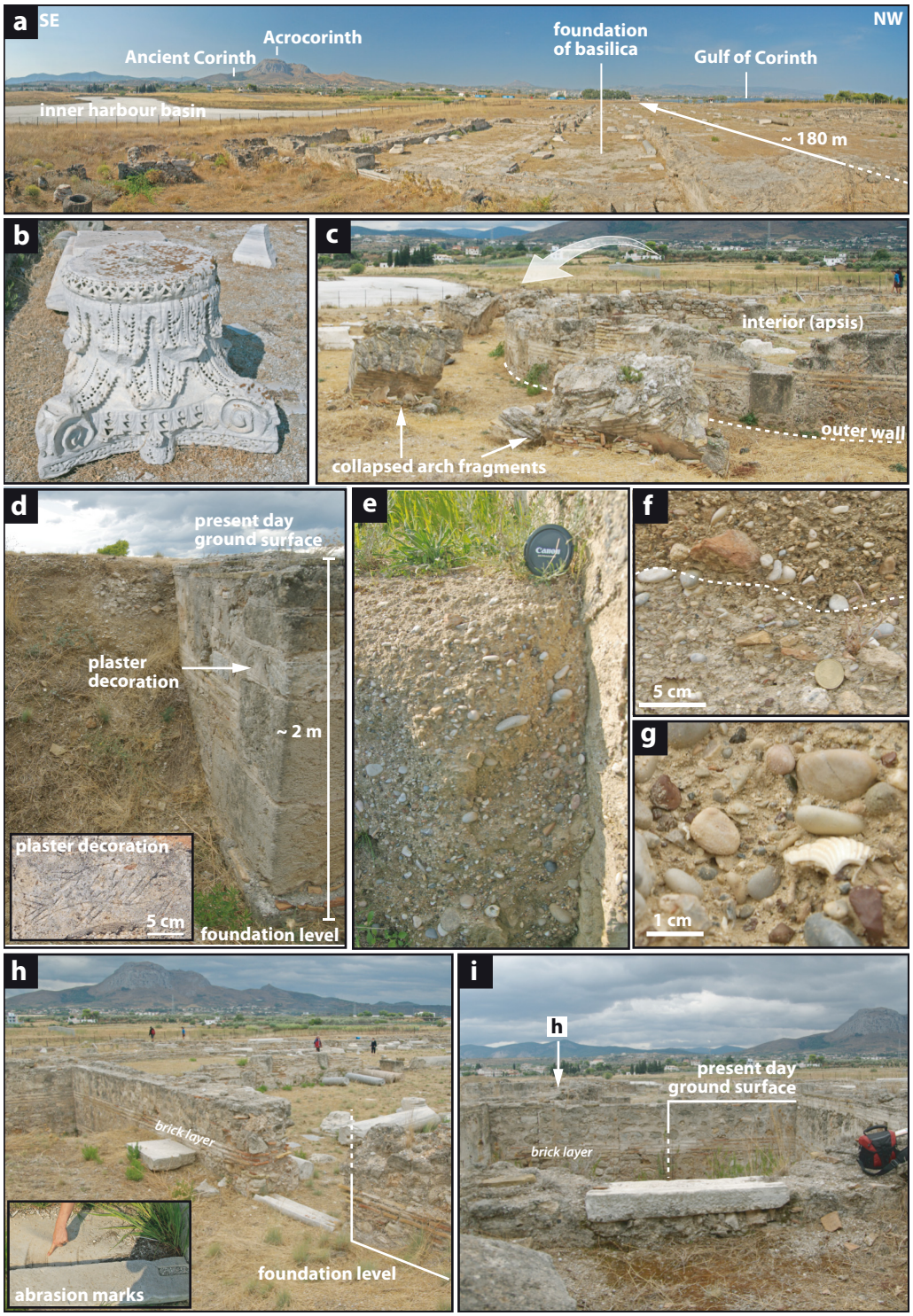

Fig. 4.7: Overview of the early Christian basilica at Lechaion (a). Columns give a late 5th century construction date (b). Collapsed arch fragments indicate a destruction of the building by earthquake influence (c). The basilica is covered by thick sandy deposits (d), incorporating abundant gravel (e), ceramic fragments (f) and Holocene marine macrofossils (g) that prove a marine origin of the sediment. Signs of soil formation within the allochthonous deposits prove long-time stable post-sedimentary conditions (f, dotted line). Archaeological findings like ***(p.t.o)***

(continuation) an in situ threshold (h) or plaster decorations (d, inlay) document that the foundation level is identical with the former ground level. A former threshold (i), re-used as door lintel after the destruction of the basilica, indicates the abrupt sedimentary burial in historical times.

well as the lack of fluvial systems, it can definitely be excluded that the remains of the building were buried during or after recent archaeological excavations or by alluvial sedimentation from the landward side. In the uppermost decimetres, the mixed terrigenous and marine sedimentary cover shows clear signs of weathering and soil formation (Fig. 4.7f, dotted line) indicating a longer time period of stable ecological conditions after deposition. Finally, several architectural features document that the building must have been rapidly buried shortly after or simultaneously to its collapse. First, the above mentioned plaster decoration along the outer walls proves that the brickwork was originally exposed to sight, thus attesting a lower ground surface for ancient times. Second, an in situ threshold encountered in the eastern part of the basilica (Fig. 4.7h) documents the foundation level to be the original ground surface during the buildings construction period. Third, a former door lintel was found that had been re-used as threshold at some point in time after the destruction of the building close to the northeastern corner (Fig. 4.7i). This archaeological observation reflects an early phase of repair during which the walking level was already elevated by 1.5 to 2 m to its present day level. The overall good preservation state of the inner basilica as well as delicate, well preserved plaster decoration of arch fragments document that the building and its inventory were not subject to mid- or even long-lasting erosion, abrasion and reworking effects but were strongly hit by a massive impulse and rapidly buried by event deposits.

Considering the geomorphological, geoarchaeological and sedimentary findings as well as the archaeological observations, it must be assumed that (i) the entire basilica was buried by one single event of high-energy character. (ii) The burial most probably occurred simultaneously to the collapse of the building and was obviously triggered by an impulse from the seaside as documented by the overall marine character of the covering deposits. (iii) A time frame for the high-energy impact is given by archaeological evidence, suggesting a 6th century AD date for the event.

4.5.2 Dredge mounds

The present day topography of the Lechaion harbour site is dominated by large sediment mounds directly adjacent to the entrance channel and eastern inner harbour basin (Fig. 1d). These mounds reach heights up to 15 m a.s.l. and were described in literature as natural dune formation or sediment obtained from dredging activities (Leake 1930, Rothaus 1995).

The mounds mainly consist of sand and gravel but incorporate also abundant ceramic fragments and marine macrofossils. It goes without saying, that grain size and sediment composition cannot be explained by natural dune formation. Further, their sedimentary composition is identical with the high-energy deposits burying the remains of the 5th century AD harbour basilica. However, the encountered coarse-grained sediments do not correspond to typical harbour deposits. Dredging in the quiescent environment of a harbour basin usually implies the removal of predominantly fine-grained homogeneous sediments to prevent the basin from silting up (Lehmann-Hartleben 1923, Marriner & Morhange 2007). It is thus concluded that the material of the dredge mounds reflects exceptional dredging after the well-protected harbour basin of Lechaion was affected by the massive input of marine gravel, sand and shells during a high-energy impact.

4.6 Spatial distribution of high-energy traces

4.6.1 Electrical resistivity tomography

The western part of the Lechaion harbour site is dominated by a plateau-like relief into which the serpentine structure of the inner harbour basin is incised by ca. 2 m (Fig. 4.1f). All over the surface of the higher ground, abundant gravel and marine molluscs as well as numerous ceramic fragments and even column drums are visible – the deposits thus being identical to the sediments burying the basilica and those building up the dredge mounds.

Electrical resistivity measurements were carried out along 5 transects in order to verify the landward extent of the high-energy deposit. South of the basilica, LEC ERT 1, 2 and 3 are radially orientated (SE-NW, E-W, NE-SW) and run from the plateau-like higher ground into the harbour basin. Transect LEC ERT 4 follows the inner harbour basin at a lower elevation in NW-SE direction whereas LEC ERT 5 runs across the plateau-like higher ground in perpendicular orientation to the coastline (N-S). In this study, results are presented from two ERT transects representative for the study area. Fig. 4.8a and Fig. 4.8b illustrate simplified model resistivity sections obtained for transects LEC ERT 2 and 5 in correlation with the schematic stratigraphy of vibracore LEC 3.

As visible in transect LEC ERT 5, the subsurface is clearly divided into two units. The upper unit is characterized by highest resistivity values (up to 1000 ohm.m) and extends at least 400 m inland. Reaching a maximum thickness of nearly 4 m in seaward direction, it can be clearly seen from Fig. 4.8a that the unit considerably thins towards inland. Along the entire transect, a sharp boundary separates this upper from a lower unit with very low resistivity values (0-30 ohm.m). In comparison with vibracore stratigraphy LEC 3, the highly conductive lower unit reflects both, the fine-grained harbour deposits as well as underlying marine sands and intercalating event layers described above (event generation I and II). Since vibracoring was only carried out inside the present-day harbour basin and not on the higher ground, the upper unit (event generation III) was not captured by the vibracore.

Transect LEC ERT 2 presents the landward elongation of LEC ERT 5, running from the higher ground into the harbour basin. While resistivity values remain high (up to 250 ohm.m) where the transect crosses the plateau, they abruptly decrease inside the harbour basin (0-30 ohm.m). Since similar results were achieved for transects ERT LEC 1 and 3, the massive high-energy layer characterizing the higher ground is obviously not preserved in the harbour basin itself. Hence, it is shown that today's visible harbour has just been excavated from a more or less closed cover of high-energy deposits in order to re-establish the navigability of the basin. The excavated material was then obviously heaped up in form of high dredge mounds.

4.6.2 Ground penetrating radar

In addition to electrical resistivity measurements, ground penetrating radar was applied to detect subsurface stratigraphic structures. Parallel to the coastline and perpendicular to LEC ERT 5, GPR measurements were carried out along three profiles across the higher ground (Fig. 4.8d).

The GPR data show that the upper sedimentary unit is characterized by strong internal undulations down to 1.5 m b.s. By interpolating between GPR profiles it turned out that the undulations document channel-like structures orientated in land-seaward direction. These channels seem to attest concentrated flow dynamics subsequent to the widespread burial of the harbour.

Hyperbolic effects in the profiles indicate that large blocks and boulders were deposited at the bases of the channels, while a more or less chaotic reflector pattern in the middle and upper parts of the profiles may be interpreted as a chaotic internal layering of the channel fill (for detailed description see KOSTER et al. 2013, this issue). Both features are evidence for high-energy flow dynamics. Due to the reduced measurement depth compared to the ERT approach and shadowing effects of the electromagnetic waves by the near-surface ground water table, the sharp contact between the upper and the lower unit as detected by ERT is not visible in the GPR data.

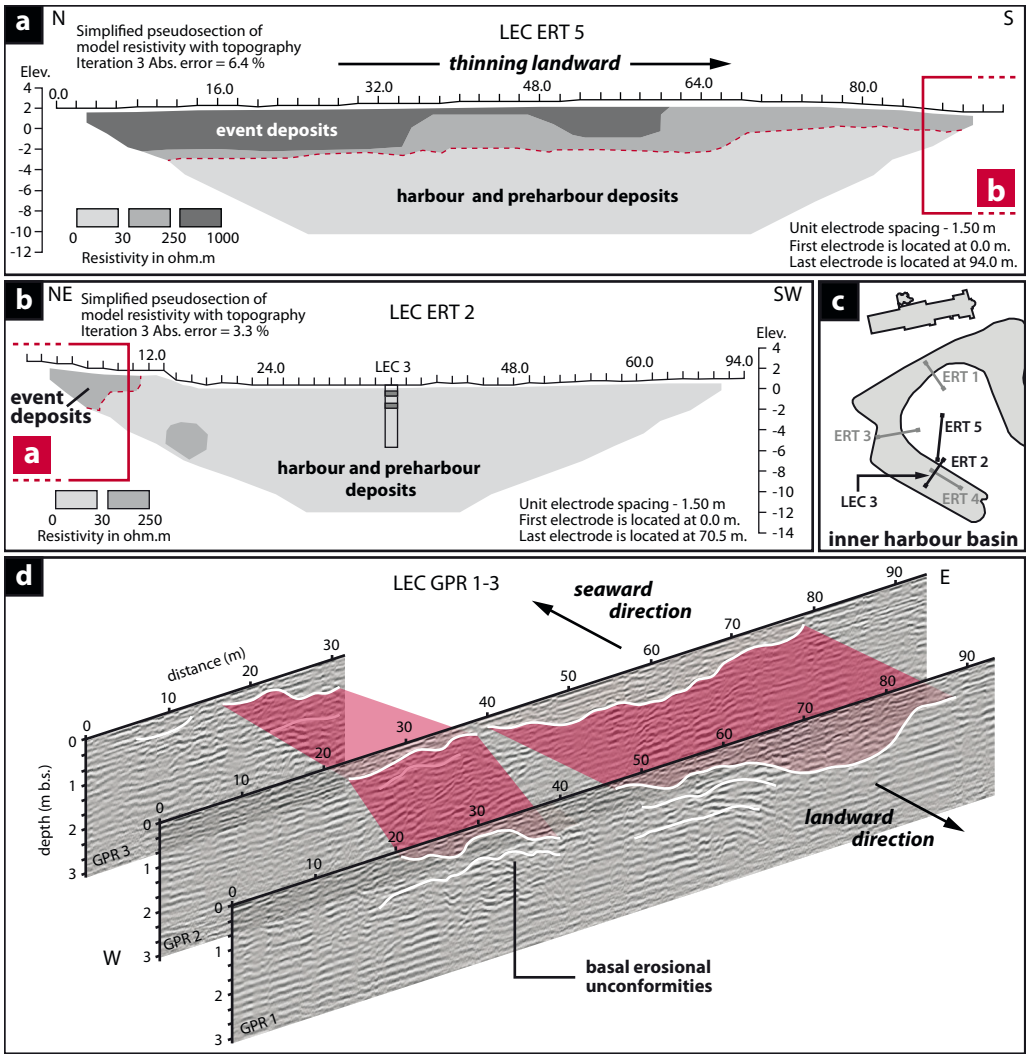

Fig. 4.8: Simplified pseudosections of modelled electrical resistivity values based on ERT measurements along transects LEC ERT 2 and LEC ERT 5 across higher grounds (a) and the inner harbour basin (b), respectively. ERT pseudosections document a sharp lower base and thinning inland of the event layer. Simplified ground penetrating radar profiles further reveal internal channel-like structures orientated in seaward direction (d). For location of vibracoring sites, ERT and GPR transects see inlay map (c) and Fig. 4.1a.

4.7 Geoarchaeological conclusions for the Lechaion harbour evolution

Using a multidisciplinary approach, extensive evidence for multiple high-energy impact was found. Therefore, the following scenario can be concluded for the Lechaion harbour site.

(i) As revealed by the local vibracore stratigraphy, the harbour of Lechaion was founded in a near-shore marine environment, probably by excavating an artificial harbour basin. The basin was enlarged at least once during its utilization.

(ii) Derived from an event stratigraphical approach, the area was hit three times by high-energy impact triggered from the sea side. The oldest event occurred prior to the harbour foundation (generation I), probably altering the coastal geomorphology. A second event affected the active harbour (generation II). The youngest event coincides with the abandonment of the site (generation III), but is only locally preserved in the present day harbour basin (core LEC 3).

(iii) In addition to the harbour stratigraphy, geoarchaeological observations, ERT and GPR measurements document a final widespread burial of the harbour area by high-energy impact of marine origin. The deposits are related to the youngest event layer encountered in vibracore LEC 3. Geoarchaeological evidence provides a 6th century AD date. Sedimentary evidence from the ancient basilica and adjacent area prove a marine origin of the event deposit as does the clear thinning landward, apparently induced by inland decreasing transport capacity of a sea-borne inundation. A subsequent erosive backflow is attested by the internal channel structures orientated in seaward direction.

(iv) The atypical sedimentary composition of dredge mounds adjacent to the entrance channel reflects dredging of high-energy deposits from the harbour basin. Regarding the fragmentary distribution of the youngest event layer inside the basin, the dredge mounds apparently originate from major post-event dredging activity rather than continuous cleaning of the harbour basin.

(v) It is thus concluded that the present day serpentine shape of the harbour basin must be regarded as a result of a latter harbour re-activation and does not necessarily correspond to the harbour basin that existed during Greek and Roman times.

4.8 Beachrock-type calcarenitic high-energy deposits in the harbour area

Along the coastline of the Lechaion Gulf, beachrock occurs at several locations close to the ancient harbour. West of the harbour, a massive beachrock complex extends 400 m along the beach, close to an industrial area. In seaward direction, the lower part of the outcrop extends below present sea level while the upper part is undercut by wave action and thus under erosion. Further inland, the upper beach is dominated by massive in situ beachrock which is intact and shows a sea-landward orientated mean inclination of 3°. It seems as if the beachrock continues towards inland, however, the area is covered by a road and an industrial zone. The thickness of the beachrock is estimated to be approximately 2 m, its upper edge reaching up to 1.30 m a.s.l. The Lechaion beachrock outcrop can be divided into a cemented lower and less consolidated upper unit. To the east of the harbour, the lower beachrock unit is represented by single large slabs surrounded by coarse beach deposits lying in shallow water. At various outcrops in the

immediate environs of Lechaion, sedimentary characteristics of the beachrock were observed that are atypical of beach deposits but rather indicate high-energy flooding impact (Fig. 4.9, VÖTT et al. 2010). The observations are as follows.

(i) At the entrance to the inner harbour basin as well as along the outer moles, patches of beachrock-type conglomerate are preserved. Cemented sand and gravel fill up the joints between man-made ashlar blocks. According to ROTHAUS (1995), this fill structure does not consist of ancient mortar but rather seems to be natural. The consolidated sand and gravel are interpreted as representative of post-depositionally cemented injection structures into an existing wall, i.e. the sediment was squeezed in between the blocks by high-energy wave impulse (Fig. 4.9e).

(ii) Close to the harbour entrance and adjacent to the dirt road along the beach, a natural cliff-like outcrop reveals clear layering, multiple fining upward sequences, imbrication structures and convolute bedding for the less consolidated upper unit of the Lechaion beachrock (Fig. 4.9d). The outcrop extends further towards the west where it passes over to the high-energy deposit burying the early Christian basilica (Sections 2.3 and 5.1). The beachrock is thus stratigraphically directly linked to the high-energy event deposit that buried both the basilica and the harbour site.

(iii) Additional evidence was found along the beach some 500 m to the west of the archaeological site of Lechaion. Here, a filled channel about 0.5 m deep and 3 m wide is currently undercut by a small cliff (Fig. 4.9c). While the lower cliff section is made up of in situ beachrock, the channel is part of the upper, less consolidated beachrock-type unit. The channel fill consists of a mixture of sand, gravel, marine shells, bone and ceramic fragments identical to the sedimentary composition described for the environs of the 5th century AD Lechaion harbour basilica. A thick fining upward sequence was found starting with large clasts at the bottom, some up to 15 cm in diameter, then passing over to gravel and finally sand at the top which suggests that the infill was rather due to a single event than to constant alluviation. It seems as if the channel exactly corresponds to those channel-type structures which were detected by GPR measurements in the harbour area (Fig. 4.8d). This site clearly shows that the beachrock along the coast is apparently part of the high-energy event layer detected in the harbour site.

(iv) Right in front of the industrial area, a cross section through the lower beachrock unit reveals a basal layer out of sand and imbricated gravel components which is unconformably overlain by two fining upward sequences deformed by convolute bedding and liquefaction (Fig. 4.9a, 4.9b). While the imbrication of gravel proves strong landward directed flow dynamics for the basal layer (SCHÄFER 2005), the sedimentary features of the upper layer clearly indicate liquefied or fluidized flow dynamics as attested for turbidity currents or sediments affected by seismic shocks (READING 1996, FÜCHTBAUER 1988). Completely atypical of a littoral environment, they are evidence of a short-term deposition of water-saturated sediments by high-energy flooding, obviously related to seismic activity.

In a summary, the Lechaion beachrock is part of the 6th century event layer that covers the early Christian basilica and wide parts of the harbour area. The beachrock must thus be regarded as cemented part of a corresponding high-energy deposit instead of lithified beach (VÖTT et al. 2010).

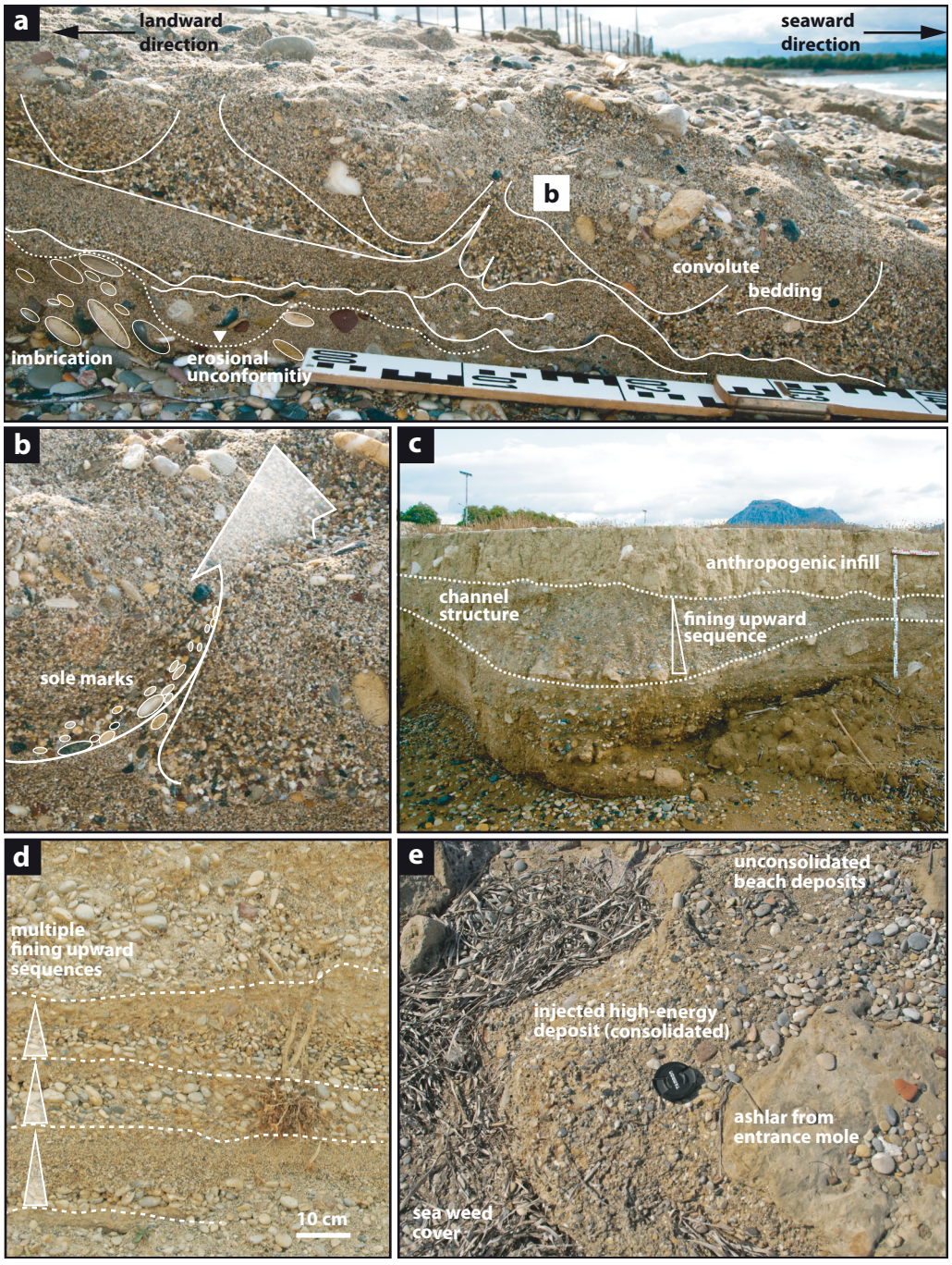

Fig. 4.9: Sedimentary characteristics of the Lechaion beachrock documenting tsunami flooding impact (Vött et al. 2010). A cross section through the lower beachrock unit reveals landward imbrication, liquefaction and convolute bedding (a, b). An erosive channel affecting the upper, less cemented beachrock unit (c) may be correlated to channel structures detected by GPR. The channel fill deposits are identical to high-energy deposits which were found widely burying the Lechaion harbour site. Multiple fining upward sequences close to the harbour entrance (d) pass over to the high-energy layer covering the Christian basilica. Injection structures (e) are visible along the moles at the harbour entrance.

4.9 Dating approaches

Within this study, 13 radiocarbon dates are presented and used as base to establish a local event-geochronostratigraphy (Tab. 4.1). Where possible, plant material instead of marine shells was selected for dating, because the spatio-temporal variability of the local marine reservoir effect is still unknown. In selected cases where sampling of marine shells was inevitable, articulated bivalve specimens were preferred to singular valves or shell fragments. This was done because articulated molluscs either died in situ or were transported alive and died during or shortly after deposition; thus they deliver the most reliable age estimate for the time of sediment deposition (Reimer & McCormac 2002, Donato et al. 2008).

A radiocarbon sandwich dating strategy was applied to time-bracket high-energy events that hit the harbour basin. Most dating samples were therefore taken from autochthonous deposits right above and/or below the event layer and not from the event layer itself in order to avoid dating of reworked material. In case it was not possible to date an event layer by the sandwich technique, best-fit solutions are suggested by cross-checking dates along the vibracore transect.

Sample LEC 1/7 PR2 yields a radiocarbon age of -220±15 BP indicating contamination with modern bomb ^{14}C. The age for sample LEC 1/7 PR2 (test) was obtained from an individual seed and constitutes the more reliable age for vibracore LEC 1. For samples LEC 3/3+ PR and LEC 1/8 PR is can be assumed that the young ages obtained are due to contamination of the sample by subrecent to modern roots. Both ages were thus excluded from further interpretation. As samples LEC 2/7 + PR, LEC 2/15+ PR and LEC 3/7+ PR consist of sea weed remains from marine aquatic environments, $\delta^{13}C$ values are much smaller than known from terrestrial plants and a marine reservoir effect was taken into account. An average marine reservoir age of 408 years is considered to calculate calendar ages for all samples of marine carbonate or marine $\delta^{13}C$ values using the Calib 6.0 software (Hughen et al. 2004, Reimer et al. 2004). Ages given in marine reservoir effect databases are still sporadic and do not consider variabilities in space (i.e. for different sedimentary environments in one and the same site) and time (i.e. for different time periods in the Holocene near-coast geological record of a specific site).

The comparison of marine and terrestrial ages from the lower unit of vibracore LEC 2 indicates a local reservoir effect slightly higher than applied. All ages retrieved from marine material must therefore be considered as maximum ages while the actual calendar age appears to be younger. Radiocarbon dates obtained from samples with $\delta^{13}C$ values typical for C3 land plants, especially wood fragments, are considered to be most reliable since reservoir effects can be excluded.

Radiocarbon dating was realised by the Radiocarbon Laboratory, University of California, Irvine (UCI) applying ^{14}C AMS. Ages inferred from other authors were carefully revised and recalibrated using the Calib 6.0 software.

4.10 Discussion

4.10.1 Tsunami events in the Lechaion Gulf

Complex geo-scientific research carried out in the ancient harbour at Lechaion revealed distinct evidence of multiple high-energy impact. Geoarchaeological findings together with geomorphological observations show that the youngest high-energy event which was trapped in the Lechaion sedimentary archive caused major devastation and the final abandonment of the harbour site.

Tab. 4.1: Radiocarbon dates of samples from the inner Lechaion harbour basin. Note: b.s. - below ground surface; b.s.l. - below sea level; Lab.No. – laboratory number; UCI - Radiocarbon Laboratory, University of California, Irvine; 1σ max;min (cal BP, cal BC/AD) - calibrated ages, 1σ range; ";" there are several possible age intervals due to multiple intersections with the calibration curve; * - marine reservoir correction with 408 years of reservoir age; a - contaminated sample, i.e. contains bomb 14C; b - δ13 value indicates aquatic plant material and a potential reservoir effect; unident. plant remain - unidentified plant remain; artic. spec. - articulated specimen; Cerastoderma gl. - Cerastoderma glaucum. Calibration based on Calib 6.0 software (Reimer et al. 2009).

Sample	Depth (m b.s.)	Depth (m b.s.l.)	Sample description	Lab. No. (UCI)	$\delta^{13}C$ (ppm)	^{14}C Age (BP)	1σ max; min (cal BP)	1σ max;min (cal BC/AD)
LEC 1/7 PR2	1.58	1.21	unident. plant remain	73821	-26,4 ± 0,1	-220 ± 15[a]	-	-
LEC 1/7 PR2 (test)	1.58	1.21	seed picked out of unident. plant remain	73836	not available	1575 ± 15	1516; 1415	434; 535 AD
LEC 1/8 PR	1.61	1.24	unident. plant remain	73822	-29,5 ± 0,1	170 ± 15	280; 7	1670; 1943 AD
LEC 1/11+ HR	2.63	2.26	wood fragment	73823	-28,5 ± 0,1	2025 ± 15	1993; 1949	44 BC; 0 AD
LEC 2/6 M	1.30	1.34	Cerastoderma glaucum, articulated specimen	73816	-1,1 ± 0,1	2285 ± 15	1925 - 1862	25 - 88 AD*
LEC 2/6+ HR	1.54	1.58	wood fragment	73824	-25,8 ± 0,1	1865 ± 15	1863; 1740	87; 210 AD
LEC 2/7+ PR	1.82	1.86	sea weed	73825	-15,2 ± 0,1[b]	2455 ± 20	2138 - 2057	189 - 108 BC*
LEC 2/9+ PR	2.50	2.54	unident. plant remain	73826	-27,8 ± 0,1	2565 ± 15	2741 - 2723	792 - 774 BC
LEC 2/15+ HR	4.79	4.83	wood fragment	73827	-25,7 ± 0,1	2505 ± 15	2712; 2511	763; 562 BC
LEC 2/15+ PR	4.74	4.78	sea weed	73828	-17,6 ± 0,1[b]	2995 ± 15	2779 - 2733	830 - 784 BC*
LEC 3/3+ PR	1.25	0.69	unident. plant remain	73829	not available	255 ± 15	305 - 293	1645 - 1657 AD
LEC 3/3+ M	1.28	0.72	Cerastoderma glaucum, articulated specimen	73817	-1,1 ± 0,1	2495 ± 15	2200 - 2107	251 - 158 BC*
LEC 3/3+ HR	1.53	0.97	wood fragment	73830	-25,1 ± 0,1	1950 ± 20	1924; 1877	26; 73 AD
LEC 3/7+ PR	2.48	1.92	unident. plant remain, probably sea weed	73831	-17,1 ± 0,1	5450 ± 20	5880 - 5791	3931 - 3842 BC*

The Corinthia coastal plain is generally characterized by a local drainage network out of several, more or less parallel torrential creeks flowing into the Lechaion Gulf. While modern Corinth is built on the Xerias river fan delta and thus is occasionally subject to flooding due to heavy rainfall, there is no torrential or other kind of alluvial system which affects the Lechaion harbour area. Moreover, high erosion rates as well as torrential flooding events are mainly restricted to side valleys further south and do not influence the coastal plain around Lechaion (Lekkas et al. 1991, Gatsis et al. 2001). By these facts alone, it can definitely be excluded that the harbour site was buried by alluvial deposits from the hinterland. Another decisive point, however, is that Holocene marine sediments and fossil fragments found incorporated in the Lechaion event sediments require sediment transport from the seaside and cannot be explained by alluvial dynamics. Finally, the ground surface rises in seaward direction documenting that the coastal topography and its sediments have been crucially controlled by impulse from the marine side.

Considering geomorphological and sedimentological features of the high-energy event deposits, all of them are well known from recent tsunami events. Basal erosional contacts have been attested for the IOT 2004 by various authors (e.g. Bahlburg & Weiss 2007). Gelfenbaum & Jaffe (2003) and Goto et al. (2011) report on fining upward sequences, incorporated rip-up clasts of older deposits as well as thinning landward of the 1998 Papua New Guinea and 2011 Japan tsunami deposits, respectively. The tsunamigenic input of marine microfauna to brackish-

lagoonal environs along the Japanese coast is documented by MINOURA et al. (1994), whereas DONATO et al. (2008) describe massive reworking of lagoonal muds by tsunami overflow in Oman.

However, many sedimentary features have also been attested for storm surges or tropical cyclones (MORTON et al. 2007). Tropical-like cyclones, so called Medicanes, occasionally occur throughout the Mediterranean. As a matter of fact, no Medicane is known to have ever directly affected the Gulf of Corinth (FITA et al. 2007, LUQUE et al. 2007, TOUS & ROMERO 2012). In the semi-enclosed Gulf of Corinth, local wind systems are dominated by winds from the E and the WSW with an average wind speed of 4 m/s during winter time. Although the wind direction coincides with the orientation of the Lechaion Gulf, average wave heights do not exceed 0.2 m (POULOS et al. 1996, SOUKISSIAN 2008). Due to the limited fetch of the gulf, winter storms are moderate and barely exceed the outer limit of the recent beach, as indicated by winter beach ridges and local small cliffs (von FREYBERG 1973, KORTEKAAS et al. 2011).

The negligible impact of winter storm events along the coast is also shown by the following facts. First, the beach zone in the Lechaion Gulf is pretty narrow and does hardly exceed widths of 20 m (Fig. 4.10a). Second, dwellings, industrial zones, hotels and camp sites have been built directly adjacent to the present day shore line (STEFATOS 2006) all along a stretch of almost 30 km with no considerable destruction of infrastructure by storm activity during the last centuries. From the analysis of tide-gauge records at Posidonia (Lechaion Gulf), extreme sea level values of 0.63 m and 0.66 m are expected to occur every 50 and 500 years, respectively (TSIMPLIS & BLACKMAN 1997). Thus, even strong storm surges are not capable of inundating the Corinthia coastal plain far inland, not to mention a fortified harbour.

Extensive high-energy deposits along the Lechaion coastline locally reach up to 400 m inland and are up to 2-4 m thick. Considering the prevailing conditions of wind and wave climate, these deposits cannot be explained by storm influence. With regard to the regional tectonic setting and considering the sedimentary features, the Lechaion high-energy event deposits rather are of tsunamigenic origin. It is thus concluded that the Lechaion harbour area has been repeatedly affected by tsunami events during its history. The present results show that the youngest tsunami caused the final destruction of the harbour facilities.

4.10.2 Beachrock-type calcarenitic tsunamites

The recent study by MOURTZAS et al. (2013) aims to reconstruct the palaeogeographical evolution of the outer harbour basin in relation to local sea level changes. The reconstruction of the relative sea level history by MOURTZAS et al. (2013) is, however, mainly based on beachrock as sea level indicator. A major problem is that the sedimentary and stratigraphical characteristics of the beachrock remain completely unconsidered.

As a consequence, MOURTZAS et al. (2013) postulate repeated phases of tectonic uplift and subsidence associated with major sea level fluctuations. This yo-yo type sea level evolution for Lechaion is in contrast to any geomorphological data from the region well known to be controlled by uplift movements (VITA-FINZI & KING 1985, PIRAZZOLI et al. 1995, KERSHAW & GUO 2001, ROBERTS et al. 2009). Since many years, there has been a controversial discussion on the doubtful use of beachrock as sea level indicator (KELLETAT 2006, 2007, KNIGHT 2007). Modern geomorphological and sedimentological beachrock studies in Greece have, moreover, provided evidence that the formation of beachrock is potentially linked to tsunami influence (VÖTT et al. 2010). In such cases, beachrock deposits are no reliable sea level indicators but rather document

the tsunami-related landward accumulation of littoral and marine deposits by high-energy impact in a specific coastal section (VÖTT et al. 2010, 2011b). As MOURTZAS et al. (2013) do not consider these issues, their sea level story as well as their palaeogeographical scenarions based on the yo-yo sea level curve are thus misleading.

Especially the Lechaion beachrock reveals many sedimentary features which document that it is the cemented part of a high-energy deposit rather than a simple cemented beach deposit (VÖTT et al. 2010). The present study further revealed strong stratigraphic correlations between tsunami deposits encountered in the Lechaion harbour and beachrock outcrops along the Lechaion coast. It is therefore conclude that the beachrock at Lechaion must be regarded as tsunamite and is out of the question to be used as reliable relative sea level indicator.

Sedimentary structures, similar to those described from the Lechaion beachrock, have been observed for consolidated as well as non-consolidated tsunami deposits. NANAYAMA & SHIGENO (2006), for example, describe imbricated gravel deposited by tsunami inundation during the 1993 Hokkaido tsunami. Since the liquefaction features described for the Lechaion beachrock require short-term interferences of water saturated sediments, it seems plausible to assume post-depositional deformation of tsunami deposits by aftershocks or further wave impact. However, in-situ liquefaction within lower parts of a water-saturated tsunamite due to dewatering can also be explained by the rapid and superimposed deposition of further tsunami deposits on top and infer convolute bedding structures (FÜCHTBAUER 1988, READING 1996).

It can be assumed that the sedimentary characteristics found in the upper, less calcified unit of the Lechaion beachrock are related to sediment deposition during tsunami backflow. Maximum sediment deposition by tsunami backflow of up to 80 cm thickness was, for instance, observed by BAHLBURG & SPISKE (2011) for the 2010 Chile tsunami. Strong backflow dynamics also explain the mixing of marine and terrestrial material during sediment transport encountered for the Lechaion tsunamite. Tsunami water backflow concentrated along topographic depressions as well as incision of erosive backflow gullies was observed by BAHLBURG & WEISS (2007) for the 2004 IOT and by BAHLBURG & SPISKE (2010) for the 2010 Chile tsunami. Further examples for beachrock-type calcified tsunamites are described for the western Peloponnese, the Ionian Islands and northwestern Greece (VÖTT et al. 2010). There, beach-rock type tsunamites revealed similar sedimentary characteristics such as fining upward sequences, load cast structures, incorporation of boulders or cemented ceramic fragments.

According to VÖTT et al. (2010), post-depositional alteration of tsunamites deposited in subaerial environments includes carbonate dissolution within the upper section of the tsunamite due to soil formation processes, subsequent downward transport of hydrogen carbonate by percolating water and final recrystallization within the lower part of the tsunamite and/or underlying substrates. Carbonate precipitation will occur around groundwater level or due to decreasing pore volume, leading to an increased incrustation (SCHEFFER & SCHACHTSCHABEL 2010, VÖTT et al. 2010). Due to carbonate dissolution by rainwater, the upper part of the tsunamite remains unconsolidated and undergoes advancing soil formation while the lower parts of the tsunamite experience a downward increase of carbonate cementation. The enrichment of calcium carbonate is also evident from the carbonate gyttja accumulated in the inner harbour basin at coring site LEC 2. Due to the ongoing relative sea level rise during the Holocene and wave action along the coastline the unconsolidated upper unit is subject to subsequent erosion whereas the well consolidated lower tsunamite section remains in situ and appears as beachrock along the Lechaion coast.

4.10.3 Establishing the Lechaion event-geochronostratigraphy

A local tsunami chronology is established for the harbour of Lechaion in order to estimate the magnitude and frequency of tsunami events for a better hazard assessment.

Tsunami generation I

Radiocarbon ages obtained for vibracore LEC 2 allowed consistent sandwich dating of tsunami generation I. While the lower sea weed meadow was dated to 830-748 cal BC and 763-562 cal AD, respectively (*termini post quos*, LEC 2/15+ PR, LEC 2/15+ HR), the upper lagoonal sediments yield a *terminus ante quem* for the tsunami event of 792-774 cal BC (LEC 2/9+ PR, Tab. 4.1). At the same time, the age obtains a *terminus ad quem* for the foundation of the ancient harbour. With regard to slightly overestimated ages of marine samples, the more reliable radiocarbon date of sample LEC 2/15+ HR indicates that tsunami generation I occurred between the early 8th and late 6th century BC, shortly before the harbour foundation.

The age of 44 cal BC - 1 cal BC/AD (LEC 1/11+ HR) obtained for the lower part of vibracore LEC 1 reveals insights into the harbour evolution rather than to the age of the underlying tsunami deposit. As the sample was taken from lagoonal deposits which still appear older and in higher elevations at site LEC 2 (Fig. 4.3), it is assumed that this date documents late 1st century BC dredging activities at coring site LEC 1 probably correlated to a latter expansion of the inner basin. For the underlying event layer, the given date merely attests a *terminus ante quem* prior to the deposition of harbour sediments. The lowermost tsunami layer at site LEC 1 correlates well with tsunami generation I deposits found at site LEC 2 and is thus assumed to belong to the same tsunami generation.

Tsunami generation II

Based on stratigraphical correlations, radiocarbon ages obtained along vibracore transect LEC 1 to 3 allow sandwich dating of event generation II.

The earliest in situ harbour deposits accumulated on top of tsunami generation II deposits at sites LEC 2 and 3 are dated to 87-210 cal AD (LEC 2/6+ HR) and 26-73 cal AD (LEC 3/3+ HR), respectively. The age inversion of sample LEC 2/6 M (25-88 cal AD) for younger harbour deposits at site LEC 2 is most probably caused by an underestimation of the marine reservoir effect. Radiocarbon dates obtained from cores LEC 2 and LEC 3 thus yield the time period 26-210 cal AD as *terminus ante quem* for tsunami generation II.

Sample LEC 3/7+ PR retrieved from the underlying unit of tsunamite generation II unfortunately yields a non-reliable age (3931-3842 cal BC, Table 4.1). Sample LEC 2/7+ PR (189-108 cal BC, Tab. 4.1) was taken from the event layer itself. The sample is supposed to have been considerably affected by re-working effects so that the retrieved age of 189-108 cal BC is regarded as *terminus post quem* (i.e. maximum age) and not as *terminus ad quem* for the event. Regarding core LEC 1, the upper event layer correlates well with tsunami generation II at site LEC 2 by sedimentary evidence. Assigning the average sedimentation rate of 0.15 mm/a found for the harbour unit at site LEC 2 to the harbour unit of core LEC 1, the late 1st or early 2nd century AD can be roughly estimated as *terminus ad quem* for the event. This goes well with radiocarbon dates presented above for sites LEC 2 and 3.

Tsunami generation III

Sediments of tsunami generation III were only found at site LEC 3. The lack of corresponding sediments at sites LEC 1 and 2 is assigned to dredging activities documented by a sudden change

from fully lagoonal to ephemerally limnic or hypersaline conditions. Tsunami event III can be time-bracketed by radiocarbon dates and geoarchaeological findings. The base of the upper lagoonal sequence found in vibracore LEC 1 was dated to 434-535 cal AD (Tab. 4.1) representing a *terminus ad* or *ante quem* for event III. This is in full accordance with ceramic fragments incorporated into the tsunami deposit as well as findings of coins found within the construction walls of the basilica documenting that the building was in use until the mid-5th or even early 6th century AD. Tsunami generation III must thus be dated to the late 5th or early 6th century AD.

4.10.4 Harbour evolution and tsunami impact

In the following, the event-geochronostratigraphy obtained for the Lechaion area os compared with the history of the harbour in order to evaluate the potential effects of tsunami impacts. Historical data is based on accounts of ancient writers and archaeological finds.

The foundation of Lechaion is generally associated to Periander, tyrant of Corinth from ca. 625-585 BC (Werner 1997). Since stratigraphical evidence and radiocarbon dates from core LEC 2 document oldest harbour deposits shortly posterior to event generation I (early 8th to late 6th century BC), the harbour environment seems to have been existing at least since Periander, probably earlier.

At site LEC 1, oldest harbour deposits were dated to the late 1st century BC. The age difference to the basal harbour sediments found at site LEC 2 apparently proves an expansion or cleaning of the Corinthian harbour, probably accompanied by dredging activity in the old harbour basin. These considerations seem plausible because historical accounts report on the re-activation of Lechaion during the Roman re-colonization of Corinth in 44 BC (Paus. 2.1.1 after Frazer 1965) and thus correlate well with the stratigraphical record.

From the 2nd to 5th century AD historical records about Lechaion are sparse. The age obtained for the upper lagoonal sequence of core LEC 1, dating to the 5th/6th century AD, however, may correlate with historic events. The harbour unit either postdates the major reconstruction and dredging of the harbour by Flavius Hermogenes from 353-358 AD (Kent 1966) or marks the re-excavation of the harbour basin after the devastating 6th century AD tsunami generation III. Neither the age range of the radiocarbon date nor the thickness of the lagoonal sedimentary unit allow a verification of the precise chronological order, though.

Considering a modern tsunami hazard assessment, it must be noted that historic tsunami catalogues do not mention a single tsunami event for the Corinthia (Hadler et al. 2012). However, the ancient harbour of Lechaion was repeatedly hit by major tsunami events. With a time lag of several centuries between major events and only one small event recorded for the 20th century AD (1981 earthquake series, Jackson et al. 1982), the tsunami hazard for the Lechaion Gulf seems to be strongly underestimated.

4.10.5 Previous studies in the light of new results from Lechaion

At Lechaion, co-seismic tectonic activity is evident from an uplifted bio-erosive notch visible along the walls of the entrance channel as well as along the quay south of the inner harbour basin (Fig. 4.1e).

Stiros et al. (1996) suggest single co-seismic uplift of the harbour site, since well-preserved, articulated fossils of *Lithophaga* sp. and *Lamellibranch* sp. were encountered in living position. A

continuous uplift would have caused shell destruction by constant wave action. By radiocarbon dating of two samples, Stiros et al. (1996) dated the co-seismic uplift to 340 ± 125 BC. In this study, for comparison reasons, all radiocarbon dates published by Stiros et al. (1996, Tab. 4.2) were recalibrated. To be on the safe side, Stiros et al. (1996) decided to retrieve control ages for each sample. Their results showed wide age discrepancies of at least 200 years for one and the same dated organism. Moreover, it is well known that dating rock-boring shells always goes along with an age overestimation as the animals incorporate old carbon from the hosting rock (Shaw et al. 2010). The revised Stiros et al. (1996) ages still cover a wide timespan from the early 5th to the late 1st century BC (Tab. 4.2). Assuming the youngest age to be the most reliable since it fits best the youngest mollusc die-off (*terminus ad/post quem*), the harbour site was not uplifted before the late 2nd to early 1st century BC as proposed by Stiros et al. (1996). Considering the obtained ages are not affected by an additional reservoir effect, the uplift would have occurred over a historical period (146-44 BC) between tsunami generations I and II, where the harbour was most probably abandoned after the Roman devastation of Corinth. Then, it has to be assumed that the event apparently would have had minor devastating effects on the harbour basin, since Lechaion was used well afterwards. Considering the obtained ages need to be corrected for an additional reservoir effect which can theoretically by as high as 2000 or so years (Shaw et al. 2010), it cannot be excluded that the co-seismic uplift was caused by the same seismic event that triggered tsunami generation II or III.

A second notch along the eastern mole of the outer harbour basin is described by Mourtzas et al. (2013) and interpreted as second uplift, but not mentioned by other authors (e.g. Rothaus 1995, Stiros 1996). Regarding the explicit W/NW exposition of the notch, it seems to be rather related to wave breaking dynamics and should not be interpreted as reliable indicator for the evolution of the local relative sea level.

The palaeogeographical scenarios for the late to post Roman harbour site given by Mourtzas et al. (2013) are highly questionableas they are based on relative sea level data derived from beachrock. Beachrock, however, is not an adequate and reliable sea level indicator.

New results on the harbour evolution are presented by Morhange et al. (2012) who recovered two sediment cores from the inner Lechaion harbour basin, one of which was analysed in detail (core 1). The stratigraphic pattern as well as the radiocarbon ages from core 1 (Morhange et al. 2012: 280f.) bear strong analogies to the stratigraphical and chronological record of vibracore LEC 2. The depth level of the early Corinthian harbour deposits described by Morhange et al. (2012) corresponds well to basal harbour deposits encountered at site LEC 2. A radiocarbon age of 729-414 cal BC (Lyon-2312 Oxa, Tab. 4.2) obtained from the sub-harbour unit provides a suitable *terminus post quem* for the harbour foundation which reasonably fits with LEC 2/15+ HR age of 763-562 cal BC (Tab. 4.1). At the same time, the date connects the sedimentary unit to tsunami generation I, dated to the early 8th to 6th century BC (Tab. 4.1).

Grain size distribution data presented by Morhange et al. (2012) for core 1 shows that coarse-grained material (gravel), atypical of harbour environments, was deposited in the harbour basin at a depth level equal to tsunami generation II. Morhange et al. (2012) further obtained a *terminus ante quem* for the coarse-grained unit of 88-215 cal AD (Tab. 4.2) which is in excellent accordance to the *terminus ante quem* obtained from tsunami generation II in this studies: 26-210 cal AD.

The upper unit of core 1 was dated by MORHANGE et al. (2012) to 900-1017 cal AD, providing a *terminus ante quem* for the abandonment of the harbour basin that corresponds well to historical and geoarchaeological evidence presented above. At the same time, the date proves the existence of a sheltered water body for the 10th century and thus limits the post-tsunami re-excavation of the harbour basin to a time period between the 6th and late 10th century AD.

MORHANGE et al. (2012) regard the active harbour site as an efficient sediment trap where tectonic uplift along with the serpentine shape of the inner basin caused increased siltation. The unfavourable setting eventually contradicts a long-term harbour use and causes the abandonment of the site (MORHANGE et al. 2012). This assumption is however in contrast to the almost continuous use of the harbour for one millennium, attested by historical reports.

Moreover, the present results indicate that the serpentine shape of the harbour basin does not correspond to the Corinthian or Roman harbour but is formed by post-tsunamigenic re-excavation. Consequently, the present-day appearance does not verify above-average sedimentation rates in ancient times. Additionally, the long-term use of Lechaion as a harbour rather supports manageable siltation dynamics of the basin.

The same scepticism is associated to effects of tectonic movements in the area as evaluated by STIROS et al. (1996) and MORHANGE et al. (2012). In case of co-seismic uplift, the harbour as local base level of erosion will be suddenly uplifted so that siltation rates consequently decrease rather than increase. A strong tectonic uplift would explain a land locking of the harbour but not the sedimentary infill in the harbour basin during or after the uplift.

Based on the presented arguments, it is concluded that neither continuous siltation nor a tectonic uplift apparently caused a considerable threat to the harbour and are therefore not responsible for the final abandonment of the site as proposed by MORHANGE et al. (2012). Stratigraphical data, sedimentological features and event-chronological correlations rather support the idea that repeated tsunami landfall caused the abandonment of the harbour at Lechaion.

Tab. 4.2: Recalibrated radiocarbon dates from STIROS et al. (1994) and MORHANGE et al. (2012). Note: a.s.l. - above sea level; 1σ max;min (cal BP, cal BC/AD) - calibrated ages, 1σ range; ";" there are several possible age intervals due to multiple intersections with the calibration curve; # - calibrated age with marine reservoir correction of 320±25 years, 2σ range; + - calibrated age according to REIMER et al. (2009), 2σ range; * - marine reservoir correction with 402 years of reservoir age. Recalibration based on Calib 6.0 software (REIMER et al. 2009).

Sample	Depth (m a.b.s.)	Description	Reference	^{14}C Age (BP)	Published age	1σ max;min (cal BC/AD)
Gif-A-90SS4-A	0.70	*Lamellibranch*	STIROS et al. (1996)	2530 ± 90	560-100 BC#	361-147 BC*
Gif-A-90SS4-B	0.70	*Lamellibranch*	STIROS et al. (1996)	2400 ± 45	340-50 BC#	151-24 BC*
Gif-A-91LE1-A	0.70	*Lithophaga*	STIROS et al. (1996)	2620 ± 50	600-340 BC#	403;260 BC*
Gif-A-91LE1-B	0.70	*Lithophaga*	STIROS et al. (1996)	2430 ± 50	360-70 BC#	184-43 BC*
Gif-A-92LE1	1.20	barnacles	MORHANGE et al. (2012)	2470 ± 45	330-46 BC+	245-90 BC*
Lyon-2378 Oxa	- 0.80	charcoal	MORHANGE et al. (2012)	1070 ± 35	895-1022 AD+	900;1017 AD
Lyon-2379 Oxa	- 1.80	wood	MORHANGE et al. (2012)	1860 ± 40	66-242 AD+	88;215 AD
Lyon-2312 Oxa	- 2.40	charcoal	MORHANGE et al. (2012)	2440 ± 30	752-407 AD+	729;414 BC

4.10.6 Tsunami impact in the wider area

In this study, evidence of repeated high-energy flooding of tsunamigenic origin is presented which affected the Lechaion harbour site. Since tsunami impacts may have a regional character, palaeotsunamis traces were also searched for offsite the Lechaion harbour area.

Outcrops at modern Corinth

About 5 km to the east of the ancient harbour, cliff-like outcrops exist along the road to modern Corinth. Today, these outcrops are concealed by modern buildings, but VON FREYBERG (1973: 145) mapped two profiles along the cliff that exposed a 0.80 m thick "conglomerate, well stratified, with brick cobbles" obviously overlying Corinthian marls with an erosional unconformity. Further west, another outcrop reveals, "gravel and sand layers with multiple cyclical alterations; with ceramic sherd", covering a coarse-grained conglomerate (VON FREYBERG 1973: 145). The sedimentary characteristics clearly speak for a tsunamigenic nature of the deposit; as similarities with the Lechaion beachrock and cliff sections are obvious there might be even stratigraphic correlations. From a sedimentological point of view, the outcrops interpreted by VON FREYBERG (1973: 145) as "Holocene terrace" apparently represent tsunamigenic deposits that most probably correlate to the devastating 6th century AD tsunami generation III.

The ancient diolkos

At the western entrance to the Corinth Canal, beachrock outcrops occur at the immediate coastline along both sides of the canal. Remaining at the same topographic level, this beachrock complex extends at minimum 300 m inland (Fig. 4.10b) and covers the paving stones of the ancient ship slipway, called *diolkos* (Fig. 4.10d). Another older beachrock compex lies severall decimetres below the *diolkos* pavement and can be traced up to 200 m inland. In places, ceramic fragments are incorporated into the beachrock (Fig. 4.10e).

Several authors (e.g. MOURTZAS & MARINOS 1994, PIRAZOLLI 2010) describe the beachrock as lithified beach and indicator for sea level changes. The constant height of the beachrock over hundreds of meters speaks against considering the unit as cemented in situ beach deposits. This is all the more true because relative sea level fluctuations would result in beach deposits at variable topographic levels. Compared to recent geomorphodynamics along the Corinthian coast (Fig. 4.10a), the beachrock additionally exceeds the maximum extension of the recent beach or storm wave activity (ca. 20 m) by far. Sedimentary characteristics comprise multiple fining upward sequences from gravel to sand as well as a landward imbrication of gravel (Fig. 4.10c). These features definitely exclude a seaward directed flow and/or sediment deposition by fluvial processes. Like the Lechaion beachrock, the *diolkos* beachrock is also subdivided into two units. Only the lower unit is calcified while the upper part is merely consolidated and thus subject to continuous erosion. By comparing the sedimentological criteria from both sites and with regard to the lateral extension, the *diolkos* beachrock must likewise be interpreted as a high-energy tsunamigenic deposit subject to post-depositional calcification.

As the beachrock-type calcarenite overlies the ancient slipway, the *diolkos* allows determining a *terminus post quem* for the high-energy event. Since the construction of the *diolkos* is assigned to Periander and historical accounts report that the slipway was in use until the 1st century AD, the age of the beachrock is about 2000 years or younger. Thus, tsunami generations II (1st-2nd century AD) and III (early 6th century AD) are suitable candidates potentially responsible for the sedimentary burial of the *diolkos*. Furthermore, the young age of the tsunami deposit obtained

by indirect archaeological age estimation again emphasizes the obviously rapid and extensive formation of beachrock by percolation already reported from other regions in the eastern Mediterranean (see VÖTT et al. 2010).

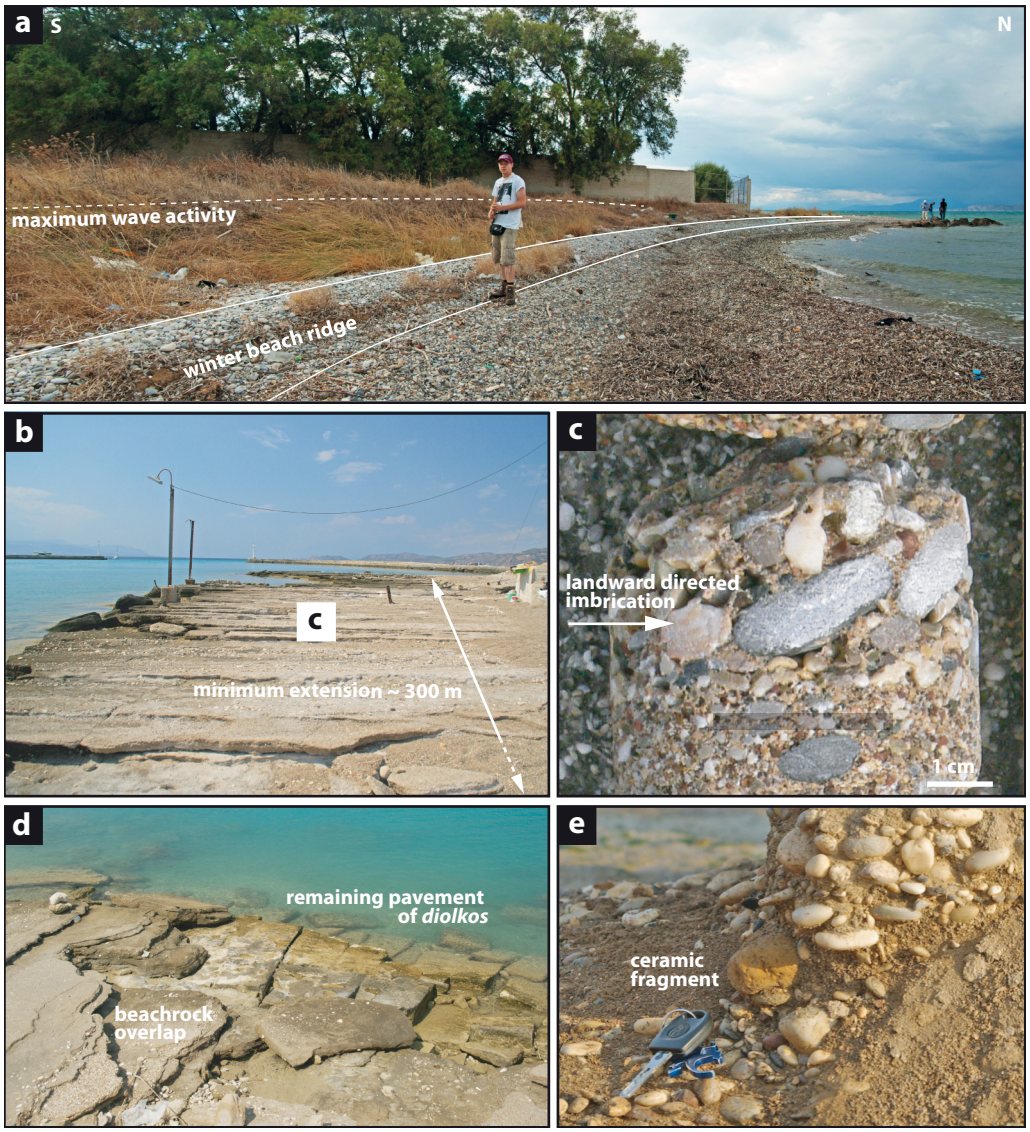

Fig. 4.10: Beachrock-type calcarenitic tsunamites at the ancient diolkos. While storm activity does not exceed the recent beach (a), beachrock-type tsunamites encountered at the western entrance of the Corinth Canal reach at least 300 m inland in a constant topographic level (b). The internal structure reveals landward imbrication of gravel (c). Covering the ancient diolkos, the beachrock-type tsunamite shows a maximum age of 2000 years (d). In some places, the cemented tsunami deposit incorporates ceramic fragments (e).

4.11 Conclusions

Based on complex and interdisciplinary geo-scientific investigations in the harbour of ancient Corinth at Lechaion by using geomorphological, geoarchaeological, sedimentological, geochemical, palaeontological and geochronological methods, the following conclusions can be made.

(i) Stratigraphical and geochronological data from the Lechaion harbour basin document that the harbour was in use at least from the early 6th century BC onwards until the 6th century AD. This is in good accordance with historical accounts.

(ii) Local stratigraphies show that the coastal region around Lechaion has been repeatedly affected by high-energy allochthonous marine sediment input and major reworking of autochthonous deposits during the past three millennia. Based on sedimentological, geomorphological and geoarchaeological evidence, these impacts are of tsunamigenic origin.

(iii) Three different generations of tsunami events were distinguished. The oldest tsunami impact (generation I) was dated to the 8th to 6th century BC and affected the area prior to the foundation of the harbour. Tsunami generations II and III hit the harbour basin in the 1st/2nd century AD and the 6th century AD, respectively. The latest event obviously caused the massive sedimentary burial and destruction of the harbour and the adjacent early Christian basilica.

(iv) The present-day shape of the harbour basin at Lechaion is the result of post-tsunamigenic dredging activities as indicated by stratigraphical evidence and dredge mounds adjacent to the harbour basin. Thus, today's serpentine configuration of the inner harbour basin does not reflect the original shape and size of the ancient harbour which has to be considered much larger. However, further fieldwork is necessary to determine the exact dimensions and geoarchaeological history of the former harbour.

(v) Beachrock outcrops near Lechaion as well as in the immediate environs of the *diolkos* at the Corinth Canal represent the lower part of a post-depositionally cemented high-energy deposit directly related to the tsunamigenic destruction of the harbour and the early Christian basilica in the 6th century AD age. The *diolkos* beachrock proves tsunamigenic impact for the wider area of Lechaion that is less than 2000 years old.

5. Palaeotsunami impact on the ancient harbour site of Kyllini (western Peloponnese, Greece) based on a multi-proxy approach

Abstract Geo-scientific and geoarchaeological studies carried out at the ancient harbour site of Kyllini (western Peloponnese, Greece) revealed distinct evidence of repeated tsunami landfall. Located in the westernmost part of the Peloponnese, the Kyllini harbour site is situated at a narrow stretch of coastal lowland along the northeastern edge of Cape Kyllini. Directly exposed to the Ionian Sea and the Hellenic Trench, the harbour holds a considerably high risk for tsunami events and thus represents an important site for palaeotsunami research. While the inner harbour basin is merely preserved as a near-coast swamp, partially submerged installations like moles, quays, breakwaters and towers clearly define the outer harbour basin. Geo-scientific studies carried out at the Kyllini harbour site comprised on-shore and near-shore vibracoring, sedimentological, geochemical and microfossil analyses of the recovered sediments as well as electrical resistivity measurements. The overall geochronological framework is based on radiocarbon dating of biogenic material and age determination of diagnostic ceramic fragments. The stratigraphical record of the harbour site reveals an autochthonous pre-harbour marine embayment on top of Pliocene bedrock. Following a first generation of high-energy impact, a coastal lake established that was then developed into an ancient harbour basin and fortified by man. Following a period of siltation, the harbour sequence is abruptly overlain by a massive layer of coarse grained marine sand, indicating a sudden high energy impact to the harbour site. Partly preserved as geoarchaeological destruction layer and post-depositionally cemented, the layer forms beachrock-type calcarenitic tsunamites. The present results suggest that the harbour site of Kyllini affected by tsunami impact in between the late 7th and early 4th cent. BC and between the 4th and 6th cent. AD. The younger event is associated with the final destruction of the harbour.

5.1 Introduction

Induced by the collision of the African and European lithospheric plates, the eastern Mediterranean and especially Greece belong to the seismo-tectonically most active regions worldwide. Along the Hellenic Arc, where the northward moving African Plate is being subducted under the Aegean microplate, movement rates reach up to 40 mm/a (Hollenstein et al. 2008a). As a result, strong earthquakes occur with high frequency and are a well-known factor for triggering tsunamis (Papazachos & Dimitriu 1991). Throughout the eastern Mediterranean, the tsunami hazard belongs to the highest worldwide since large water depth, narrow shelf zones and short distances from shore to shore encourage major events (Tselentis et al. 2010). Concerning western Greece, coastlines that are exposed to the Hellenic Arc must be considered as particularly threatened by tsunami hazard. Accordingly, geo-scientific studies provide convincing evidence, that coastal areas along the Ionian Islands or the western Peloponnese have repeatedly been affected by major tsunami events (e.g. Vött et al. 2009a, 2009b, 2011a, Röbke et al. 2013, Willershäuser et al. 2013, Scheffers et al. 2008).

Historic accounts such as the one by Ammianus Marcellinus, who reports on the 365 AD tsunami, repeatedly describe tsunami impact along the Peloponnesian shores (Amm. Mar. 26.10.15-19 after Rolfe 1940). Compared to adjacent areas, however, the historical record especially for the northwestern Peloponnese is sparse and merely comprises younger events and/or those that

had more or less devastating effects on larger settlements (Hadler et al. 2012). In order to better assess the hazard potential of an area and to prepare for future events, it is however inevitable, to gather sufficient data on the frequency and effects of palaeotsunami events. Investigations on recent tsunami impacts (e.g. Japan 2011) revealed that areas once affected by palaeotsunami impact are highly prone to future events (Goto et al. 2011). Thus, to better understand the historically known tsunami risk for an area, it is necessary to fill in the gaps in the historical record by geo-scientific studies.

In this respect there is the need to search for geo-archives that show high-quality and preferably complete conservation of sedimentary traces of previous events. Ancient harbour basins have turned out to be such suitable geo-archives since they provide sheltered and quiescent near-coast environments that act as efficient sediment traps for tsunami deposits.

With regard to the tsunami hazard of the northwestern Peloponnese and to allow a reliable risk assessment and mitigation strategies, the main objectives of the study were (i) to establish a stratigraphical record for the Kyllini harbour site in order (ii) to decipher potential palaeo-tsunami impacts and (iii) to assess their effects on the ancient settlement as well as on the coastal evolution. Concerning geoarchaeological aspects, we additionally aimed at (iv) reconstructing the evolution of the harbour site through space and time and (iv) correlating geoarchaeological data on the harbour evolution with archaeological findings and historical reports.

5.2 Natural setting and geoarchaeological background

The Kyllini peninsula is the westernmost promontory of the entire Peloponnese. Adjacent to the headland, the Gulf of Kyllini and the Chelonitis Gulf extend to the north and south, respectively, while the Strait of Zakynthos bounds the peninsula to the west (Maroukian et al. 2000). The hilly landscape of the area consists of alternating Pliocene marine, brackish and freshwater deposits that are uplifted by salt diapirism since the Miocene (IGME 1969, Kowalczyk & Winter 1979). The headland is connected to the mainland of the Peloponnese by the low-lying floodplains of the Peneios river, consisting of Holocene alluvial deposits (IGME 1969, Raphael 1973, Maroukian et al. 2000).

The ancient harbour of Kyllini is located at the northernmost point of the Kyllini Peninsula, directly adjacent to the modern village and harbour (Fig. 5.1). Remains of a medieval fortress are located on top of the bedrock ridge to the southwest of the harbour. At several locations along the coastline, dune fields and beachrock-type consolidated sediments occur (IGME 1969, Mariolakos et al. 1991). Annual accumulation and erosion of seaweed lead to rapid changes in the coastal constellation. To the northwest of the harbour, high cliffs with narrow beaches face the Ionian Sea. Since dominating wave dynamics easily erode the poorly consolidated soft Pliocene rocks, the recent cliff retreat is fast and already affects the ancient fortress, as documented by fallen wall fragments scattered at the foot of the cliff (Fig. 5.2d-f., Maroukian et al. 2000).

Due to the topographic constellation (Fig. 5.1), Kyllini has been a favourable strategic spot for a long time. While only few locations along the coastline of the western Peloponnese provide a sheltered anchorage for ships, the sheltered embayment at Kyllini offers both a well defendable settlement site and a protected harbour which, by archaeological and literary evidence has been used at least since the 5th century BC.

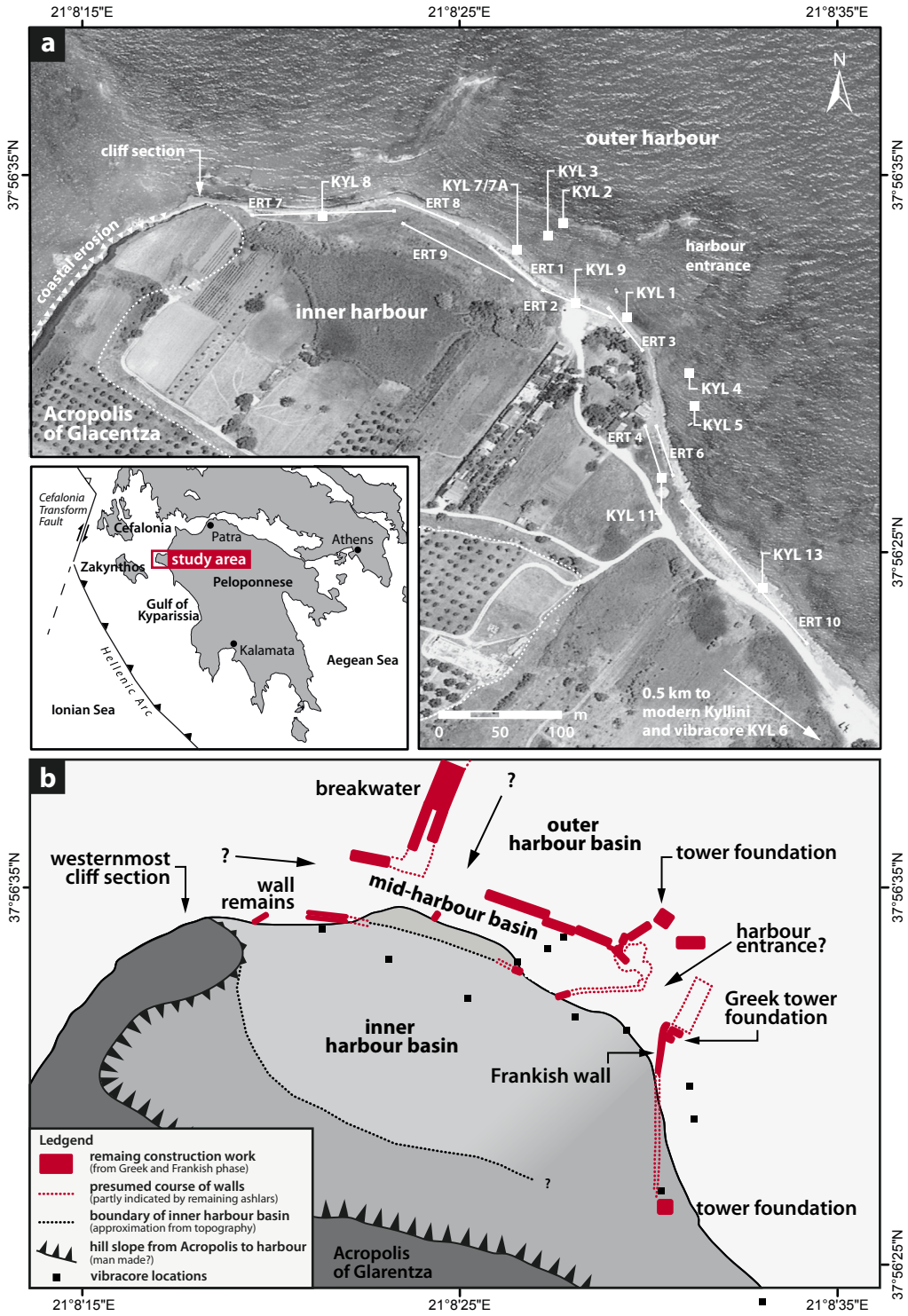

Fig. 5.1: Overview of the Kyllini harbour site including locations of vibracores and ERT transects (a) as well as archaeological remains of the Classical and Frankish harbour (b). The local topography provides sheltered conditions and makes the site a favourable anchorage. Maps modified after Google Earth 2009 and MORGAN 2009.

5.2.1 Historical accounts on the Kyllini harbour site

The ancient harbour of Kyllini belongs to the territory of Elis that was controlled by the powerful eponymous poleis. Among others, Elis held the sanctuary of Olympia and thus hosted the Olympic Games (Hansen & Nielsen 2004). The ancient and the Frankish Kyllini, named Glarentza, are well known from archaeological finds of coins that come from the Hellenistic to Roman and from the Medieval period, respectively (EBA 2005).

While *Κυλληνιον* is already mentioned in Homer's Iliad (Hom. 15.515 after Murray 1924), Thukydides is the first to report on the Classical harbour in the mid-5th cent. BC when it was burned by the Corcyrans for the Eleans supported the Corinthians with ships and money (Thuk. 1.30 after Landmann 2010, Gehrke & Schneider 2006). According to his descriptions, Kyllini was the main shipyard of Elis, which implies a harbour of already considerable size with shipsheds. Also, the harbour facilities must have been strongly fortified since Thukydides denotes the port as *επινειον* (engl. *epineion*, Servais 1961, Thuk. 1.30 after Jones & Powell 1942).

During Classical to Hellenistic times, city and harbour maintain their significant strategic role, still being one of only few locations along the western Peloponnesian shoreline that *"affords ships a suitable anchorage"* (Strabo 8.3.4. after Jones 1927). As a consequence, it is quite often affected by military conflicts. The harbour is repeatedly mentioned (429 BC, 427 BC) as the naval base for the Spartan fleet during the Peloponnesian War (431-404 BC, Thuk. 2.84/86, 3.69 after Landmann 2010). In 398 BC, in order to end the war between Elis and Sparta, the Eleans *"agreed to tear down the walls of Phea and Cyllene"* (Paus. 3.8.5 after Jones et al. 1918, Xen. 3.2.30 after Brownson 1921, Servais 1961). During the 3rd war of the Diadochi, however, Kyllini must have been fully restored. Diodorus Siculus reports that it was repeatedly under siege (314 BC, 312 BC) or recovered by the rivalling Diadochs (Diod. Sic. 19.66.1/2, 19.87.3 after Geer 1954, Servais 1961, Gehrke & Schneider 2006). About a century later, prior to the 1st Macedonian War, the Eleans were "*carefully strengthening*" Kyllini against the threat of being besieged by the Macedonian king Philipp V (Polyb. 4.9.1, 5.3.1 after Paton 1922, 1923), which potentially includes another reinforcement of the fortification walls. Titus Livius, who reports 15 Roman ships and four thousand armed man landing at Kyllini in 208 BC during the 1st Macedonian War, underlines the significant role of Kyllini in ancient warfare (Tit. Liv. 27.32 after Edmonds 1850, Servais 1961). As the major port for Elis, it must also be assumed that the harbour of Kyllini also served as a landing for a great number of spectators visiting the Olympic games (Hansen & Nielsen 2004, FIA 2013).

In Roman times, historical accounts of Strabo and Pausanias still refer to Kyllini as *επινειον*-type naval station of Elis but also note a considerable trading activity (Pausanias 6.26.4-5, 8.6.8 after Jones et al. 1918, Strabo 8.3.5 after Jones 1927, Gehrke & Schneider 2006, Ptol. 3.14.30 after Stückelberg 2006).

For about one millennium, not much is known about Kyllini. It was not before the early 13th century AD, that the site came under Frankish possession and the castle of Glarentza was built (Traquair 1906/07, Bon 1969). The ancient harbour facilities were partly re-established as demonstrated by ancient Greek foundations below Frankish walls (Pakkanen et al. 2010). Under the Frankish Rule, Kyllini (Glarentza) became the *"first town in Achaia"* (Traquair 1906/07: 276). For about two centuries, Kyllini was a flourishing harbour of major economic and strategic importance (Bon 1969, EBA 2006). At the beginning of the 15th cent. AD, however, Glarentza was

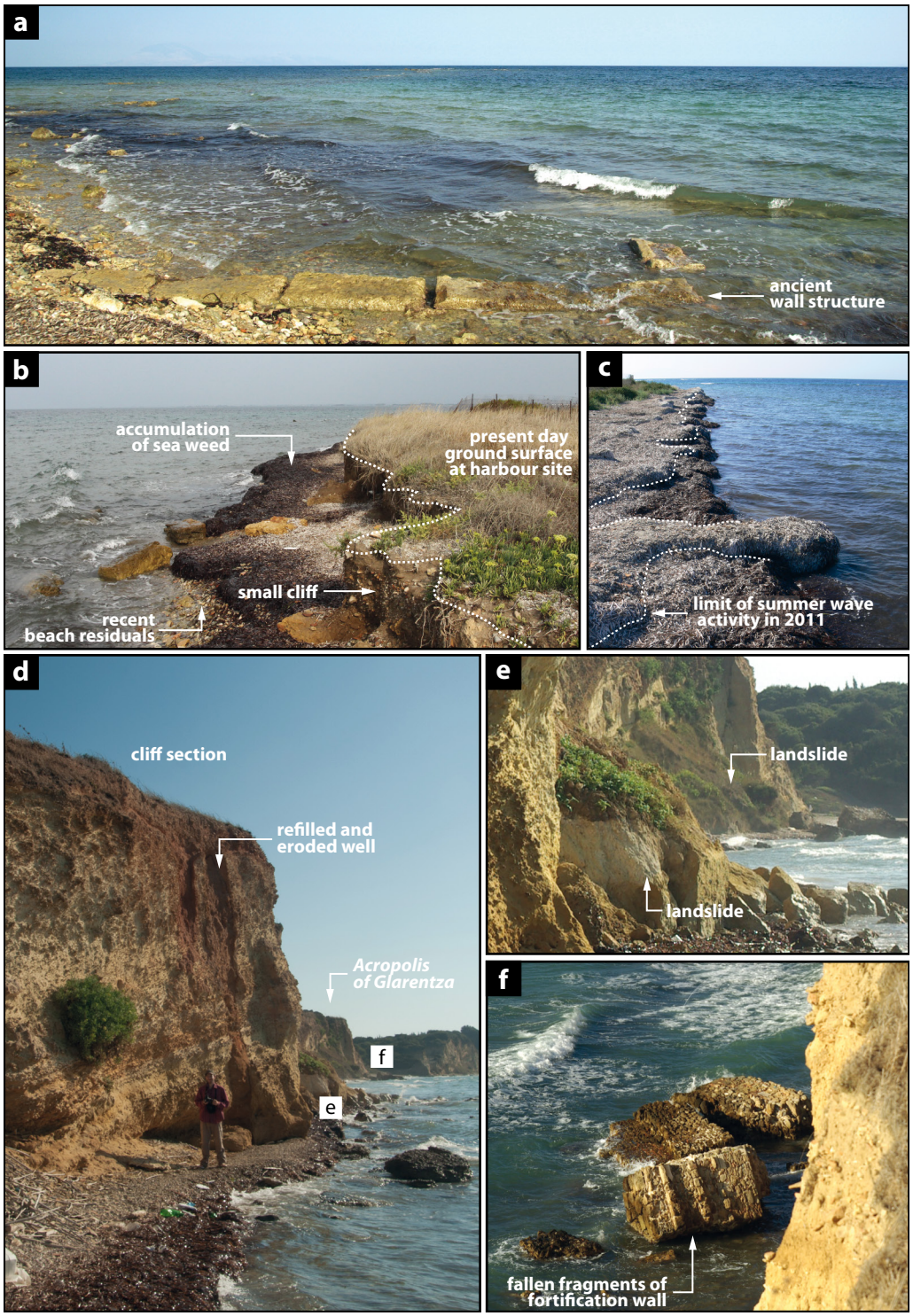

Fig. 5.2: Recent coastal dynamics at the Kyllini harbour site (a). Constant erosion has formed a small cliff (0.5-1.0 m high), that is mostly inactive during summertime (b). The annual accumulation of seaweed along the shores of Kyllini protects the harbour area from erosion (c). West of the harbour, the Kyllini peninsula is bound by a steep cliff coast (d). Strong erosion and rapid cliff retreat are visible from numerous landslides (e) which also affect the medieval fortress of Glarentza (f).

repeatedly conquered (Traquair 1906/07, FIA 2013). In order to prevent it from falling into the enemy's hands, the Byzantine emperor Constantinos Palaiologos ordered the slighting of Kyllini's fortification wall in 1431 AD (Sphrantzes after Phillipides 1980). Although the destruction of walls and towers probably also implies a destruction of the Frankish harbour facilities, historical accounts document on-going trading activity. Without fortification the significance of the Kyllini fortress gradually declined towards the mid-15th AD century when it was replaced by the well-fortified fortress of Chlemoutsi (Schmitt 1995).

Travel accounts from the early 19th cent. AD merely refer to Kyllini as anchorage for small ships from Zakynthos with adjacent *"custom-house and a few sheds, or magazines"* (Chandler 1817: 318). While of the ancient settlement *"some masses of wall and other vestiges remain"*, the harbour itself is described as *"chocked up"* (Chandler 1817: 319, Leake 1830).

5.2.2 Recent archaeological studies

Recently, coastal and underwater investigated at the ancient harbour site of Kyllini are conducted within the Kyllene Harbour Project, carried out by the Finnish Institute at Athens (FIA 2013).

Archaeological remains that are still visible at the harbour site allow a rough visualisation of the ancient facilities (Fig. 5.3, Morgan 2008). From its basic structure, the harbour was separated into different basins. While the existence of an inner basin can merely be expected from the present-day topography and swamp-like conditions in the lowland embayed between the acropolis of Glarentza and the recent coastline (Fig. 5.3a), an outer harbour is well defined by remaining harbour installations. In the shallow water off the modern coastline, submerged walls, moles and tower foundations are well preserved (Fig. 5.3b-c). In the north-western harbour area, a massive mole runs perpendicular to the recent beach, while narrower structures that parallel the coastline form some kind of mid-harbour basin. In some places, massive double walls run obliquely to the beach were they are covered by sediments so that their further course remains unclear (Morgan 2009, FIA 2013). It seems, though, as if these walls separate the mid-basin from the inner harbour (Figs. 5.1 and 5.3e). No archaeological remains are visible in the central area of the inner harbour basin. Its maximum extension is merely defined by the rising terrain of the surrounding slopes. While the outer harbour is mostly submerged, the present day surface of the inner basin lies about 1 m a.s.l. (above sea level) along the present beach but slightly declines in landward direction.

The harbour basins were probably accessible by three different entrances (Fig. 5.1b), whereby only the northeastern entrance seems to be ascertained since it was secured by towers and additional walls, opening towards the inner basin (Morgan 2009). Assuming a mid-harbour basin, it is likely that further entrances existed to the north and/or the west.

Regarding the age of the archaeological remains, most visible structures date to the Frankish period and indicate a well-fortified harbour site during Medieval times (EBA 2005). Many facilities are, however, constructed on top of ancient Greek harbour remains. At the northeastern harbour entrance for instance, a Frankish wall connects a polygonal Frankish tower, probably founded in water on wooden stakes, with an ancient Greek tower foundation, built-over by Frankish constructions (Fig. 5.3f, Morgan 2009, FIA 2013).

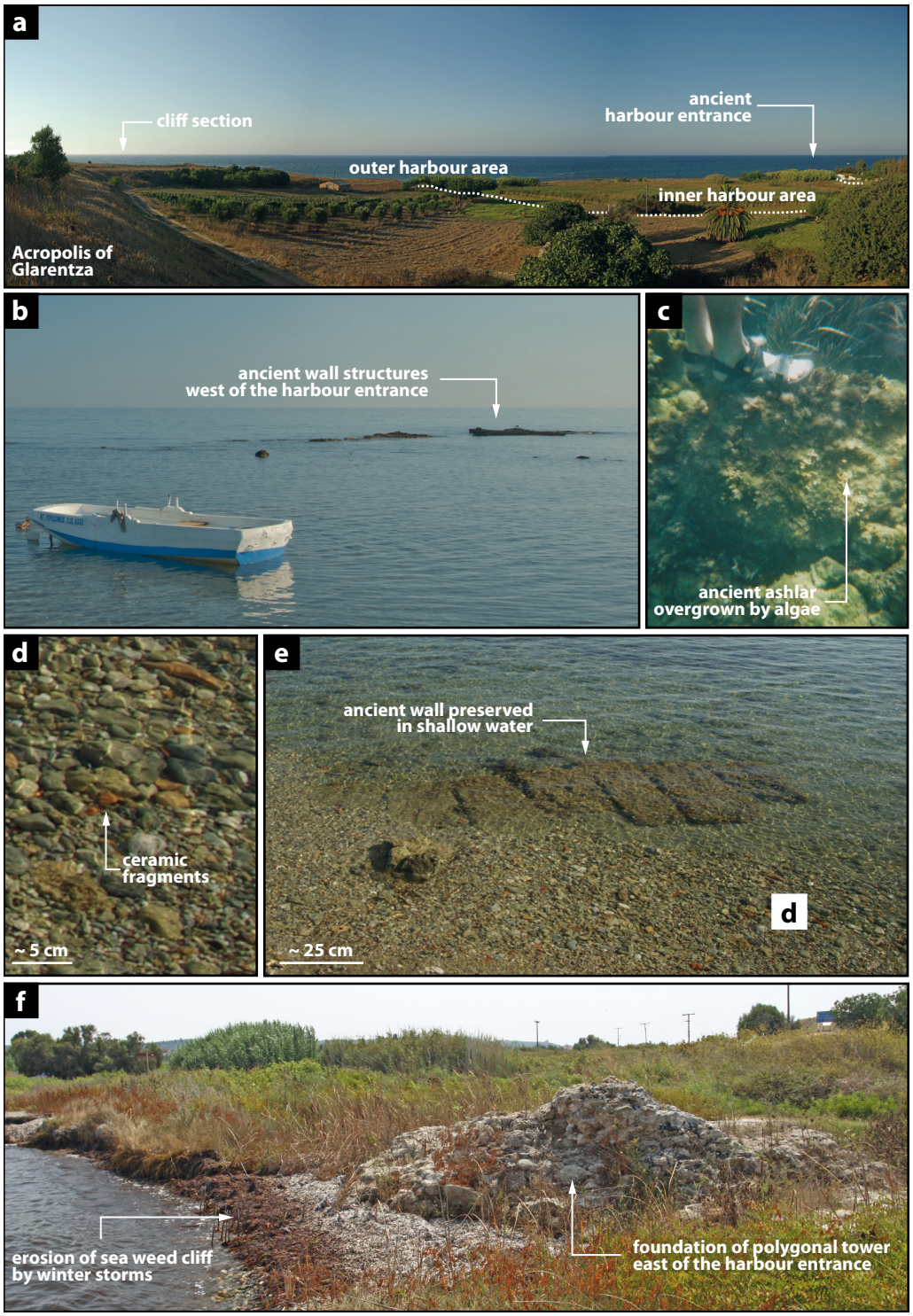

Fig. 5.3: Visible remains of the ancient Kyllini harbour site. Today, the inner harbour basin appears as coastal lowland (a), while remains of the outer harbour lie off the recent coastline in shallow water depth (b, c). Along the recent coastline, numerous ceramic fragments are incorporated to the gravely beach (d). Remaining walls that run in landward direction are covered by those beach deposits (e). The foundation of an polygonal tower marks the eastern fortification of the harbours that has equally been connected to the city wall (f).

5.3 Methods

This study is based on a multidisciplinary approach combining a broad variety of geo-scientific methods in the context of archaeological observations.

Field work

On-site geo-scientific studies are based on vibracoring using an Atlas Copco Cobra mk pro coring device with core diameters of 3 cm, 5 cm and 6 cm. In total, 11 vibracores with a maximum coring depth of 9 m below surface (m b.s.) were drilled along the recent coastline (beach), partly also in the shallow water of the outer harbour basin. Vibracores were photographed, described and sampled with regard to different stratigraphical units. The core description considers grain size, colour of sediment and content of calcium carbonate as well as macrofossil and plant remains, ceramic fragments and further sedimentological and pedological features (Ad-hoc-Arbeitsgruppe Boden 2005).

Geophysical methods like electrical resistivity tomography (ERT) allowed to reconstruct the subsurface stratigraphy. They also helped to detect or track archaeological remains, e.g. harbour walls, or the local bedrock topography. At the Kyllini harbour site, 10 ERT transects were measured parallel to the recent coastline using a multi-electrode geo-electrical unit (type Iris Instruments, Syscal R1 Plus Switch 48). Position and elevation data for each vibracoring site and ERT transect were measured using a Topcon HiPer Pro DGPS device (handheld type FC-200).

Laboratory analyses

Sediment samples were analysed for standard geochemical parameters such as pH-value, electrical conductivity, loss on ignition and content of calcium carbonate. Additionally, a handheld XRF spectrometer (type Niton XL3t 900s GOLDD, calibration mode SOIL) was used to determine a detailed geochemical profile for each stratigraphical unit. In order to eliminate potential influences of moisture, grain size or inhomogenities, sediment samples from vibracore KYL 7A were dried, finely grounded using a ball mill and prepared in sample cups. To obtain mean values for element concentrations, samples were then measured three times for 30.5 sec with an average resolution of 5 cm. Magnetic susceptibility measurements were carried out using a Bartington Instruments MS3 Magnetic Susceptibility meter and a MS2K Surface Sensor (24.5 mm² response area, 8 mm response depth). Samples were measured for 1 sec and deviations were controlled by means of a standard sample.

Grain size analyses were conducted for selected vibracores in order to characterize the depositional environment of each stratigraphical unit. The proportion of each grain size fractions was determined according to Köhn (Blume et al. 2010).

Microfossil analyses were carried out for samples from vibracore KYL 7A to distinguish between freshwater, brackish or marine environments. Sediment samples of 15 ml were extracted from each stratigraphical unit, partly pretreated with H_2O_2 (3%) and fractioned by wet-sieving (< 125 µm, 125-250 µm, 250-400 µm and > 400 µm). Foraminifera were then picked from residual sediments using a stereo microscope (type Nikon SMZ 745T) and photo-documented using a light-polarizing microscope (type Nikon Eclipse 50i POL with digital camera type Digital Sight DS-FI2). Photos were processed using the NIS Elements Basic Research 4 software. Foraminifera were identified to group or – if possible – to species level. Identification was mainly based on Loeblich & Tappan (1988) and Cimerman & Langer (1991).

Dating approach

The local geochronostratigraphy is based on ^{14}C-AMS dating of plant remains or biogenic calcium carbonate. Radiocarbon dating was accomplished by the Leibniz-Laboratory for Radiometric Dating and Isotope Research, Christian-Albrechts-University, Kiel (KIA). Archaeological age determination of diagnostic ceramic fragments as well as architectural remains provided further data for the chronostratigraphy of the harbour evolution.

5.4 Sedimentological and geoarchaeological investigations at the Kyllini harbour site

In the area of the inner and outer harbour basin, 6 vibracores were drilled (KYL 1-3, 7-9). Five additional vibracores were drilled along the south-east trending beach (KYL 4, 5, 11 and 13) and close to the modern settlement (KYL 6), for location of coring sites see Fig. 5.1). In this paper, we present detailed data on the harbour basin stratigraphy and the event stratigraphical record.

5.4.1 The stratigraphical record of the Kyllini harbour site

In the following, selected stratigraphical records retrieved from different vibracoring sites within and without the archaeological complex are presented (for vibracore locations see Fig. 5.1).

The inner harbour basin stratigraphy

Vibracore KYL 8 (ground surface at 0.65 m a.s.l., N 37°56’32.2”, E 21°08’24.4”) was drilled in the outermost seaward area of the presumed inner harbour basin close to the recent coastline.

The basal unit of KYL 8 is dominated by partly lithified, sandy bedrock (6.00-4.78 m b.s). Subsequently, medium grey sand documents the establishment of marine conditions (4.78-3.74 m b.s.) associated with a shallow embayment. At the site of the test core, marine deposits even reach down to 7.50 m b.s.

An increasing silt content indicates more quiescent conditions (KYL 8: 3.74-3.68 m b.s.). In a test core stratigraphy recovered close to site KYL 8, a unit of homogeneous sand again documents marine influence associated to increased sedimentary dynamics. An abruptly following unit of light-grey, sandy to clayey silt indicates the establishment of a quiescent, probably limnic environment. The sharp basal contact of the unit documents a rapid closure of the marine embayment and a cut-off from shallow marine conditions. Subsequently, clayey-silty sediments including seaweed remains and marine macrofossils testify to the gradual transition to a lagoonal environment that corresponds well with the depositional conditions typical of harbour basins. At site KYL 8, a sharp contact also marks the abrupt onset of lagoonal conditions (3.68-2.94 m b.s.) subsequently to the quiescent marine environment. Plant and animal remains like olive pits, nutshells or pincers, as well as ceramic sherds or wooden plank fragments with attached calcified worm tubes were found incorporated into the lagoonal facies. A constantly growing amount of seaweed and increasing content of organic substance in the upper lagoonal unit documents the gradual siltation of the inner harbour basin (KYL 8: 2.94-2.70 m b.s.).

Following a sharp erosional contact, the quiescent harbour deposits are covered by coarse-grained marine sand (2.70-0.55 m b.s.) indicating a sudden environmental change towards high-energy conditions. At the base of the sand unit, underlying lagoonal deposits were found strongly reworked partly appearing as rip-up clasts. The entire unit incorporates numerous *Cerithium* sp. gastropods and shows a fining upward grain size distribution. Towards the top, the sand unit passes over to silt-dominated colluvial deposits (0.55-0.00 m b.s.).

The mid-harbour basin stratigraphy

Vibracores KYL 7/7A (ground surface at 0.77 m a.s.l., N 37°56'32.7" E 21°08'25.7") and KYL 3 (ground surface at -0.87 m a.s.l., N 37°56'33.3" E 21°08'26.3") show a similar stratigraphical record. Here, stratigraphic details of core KYL 7/7A are presented (Fig. 5.4a).

The base of core KYL 7/7A is dominated by grey, fine to medium sand deposited in a shallow marine environment (7.00-4.88 m b.s.). Subsequently, light grey silt indicates the formation of quiescent conditions (4.93-4.80 m b.s.l.). This unit is, however, covered by alternating sequences of sand, clayey silt and organic material documenting a temporary and cyclic alternation of high- and low-energetic depositional conditions (4.80-4.16 m b.s.). On top of this sequence, light grey clayey to silty limnic deposits indicate the rapid formation of a coastal lake were found (4.16-3.80 m b.s.), covered by lagoonal mud corresponding to harbour deposits (3.80-3.50 m b.s.). Towards the top, abundant seaweed and organic material indicates a short period of siltation (3.43-3.22 m b.s.). Then, silty sand with shell debris and seaweed documents a gradual change from lagoonal back to low-energy shallow marine conditions (3.22-1.90 m b.s.). Subsequently follows, on top of an erosional contact (Fig. 5.4c) and following a thin shell debris layer (1.93-1.85 m b.s.), grey, medium to coarse marine sand including numerous specimens of *Cerithium* sp. (1.90-0.82 m b.s.). While the lower part of the unit is characterized by quite homogenous sand (1.85-1.57 m b.s.), the middle section contains rip up clasts and reveals repeated fining upward sequences (Fig. 5.4b) from coarse sand to organic rich layers (1.57-1.13 m b.s.). The sediment colour changes from grey to rust-coloured, thus indicating that the material was partly deposited above sea level (1.13-0.82 m b.s.). Successively, the sandy unit is covered by colluvial deposits (0.82-0.50 m b.s.). Gravel on top of the profile is assumed to be associated to a dirt road along the beach (0.50-0.31 m b.s.).

The harbour entrance stratigraphy

Vibracoring sites KYL 9 (ground surface at 0.55 m a.s.l, N 37°56'31.8" E 21°08'27.2") and KYL 1 (ground surface at -0.41 m a.s.l., N 37°56'31.4" E 21°08'28.7") are directly located in the presumed main entrance to the inner harbour basin (Fig. 5.1a).

The lower stratigraphical record of KYL 9 shows a shallow marine sand and silt including abundant seaweed (5.00-2.89 m b.s.). From 4.00-3.74 m b.s., the seaweed meadow suddenly disappears and increasing amounts of silt and numerous marine molluscs point to more quiescent conditions (2.89-2.50 m b.s.). This unit may therefore be correlated with the ancient harbour basin. Subsequently, shallow marine conditions are re-established as indicated by the increase of sand (2.50-1.79 m b.s.). Following an erosive unconformity, a thick layer of medium sand including marine mollusc fragments, large gravels and ceramic sherds documents a rapid environmental change from predominantly low- to higher-energetic conditions (1.79-0.17 m b.s.). From 0.82 m b.s. onwards, the beige to rust-coloured sediment documents a deposition partially above sea level. The upper part of the profile consists of fine-grained colluvial deposits, strongly influenced by anthropogenic land use activities (0.17-0.00 m b.s.).

The stratigraphical record outside the harbour area

Vibracoring site KYL 11 (ground surface at 0.39 m a.s.l., N 37°56'27.6" E 21°08'29.6") lies next to the foundation of an ancient tower, while site KYL 5 (ground surface at -0.96 m a.s.l., N 37°56'28.8" E 21°08'30.6") was drilled in the shallow water some 25 m away from the recent shoreline.

At site KYL 11, the local bedrock was found only 4 m below the present day ground surface (6.00-4.91 m b.s.) followed by shallow marine deposits (4.91-2.44 m b.s.) with predominant medium

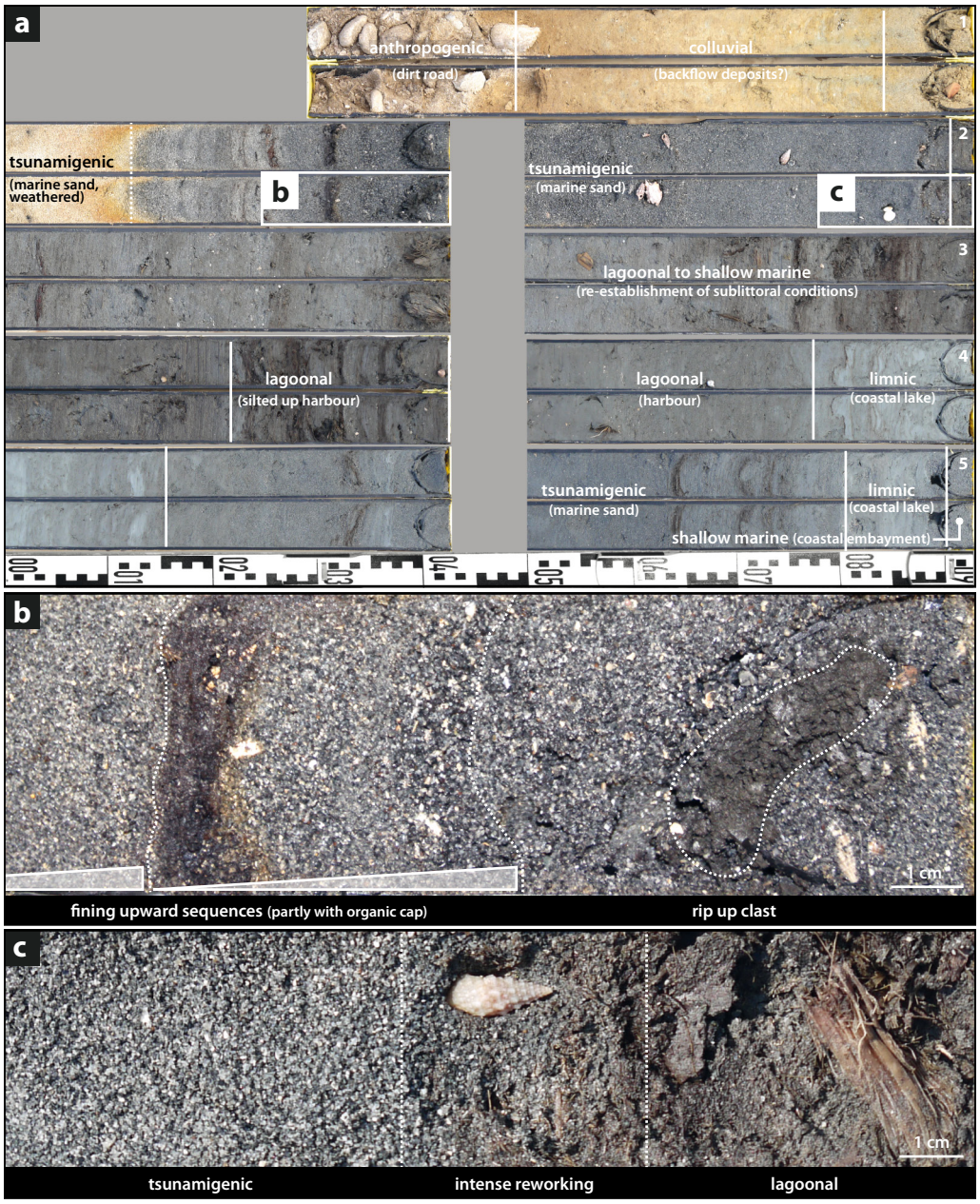

Fig. 5.4: Simplified facies profile of vibracore KYL 7A drilled in the mid-harbour basin (a). The detailed view shows rip up clasts incorporated to the high-energy event deposit (b) by erosion of underlying shallow marine to lagoonal deposits (c). Multiple fining upward sequences document repeated inflow and subsequently decreasing flow velocities. Note that the lower two meters (5.00-7.00 m) are not depicted in the photo.

sand that indicates moderate energetic conditions similar to present day situation. From 2.44-2.22 m b.s. the amount of silt increased, while the subsequent unit is characterized by coarse sand and gravel with few seaweed remains and numerous mollusc fragments (2.22-0.79 m b.s.) documenting a considerable change towards high-energy conditions. Subsequent medium sand and a thick layer of seaweed (0.79-0.50 m b.s.) then show the establishment of shallow littoral conditions. In the upper part of the profile, brown sand reflects the present day terrestrial near-shore conditions (0.50-0.00 m b.s.).

Vibracore KYL 5 largely reflects the palaeogeographical evolution depicted in core KYL 11. Coarse sand, gravel, shell debris and ceramic fragments also indicate an abrupt onset of high-energy conditions in the upper part of the vibracore profile (1.48-0.70 m b.s.).

5.4.2 The palaeogeographical evolution and spatial extent of the Kyllini harbour basin

Across the Kyllini harbour site, the described vibracores are arranged in two transects, that allow a spatial correlation of facies types distinguished in the stratigraphical record. Vibracore transect A (Fig. 5.5) begins in the north-westernmost part of the harbour site and assumes a V-shaped course in southeastern and northeastern direction, respectively. Vibracore transect B (Fig. 5.6) runs parallel to the coastline in southeastern direction (for vibracore locations see Fig. 5.1a).

Vibracore transect A shows that the Kyllini harbour site is located in a natural depression of the Pliocene bedrock. While the bedrock rises at the edges of the harbour area (KYL 8), it submerges in the direction of the central basin in seaward direction (KYL 3). Due to the relative sea level rise, a shallow marine pre-harbour environment subsequently developed on top of the bedrock.

Along transect A, mid-energetic shallow marine environment gradually got under more quiescent conditions, probably due to the initial eastward progradation of a sand spit. Later, marine deposits were replaced by sediments of a coastal lake that precedes the lagoonal harbour facies. Vibracore stratigraphies thus show that the local palaeogeography already provided some sheltered anchorage that has been subsequently extended and fortified as harbour place. Stratigraphical data further suggest that the harbour was divided into different harbour basins, separated from each other by massive walls.

Initially, an equally quiescent harbour environment was recovered at several vibracoring sites. Possibly, surrounding walls created environmental conditions disconnected from the open sea. At site KYL 8, the harbour basin is then gradually affected by siltation and the establishment of semi-terrestrial conditions while corresponding stratigraphical sections in cores KYL 7/7A and KYL 3 document increasing wave dynamics and a sudden shift from lagoonal to shallow marine conditions. This contrasting palaeo-environmental development suggests a harbour division in at least two different basins, which is supported by massive double wall structures encountered near coring sites KYL 8 and KYL 7 (Fig. 1). The first basin could correspond to the well-protected innermost harbour basin. The second basin, on the contrary, represents an outer harbour section increasingly influenced by shallow marine dynamics probably related to the constantly rising sea level and/or high-energy wave impact.

Along vibracore transect B, shallow marine sequences encountered at sites KYL 1 and KYL 9 indicate sheltered conditions but also a constant marine influence. Since the sedimentary facies documents some kind of transition zone between the quiescent inner basin and a wave dominated marine environment, the stratigraphical record fits well the suggested walled entrance situation.

Further to the southeast, the natural near-shore environment represented by cores KYL 5 and 11 seems to be only little affected by the harbour facilities. Sediments recovered from these sites do rather mirror present-day environmental conditions. Therefore, this area must have been located outside the ancient harbour. Since site KYL 11 lies next to a massive wall connecting two towers along the harbour entrance, more quiescent conditions are temporarily established. Outer harbour facilities do obviously reflect the palaegeographical setting as the local bedrock is close to ground surface at the site of the tower and submerges in the direction of the harbour basin (Fig. 5.6).

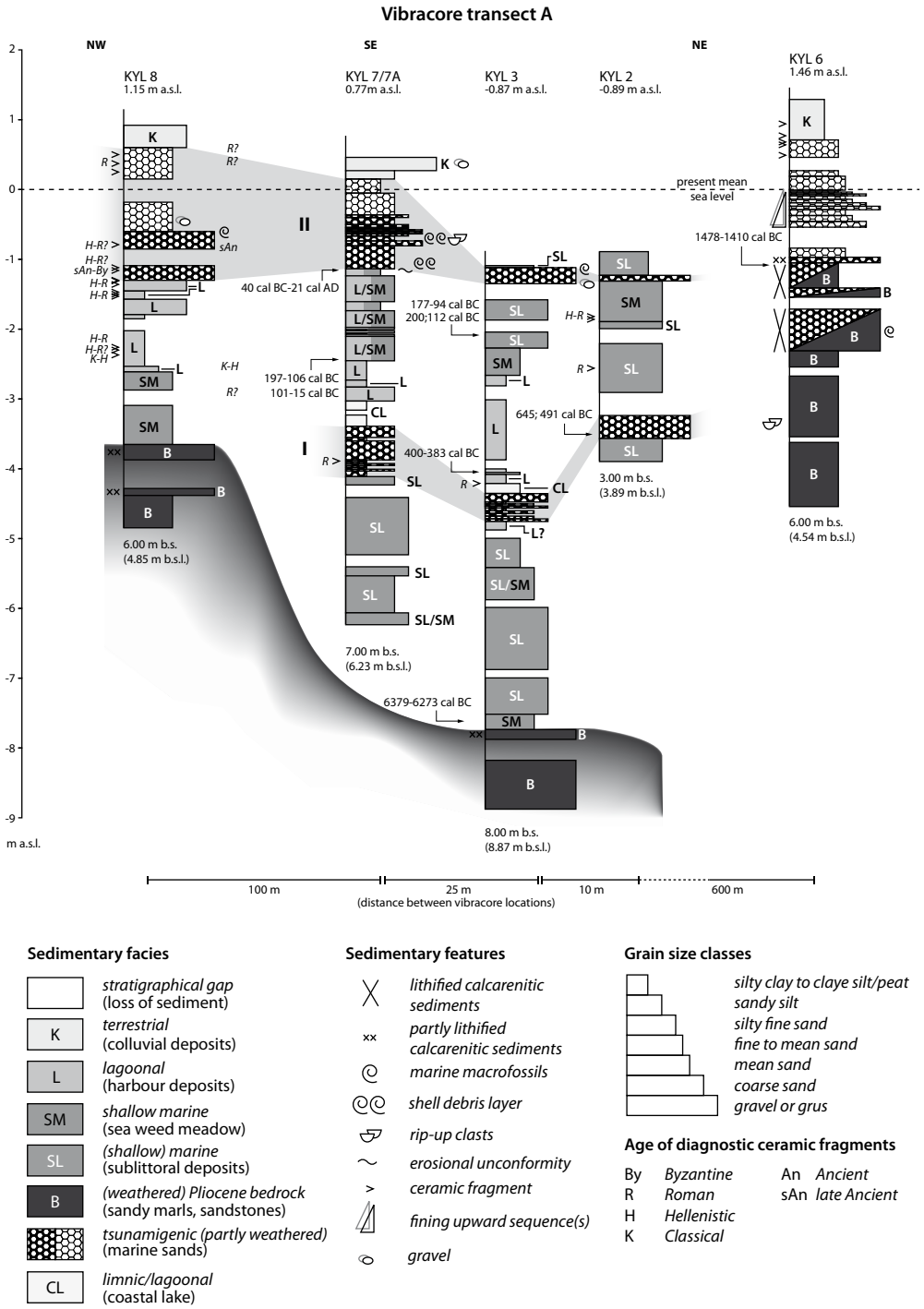

Fig. 5.5: Stratigraphies, facies distribution and geochronostratigraphy for vibracore transect A. For location of vibracores see Fig. 5.1. Details on radiocarbon ages are presented in Tab. 5.1.

5.4.3 Evidence of high-energy impact and event-stratigraphical correlations

The stratigraphical record of the Kyllini harbour site does not only offer information on the evolution of the ancient harbour. Also, the sedimentary sequence provides distinct evidence that the area has repeatedly been affected by the impact of high-energy wave events. Along vibracore transects A and B, an event-stratigraphical approach allows to correlate high-energy event facies.

According to the presented data, Kyllini was hit by at least two high-energy impacts. A first event generation (I) affected the site prior to the foundation of the ancient harbour. At sites KYL 3 and KYL 7/7A, autochtonous conditions were abruptly interfered by high-energy impact; multiple fining upward sequences that consist of alternating layers of sand, silt, clay and organic substance were suddenly deposited in the quiescent environment documenting repeated rapid inflow of a sediment-loaded mass of water and a fast decline in flow velocity. Well-developed mud-caps (Fig. 5.4a) reflect short-term stagnation of the water prior to backflow. The underlying low-energy deposits have been reworked due to increasing flow dynamics.

All along transect A, the upper limit of the event layer is characterized by a sharp contact. Subsequent to event generation I, the former shallow marine embayment was abruptly disconnected from the open sea and transformed into a coastal lake. As major consequence for the Kyllini harbour site, the high-energy event-related reorganisation of the coastline obviously created the initial conditions that subsequently led to the foundation of the harbour.

The high-energy layer associated with event generation I is hardly traceable along vibracore transect B. Here, the event affected already more or less wave-dominated environments that impede the identification of event-related allochthonous sediments. Only vibracores KYL 9 and KYL 1 allow an event-stratigraphical correlation with transect A.

Across the entire Kyllini harbour site, the impact of a second high-energy event (II) is evident from the stratigraphical records. Along transect A, event generation II interferes semi-terrestrial conditions of the silted up inner harbour basin as well as shallow marine conditions in the seaward basin. For this younger high-energy impact, the sedimentary record at site KYL 7/7A reveals a similar deposition pattern as the one found for event generation I. Low-energetic silty to sandy deposits associated to growing up seaweed meadows are unconformably overlain by a thick layer of marine sand, attesting an abrupt environmental change towards temporary high-energetic conditions. The upper limit of the autochthonous fine-grained deposits exhibits sedimentary features of strong erosion and significant reworking. At site KYL 7/7A, a basal shell debris layer additionally marks the erosional contact. Following homogenous sand, rip up clasts are embedded in the sediment (Fig. 5.4b). The overall content of marine macrofossil fragments is high, especially incorporating numerous specimens of *Cerithium vulgatum* that do not appear in the autochthonous shallow marine deposits. Since *C. vulgatum* prefers shallow water but sandy sediments (Poppe & Goto 1991), it can be assumed that the allochthonous deposits originate from the nearby offshore coastal area outside the harbour and were dislocated by high-energy wave impact. Alternating layers of fining upward sequences from coarse to fine sand and organic substance again indicate repeated inflow and subsequent stagnation of a sediment loaded mass of water. As the ancient harbour was fortified with massive walls and thus acted as a sediment trap, successive high-energy waves eventually “swashed” into the basin and led to sediment deposition. The remaining harbour facilities then prevented rapid water run off so that mud-caps and layers of organic substance were deposited and conserved. At sites KYL 2 and KYL 3, the deposits of event generation II are thin, which may either be explained by erosion due to recent wave action or by dredging activities.

Another sedimentary feature of event generation II is visible along transect A. High-energy event-related marine sediments were partly deposited above sea level and were subsequently subject to subaerial weathering as attested by the rusty sediment colour (see Fig. 5.4a, KYL 7A from 1.13 m b.s. onwards). As the data shows, wide areas of the ancient harbour basin were buried.

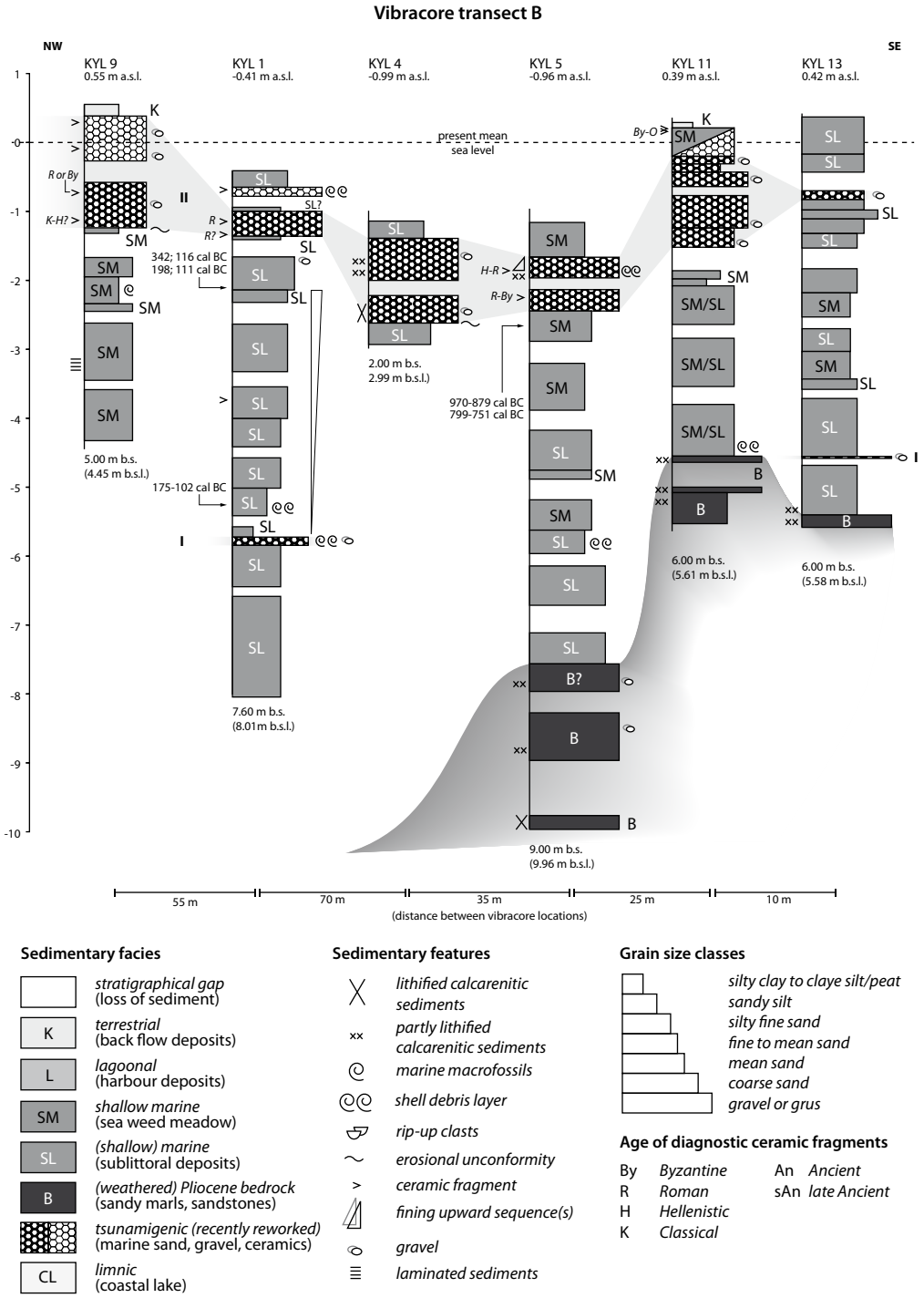

Fig. 5.6: Stratigraphies, facies distribution and geochronostratigraphy for vibracore transect B. For location of vibracores see Fig. 5.1. Details on radiocarbon ages are presented in Tab. 5.1.

Event generation II deposits were also recovered from vibracoring site KYL 6 (1.46 m a.s.l., N 37°56'14.2'' E 21°08'34.3''), drilled in the vicinity of modern Kyllini (Fig. 5.1a) some 600 m distant from the ancient harbour. Here, the bedrock is, on top of an erosional unconformity, overlain by a high-energy event deposit including marine macrofossils and ceramic fragments. The upper part features multiple fining upward sequences. The fact that the upper part of the event deposits

are dark yellow to rust-coloured is explained by postdepositional subaerial weathering. Event generation II did thus not only affect the ancient harbour site but also hit the surrounding coastal area.

Along transect B, event generation II is preserved as noticeable interference of the shallow marine environment. While autochthonous conditions are characterized by mean sand including seaweed, the event layer is characterized by abundant gravel, shell debris and ceramic fragments. For offshore vibracoring sites, a re-establishment or the former environmental conditions is observed (i.e. KYL 1, KYL 4, KYL 5). It remains unclear, though, whether marine conditions naturally recurred posterior to the event or are the result of modern coastal erosion.

5.5 Evidence of high-energy impact derived from multi-proxy analyses

Different palaeoenvironmental proxies provide significant information on the geochemical fingerprint of sedimentary facies as they help to distinguish between autochthonous and allochthonous sediments. In this study, different methods were applied to to verify high-energy impact to the Kyllini harbour site. Being a key site for both the harbour evolution and reconstruction of event-generations I and II, detailed multi-proxy analyses were carried out for sediments from vibracoring site KYL 7A.

5.5.1 Grain size analysis of vibracore KYL 7A

The grain size distribution of each facies is directly related to the energetic environment (Reineck & Singh 1980, Schäfer 2005). According to Walther's law of the correlation of facies, a gradual shift of different laterally associated depositional environments will inevitably results in an equally gradual vertical sequence. Erosive events must hence be assumed where unconformities and abrupt alterations occur (Walther 1894). The calculation of an energetic ratio for each facies additionally emphasizes abrupt changes (Willershäuser et al. 2013). Low-energy marine embayments or harbour basins are characterized by fine-grained deposits (Füchtbauer 1988, Marriner & Morhange et al. 2007). Therefore, high-energy input of allochthonous sediments is supposed to be well traceable in the stratigraphical record. Grain size data for vibracore KYL 7 is presented in Fig. 5.7.

Grain size distributions as well as the calculated energetic ratio for KYL 7 provide evidence on gradual and abrupt changes of the palaeo-environment at the Kyllini harbour site (Fig. 5.7). Autochthonous sedimentation conditions of the pre-harbour, harbour and also post-harbour environment are characterized by fine grained sediments and thus show a rather low energetic index. On the contrary, coarse grained high-energy deposits show highest values of the sand+gravel to silt+clay ratio. Abrupt changes of the energetic ratio emphasize the temporary character of the high-energy deposits.

5.5.2 Microfossil analysis of vibracore KYL 7A

Due to their good preservation potential in the stratigraphical record, the analysis of foraminiferal assemblages in sediment samples provides a valuable tool to reconstruct the palaeo-environmental evolution (Gupta 2002, Fiorini 2004). However, rapid or catastrophic alterations of an ecosystem may strongly affect the foraminiferal community (Mamo et al. 2009). In coastal environments, single high-energy events like storm surges or tsunamis can already initiate considerable changes of the environmental conditions. Such events are quite often accompanied

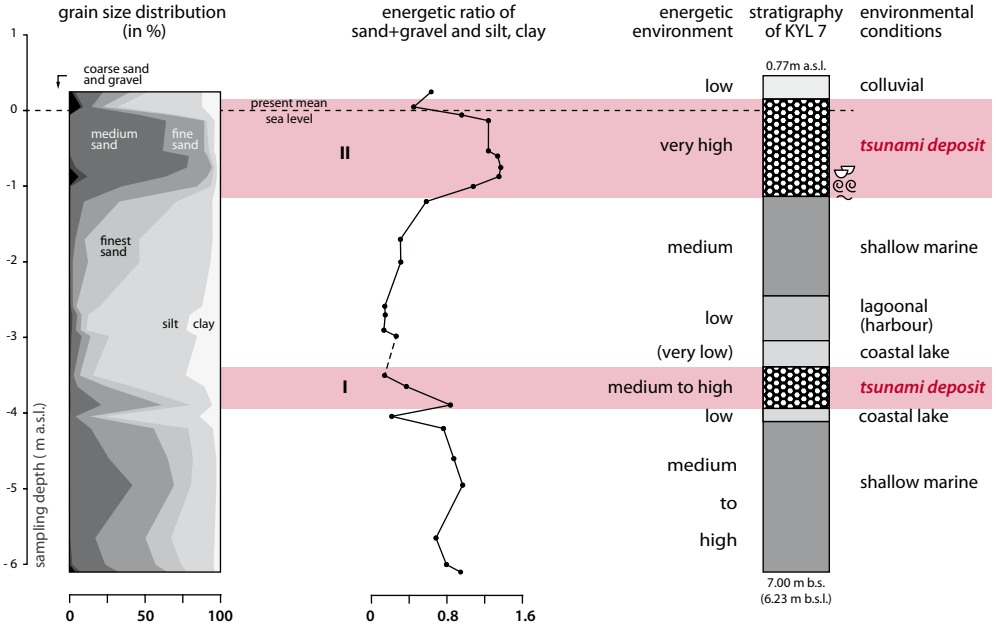

Fig. 5.7: Results of grain size analyses for samples from vibracore KYL 7. Event deposits are characterized by a sudden shift towards coarser grain sizes, while in situ deposits are mostly silt dominated. The energetic ratio emphasizes the abrupt increase in transport energy that goes along with both event layers.

by a clear disturbance of the foraminiferal assemblage preserved in the stratigraphical record (e.g. Alvarez-Zarikian et al. 2008, Pilarczyk et al. 2012 , Hadler et al. 2013, Willershäuser et al. 2013).

With regard to the facies pattern of vibracore KYL 7A, 29 sediment samples were analysed for their foraminiferal assemblages (Fig. 5.8). A total number of 75 species were identified (Loeblich & Tappan 1988, Cimerman & Langer 1991).

At the shallow marine base of the profile, the foraminiferal assemblage is characterized by a medium to high diversity but low abundance. Dominating species comprise *Ammonia beccarii*, *Orbulina universa* and *Planorbulina mediterranensis*. The assemblage mirrors a near-coast shallow marine environment (Murray 1991, 2006). Living attached to vegetation, the occurrence of *P. mediterranensis* indicates the increased presence of *Posidonia* and therefore reflects more quiescent conditions. The planktonic *O. universa* reflects slightly increased water depths (Gupta 2002).

Planktonic foraminifera like *Lagena* sp. or *Fursenkonia* sp. found within the overlying marine sand require growing water depth. Moreover, *Quinqueloculina seminula* and also *Elphidium* sp., *Asterigerinata mamilla, Rosalina* sp., *Cibicides* sp. and *Massilina secans* emphasize the fully marine character of the facies (Murray 1973, 1991, 2006, Di Bella et al. 2011). The encountered foraminiferal assemblage documents the high-energy input of allochthonous sediments from adjacent seaward environments into a near-coast marine embayment. Especially the incorporation of planktonic species that do not occur in the pre- and post-event deposits proves the allochthonous nature of the sediments.

Decreasing diversity and abundance of foraminifera mark the event-associated establishment of a quiescent water body. The foraminiferal distribution and the presence of saltwater-bearing species show that is is rather a pre-harbour lagoon, separated from open marine conditions, than a coastal lake. Dominating species are *Adelosina carinata-striata*, *Miliolinella sp.*, *A. parkinsonia* and *A. beccarii* as well as *P. mediterranesis*.

The subsequent harbour facies is marked by the sudden and rapid decrease in diversity. In the lower harbour facies, stress tolerant species like *A. tepida*, *Triloculina trigonula*, *Pseudotriloculina* sp. and *Haynesina* sp. represent about 2/3 of the total assemblage. While *Haynesina* sp. prefers brackish conditions, *A. tepida* also tolerates extreme environmental conditions like (i.e. temperature changes, hypersaline or anoxic water) that often occur in harbour basins Gupta 2002, Fiorini 2004, Marriner & Morhange 2007). In the upper part of the harbour facies, extreme conditions obviously intensify, as diversity and abundance of *A. tepida* and *Haynesina* sp. decrease. *Triloculina* sp., however, even tolerates hypersaline conditions (Murray 2006). Species associated with normal or shallow marine environments like *Rosalina bradyi* and *Elphidium crispum* are absent (Murray 1991).

Subsequently, microfossil assemblages document the re-establishment of shallow marine conditions. A sudden rise in the diversity is accompanied by the establishment of a shallow marine seaweed habitat. While *T. trigonula* still occurs in large numbers, the presence of *Quinqueloculina* sp. emphasizes the return of marine conditions. Abundant specimens of *Massilina secans* document prevailing shallow water conditions with a water depth of only a few meters (Murray 2006). *Bulimina marginata* documents rather quiescent conditions (Gupta 2002). Warm water planktonic species like *Peneroplis pertusus* or *Rosalina globularis* that browse around seaweed and algae also emphasize a near-shore environment dominated by seaweed meadows (Murray 1991, 2006). The assemblage further includes numerous foraminifera associated with Mediterranean seaweed habitats of slightly increased salinity, like *Asteriginata mamilla*, *Elphidium advenum*, *Rosalina* sp., *Cibicides* sp., *P. mediterranensis*, *Vertebralina* sp. or *Cyclocibicides* sp. (Gupta 2002, Fiorini 2004, Murray 2006). To the upper part of the facies, a high diversity and overall high abundance of species indicates a fully established marine habitat with stable palaeo-environmental conditions (Bernasconi et al. 2006).

Towards the top of the shallow marine facies, a shift in the foraminiferal assemblage documents a sudden increase of sessile species like *Sorites orbiculus*, *Planorbulina mediterranensis* or *Peneroplis planatus* that cling to the leaves or rhizomes of *Posidonia* (Murray 1973, Gupta 2002). Together with sedimentary characteristics, the encountered foraminiferal assemblage thus proves the allochthonous sediment input from nearby shallow marine environments caused by strong overflow dynamics and intense reworking of the seafloor. Omnipresent species like *A. beccarii* or *T. trigonula* still persist.

The foraminiferal assemblage of the facies associated with event generation II provides further evidence for a marine-borne, high energy impact to the study area as several significant breaks occur in the species distribution. The input of allochthonous sediments is among others marked by the sudden occurrence of *S. orbiculus* and *P. mediterranensis*.

According to Gupta (2002), *S. orbiculus* is generally immobile and attached to *Posidonia*. The species avoids high-energetic conditions and commonly occurs in shallow lagoonal environs (Murray 2006). As indicator for low-energy conditions, the high amount of *S. orbiculus* contradicts the coarse-grained sandy composition of the facies that reflects high-energy conditions. In the

Fig. 5.8: Results of foraminiferal analyses of selected sediment samples from vibracore KYL 7A. Some omnipresent specimens of Adelosina sp., Ammonia sp., Bolovina sp., Brizalina sp., Bulimina sp., Cibicides sp., Cycloforina sp., Elphidium sp., Fissurina sp., Globigerina sp., Massilina sp., Milliolinella sp., Nonion sp., Polymorphina sp., Quinqueloculina sp., Rosalina sp., Sigmoilinita sp., Siphonaperta sp., Spirillina sp., Spiroloculina sp. and Triloculina sp. are not regarded as decisively indicative and are not included in the figure.

upper part of the event deposit, diversity is again low with dominating *A. beccarii* and *O. universa*. The re-appearance of several species associated with seaweed habitats in sample 18 is due to a layer of organic substance incorporated in the event deposit. Predominance of the planktonic *O. universa* may be related to slightly increased water depths. As the species is predominant, the allochthonous sediments may originate in nearby deeper marine environments. Strong pyritization effects indicate a post-depositional alteration under anoxic conditions. Towards the top of the unit, the total amount of foraminifera strongly declines due to the constant weathering of the deposit.

In a summary view, the assignment of specific foraminiferal species to distinct palaeo-environments additionally allowed estimating the source areas for event-displaced deposits. Results for both event layers point to a dislocation of sediments from nearby offshore environments and thus indicate short transport distances. It must be emphasized, that the foraminiferal spectra of event-related facies do not necessarily comprise "exotic" species from distal or deep water environments as commonly proposed (e.g. Mamo et al 2009) but rather reflect the dislocation of reworked sediments from adjacent areas.

5.5.3 XRF measurements

As different environmental factors are related to specific chemical components, different sedimentary facies hold characteristic geochemical profiles depending on the local conditions at the time of sediment deposition.

Terrestrial settings are basically influenced by weathering and pedogenic processes so that the concentrations of elements like Fe or Ti are increased, while Ca is affected by rapid dissipation. Marine environs are, on the contrary, influenced by the production of calcium carbonate ($CaCO_3$) by marine organisms (e.g. molluscs, gastropods, foraminifera) so that marine sediments are generally enriched in calcium (Ca). Lagoonal sediments reveal terrestrial as well as marine characteristics and indicators of eutrophication such as the content of sodium (K), related to a high content of clay minerals in lagoonal deposits (Albarède 2009, Scheffer & Schachtschabel 2010). Since major marine flooding events are often accompanied by a significant landward dislocation of sediments, allochthonous high-energy deposits may leave a distinct geochemical fingerprint in the stratigraphical record of the respective geo-archive (Vött et al. 2011a, 2011b).

Selected element concentrations measured for vibracore KYL 7A are illustrated in Fig. 5.9. Autochthonous shallow marine sediments are characterized by medium Ca concentrations and low contents of Fe, Ti and K, whereas autochthonous limnic/lagoonal deposits show inverse concentrations. At the transition from a natural coastal lake to lagoonal environment, the temporary inversion probably marks the opening of the coastal lake during harbour construction. Harbour sediments are characterized by maximum Fe, K and Pb concentrations and a comparatively low Ca content. Contamination of ancient harbour with lead during Greek and Roman times is known for many other harbour sites (see Le Roux et al. for Marseille or Hadler et al. 2013 for Lechaion). In Kyllini, the strong Pb increase marks the transition of a natural coastal lake into an artificial harbour basin; once abandoned, shallow marine conditions were re-established and the Pb values decrease. Following the harbour facies, the geochemical signature documents a transition back to shallow marine condition. While terrestrial indicators constantly decline, the increasing marine influence is accompanied by slightly increasing Ca values.

Event generations I and II are clearly distinguishable by their significant geochemical record. Event generation I reflects a geochemical fingerprint, already described for the shallow marine environment at the very base of the profile as event deposits originate from the nearby coastal zone. The geochemical signature of event generation II is characterized by maximum Ca concentrations, while terrestrial indicators (especially Ti) are reduced to low concentrations. The peak at 0.63 m b.s.l. is due to rip up clasts out of underlying material. In the upper part of the profile the geochemical signature documents constant weathering due to sediment deposition above sea level. Since vibracoring site KYL 7A is located directly adjacent to the recent coastline, the uppermost facies is geochemically influenced by spray water due to marine wave dynamics.

5.5.4 Magnetic susceptibility

Magnetic susceptibility allows assigning another geochemical fingerprint to different sedimentary facies. Weathered terrestrial or lagoonal deposits usually bear a high magnetisability, while marine sediments are generally enriched in diamagnetic components like quartz sand or calcium carbonate (Dearing 1999, Scheffer & Schachtschabel 2010).

For the stratigraphical record of vibracore KYL 7A, the magnetic susceptibility reaches maximum values where quiescent depositional conditions are predominant (Fig. 5.9). High values are associated to coastal lake, lagoonal and harbour facies. This is mostly due to the high content of Fe-rich clay minerals and magnetic minerals originating from terrigenous weathering. On the contrary, marine facies are characterized by low susceptibility values.

Intersecting coastal lake deposits, event generation I is marked by contrasting low values. Covering a shallow marine facies, event generation II deposits are not well discernible in the magnetic susceptibility curve. Maximum values were only obtained for weathered high-energy deposits and covering colluvisol material.

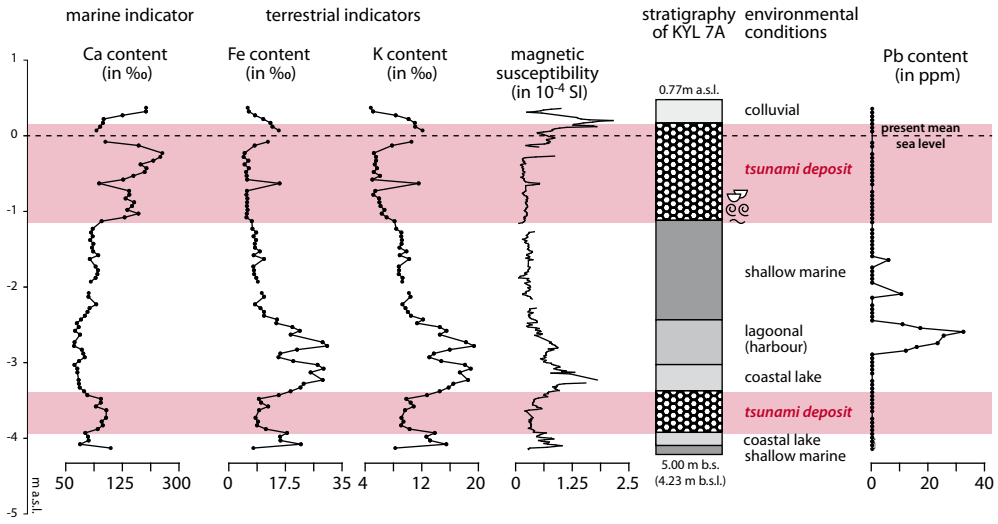

Fig. 5.9: Results of XRF analyses and magnetic susceptibility measurements for vibracore KYL 7A. While autochthonous facies document near-shore, quiescent environmental conditions (Fe, K, Ti), allochthonous deposits show a marine fingerprint (Ca). Harbour deposits are detectible by increased Pb values due to anthropogenic influences on the ecosystem.

5.6 Spatial distribution of high-energy traces

5.6.1 Electrical resistivity tomography

Across the Kyllini harbour site, electrical resistivity tomography (ERT) was carried out along 10 transects parallel to the recent coastline. ERT transects cover a coastal stretch of about 550 m from the westernmost harbour area up to the present day beach close to the modern settlement (for ERT locations see Fig. 5.10). By correlating results from ERT with associated vibracore stratigraphies, the determination of facies-related resistivity spectra allows to evaluate the general subsurface structure and to trace the spatial extent of the harbour facies.

In transects KYL ERT 9 and KYL ERT 4 (Fig. 5.10a-b) fine-grained harbour deposits are well traceable by lowest resistivity values (ca. 0-5 ohm.m). Stratigraphical verification is given by a test core. Low resistivity values were also found for recent marine/littoral deposits close to the present surface, where the influence of saltwater is high (KYL ERT 4 and 10, Fig. 5.10b-c). Pre-harbour marine sediments show slightly increased resistivity values (ca. 5-30 ohm.m).

In the eastern part of the harbour, transect KYL ERT 4 revealed a massive square structure with highest resistivity values (Fig. 5.10b) that separates the harbour facies from adjacent marine deposits (ca. 5-40 ohm.m, KYL 11). This structure, located between two tower foundations, is most probably part of the ancient fortification wall that surrounded the harbour (see also transect KYL ERT 6, Fig. 5.1b). However, the detected wall runs oblique to the presumed course of the Frankish fortification wall (Fig. 5.1b). Further southeast of the wall and adjacent fortification tower, the consistent distribution of mean resistivity values (ca. 5-40 ohm.m) in transect KYL ERT 10 documents on-going marine conditions as detected in vibracore KYL 13. Results from ERT confirm the assumed extent of the harbour basin bounded by the detected wall structure.

From vibracore transects A and B it is known that the bedrock topography has favoured the foundation of the harbour. However, local bedrock (silt- and sandstones of Pliocene age) is hardly detectible by ERT (Figs. 5.10a-c and 5.5) because its grain size is similar to overlying marine deposits. Lowest values at the very base of KYL ERT 9 are probably caused by emerging marls.

While deposits of event generation I – due to their limited thickness and the restricted resolution of ERT measurements – are not discernible in ERT pseudosections, deposits of event generation II deposits - partly deposited above present mean sea level and containing larger amounts of gravel – are well detectible in transects KYL ERT 9 and KYL ERT 7 as the uppermost unit of higher resistivity values (Fig. Xa,d). The strong gradient from underlying low-resistivity values to event-associated higher resistivities documents the abrupt onset of the event deposit. Local variations in distribution and thickness are probably associated with overwash dynamics. Where the layer comprises finer components, resistivity values decrease (KYL ERT 7, Fig. 5.10d). Outside the harbour area, event generation II deposits are not well discernible by ERT (KYL ERT 4, Fig. 5.10b) as they intersect shallow marine deposits.

5.6.2 Geoarchaeological destruction layer

The coast to the west of the Kyllini harbour site is characterized by a cliff, up to 4 m high. Event generation II deposits can be followed from the assumed harbour entrance over 250 m towards the west on higher ground up to 1 m a.s.l., showing a thickness between 0.1 m and 1.5 m (Fig. 5.11a). At different outcrops, the sedimentary characteristics prove the high-energy character of the layer.

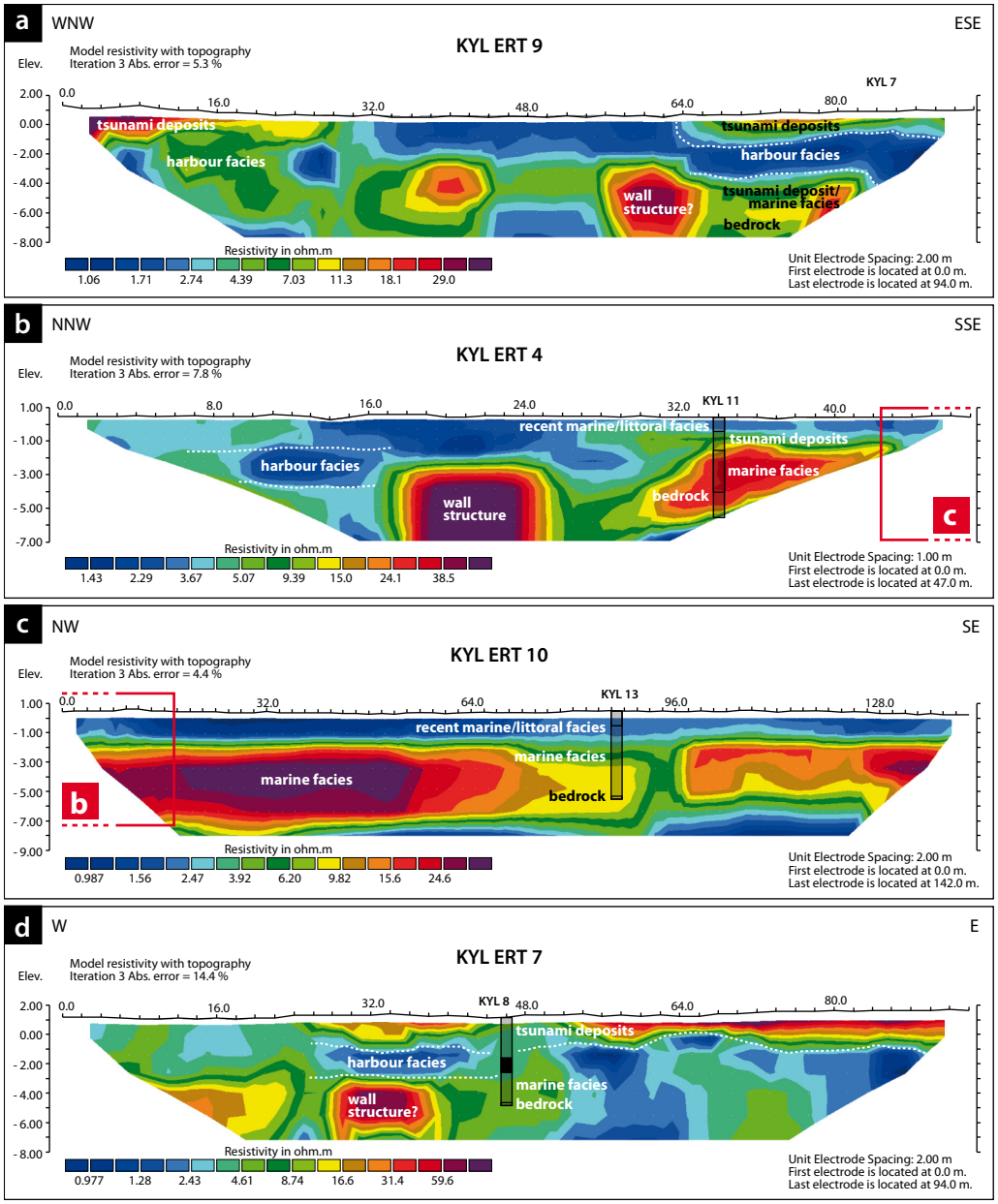

Fig. 5.10: Pseudosections of modelled electrical resistivity values based on ERT measurements in the Kyllini harbour site. Lowest resistivity values characterize the harbour facies (a). A massive wall structure (b) separates the harbour basin from a marine environment to the east of the ancient harbour (c). Event generation II occurs as thick sediment sheet with high resistivity values that covers the harbour facies (d). For location of ERT transects and vibracores see Fig. 5.1.

Well rounded gravel components are incorporated into a silty to sandy matrix and mixed with abundant angular ceramic fragments, numerous marine macrofossils and many bone fragments (Fig. 5.11b). In places, the deposit contains large ashlars possibly originating from ancient harbour installations. Since there is no river or creek discharging in the study area, a fluvial deposition of the well rounded gravel must be excluded, while the high content of marine macrofossils documents a sea-born origin of the deposit. The massive occurrence of sherds and bones, however, indicates a major terrestrial component. Since the deposit obviously derives

from diametrically opposed sedimentary environments, the site must have been affected by high-energy transenvironmental geomorphodynamics.

The overall multimodal grain size distribution of the event deposit implies the simultaneous transport and deposition of coarse- and fine-grained components for instance by sheet floods or mud flows, generally characterized by a water-saturated matrix (Reineck & Singh 1980, Schäfer 2005). Angular-shaped ceramic fragments and numerous well-preserved marine macrofossils additionally point to a short transport distance and rapid deposition, as long-term littoral processes would have rounded sherds and destroyed or abraded macrofossils.

In places, channel-like structures can be seen incised at right angles to the cliff, thus being orientated in seaward direction (Fig. 5.11c). The channel-infill out of larger ceramic fragments as well as gravel components is horizontally adjusted resulting from a high level of water saturation during transportation and strong flow dynamics (Schäfer 2005).

Multiple sandy sequences sharply overlie a palaeosol and occupation layer. The sediments show a laminated structure with fining upward cycles from sand to clay and include abundant shell debris and intraclasts. Within the sandy layer, channel structures with undulating bases are incised and filled with gravel, ceramic sherds, marine molluscs and bones (Fig. 5.11b). The top of the lower channel is covered by sand documenting repeated and cyclic widespread sedimentation (laminated sand layer) and linear erosion (channel structure). In the vicinity, the layer covers the remains of an ancient wall foundation (Fig. 5.11d).

Considering the geoarchaeological findings along the recent cliff and with regard to the archaeological remains of harbour installations, it is obvious that (i) the extensive distribution of the deposit, (ii) the mixture of marine and terrestrial components, (iii) the average grain size and bad sorting, (iv) the short-distance transport and rapid deposition as well as (v) simultaneous erosive effects are due to a widespread marine-borne high-energy impact to the Kyllini harbour site.

5.6.3 Beachrock-type calcarenitic high-energy deposits in the harbour area

Along the Kyllini harbour site, strong winter storms lead to constant erosion of the coastal cliff. Consequently, all-day coastal dynamics cause considerable reworking of high-energy event deposits incorporated in the cliff. As a result, coarse components like gravel or stones (up to 0.3 m in diameter) and also large ceramic fragments accumulate along the beach.

In some places, however, event deposits including ceramic fragments and abundant gravel are cemented by a carbonate matrix and exposed in the form of widespread beachrock-type conglomeratic slabs (Fig. 5.12a). Where cliff retreat continues, beachrock slabs break down and are embedded in the present-day littoral deposits. Ashlars incorporated into the beachrock-type deposits provide a *terminus post quem* for the formation of the high-energy unit (Fig. 5.12b-c, Vött et al. 2010).

Along the coast of the Kyllini peninsula, further outcrops of beachrock-type deposit were described as cemented beach and used as indicator to reconstruct sea level changes (Maroukian et al. 2000). For the Kyllini harbour site, it must be emphasized that the beachrock is associated to event-related high-energy dynamics. The beachrock must therefore not be regarded as lithified beach; it rather testifies to short-term event-related sea level rise.

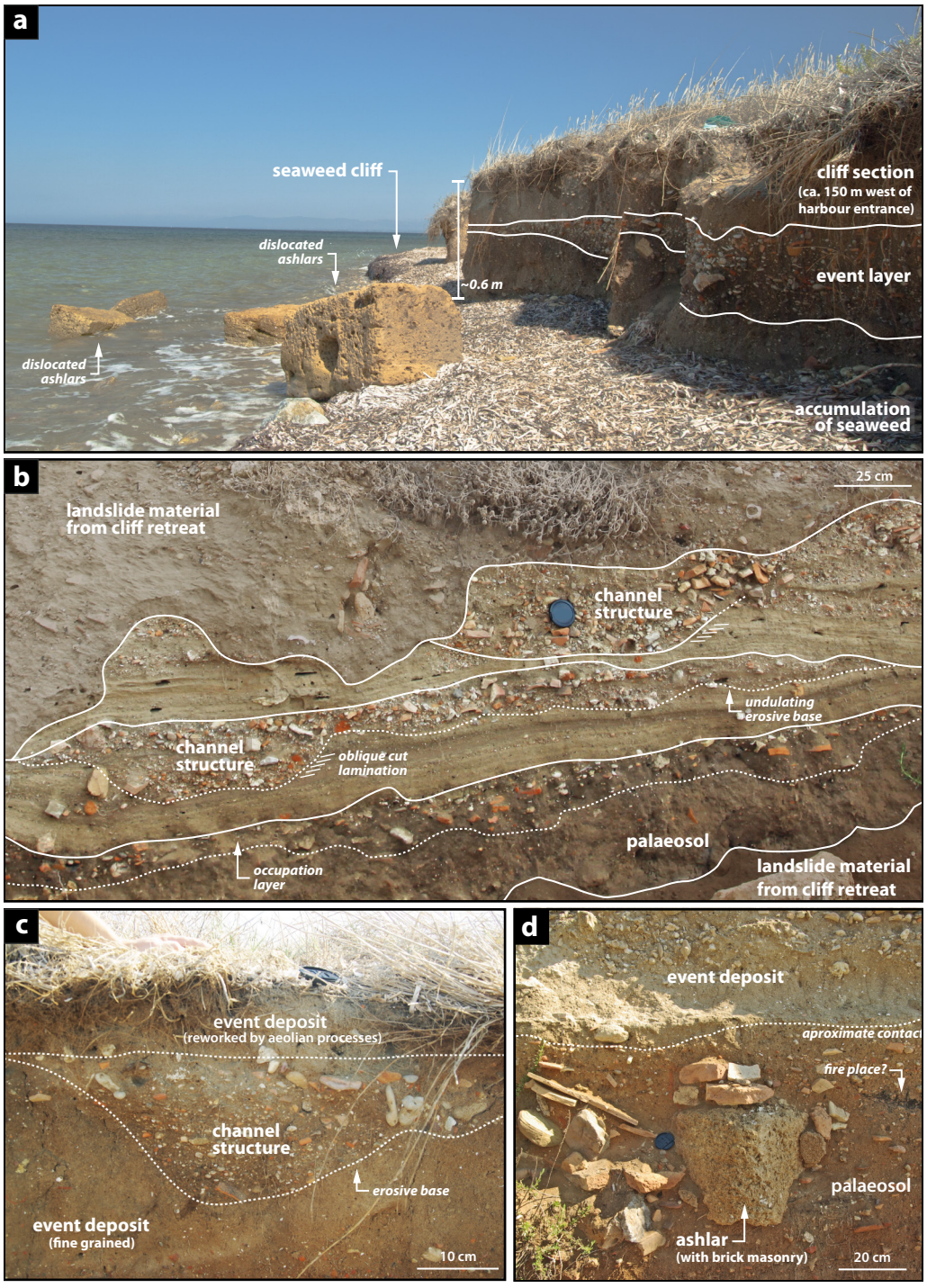

Fig. 5.11: Cliff section with geoarchaeological destruction layer to the west of the harbour entrance (a). In the westernmost part of the harbour, the layer overlies a palaeosol and occupation layer (b) with foundation remains (d). Sedimentary characteristics comprise lamination and fining upward-sequences (b). Seaward orientated channel structures are incised in the destruction layer. The channel fill comprises a mixture of terrestrial and marine deposits, including gravel, ceramic fragments and marine molluscs (b, c).

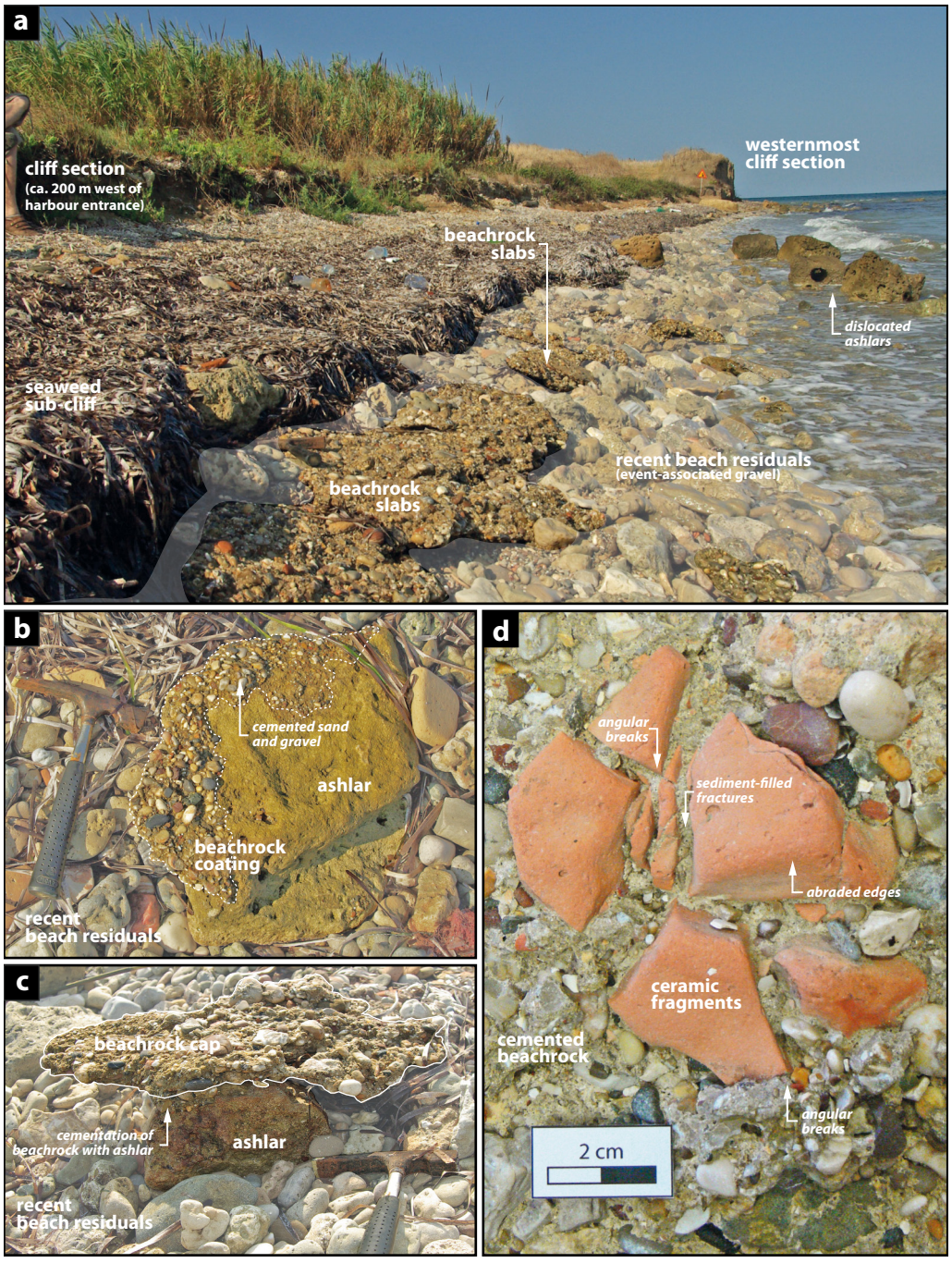

Fig. 5.12: Beachrock deposits at the Kyllini harbour site. Where the geoarchaeological destruction layer has been calcified posterior to deposition, calcarenitic beachrock-type slabs are exposed along the beach due to constant coastal erosion (a). Large ashlars that are incorporated into the beachrock slabs indicate high-energy deposition (b,c). Angular ceramic fragments with sediment-filled cracks in between document that destruction and deposition of the sherd were coincident (d).

5.7 Dating approaches

In order to establish a local event-geochronostratigraphy, 14 radiocarbon ages retrieved from six different vibracore locations are presented in this paper (Tab. 5.1). Non-marine plant material was preferred for dating, since the unknown spatio-temporal variability of the local marine reservoir effect still leads to considerable age deviations for marine samples (Reimer & McCormack 2002).

Dating samples were taken in maximal approximation to the upper and/or lower stratigraphical contacts. Samples taken from high-energy deposits merely provide a *terminus ad* or *post quem* (maximum age) for the event. If material for dating is retrieved beneath an erosive contact, the sample also yields a *terminus post quem* but the erosional hiatus remains unknown.

About half of the samples taken for radiocarbon dating consist of seaweed remains (KYL 2/8 PR, KYL 5/5, KYL 6/13+, PR KYL 7/12 PR). The unidentified plant remains of samples KYL 3/20+ PR must also be considered as seaweed since plant material from marine aquatic environments exhibits much smaller $\delta^{13}C$ values than known from terrestrial plants (Geyh 2005). For samples that feature marine $\delta^{13}C$ values, a marine reservoir effect was taken into account.

Due to the fact that the influence of spatial variations of the sedimentary environment or temporal variabilites of carbonate exchange on the marine reservoir age are still unknown, reservoir ages given in recent databases do only mirror local conditions for a specific time and are thus not transferable to other regions. Therefore, an average marine reservoir age of 408 years was used to calculate calendar ages using the Calib 6.0 software (Hughen et al. 2004, Reimer et al. 2004).

Tab. 5.1: Radiocarbon dates of samples from the outer Kyllini harbor site. Note: b.s – below ground surface; b.s.l. – below sea level; Lab.No. – laboratory number; KIA - Leibniz-Laboratory for Radiometric Dating and Isotope Research, Christian-Albrechts-University, Kiel; 1σ max;min (cal BP, cal BC/AD) – calibrated ages, 1σ range; ";" – there are several possible ages intervals due to multiple intersection with the calibration curve; * - marine reservoir correction with 408 years of reservoir age; a – comparative measurement of second prepared sample portion; b – significant age differences of > 2σ between original and comparative measurement; c – δ^{13} value indicates aquatic plant remain. Calibration based on Calib 6.0 software (Reimer et al. 2009).

Sample	Depth (m b.s.)	Depth (m b.s.l.)	Sample description	Lab. No. (KIA)	$\delta^{13}C$ (ppm)	^{14}C Age (BP)	1σ max; min (cal BP)	1σ max;min (cal BC/AD)
KYL 1/12+ PR	1.70	2.11	unident. plant remain	45997-1	-22.03 ± 0.11	2140 ± 25	2292; 2066	342; 116 BC
KYL 1/12+ PR[a]	1.70	2.11	unident. plant remain	45997-2	-21.69 ± 0.19	2125 ± 25	2148; 2061	198; 111 BC
KYL 1/17+ PR	4.85	5.26	unident. plant remain	45998	-26.80 ± 0.14	2110 ± 20	2125 – 2052	175 - 102 BC
KYL 2/8 PR	2.54	3.43	sea weed	45999	-15.52 ± 0.15[c]	2775 ± 25	2595; 2441	645; 491 BC*
KYL 3/4 HR	1.33	2.20	wood fragment	46000-1	-25.04 ± 0.11	2110 ± 25	2127 – 2044	177 - 94 BC
KYL 3/4 HR[a]	1.33	2.20	wood fragment	46000-2	-24.25 ± 0.20	2130 ± 25	2150; 2062	200; 112 BC
KYL 3/10 HR	3.29	4.16	wood fragment	46001	-30.41 ± 0.16	2310 ± 25	2350 – 2333	400 - 383 BC
KYL 3/20+ PR	6.86	7.73	unident. plant remain	46002	-15.20 ± 0.10[c]	7805 ± 40	8329 – 8223	6379 - 6273 BC*
KYL 5/5	1.625	2.585	sea weed	46003-1	-14.40 ± 0.09[c]	3100 ± 25	2920 – 2829	970 - 879 BC*
KYL 5/5[a]	1.625	2.585	sea weed	46003-2	-13.15 ± 0.27[c]	2945 ± 30[b]	2749 – 2701	799 - 751 BC*
KYL 6/13+ PR	2.545	1.085	sea weed	46004	-16.56 ± 0.21[c]	3510 ± 25	3428 – 3360	1478 - 1410 BC*
KYL 7/10 PR	1.98	1.21	wood/bone fragment	46005	-27.10 ± 0.11	2005 ± 25	1990 – 1929	40 BC - 21 AD
KYL 7/12 PR	3.325	2.555	sea weed	46006-1	-14.43 ± 0.12[c]	2460 ± 25	2147 – 2056	197 - 106 BC*
KYL 7/12 PR[a]	3.325	2.555	sea weed	46006-2	-14.36 ± 0.17[c]	2380 ± 20[b]	2051 – 1965	101-15 BC*

According to Wagner (1995) and Geyh (2005), reservoir effects for samples from C3 land plants, especially wood or charcoal, are negligible. $\delta^{13}C$ values obtained for samples KYL 1/12+ PR and KYL 1/17+ PR are typical of C3 land plants and therefore indicate a terrestrial origin. Samples KYL 3/4 HR, KYL 3/10 HR and KYL 7/10 PR also provide reliable ages for they comprised macroscopic wood fragments, as approved by the respective $\delta^{13}C$ values. For samples KYL 1/12+ PR, KYL 3/4 HR, KYL 5/5 and KYL 7/12 PR, additional radiocarbon ages have been retrieved from comparative measurements of a second prepared portion of the same sample. While samples KYL 1/12+ PR[a] and KYL 3/4 HR[a] provide consistent dating results within the fault tolerance, there are significant age differences (> 2σ) between the original and comparative measurement concerning samples KYL 5/5[a] and KYL 7/12 PR[a].

Across the Kyllini harbour site, 38 ceramic fragments were recovered from 10 different vibracores. 29 diagnostic sherds were ascribed to historical periods. The majority of ceramic finds date to Hellenistic to Roman times which fits well with the early phase of harbour usage.

5.8 Discussion

5.8.1 Tsunami impact at the Kyllini harbour site

For the Kyllini harbour site, detailed geo-scientific studies and geoarchaeological observations document repeated high-energy impact that influenced the foundation and history of the ancient harbour. The following geomorphological and geoarchaeological traces as well as detailed multi-proxy evidence reflect repeated marine-borne high-energy wave events.

(i) Pre-existing low-energy environments were repeatedly interrupted by the input of coarse-grained allochthonous deposits that exceed the prevailing energetic potential and document high-energy impact.

(ii) Basal erosional unconformities and rip up-clasts of eroded underlying deposits indicate that event was of abrupt temporary and high-energy character.

(iii) Several fining upward sequences from sand to silt with mud caps, partially being eroded, document repeated inflow, subsequent stagnation and backflow of water masses.

(iv) Sudden environmental changes took place after high-energy events, e.g. transitions from marine to lagoonal/limnic conditions or vice versa. As gradual environmental changes cause gradual transitions, abrupt changes are associated with extreme events.

(v) Geochemical and microfaunal data document the input of allochthonous marine deposits into a harbour basin and/or shallow marine environment.

(vi) In the inner harbour basin, a massive allochthonous sand layer covers quiescent lagoonal to semi-terrestrial deposits on top of a sharp erosional contact.

(vii) A geoarchaeological destruction layer that incorporates marine as well as terrestrial components extends about 250 m across the harbour area and covers ancient harbour facilities. Elevation, average grain size, thickness and lateral extent exceed by far recent coastal dynamics and document the widespread high-energy flooding of the harbour area. Angular ceramic fragments and intact shells exclude gradual sediment transport and reworking by littoral and/or colluvial processes but rather indicate a short transport distances and high-impulse sediment deposition within a short time period.

Throughout the year, prevailing winds from western and northwestern directions dominate the Ionian Sea and western Greece (Hofrichter 2002). As the propagation of wind-generated waves is a function of the respective wind directions, the (north-)westward orientated Kyllini Peninsula may especially be exposed to storm activity.

However, this area is quite well protected by the Ionian Islands with their high mountain ridges reaching up to 1600 m above sea level (Mt. Ainos/Cefalonia, Orama Ed. 2011) and forming kind of a protection shield for the inner Ionian Sea. Due to the restricted fetch (about 50 km), average wave heights along the coastline of the northwestern Peloponnese do not exceed 0.9 m during the winter month (Soukissian et al. 2008). On the contrary, maximum observed wave heights in the open Ionian Sea may reach 6-7 m with a maximum average wave height during winter is 1.8 m (Medatlas Group 2004, Soukissian et al. 2008)

Exceptional storm events of hurricane-like character occasionally develop in the Mediterranean (Fita et al. 2007). Known as so called Medicanes, these storms generally develop in the western Mediterranean and are accompanied by strong precipitation, heavy wind gusts and occasional flooding of low-lying coastal areas (Luque et al. 2007, Lionello et al. 2006, Tous et al. 2010). They also occur in the Ionian Sea (e.g. in 1995, Pytharoulis et al. 2000) but generally proceed in southeastern direction towards Africa and the Levante.

Palaeotempestological studies in the Mediterranean so far documented erosional damages of locally considerable dimensions at littoral dunes or coastal barriers (e.g. Ghionis et al. 2008). Geo-scientific studies on storm events (e.g. Andrade et al. 2004, Sabatier et al. 2008, 2010), also provided evidence of allochthonous thin layers of sandy storm deposits found, for instance, in near-shore littoral or lagoonal environments. However, only minor and locally limited landward transport of coarse-grained sediments (sand, silt) even during strong storm events is described (e.g. Sabatier et al. 2010). Additionally, it has been observed that even during strongest storms sea level maxima merely reach about +1 m (Krestenitis et al. 2011). Thus, major modifications of coastlines and lagoonal systems in the Mediterranean seem to be subject to repeated storm impact and do not occur during single events (Andrade et al. 2004). Consequently, neither winter storms nor Medicanes are suitable candidates to explain the abrupt environmental changes and sedimentary characteristics of high-energy deposits found at the Kyllini harbour site.

However, for the coastal area of the Kyllini peninsula a considerable tsunami risk arises from two different sources. Events may either develop on a supra-regional scale triggered along the Hellenic Arc, or may occur on a regional to local scale triggered by local tectonic fault systems (Papazachos & Dimitriu 1991, Maroukian et al. 2000). Offshore Kyllini, two major active normal faults paralleled the north-south trending graben of the Zakynthos Strait. As a consequence, the area shows a high seismic activity with a common occurrence of strong earthquakes, in cases associated with considerable vertical displacements (e.g. in 1953 along the eastern coastline of Zakynthos and Cefalonia, Brooks & Ferentinos 1984). For the 20th cent., Maroukian et al. (2000) list five earthquakes with magnitudes of M > 5.5. Many earthquakes caused local tsunami events as documented by historical records, e.g. in 1633 AD or 1820 AD (Maroukian et al. 2000).

For the Kyllini coastal area, submarine mass movements have to be taken into consideration as another factor that enhances the tsunami hazard. Their occurrence is frequent, triggered either by earthquakes or salt diapirism affecting the slopes of the Zakynthos graben system. Once induced, these slope failures may induce a chain reaction and cause further mass movements (Ferentinos et al. 1985).

For both, supra-regional or local events, tsunami waves will additionally be amplified by the submarine relief of the Zakynthos Strait and the coastal constellation of the Kyllini peninsula (Fig. 5.13). The Zakynthos graben system is subdivided in two parts, a steep sloped canyon that extends from Cape Katakolo in northern direction to the Kyllini promontory and the adjacent basin-like Zakynthos valley (Ferentinos et al. 1985, Maroukian et al. 2000). Since the canyon narrows from 23 km in the south to 8 km in the north and the water depth decreases in the same direction from 1800 m to 200 m, the structure features a remarkably funnel-like shape directly pointed at the Kyllini peninsula (Fig. 5.13., Ferentinos et al. 1985). Generally, decreasing water depth will cause increasing wave heights of approaching tsunami waters, while a constantly decreasing flow range may simultaneously lead to local channelling effects and increasing flow velocity (Sugawara et al. 2008).

Numerical simulation of tsunami wave propagation in the Gulf of Kyparissia by Röbke et al. (2013) shows that apart from the regional bathymetry, the local coastal constellation additionally affects tsunami wave dynamics. Although the Kyllini harbour site is situated in a leeward position for tsunami waves approaching from the south or west, strong refraction effects at the northern Kyllini peninsula (Fig. 5.13, inlay) are expected to redirect any approaching wave towards the southeast and cause flooding of the adjacent coastal areas (Ahnert 2009, Röbke et al. 2013).

Macro-scale consequences of tsunami impact on coastal systems

Tsunamis may cause major changes to established coastal constellations (Richmond et al. 2012). For example, tsunami waves are well capable of breaching coastal barriers and inundate lagoonal systems (e.g. Donato et al. 2008). In case of the 2011 Japan tsunami, breaching of a coastal barrier was associated with massive scouring on the landward side causing the establishment of a coastal lake (Tanaka et al. 2012).

Recent tsunami events also cause major damage to coastal infrastructure, as seen during the 2004 IOT or the 2011 Japan event and leave massive destruction layers incorporating cultural debris (Mimura et al. 2011). Comparable to the geoarchaeological destruction layer described from Kyllini, the modern equivalent consist of marine sediments mixed with building debris, everyday objects and organic remains. Channel structures in the event layer as visible along the Kyllini cliff section have also been observed for recent events, where backflow dynamics caused the incision of gullies up to 1 m in depth. Also, a bi-/multimodal grain size distribution and poor sorting of tsunami sediments, as observed for the channel fill, have been ascribed to backflow deposits Bahlburg & Spiske (2012).

Micro-scale characteristic features of tsunami sediments

Depending on the local topography, recent tsunami deposits are often deposited with a far landward extent (Gelfenbaum & Jaffe 2003) and associated sediments frequently overly the pre-tsunami surface with an erosional basal contact (Bahlburg & Weiss 2007). Comparable sharp contacts at the base of event layers were found at the Kyllini harbour site.

Different sedimentary structures observed for tsunami-associated deposits in the study area have also been found for recent tsunami sediments. Characteristic features comprise fining upward sequences (Gelfenbaum & Jaffe 2003), a distinct layering (parallel-laminated) (Bahlburg & Weiss 2007) caused by shifting flow dynamics and rip up-clasts, mud caps and organic caps as indicators of intense reworking and stagnation of flow velocities (Gelfenbaum & Jaffe 2003, Chague-Goff et al. 2011). A disturbed or atypical macro- and microfossil content)

or characteristic geochemical patterns as described for the Kyllini site have also been attested for recent tsunami deposits (Bahlburg & Weiss 2007, Donato et al. 2008, Chague-Goff et al. 2011, 2012).

Against the background of the local geomorphological setting as well as the sedimentary, geochemical and microfaunal characteristics of the event layers originating from the seaside, the repeated high-energy impact on the ancient harbour site of Kyllini must be of tsunamigenic origin. For the Ionian Sea and the western Peloponnese, Vött et al. (2011b) and Willershäuser et al. (2013) provide similar evidence of palaeotsunami impact.

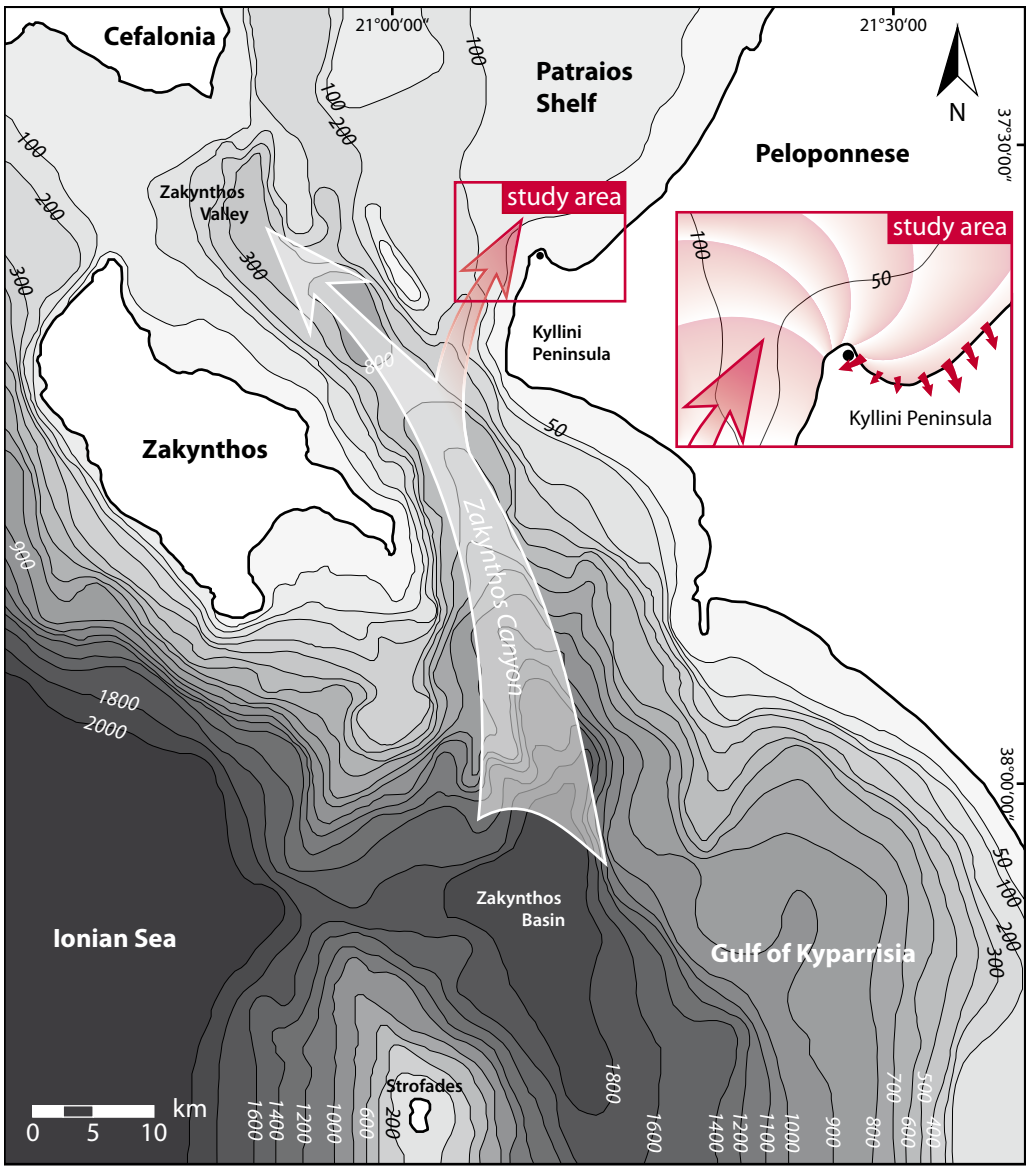

Fig. 5.13: Bathymetrical constellation offshore Kyllini. Refraction of tsunami waves along the peninsula will cause flooding of the harbour site (inlay). Map modified after Ferentinos et al. (1985), scenario modified after Röbke et al. (2013).

5.8.2 Geoarchaeological evidence of tsunami impact – beachrock-type tsunamites

Based on detailed geo-scientific findings in several coastal sections of western Greece, beachrock-type calcarenitic deposits were identified as high-energy deposit related to tsunami impact (VÖTT et al. 2010, HADLER et al. 2013). Post-depositional decalcification of ex-situ marine sediments followed by subsequent recrystallization cause the cementation of parts of the tsunamigenic sediments (VÖTT et al. 2010).

Concerning the Kyllini beachrock, this study provides distinct evidence that the local outcrops do not present lithified beach deposits but exhibit features related to tsunami impact.

(i) The Kyllini beachrock is in perfect stratigraphical correlation with high-energy tsunami deposits visible along the Kyllini cliff and in different vibracore stratigraphies.

(ii) At present, the beachrock isin a state of subsequent destruction due to littoral wave action. No recent beachrock formation can be observed.

(iii) Sherds found embedded in the beachrock provide evidence for a rapid deposition without further reworking (Fig. 5.12d). While loose ceramic fragments along the beach are exposed to wave action and appear well rounded (FÜCHTBAUER 1988), fragments in the beachrock show angular breaks and have thus not been reworked prior to or after deposition.

(iv) The Kyllini beachrock even contains matching ceramic fragments in the state of breakage (Fig. 5.12d). As the cracks between the fragments are filled with sediment, the sherd obviously broke when being incorporated into the deposit without further reworking.

The stratigraphical correlation of the Kyllini beachrock with nearby high-energy event deposits proves it to represent a lithified section of a complex tsunamite unit. Post-depositional cementation of the event layer visible along the cliff obviously led to beachrock formation, while present-day wave action uncovers the lithified parts and erodes the non-calcified sediments above and below. Due to its event-related origin, the calcarenitic beachrock-type tsunamite at Kyllini must not be used as sea level indicator (VÖTT et al. 2010, HADLER et al. 2013).

5.8.3 Tsunami impact and the Kyllini harbour evolution - establishing a local geochronostratigraphy

Radiocarbon ages as well as age estimations obtained for diagnostic ceramic fragments from the Kyllini harbour site were used to establish a local event-geochronostratigraphy.

Tsunami generation I and the time of harbour use

For tsunami generation I, sample KYL 2/8 PR yielded 645-491 cal BC as *terminus ad* or *post quem*. Moreover, sample KYL 3/10 HR yielded 400-383 cal BC as terminus ante quem for the same impact. As the sample was retrieved from the lowermost lagoonal-type harbour deposit, this radiocarbon age also provides a *terminus ad* or *ante quem* for the foundation of the harbour site that fits well the historical reports about an active harbour from the beginning of the 5th century BC onwards. Diagnostic ceramic fragments from the lowermost harbour deposit at site KYL 8 and a test core close by were assigned to the Classical to Hellenistic period (5th to 3rd cent. BC) representing a corresponding *terminus ad* or *ante quem* for the beginning of the Kyllini harbour (Fig. 5.14). Tsunami generation I preceded the foundation of the harbour and, according to the presented dates, hit the coastal embayment at Kyllini between the mid 7th and early 4th cent. BC.

Since the majority of ceramic fragments originates from the Hellenistic to Roman period, the most intense phase of harbour usage in ancient times obviously occurred between the 4th and 1st cent. BC.

Concerning the mid-harbour basin, the observed transition from sheltered harbour to shallow marine conditions was dated to 177-94 cal BC and 200-112 cal BC (sample KYL 3/4 HR) and 197-106 cal BC and 101-15 cal BC (sample KYL 7/12 PR). As the latter sample comes from the very contact between the lagoonal and shallow marine facies, this age provides the besit-fit *terminus ad quem* for the end of the sheltered harbour. A thick layer of homogeneous marine sand in the harbour entrance at coring site KYL 1 was deposited during a very short time period. While the lower part was dated to 175-102 cal BC (sample KYL 1/17+ PR), the upper section was dated to 342-116 cal BC and 198-111 cal BC (sample KYL 1/12+ PR. With regard to the sudden environmental change that simultaneously affected the mid-harbour basin and considering that consistent stratigraphical interferences have not been found elsewhere, it has to be assumed that this massive depositional event was caused by the destruction of protecting harbour infrastructure (i.e. walls or moles) so that shallow marine conditions were re-established.

Tsunami generation II

Sample KYL 7/10 PR yielded 40 cal BC-21 cal AD as *terminus post quem* for tsunami generation II. Since the degree of tsunamigenic erosion remains unknown, the date must be considered as maximum age. Diagnostic ceramic fragments incorporated in the event layer provide another *terminus ad* or *post quem* for the tsunami that is consistent with radiocarbon dating indicating an event during Roman to Byzantine times (samples KYL 5/3+ K, KYL 9/4+ K, KYL 8/6+ K3, sample from test core). The youngest diagnostic sherd was dated to the 4th to 6th cent. AD (Tab. 5.2, Fig. 5.14). Therefore, a 4th to 6th cent. AD age seems to be most plausible for tsunami generation II. In correlation to historical accounts on major tsunami events, tsunami generation II may be associated with the 365 AD or 522/551 AD tsunami events (Ambrasey 2009).

5.8.4 Evaluating the Kyllini harbour site as geo-archive for palaeotsunami research

In order to best assess the hazard potential of a coastal area, the maximum time span of a geo-archive is relevant to gain a most complete palaeotsunami record. As derived from the presented results and in accordance to historical accounts, the foundation of the Kyllini harbour site dates to the late 5th century BC. Already affected by siltation in the 1st cent. BC/AD, geo-scientific studies document a final destruction of the Greek harbour site by tsunami impact between the 4th and 6th cent. AD. Accordingly, the ancient harbour was used between 400 and 800 years at a maximum.

Based on the present results, major tsunami events at Kyllini seem to recur every 1000 years. The local return period thus exceeds the phase of harbour usage by far. However, earliest marine deposits at the Kyllini harbour site were dated to 6.4-6.3 ka cal BC (Fig. 5.5, Tab. 5.1) thus providing a stratigraphical record of more than 8000 years. Evidence of early tsunami impact is most likely preserved at vibracoring site KYL 6, where a thick basal deposit incorporating marine macrofossils overlies the local bedrock (Fig. 5.5). Dated to around 1500 BC (*terminus ad* or *post quem*), the deposit fits the estimated local return rate of 1000 years. As shallow marine environments generally provide a minor preservation potential, no further traces of tsunami impact are preserved in the lower marine deposits at the harbour site. It can thus be stated that the harbour basin itself – although it comprises only a restricted time span – provides a better

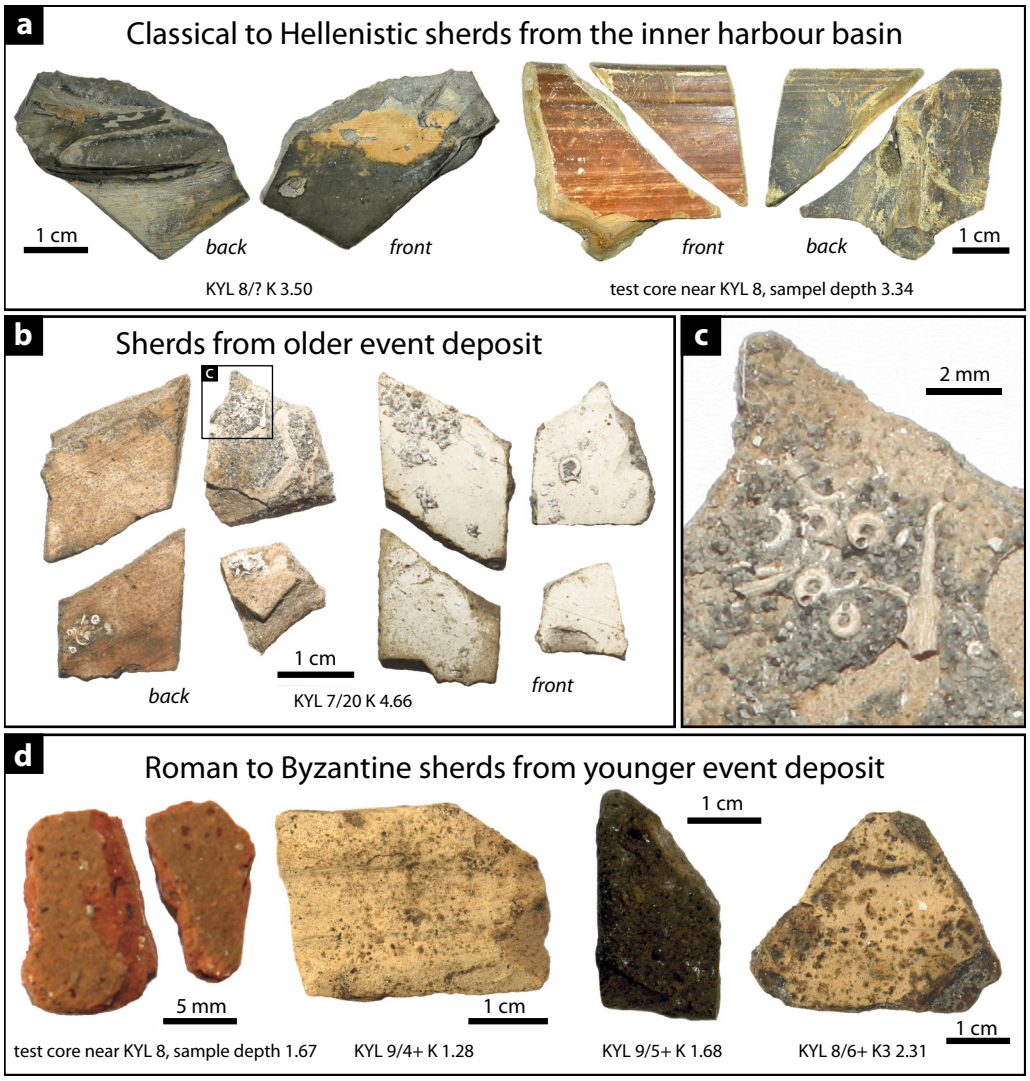

Fig. 5.14: Ceramic fragments encountered at the Kyllini harbour site. Classical to Hellenistic sherds provide evidence of a 5th cent. BC foundation of the harbour (a). Sherds incorporated to the older event deposit (b,c). Roman to Byzantine sherds from the 4th – 6th cent. AD provide a terminus post quem for the younger tsunami generation (d).

preservation potential for palaeotsunami traces as the pre-harbour natural embayment.

In a supra-regional context, the different tsunami generations encountered in the Kyllini harbour basin are quite likely related to known major events and tsunamites published for the Ionian Sea. While tsunami generation I is probably associated to a supra-regional event that affected Cefalonia (Willershäuser et al. 2013) as well as Sicily (Smedile et al. 2011), tsunami generation II seems to be related to the 365 AD or 551 AD tsunami that are attested by geo-scientific evidence throughout the eastern Mediterranean (e.g. Pirazzoli et al. 1996, Bernasconi et al. 2006, Vött et al. 2009b, 2011b, Smedile et al. 2011). Although local tectonics bear a significant potential for tsunami events, it seems that only traces of supra-regional tsunami impact are preserved in the geo-archive of Kyllini. It is thus concluded, that local events – although they occur more frequently – constitute a minor hazard than supra-regional mega tsunamis.

Like other harbour sites (e.g. Pheia, VÖTT et al. 2011b, Yenikapı, BONY et al. 2012, or Lechaion, HADLER et al. 2013), the destruction of the Greek harbour facilities at Kyllini is closely related to palaeotsunami impact. On the other hand, tsunami-generated coastal changes in the first place favour the foundation of the harbour. Kyllini thus emphasizes the close interdependency of ancient settlements and palaeotsunami events and provides valuable results for palaeotsunami research.

5.9 Conclusions

(i) Repeated tsunami impact on the Kyllini harbour site was identified from sedimentological, geomorphological, geochemical and microfossil analyses of selected sediment samples from the Holocene stratigraphical record.

(ii) Tsunami generation I hit the coast between the mid 7th to early 4th cent. BC while tsunami generation II took place between the 4th and 6th cent. AD or later.

(iii) Major tsunami events seem to recur in an average period of around 5 centuries.

(iv) In accordance to historical accounts, the Kyllini harbour started to operate in the 5th cent. BC. The harbour was built shortly after event generation I took place and is probably associated with a tsunamigenic modification of the coastline that caused the formation of a coastal lake/lagoon. The harbour was in use at least until the 1st cent. AD.

(v) Starting in the 2nd cent. BC, the mid-harbour basin and the harbour entrance channel experienced strong siltation due to the probable destruction of protecting harbour installations.

(vi) Posterior to siltation, the inner harbour basin has been subject to tsunamigenic burial by event generation II. Weathering of the tsunami deposits documents the final transition from lagoonal to terrestrial conditions.

(vii) No evidence of a re-activation during Frankish time was found in the inner harbour basin. We must therefore conclude that during the Frankish period, the inner harbour basin was still blocked as a consequence of tsunami impact II and harbour usage was limited to the mid- and outer basins.

(viii) In the mid- and outer harbour basin, merely thin layers of event generation II are preserved. Exposed on the recent sea floor, the event layer has either been eroded by constant wave action and longshore drift or excavated by dredging activity during the Frankish period.

(ix) In a synoptic view, the history of the ancient harbour site of Kyllini is closely related to tsunami impact, since the foundation as well as destruction of the inner harbour basin are preceded and followed by tsunami events.

6. The significance of ancient harbours for palaeotsunami research - a synoptic view

Throughout the eastern Mediterranean Sea, the constant threat of tsunami impact has been reviewed within this study (*Chapter 1*). The analysis of historical records about tsunami events in the Ionian Sea and the Gulf of Corinth (*Chapter 2*) clearly emphasized the need for further geo-scientific research in order to enable a reliable assessment of the tsunami risk along eastern Mediterranean shores. To estimate the frequency of major tsunami events and to evaluate their effects on (ancient) coastal settlements in the Ionian Sea, the Gulf of Corinth and along the W-Peloponnesian coastline, the ancient harbour sites of Krane (*Chapter 3*), Lechaion (*Chapter 4*) and Kyllini (*Chapter 5*) proved to be valuable geo-archives for palaeotsunami research. In the following, the obtained results are compared in a synoptic view to assess the significance and applicability of ancient harbour sites in terms of palaeotsunami research and tsunami hazard assessment.

6.1 The influence of coastal geomorphologies on the local tsunami hazard

The conservation and detection of palaeotsunami traces in geo-archives is a basis for geo-scientific palaeotsunami research. Regarding ancient harbour sites, the probability of detecting traces of palaeotsunami events in the stratigraphical record is the higher, the more a site is endangered by tsunami hazard. As distinct high-energy event-related deposits were identified from the stratigraphical record of Krane, Lechaion and Kyllini, the selected harbour sites seem to be especially prone to tsunamigenic impact. As demonstrated by recent events (e.g. Chile 2010, Japan 2011), both the coastal constellation and the local geomorphological setting have a major influence on the intensity of tsunami landfall in terms of inundation and maximum run-up. Thus, the risk of tsunami impact always has to be reviewed in reference to a study areas' local setting.

In the study area of Krane, the funnel shaped entrance to the Gulf of Argostoli already causes an amplification of approaching waves, whereas refraction effects at Cape Theodorou further intensify the tsunami hazard, even for well-protected embayments like the Koutavos Bay (Chapter 3). The narrow passage to the inner bay may cause an impoundment of water in the rearmost part of the lagoon and consequently lead to a flooding of the adjacent Koutavos coastal plain.

Although the harbour site of Lechaion is situated in the tectonically less active part of the Corinthian Gulf, earthquakes and submarine slides triggered by offshore faults as well as steep submarine slopes at the entrance to the Lechaion Gulf enhance the risk of tsunami events (Chapter 4). Waves that propagate through the Lechaion Gulf from the north(-west) will inevitably inundate the low-lying coastal plain of the Corinthia in the south.

At Kyllini, the tsunami hazard is related to the local as well as supraregional tectonic constellation. In each case, however, the cape-like structure of the Kyllini peninsula will lead to strong wave refraction that redirects any approaching wave in the direction of the harbour site (Chapter 5). Even though situated in one of the most sheltered locations along the Peloponnese, the regional geomorphological constellation puts a major tsunami risk on the harbour site of Kyllini.

In comparison, it has to be stated that although each study area is characterized by individual coastal settings that differ considerably from one another, the coastal constellation of every harbour site seems to increase the risk of major tsunami impact. As similar effects must be expected for other coastal areas, the implication for tsunami risk assessment must be, that, apart from an exposition to tectonically active zones, the local topography has to be considered when evaluation strategies in hazard management.

6.2 Evaluating the palaeotsunami record of ancient harbour basin stratigraphies

By comprehensive geo-scientific investigations, four different generations of tsunamigenic impact have been identified for the ancient harbour site of Krane, while the stratigraphical record at Lechaion provided evidence of three high-energy interferences. At Kyllini, traces of tsunami impact were at least found twice. With the exception of Krane, the geo-archives provide significant traces of tsunami impact that affected the shallow marine pre-harbour as well as lagoonal harbour environments. No traces of tsunami impact are evident in the post-harbour environments at Lechaion and Kyllini. In case of Krane, consistent natural lagoonal conditions impede a sedimentary differentiation between pre-harbour, harbour or post-harbour environments.

Sedimentary evidence of tsunami impact derived from the pre-harbour shallow marine environs of Lechaion and Kyllini, comprises (i) the input of allochthonous marine sediments as well as (ii) significantly disturbed microfaunal assemblages with an increased amount of planktonic species and/or species from deeper water. At Krane, (iii) shell debris layers associated with high-energy impact repeatedly intersect alluvial fan deposits in the vicinity of the lagoonal embayment.

Traces of tsunami impact derived from the harbour basin and lagoonal facies at Lechaion and Krane, respectively, comprise (iv) strongly reworked autochthonous deposits as well as (v) the input of coarse grained deposits like sand, stones or gravel. Additionally, (vi) grain size analyses and (vii) geochemical ratios emphasize the high-energy character and marine origin of the event deposits encountered at both study areas. At Kyllini, no tsunamigenic deposits were found intersecting the harbour facies.

Nevertheless, (viii) a thick geoarchaeological destruction layer that comprises marine as well as terrestrial and anthropogenic components (marine fossils, gravel, charcoal, bones, and ceramic fragments) overlies the harbour facies at Lechaion and Kyllini. At both sites, the lower part of the destruction layer (ix) is subject to post-depositional solution and subsequent precipitation of calcium carbonate. As a result, (x) beachrock-type calcarenitic tsunamites occur along the recent coastlines of Lechaion and Kyllini.

6.3 The applicability of ancient harbour basin stratigraphies for tsunami risk assessment

Unlike most natural near-coast geo-archives (e.g. lagoons or back-beach swamps), the preservation of high-energy traces in harbour basins as well as the reliability of the palaeotsunami record are closely related to human interferences (?). This fact must especially where the stratigraphical record of ancient harbour basins is evaluated for palaeotsunami research.

As the existence of most harbour basins is bound to human settlement activity and maintenance of the harbour site, the time span that is covered by a harbour's stratigraphical record is closely related to the political and economic significance of the associated settlement. In order to assess

the probability of future events, the availability of long-term data is particularly significant to calculate reliable return rates since major tsunamis can be rare events that probably occur every 500 or 1000 years (Chapter 2). Thus, another factor that has to be considered where ancient harbours are used as palaeotsunami geo-archive is the maximum period of time the respective archive covers. Historical accounts on the specific site may provide a first approximation to the timeframe of active harbour usage.

For Krane, only little historical evidence is given on the usage of the harbour. Although the Bay of Koutavos has most probably been used for centuries as a sheltered natural anchorage, merely 200 years of harbour activity are attested for the ancient settlement (Fig. 6.1, Chapter 3). Thus, the active phase of harbour usage is by far too short to estimate reliable return rates for major events. Nevertheless, the natural character of the harbour site with a continuous lagoonal environment provides suitable “harbour-like” conditions throughout the past six millennia.

For the Lechaion geo-archive, historical accounts as well as geo-scientific evidence attest an active harbour usage for at least 1000 years (Fig. 6.1, Chapter 4). From a statistical point of view, the harbour basin has quite likely been struck by a tsunami event of millennial character. In Kyllini, geo-scientific studies provide evidence of a harbour basin used for about five centuries during Classical to Hellenistic times, but no sediments of the literary well known and by archaeological evidence attested Frankish harbour phase were found. From the present data, the time span of the archive is obviously limited to about five centuries, although nearly twice the timespan had to be expected from literary descriptions.

Apart from a limited time span, dredging activity in historic times may disturb or even delete all traces of tsunami impact that occurred during the active phase of harbour usage. In case of artificially laid out harbour sites, the initial excavation of the basin during harbour foundation may additionally delete potential traces of tsunami impact preserved in the pre-harbour natural environment. Hence, event layers identified from the stratigraphical record must always be considered as a minimum of tsunamigenic interferences, where the stratigraphical record of a harbour sites provides any evidence of digging and/or dredging.

Apart from anthropogenic dredging activity, harbour installations also affect the preservation potential of palaeotsunami traces. Where fortifications protect harbour sites from storm activity, most likely the surrounding walls also provide shelter against minor tsunami events that – as a consequence – will not be recorded in the geo-archive. Although harbour resonance induced by minor events may cause a disturbance in the stratigraphical record, the associated event layer will be hard to identify when harbour deposits are reworked but no allochthonous sediments are deposited.

In case of Krane, the stratigraphical record of the harbour site seems to be least restricted to and influenced by human settlement activity, since the geo-archive is located in a natural lagoonal embayment. Derived from archaeological evidence and historical records, a fortified harbour at Krane existed – if at all – for only two centuries (Fig. 6.1), so most likely no artificial barriers (e.g. fortification walls) impede the impact of tsunami events to the embayment. Regarding the restricted settlement activity at Krane and the continuous existence of the quiescent lagoonal system, only minor anthropogenic disturbances of the stratigraphical record must be expected. In contrast, Lechaion and Kyllini are described as strongly fortified by walls and were thus most likely protected against minor tsunami events. Nevertheless, the isolated and sheltered location of the natural harbour at Krane restricts the input of marine sediments to the archive. While

major events were clearly identified by reworking of autochthonous lagoonal deposits and in cases even the input of marine sand, smaller events have probably been overlooked as they are likely to leave only minor traces of disturbance. Lechaion and Kyllini, on the other hand, are directly exposed to the marine environs of the Gulf of Corinth and the Ionian Sea, respectively, so that major tsunami events are expected to leave a distinct and easy recognizable marine signal in the stratigraphical record of each harbour site.

In terms of stratigraphical completeness, the most reliable sedimentary record can probably be assumed for Krane, since a dredging of the natural lagoonal environment seems quite unlikely. Obvious traces of dredging activity were merely identified for Lechaion. As derived from stratigraphical correlations, especially the Roman re-foundation of Corinth in the 1st cent. BC must be associated with the extension and simultaneous dredging of the harbour basin (Chapter 5). At Kyllini, apparently no dredging has been carried out in the inner harbour basin whereas the mid-harbour basin has obviously been cleaned during the Frankish usage of the harbour (Chapter 5).

In a summary, it can be stated that despite all anthropogenic activity, distinct sedimentary traces of tsunami impact are preserved at each study area. The selected ancient harbours proved to be particularly suitable to decide, whether an area has already been subject to tsunamigenic impact and may thus be threatened by future events. With regard to the completeness – and by association the reliability – of the palaeotsunami record recovered from the respective geo-archive, one has to keep in mind that every study area is subject to the specific natural setting and settlement history. Whether the local geomorphology or anthropogenic activity determine and/or modify the palaeotsunami record of a geo-archive, it will hardly be possible to establish a site-specific palaeotsunami history without a gap. Either way, a harbour site will only provide the minimum number of tsunami landfall for the respective coastal area. As a basis for future tsunami risk assessment, the different event generations detected in the harbour basins of Krane, Lechaion and Kyllini must always be regarded as minimal while the actual hazard potential may as well exceed the evaluated risk. Tsunami return periods calculated from harbour basin stratigraphies thus only provide a maximum timespan between major events.

6.4 The tsunami history of Krane, Lechaion and Kyllini in a supra-regional context

As illustrated above, single geo-archives are hardly ever capable to provide a continuous record of the local palaeotsunami history. It is the correlation of different archives from various study areas that successively fills in the gaps in the chronology of palaeotsunami events, especially in terms of major supra-regional impacts. Traces of tsunami impact deciphered within this study cover a time span from 4000 BC onwards. In the following, results are compared to palaeotsunami events known from historical records or identified for different coastal areas in the eastern Mediterranean by geo-scientific studies (see Fig. 6.1).

As expected from the coastal constellation in the Gulf of Argostoli (Chapter 3), the local tsunami chronology for ancient Krane seems in good accordance to palaeotsunami signals from the nearby coastal plain of Lixouri (Paliki peninsula/Cefalonia, Willershäuser et al. 2013). Oldest traces of tsunami impact that were encountered at Koutavos as well as Lixouri are also suitable candidates for supra-regional events that occurred around 4300 BC and 2900 BC, respectively. Potentially correlating traces of tsunami impact are attested for different coastal areas in northern

Akarnania (Vött et al. 2011a, May et al. 2007). The older tsunami candidate obviously also hit the western Peloponnese, as indicated by related tsunamites encountered at Pheia, the ancient harbour site of Olympia (Vött et al. 2011b). It must be noted, however, that no comparable evidence has been found for Kyllini.

Dated to around 1600 BC (Friedrich et al. 2006), the eruption of Thera (Santorini) is associated with a supra-regional tsunami that affected wide areas of the eastern Mediterranean. Geo-scientific evidence of the associated tsunami was found for Caesarea Maritima (Goodman-Tchernov et al. 2009) and probably also Sicily (Smedile et al. 2011). At Kyllini, the oldest event deposit was dated to around 1500 BC and therefore – even within the dating inaccuracy – rather postdates the Santorini tsunami.

For a younger event generation that hit the Bay of Koutavos sometime posterior to the 8th cent. BC, radiocarbon ages merely provide rough *termini post quos* that impede a reliable correlation with other study areas. Comparable tsunami signatures were identified for the Bay of Lixouri by Willershäuser et al. (2013). Furthermore, Smedile et al. (2011) found temporally consistent event layers in eastern Sicily (Augusta Bay,) that possibly attest a supra-regional character of the tsunami, probably generated in the open Ionian Sea. Within the limit of dating insecurities, oldest traces of tsunami impact found for Kyllini may also correspond to a supra-regional post-8th cent. BC event. As the tsunami deposit at Kyllini definitely predates the harbour foundation, the impact could have most likely occurred around the 6th cent. BC. In this case, the tsunami-related destruction of Krane in the late 3rd cent. BC seems rather unlikely, though. Nevertheless, around 300 BC tsunami impact is attested for Akarnania (Vött et al. 2009b) and Sicily (Smedile et al. 2011) that probably affected Cefalonia as well.

Temporary consistent traces of tsunami impact for the 8th-6th cent. BC were also identified for the Lechaion harbour site. Even though tsunami waves are known to propagate from the Ionian Sea into the Gulf of Corinth, the isolated location in the easternmost part of the gulf rather suggests an independent local event-geochronology for the study area. The same is true for the 1st cent. AD event encountered at Lechaion which should as well be regarded as local.

Throughout the eastern Mediterranean, geo-scientific studies increasingly identify sedimentary traces of the 365 AD mega-tsunami, well described by ancient literary sources. Associated deposits were found for northwester Greece (Akarnania, Vött et al. 2009b), the Peloponnese (Vött et al. 2011b), Crete (Pirazzoli 1992) and eastern Sicily (Smedile et al. 2011) but also along the north African coast, e.g. for the ancient harbour of Alexandria (Stanley & Bernasconi 2006). Within this study, the mega tsunami may be related to the destruction of Kyllini, where the youngest tsunami generation has been dates to the 4th to 6th cent. AD. Due to dating inaccuracies, the tsunamigenic destruction of the harbour may equally be associated with a series of earthquake clustering from the 4th to 6th century BC (Early Byzantine tectonic paroxysm, Pirazzoli et al. 1996). Evidence of increased tsunami landfall on a local as well as supra-regional scale dating to around 551 AD was for example identified for the harbour of Caesarea Maritima (Goodmann-Tchernov et al. 2009), Yenikapı (Bony et al. 2012) or Pheia (Vött 2011b). Within this study, coinciding tsunami deposits were found for the ancient harbours of Lechaion (chapter 4) and probably also Kyllini (chapter 5). In cases, the isolated locations of the different harbours (e.g. Lechaion, Yenikapı) rather exclude the influence of a supra-regional mega tsunami, while evidence from Pheia, Kyllini and probably even Caesarea Maritima support an event of supra-regional character.

The youngest event identified within this study affected ancient Krane around 900 AD or later. Temporally coinciding tsunami deposits are published for the nearby coastal plain of Lixouri (WILLERSHÄUSER et al. 2013), Akarnania (VÖTT et al. 2009a) and again Sicily (SMEDILE et al. 2011). Thus, the youngest event again seems to be of (supra-)regional character.

In a summary it can be stated, that the studied harbour sites of Krane and Kyllini obviously provide traces of major supra-regional tsunami events whereas Lechaion was rather subject to local events.

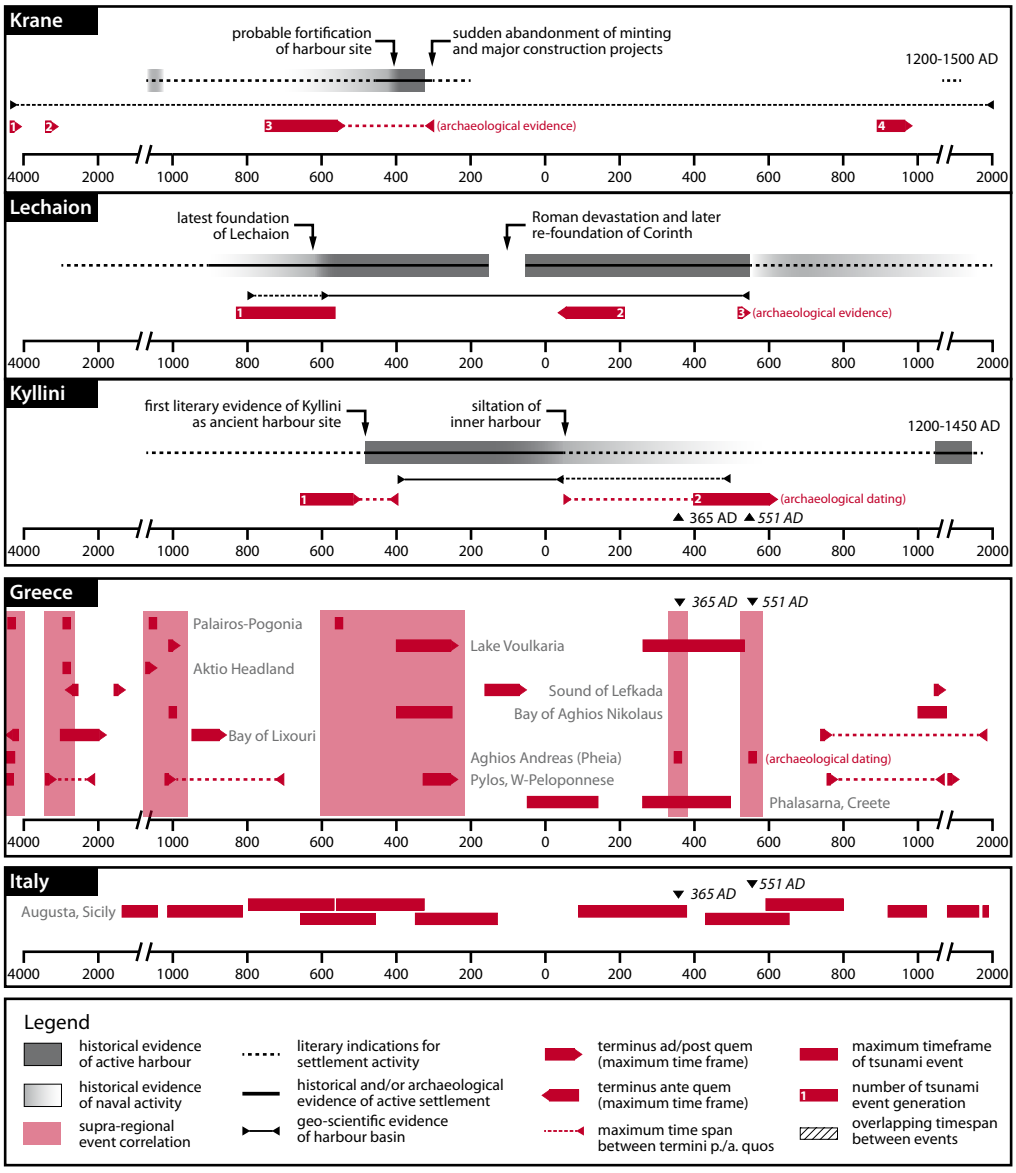

Fig. 6.1: Geo-scientific traces of tsunami impact for the Ionian Sea (compiled after Pirazzoli et al. 1992, May et al. 2007, Smedile et al. 2011, Vött et al. 2009a, 2009b, 2011a, 2011b, Willershäuser et al. 2013).

6.5 Palaeotsunami impact and ancient settlements

The severe consequences of major tsunami impact on coastal area were strikingly demonstrated by recent events (i.e. Japan 2011). Comparable effects of palaeotsunami impact can be assumed for ancient coastal settlements and associated infrastructure, i.e. harbour facilities). Although literary evidence on such events is sparse, two out of three harbour sites investigated within this study were certainly destroyed by major tsunami events. At Lechaion as well as at Kyllini, the widespread tsunamigenic burial of harbour basin caused the final abandonment of the site. In case of Krane, the relationship between tsunami impact and ancient settlement activity remains unclear.

Besides devastating effects, palaeotsunami events also turned out to be advantageous for ancient settlement activities. At Lechaion and Kyllini, major tsunami events precede the foundation of both harbour sites (Figs. 4.3, 5.5 and 6.1). As derived from the respective stratigraphical sequences, the high-energy impact has in each case been related to significant modifications of the ancient coastline. Posterior to the event generation I, the shallow marine environment at Kyllini changed into a coastal lake – the predecessor of the later harbour basin. At Lechaion, tsunamigenic sediment deposition obviously formed a coastal barrier with an adjacent shallow marine depression that favoured the foundation and excavation of an artificial harbour basin.

Considering the historical record available for each harbour site, is must be noted that even for well documented sites like Lechaion, no ancient account is known that report on tsunamigenic impact, not to mention the destruction of the site. Whether or not an account was written, the geo-scientific evidence presented within this study again emphasizes the wide gap in the historical record. Additionally, it stresses the need for further geo-scientific studies to better assess the consequences of palaeotsunami events as well as the risk of future impacts.

6.6 Perspectives

The present study aimed (i) at the identification of palaeotsunami traces in ancient harbour basins of the eastern Mediterranean, in order (ii) to establish a local event-geochronology and (iii) to evaluate the vulnerability and hazard potential for different coastal areas. In view of the fact that the fragmentary historical record on tsunami events neither provides a reliable base to sufficiently recognize areas tsunami risk nor allows the development of appropriate risk mitigation strategies, geo-scientific evidence of palaeotsunami events in the eastern Mediterranean becomes increasingly significant.

As the present results show, ancient harbours are well capable of preserving evidence of major tsunami impact and thus provide valuable geo-archives to complement our knowledge on the occurrence and frequency of palaeotsunami events. However, most harbours in the Mediterranean were so far not investigated against the background of tsunami impact. Thus, our knowledge on the influence of tsunami hazard on ancient settlements still remains sparse. In terms of present day risk assessment, the estimation of effects of previous tsunami impact may provide a valuable basis for the establishment of prevention measures, though. Comprehensive research on tsunami events based on ancient harbour sites is a promising approach and should hence be intensified, especially for areas not yet in the focus of tsunami hazard.

However, it will most likely remain difficult to gather comprehensive data on the vulnerability of coastal areas by geo-scientific investigation alone, e.g. due to missing archives, bad preservation

potential or high settlement density. Here, the numerical simulation of tsunami events based on field evidence may provide an area-wide assessment of the tsunami risk and enable mitigation strategies were needed. With the increasing future use of Mediterranean coastal areas either for settlement, recreation or economic purpose, a reliable hazard assessment and prevention for highly tsunamigenic areas like the eastern Mediterranean seem more important than ever.

References

Åberg, G., Charalampides, G., Fosse, G. & Hjelmseth, H. (2001): The use of Pb isotopes to differentiate between contemporary and ancient sources of pollution in Greece. – Atmospheric Environment 35: 4609-4615.

Ad-hoc-Arbeitsgruppe Boden (2005): Bodenkundliche Kartieranleitung. – Schweizerbart, Stuttgart, 438 pp.

Ahnert, F. (2009): Einführung in die Geomorphologie. – UTB, Stuttgart: 393 pp.

Albarède, F. (2009): Geochemistry. An Introduction. – Cambridge University Press, Cambridge: 342 pp.

Alvarez-Zarikian, C.A., Soter, S., & Katsonopoulou, D. (2008): Recurrent Submergence and Uplift in the Area of Ancient Helike, Gulf of Corinth, Greece: Microfaunal and Archaeological Evidence. – Journal of Coastal Research 24 (1A): 110-125.

Ambrasey, N. (2009): Earthquakes in the Mediterranean and Middle East. A multidisciplinary study of seismicity up to 1900. – Cambridge University Press, Cambridge, 968 pp.

Ambrasey, N. & Synolakis, C. (2010): Tsunami Catalogs for the Eastern Mediterranean, revisited. – Journal of Earthquake engineering 14: 309-330.

Ambrasey, N.N. & Jackson, J.A. (1997): Seismicity and strain in the Gulf of Corinth (Greece) since 1694. – Journal of Earthquake Engineering 1 (3): 433-474.

Andrade, C., Freitas, M.C., Moreno, J. & Craveiro, S.C. (2004): Stratigraphical evidence of Late Holocene barrier breaching and extreme storms in lagoonal sediments of Ria Formosa, Algarve, Portugal. – Marine Geology 210: 339-362.

Antonopoulos, J. (1979): Catalogue of tsunamis in the Eastern Mediterranean from Antiquity to present times. – Annali die Geofisica 32: 113-130.

Antonopoulos, J. (1980a): Data from investigation on seismic sea-waves events in the Eastern Mediterranean from the Birth of Christ to 500 AD. Part 1. – Annali di Geofisica 33 (1): 141-161.

Antonopoulos, J. (1980b): Data from investigation on seismic sea-waves events in the Eastern Mediterranean from 500 to 1000 AD. Part 2. – Annali di Geofisica 33 (1): 163-178.

Antonopoulos, J. (1980c): Data from investigation on seismic sea-waves events in the Eastern Mediterranean from 1000 to 1500 AD. Part 3. – Annali di Geofisica 33 (1): 179-198.

Antonopoulos, J. (1980d): Data from investigation on seismic sea-waves events in the Eastern Mediterranean from 1500 to 1800 AD. Part 4. – Annali di Geofisica 33 (1): 199-214.

Antonopoulos, J. (1980e): Data from investigation on seismic sea-waves events in the Eastern Mediterranean from 1800 to 1900 AD. Part 5. – Annali di Geofisica 33 (1): 215-230.

Antonopoulos, J. (1980f): Data from investigation on seismic sea-waves events in the Eastern Mediterranean from 1900 to 1980 AD. Part 6. – Annali di Geofisica 33 (1): 231-248.

Avallone, A., Briole, P., Agatza-Balodimou, A.M., Billiris, H., Charade, O., Mitsakaki, C., Nercessian, A., Papazissi, K., Paradissis, D. & Veis, G. (2004): Analysis of eleven years of deformation measured by GPS in the Corinth Rift Laboratory area. – Comptes Rendus Géosciences 336 (4-5): 301-311.

Bahlburg, H. & Spiske, M. (2010): The February 27, 2010 Chile Tsunami. Sedimentology of runup and backflow deposits at Isla Mocha. – American Geophysical Union, Abstract #OS42B-06.

Bahlburg, H. & Spiske, M. (2011): Sedimentology of tsunami inflow and backflow deposits: key differences revealed in a modern example. – Sedimentology 59 (3): 1063-1086.

Bahlburg, H. & Weiss, R. (2007): Sedimentology of the December 26, 2004, Sumatra tsunami deposits in eastern India (Tamil Nadu) and Kenya. – International Journal of Earth Sciences 96 (6): 1195-1209.

Becker, J. (1998): Paulus. Der Apostel der Völker. – UTB, Stuttgart, 524 pp.

Bell, R. E., McNeill, L.C., Bull, J.M., Henstock, T.J., Collier, R.E.L. & Leeder, M.R. (2009): Fault architecture, basin structure and evolution of the Gulf of Corinth Rift, central Greece. – Basin Research 21 (6): 824-855.

Bernasconi, M.P., Melis, R. & Stanley, J.D. (2006): Benthic biofacies to interpret Holocene environmental changes and human impact in Alexandria's Eastern Harbour, Egypt. – The Holocene 116 (8): 1163-1176.

Biedermann, G. (1887): Die Insel Kephallenia im Altertum. Dissertation. Hohe philosophische Facultät der Universität Würzburg. – Akademische Buchdruckerei von F. Straub, München, 104 pp.

Blackman, D.J. (1982): Ancient harbours in the Mediterranean. Part 2. – The International Journal of Nautical Archaeology and Underwater Exploration 11 (3): 185-211.

Blaquiere, E. (1825): Narrative of a second visit to Greece. – G. B. Whittaker, London, 342 pp.

Blegen, C.W. (1920): Corinth in prehistoric times. – American Journal of Archaeology 24 (1): 1-13.

Blume, H.-P., Stahr, K. & Leinweber, P. (2011): Bodenkundliches Praktikum. Eine Einführung in pedologisches Arbeiten für Ökologen, insbesondere Land- und Forstwirte, und für Geowissenschaftler. – Spektrum Akademischer Verlag, Heidelberg, 255.

Bon, A. (1969): La more franque. Recherches historiques, topographiques et archéologiques sur la principauté d'Achaie (1205-1430). – Boccard, Paris, 746 pp.

Bony, G., Marriner, N., Morhange, C., Kaniewski, D. & Dogan, P. (2012): A high-energy deposit in the Byzantine harbour of Yenikapi, Istanbul (Turkey). – Quaternery International 266: 117-130.

Bourouis, S. & Cornet, F.H. (2009): Microseismic activity and fluid fault interactions: some results from the Corinth Rift Laboratory (CRL), Greece. – Geophysical Journal International 178: 561-580.

Brockhaus, F.A. (Hrsg.): Allgemeine deutsche Real-Encyklopädie für gebildete Stände (Conversations-Lexikon). Bd. 8. – Brockhaus, Leipzig, 1003 pp.

Brooks, M. & Ferentinos, G. (1984): Tectonics and sedimentation in the Gulf of Corinth and the Zakynthos and Keffalinia channels, western Greece. – Tectonophysics 101: 25-54.

Brownson, C.L. (ed.) (1918): Xenophon, Hellenica. – Harvard University Press, Cambridge, 395 pp.

Brückner, H., Müllenhoff, M., Gehrels, R., Herda, A., Knipping, M. & Vött, A. (2006): From archipelago to floodplain – geographical and ecological changes in Miletus and its environs during the past six millennia (Western Anatolia, Turkey). – Zeitschrift für Geomorphologie N. F. Suppl. Vol. 142: 63-83.

Burke, L., Kura, Y., Kassem, K., Revenga, C., Spalding, M. & McAllister, D. (2001): Coastal Ecosystems. Pilot Analysis of Global Ecosystems. – World Resources Institute, Washington, 93 pp.

Cavaleri, L. (2005): The wind and wave atlas of the Mediterranean Sea – the calibration phase. – Advances in Geosciences 2: 255-257.

Chandler, R. (1817): Travels in Asia Minor and Greece. – Booker and Priestley, London, 334 pp.

Charalampakis, M., Stefatos, A., Hasiotis, T. & Ferentinos, G. (2007a): Submarine mass movements on an active fault system in the central Gulf of Corinth. – Advances in Natural and Technological Hazards Research 27: 67-76.

Charalampakis, M., Stefatos, A., Mpourdopoulos, K. & Ferentinos, G. (2007b): Towards the mitigation of the tsunami risk by submarine mass failures in the Gulf of Corinth: The Xylocastro resort town case study. – Advances in Natural and Technological Hazards Research 27: 367-376.

Cimerman, F. & Langer, M.R. (1991): Mediterranean foraminifera. – Slovenska Akademija Znanosti in Umetnosti, Razred za Naravoslovne Vede 30, Ljubljana, 118 pp.

Clément, C., Hirn, A., Charvis, P., Sachpazi, M. & Marnelis, F. (2000): Seismic structure and the active Hellenic subduction in the Ionian islands. – Tectonophysics 329: 141-156.

Cocard, M., Kahle, H.-G., Peter, Y., Geiger, A., Veis, G., Felekis, S., Paradissis, D. & Billiris, H. (1999): New constraints on the rapid crustal motion of the Aegean region: recent results inferred from GPS measurements (1993-1998) across the Wetern Hellenic Arc, Greece. – Earth and Planetary Science Letters 172: 39-47.

Crawley, R. (2009): Thucydides. The history of the Peloponnesian War. – EBook #7142, Project Gutenberg. http://www.gutenberg.org/files/7142/7142-h/7142-h.htm#2HCH0011. (latest access: 01/2012).

Crossland, J., Kremer, H.H., Lindeboom, H.J., Marshall Crossland, J.I. & Le Tissier, M.D.A. (eds.) (2005): Coastal Fluxes in the Anthropocene. The Land-Ocean Interactions in the Coastal Zone Project of the International Geosphere-Biosphere Programme. – Springer, Berlin/ Heidelberg, 232 pp.

Dahlheim, W. (1997): Die griechisch-römische Antike. Bd. 1. – UTB/Ferdinand Schöningh, Paderborn, 368 pp.

Dawson, A. & Shi, S. (2000): Tsunami deposits. – Pure and Applied Geophysics 157: 875-897.

Dearing, J. (1999): Environmental Magnetic Susceptibility. Using a Bartington MS2 System. – Chi Publications, Kenilworth, 111 pp.

De Martini, P. M., Barbano, M.S., Smedile, A., Gerardi, F., Pantosti, D., Del Carlo, P. & Pirrotta, C. (2010): A unique 4000 year long geological record of multiple tsunami inundations in the Augusta Bay (eastern Sicily, Italy). – Marine Geology 276 (1-4): 42-57.

Di Bella, L., Bellotti, P., Frezza, V., Bergamin, L. & Carboni, M.G. (2011): Bentic foraminiferal assemblages of the imperial harbour of Claudius (Rome): Further palaeoenvironmental and geoarchaeological evidences. – The Holocene 21 (8): 1245-1259.

Donato, S.V., Reinhardt, E.G., Boyce, J. I., Rothaus, R. & Vosmer, T. (2008): Identifying tsunami deposits using bivalve shell taphonomy. – Geology 36 (3): 199-202.

Doutsos, T. & Kokkalas, S. (2001): Stress and deformation patterns in the Aegean region. – Journal of Structural Geology 23 (2-3): 455-472.

EBA – 6TH EPHORATE OF BYZANTINE ANTIQUITIES (2005): Clarence/ Γλαρεντοζας. – Hellenic Ministry of Culture, Athens, 56 pp.

EDMONDS, C. (1850): Livy. The History of Rome by Titus Livius. – David MaKay, Philadelphia.

ENGEL, M., KNIPPING, M., BRÜCKNER, H., KIDERLEN, M. & KRAFT, J.C. (2009): Reconstructing middle to late Holocene palaeogeographies of the lower Messenian plain (southwestern Peloponnese, Greece): Coastline migration, vegetation history, and sea level change. – Palaeogeography, Palaeoclimatology, Palaeoecology 284: 257-270.

FERENTINOS, G., COLLINS, M.B., PATTIARATCHI, C.B. & TAYLOR, P.G. (1985): Mechanisms of sediment transport and dispersion in a tectonically active submarine valley/canyon system: Zakynthos Straits, NW Hellenic Trench. – Marine Geology 65: 243-269.

FIA – THE FINNISH INSTITUTE AT ATHENS (2013): Kyllene Harbour Project. – Internet: http://www.finninstitute.gr/en/kyllene (19.07.2013).

FIORINI, F. (2004): Benthic foraminiferal associations from Upper Quaternary deposits of southeastern Po Plain, Italy. – Micropaleontolgy 50 (1): 45-58.

FITA, L., ROMERO, R., LUQUE, A., EMANUEL, K., & RAMIS, C. (2007): Analysis of the environments of seven Mediterranean tropical-like storms using an axisymmetric, nonhydrostatic, cloud resolving model. – Natural Hazards and Earth System Science 7 (1): 41-56.

FOUACHE, E., GHILARDI, M., VOUVALIDIS, K., SYRIDES, G., STYLLAS, G., KUNESCH, S. & STIROS, S. (2008): Contribution on the Holocene Reconstruction of Thessaloniki Coastal Plain, Greece. – Journal of Coastal Research 24 (5):1161-1173.

FOWLER, H.N. & STILLWELL, R. (1932): Corinth. Introduction, topography, architecture. – Harvard University Press, Cambridge, 239 pp.

FRAZER, J.G. (1965): Pausania's description of Greece. – Biblio and Tanne, New York, 652 pp.

FREYBERG, B. VON (1973): Geologie des Isthmus von Korinth. – Erlanger Geologische Abhandlungen 95: 1-183.

FRIEDRICH, W. L., KROMER, B., FRIEDRICH, M., HEINEMEIER, J., PFEIFFER, T., & TALAMO, S. (2006): Santorini eruption radiocarbon dated to 1627-1600 BC. – Science 312 (5773): 548-548.

FÜCHTBAUER, H. (ed.) ([4]1988): Sedimente und Sedimentgesteine. – Schweizerbart, Stuttgart, 1141 pp.

GALANOPOULOS, A.G. (1960): Tsunamis Observed on the coasts of Greece from Antiquity to present times. – Annali di Geofisica 13 (3-4): 369-386.

GATSIS, I., PAVLOPOULOS, A. & PARCHARIDIS, I. (2001): Geomorphological observations and related natural hazards using merged remotely sensed data: a case study in the Corinthos area (NE Peloponnese, S. Greece). – Geografisker Annaler 83A (4): 217-228.

GEER, R.M. (1954): Diodorus Siculus. Library of History. Volume X. – Harvard University Press, Cambridge, 480 pp.

GEHRKE, H.-J. & SCHNEIDER, H. (2006): Geschichte der Antike. Ein Studienbuch. – Verlag J.B. Metzler, Stuttgart/Weimar, 657 pp.

GEHRKE, H.-J. & WIRBELAUER, E. (2004): Akarnania and adjacent areas. – In Hansen, M.H. & Nielsen, T.H. (eds.): An inventory of Archaic and Classical Poleis. Oxford University Press, Oxford, pp. 351-378.

GELFENBAUM, G. & JAFFE, B. (2003): Erosion and Sedimentation from the 15 July, 1998 Papua New Guinea Tsunami. – Pure and Applied Geophysics 160 (10-11): 1969-1999.

Gerardi, F., Barbano, M. S., de Martini, P. M. & Pantosti, D. (2008): Discrimination of tsunami sources (earthquake vs. landslide) on the basis of historical data in eastern Sicily and southern Calabria. – Bulletin of the Seismological Society of America 98 (6): 2795-2805.

Ghilardi, M., Kunesch, S,. Styllas, M. & Fouache E. (2008): Reconstruction of mid-Holocene sedimentary environments in the central part of the Thessaloniki plain (Greece), based on microfaunal identification, magnetic susceptibility and grain-size analyses. – Geomorphology 97: 617-630.

Ghionis, G., Poulos, S., Kampanis, N., Verikiou, E., Karditsa, A., Alexandrakis, G., & Andris, P. (2008): The effects of a severe storm event on the NW coast of Lefkada Island, Ionian Sea (Greece). – Geophysical Research Abstracts 10.

Giraudi, C. (2009): Late Holocene Evolution of Tiber River Delta and Geoarchaeology of Claudius and Trajan Harbor, Rome. – Geoarchaeology: An International Journal 24 (3): 371-382.

Goiran, J.P. (2010): Palaeoenvironmental reconstruction of the ancient harbours of Rome: Claudius and Trajan's marine harbours on the Tiber delta. – Quaternary International 216: 3-13.

Goiran, J.P., Pavlopoulos, K.P., Fouache, E., Triantaphyllou, M. & Etienne, R. (2011): Piraeus, the ancient island of Athens: Evidence from Holocene sediments and historical archives. – Geology 39 (6): 531-534.

Goodman-Tchernov, B.N., Dey, H.W., Reinhardt, E.G., McCoy, F. & Mart, Y. (2009): Tsunami waves generated by the Santorini eruption reached Eastern Mediterranean shores. – Geology 37 (19): 943-946.

Gornitz, V. (2005): Natural hazards. – In: Schwartz, M. (ed., 2005): Encyclopedia of Coastal Science. Springer, Dordrecht: 678-684.

Goto, K., Chagué-Goff, C., Fujino, S., Goff, J., Jaffe, B., Nishimura, Y., Richmond, B., Sugawara, D., Szczucinski, W., Tappin, D.R., Witter, R. C. & Yulianto, E. (2011): New insights of tsunami hazard from the 2011 Tohoku-oki event. – Marine Geology 290 (1-4): 46-50.

Gowland, W. (1901): The Early Metallurgy of Silver and Lead: Part I., Lead. – Archaeologia 52 (2): 359-422.

Graham, A. J. (1964): Colony and mother city in ancient Greece. – Manchester University Press, Manchester, 259 pp.

Guidoboni, E. (1994): Catalogue of ancient earthquakes in the Mediterranean area up to the 10th century. – SGA, Roma, 504 pp.

Guidoboni, E. & Comastri, A. (2005): Catalogue of earthquakes and tsunamis in the Mediterranean area from the 11th to the 15th century. – SGA, Roma, 1037 pp.

Guidoboni, E. & Ebel, J. E. (2009): Earthquakes and tsunami in the past. A guide to techniques in historical seismology. – Cambridge University Press, Cambridge, 602 pp.

Gupta, B.K.S. (ed.) (2002): Modern foraminifera. – Kluwer Academic Publisher, Dordrecht, 371 pp.

Hadler, H., Vött, A., Brückner, H., Bareth, G., Ntageretzis, K., Warnecke, H. & Willershäuser, T. (2011a): The harbour of ancient Krane, Kutavos Bay (Cefalonia, Greece) – an excellent geo-archive for palaeo-tsunami research. – Coastline Reports 17: 111-122.

Hadler, H., Vött, A., Koster, B., Mathes-Schmidt, M., Mattern, T., Ntageretzis, K., Reicherter, K., Sakellariou, D. & Willershäuser, T. (2011b): Lechaion, the ancient harbour of Corinth (Peloponnese, Greece) destroyed by tsunamigenic impact. – 2nd INQUA-IGCP-567 International Workshop on Active Tectonics, Earthquake Geology, Archaeology and Engineering, Corinth, Greece: 70-73.

Hadler, H., Willershäuser, T., Ntageretzis, K., Henning, P., Vött, A. (2012): Catalogue entries and non-entries of earthquake and tsunami events in the Ionian Sea and the Gulf of Corinth (eastern Mediterranean, Greece) and their interpretation with regard to palaeotsunami research. – Bremer Beiträge zur Geographie und Raumplanung 44: 1-15.

Hadler, H., Vött, A., Koster, B., Mathes-Schmidt, M., Mattern, T., Ntageretzis, K., Reicherter, K. & Willershäuser, T. (2013): Multiple late-Holocene tsunami landfall in the eastern gulf of corinth recorded in the palaeotsunami geo-archive at Lechaion, harbour of ancient Corinth (Peloponnese, Greece). – Zeitschrift für Geomorphologie N.F. Suppl. 57 (4): 139-180.

Hamilton, H.C. & Falconer, W. (1903): The Geography of Strabo. Literally translated, with notes, in three volumes. – George Bells & Sons, London.

Hansen, M.H. & Nielsen, T.H. (2004): An inventory of Archaic and Classical poleis. – Oxford University Press, New York, 1396 pp.

Hasiotis, T., Papatheodorou, G., Bouckovalas, G., Corbau C. & Ferentinos, G. (2002): Earthquake-induced coastal sediment instabilities in the western Gulf of Corinth, Greece. – Marine Geology 186: 319-335.

Haslinger, F., Kissling, E., Ansorge, J., Hatzfeld, D., Papadimitriou, E., Karakostas, V., Makropoulos, K., Kahle, H.-G. & Peter, Y. (1999): 3D crustal structure from local earthquake tomography around the Gulf of Arta (Ionian region, NW Greece). – Tectonophysics 304: 201-218.

Hayward, C.L. (2003): The Geology of the Corinthia. – In: Williams, C.K. & Bookidis, N. (eds.): Corinth: the centenary 1896-1996. – American School of Classical Studies at Athens, Athens, 474 pp.

Higgins, M.D. & Higgins, R. (1996): A geological companion to Greece and the Aegean. – Duckworth, London, 256 pp.

Hofrichter, R. (ed.) (2002): Das Mittelmeer. Fauna, Flora, Ökologie. Band I: Allgemeiner Teil – Spektrum Akademischer Verlag, Heidelberg/Berlin, 2002, 608.

Hollenstein, C., Müller, M.D., Geiger, A. & Kahle, H.G. (2008a): Crustal motion and deformation in Greece from a decade of GPS measurements, 1993-2003. – Tectonophysics 449 (1-4): 17-40.

Hollenstein, C., Müller, M.D., Geiger, A. & Kahle, H.G. (2008b): GPS-derived coseismic displacements associated with the 2001 Skyros and 2003 Lefkada earthquakes in Greece. – Bulletin of the Seismological Society of America 98 (1): 149-161.

Hong, S., Candelone, J.-P., Patterson, C.C. & Boutron, C.F. (1994): Greenland ice evidence of hemispheric lead pollution two millennia ago by Greek and Roman Civilizations. – Science 265: 1841-1843.

Hoshiba, M. & Ozaki, T. (2014): Earthquake Early Warning and Tsunami Warning of the Japan Meteorological Agency, and their Performance in the 2011 off the Pacific Coast of tohoku Earthquake (M_w 9.0). – In: Wenzel, F. & Zschau, J. (eds., 2014): Early Warning for Geological Disasters. Springer, Heidelberg: 1-28.

Howarth, R.J. & Murray, J.W. (1969): The Foraminiferida of Christchurch Harbour, England: a reappraisal using multivariate techniques. – Journal of Paleontology 43 (3): 660-675.

Hughen, K.A., Baillie, M.G.L., Bard, E., Beck, J.W., Bertrand, C.J.H., Blackwell, P.G., Buck, C.e., Burr, G.S., Cutler, K.B., Damon, P.E., Edwards, R.L., Fairbanks, R.G., Friedrich, M., Guilderson, T.P., Kromer, B., McCormac, G., Manning, S., Ramsey, C.B., Reimer, P.J., Reimer, R.W., Remmele, S., Southon, J.R., Stuiver, M., Talamo, S., Taylor, F.W., van der Plicht, J. & Weyhenmeyer, C.E. (2004): Marine04 marine radiocarbon age calibration, 0-26 cal kyr BP. – Radiocarbon 46 (3): 1059-1086.

IGME – Institute of Geology and Mineral Exploration (1972): Geological map of Greece 1:50.000. Sheet Korinthos. – Athens.

IGME – Institute of Geology and Mineral Exploration (1985): Geological map of Greece, 1:50.000. Sheet Cephalonia Island (southern part). – Athens.

Jackson, J.A., Gagnepain, J., Houseman, G., King, G.C.P., Papadimitriou, P., Soufleris, C. & Virieux, J. (1982): Seismicity, normal faulting, and the geomorphological development of the Gulf of Corinth (Greece): the Corinth earthquakes of February and March 1981. – Earth and Planetary Science Letters 57 (2): 377-397.

Jones, H.L. (1927): Strabo. Geography. Vol. 4. Books 8-9. – Harvard University Press, Cambridge: 480 pp.

Jones, H.S. & Powell, J.E. (eds., 1942): Thucydides. Historiae Vol. I. – Oxford University Press, USA: 350 pp.

Jones, W.H.S., Litt, D. & Ormerod, H.A. (1918): Pausanias. Pausanias Descriptions of Greece. – Harvard University Press, London.

Kelletat, D. (2006) Beachrock as Sea-Level Indicator? Remarks from a Geomorphological Point of View. – In: Journal of Coastal Research 22 (6): 1558-1564.

Kelletat, D. (2007): Reply to: Knight, J. (2007): Beachrock Reconsidered. Discussion of: Kelletat, D. (2006). Beachrock as Sea-Level Indicator? Remarks from a Geomorphological Point of View, Journal of Coastal Research, 22(6), 1558–1564. – In: Journal of Coastal Research 23(4): 1074-1078.

Kent, J.H. (1966): The Inscriptions: 1926-1950. – American School of Classical Studies at Athens, Athens, 64 pp.

Keraudren, B. & Sorel, D. (1987): The terraces of Corinth (Greece) – a detailed record of eustatic sea-level variations during the last 500,000 years. – Marine Geology 77: 99-107.

Kershaw, S. & Guo, L. (2001): Marine notches in coastal cliffs: Indicators of relative sea-level change, Perachora Peninsula, central Greece. – Marine Geology 179: 213-228.

Knight, J. (2007): Beachrock Reconsidered. Discussion of: Kelletat, D. (2006): Beachrock as Sea-Level Indicator? Remarks from a Geomorphological Point of View. Journal of Coastal Research, 22(6), 1558–1564. – In: Journal of Coastal Research 23 (4): 1074-1078.

Kortekaas, S. & Dawson, A.G. (2007): Distinguishing tsunami and storm deposits: an example from Martinhal, SW Portugal. – Sedimentary Geology 200 (3): 208-221.

Kortekaas, S., Papadopoulos, G.A., Ganas, A., Cundy, A.B. & Diakantoni, A. (2011): Geological identification of historical tsunamis in the Gulf of Corinth, Central Greece. – Natural Hazards and Earth System Sciences 11 (7): 2029-2041.

Koster, B., Hadler, H., Vött, A., Reicherter, K. & Grützner, C. (2013): Application of GPR for visualising spatial distribution and internal structures of tsunami deposits: Case studies from Spain and Greece. – Zeitschrift für Geomorphologie N.F. Suppl. DOI: http://dx.doi.org/10.1127/0372-8854/2013/S-00151

Koukouvelas, I., Mpresiakas, A., Sokos, E. & Doutsos, T. (1996): The tectonic setting and earthquake ground hazards of the 1993 Pyrgos earthquake, Peloponnese, Greece. – Journal of the Geological Society 153: 39-49.

Kowalczyk, G. & Winter, K. (1979): Die geologische Entwicklung der Kyllini-Halbinsel im Neogen und Quartär (West Peloponnes, Griechenland. – Zeitschrift der Deutschen Geologischen Gesellschaft 130: 323-346.

Krautheimer, R. (1989): Early Christian and Byzantine Architecture. – Penguin Books, London, 556 pp.

Krestenitis, Y. N., Androulidakis, Y. S., Kontos, Y. N., & Georgakopoulos, G. (2011): Coastal inundation in the north-eastern mediterranean coastal zone due to storm surge events. - Journal of Coastal Conservation 15 (3): 353-368.

Labonne, M., Ben Othmann, D. & Luck, J.-M. (1998): Recent and past anthropogenic impact on a Mediterranean lagoon: Lead isotope constraints from mussel shells. – Applied Geochemistry 13 (7): 885-892.

Lagios, E. Sakkas, V. Papadimitriou, P. Parcharidis, I. Damiata, B.N. Chousianitis, K. & Vassilopoulou, S. (2007): Crustal deformation in the Central Ionian Islands (Greece): Results from DGPS and DInSAR analyses (1995-2006). – Tectonophysics 444: 119-145.

Landmann, G.P. (2010): Thukydides. Der Peloponnesische Krieg. – Artemis & Winkler, Düsseldorf, 644 pp.

Leake, W.M. (1930): Travels in the Morea. Vol. III. – John Murray, London, 476 pp.

Lee, J.J. & Raichlen, F. (1971): Wave induced oscillations in harbours with connected basins. – California Institute of Technology, Pasadena, 135 pp.

Lehmann-Hartleben, K. (1923): Die antiken Hafenanlagen des Mittelmeeres. – Scientia Verlag, Aalen, 304 pp.

Lekkas, E., Lozios, S., Skourtsos, e. & Kranis, H. (1991): Floods, geodynamic environment and human intervention. The case of Corinth (Greece). – Computational Mechanics Publications 2: 135-144.

Le Roux, G., Véron, A. & Morhange, C. (2005): Lead pollution in the ancient harbours of Marseille. – Méditerranée 1 (2): 31-35.

Lewis, M.J.T. (2001): Railways in the Greek and Roman world. – In: Guy, A. & Rees, J. (eds.): Early Railways. A selection of papers from the first International Early Railways Conference. 360 pp.

Lionello, P., Bhend, J., Buzzi, A., Della-Marta, P.M., Krichak, S.O., Jansà, A., Maheras, P., Sanna, A., Trigo, I.F. & Trigo, R. (xxx): Cyclones in the Mediterranean Region: Climatology and Effects on the environment. – Developments in Earth and Environmental Sciences 4: 325-372.

Loeblich, A.R. & Tappan, H.N. (1988): Foraminiferal genera and their classification. – Springer US, New York, 970 pp.

Lohmann, H. (2013): Der diolkos von Korinth. Eine antike Schiffsschleppe? - In: Niemeier, W.D. & Kissas, N. (eds.): The Corinthia and the Northeast Peloponnesus. Topography and History from Prehistoric Until the End of Antiquity. Deutsches Archaeologisches Institut, Berlin (in opress).

Louvari, E., Kiratzi, A.A. & Papazachos, B.C. (1999): The Cephalonia Transform Fault and its extension to western Lefkada Island (Greece). – Tectonophysics 308: 223-236.

Luque, A., Fita, L., Romero, R. & Alonso, S. (2007): Tropical-like Mediterranean storms: an analysis from satellite. – EUMET-SAT 07 proceedings.

Lykousis, V., Sakellariou, D., Rousakis, G., Alexandri, S., Kaberi, H., Nomikou, P., Georgiou & Balas, D. (2007): Sediment failure processes in active grabens: the western Gulf of Corinth (Greece). – Advances in Natural and Technological Hazards Research 27: 297-308.

MacDonald, B.R. (1986): The diolkos. – The Journal of Hellenic Studies 106: 191-195.

Mamo, B., Strotz, L. & Dominey-Howes, D. (2009): Tsunami sediments and their foraminiferal assemblages. – Earth-Science Reviews 96 (4): 263-278.

Mariolakos, H., Lekkas, E., Danamos, G., Logos, E., Fountoulis, I. & Adamopoulou, E. (1991): Νεοτεκτονικη εξελιξη της χερσονησου της Κυλληνης (Βδ. Πελοποννησος). – Bulltin of the Geological Society of Greece (15) 3: 163-176. (in greek)

Marriner, N. & Morhange, C. (2007): Geoscience of ancient Mediterranean harbours. – Earth-Science Reviews 80 (3-4): 137-194.

Maroukian, H., Gaki-Papanastassiou, K., Papanastassioi, D. & Palyvos, N. (2000): Geomorphological Observations in the Coastal Zone of Kyllini Peninsula, NW-Peloponnesus-Greece, and their Relation to the Seismotectonic Regime of the Area. – Journal of Coastal Research 16 (3): 853-863.

Marriner, N. & Morhange, C. (2007): Geoscience of ancient Mediterranean harbours. – Earth-Science Reviews 80 (3-4): 137-194.

Marriner, N., Morhange, C. & Goiran, J.P. (2010): Coastal and ancient harbour geoarchaeology. – Geology Today 26 (1): 21-27.

Martinez, F.M. & Naverac, V.S. (1988): An experimental study of harbour resonance phenomena. – Coastal Engineering Proceedings 1 (21): 270-280.

Mastronuzzi, G. & Sanso, P. (2012): The role of strong earthquakes and tsunami in the Late Holocene evolution of the Fortore River coastal plain (Apulia, Italy): A synthesis. – Geomorphology 138: 89-99.

May, S. M., Vött, A., Brückner, H., & Brockmüller, S. (2007): Evidence of tsunamigenic impact on Actio headland near Preveza, NW Greece. – Coastline Reports 9: 115-125.

May, S. M., Vött, A., Brückner, H., Grapmayer, R., Handl M. & Wennrich, V. (2012): The Lefkada barrier and beachrock system (NW Greece) – controls on coastal evolution and the significance of extreme events. – Geomorphology 139/140: 330-347.

Medatlas Group (2004): Wind and wave atlas of the Mediterranean Sea. – Western European Union, WEAO Research Cell.

Mee, L. (2012): Between the Devil and the deep Blue Sea: The coastal zone in an Era of globalization. – Estuarine, Coastal and Shelf Science 96: 1-8.

Mimura, N., Yasuhara, K., Kawagoe, S., Yokoki, H., & Kazama, S. (2011): Damage from the Great East Japan Earthquake and Tsunami - A quick report. – Mitigation and adaptation strategies for global change 16 (7): 803-818.

Minoura, K., Nakaya, S. & Uchida, M. (1994): Tsunami deposits in a lacustrine sequence of the Sanriku coast, northeast Japan. – Sedimentary Geology 89 (1-2): 25-31.

Minoura, K., Imamura, F., Sugawara, D., Kono,Y. & Iwashita, T. (2001): The 869 Jogan tsunami deposit and recurrence interval of large-scale tsunami on the Pacific coast of northeast Japan. – Journal of Natural Disaster Science 23 (2): 83-88.

Morgan, C. (2008): Eleia. – Archaeological Reports 54: 41-43.

Morgan, C. (2009): Eleia including Triphyllia. – Archaeological Reports 55: 37-39.

Morhange, C. & Marriner, N. (2010): Paleo-hazards in the coastal Mediterranean: a geoarchaeological approach. – In: Martini, I.P. & Chesworth W. (eds.): Landscapes and societies. Selected cases. – Springer, Dordrecht/Heidelberg/London/New York, pp. 223-234.

Morhange, C., Pirazzoli, P.A., Evelpidou, N. & Marriner, N. (2012): Late Holocene Uplift and the Silting Up of Lechaion, the Western Harbor of Ancient Corinth, Greece. – Geoarchaeology 27 (3): 278-283.

Morton, R., Gelfenbaum, G. & Jaffe, B.E. (2007): Physical criteria for distinguishing sandy tsunami and storm deposits using modern examples. – Sedimentary Geology 200 (3): 184-207.

Moschopoulos, G.N. & Marabegia-Kosta, K. (2007): The Argostoli Earthquake 1953. Beginning and end of a town (in Greek).

Mourtzas, N.D. & Marinos, P.G. (1994): Upper Holocene sea-level changes. Palaeogeographic evolution and its impact on coastal archaeological sites and monuments. – Environmental Geology 23 (1): 1-13.

Mourtzas, N.D., Kissas, C. & Kolaiti, E. (2013): Archaeological and Geomorphological Indicators of the Historical Sea Level Changes and the related Palaeogeographical Reconstruction of the Ancient Foreharbour of Lechaion, E Corinth Gulf (Greece). – Quaternary International (in press).

Müllenhoff, M. (2005): Geoarchäologische, sedimentologische und morphodynamische Untersuchungen im Mündungsgebiet des Büyük Menderes (Mäander), Westtürkei. – Marburger Geographische Schriften 141.

Münchener Rück (2013): NATCATSERVICE. Bedeutende NAturkatastrophen seit 1980. - http://www.munichre.com/de/reinsurance/business/non-life/georisks/natcatservice/significant_natural_catastrophes.aspx (latest access: 12/2013).

Murray, A.T. (1924): Homer. The Illiad. – Harvard University Press, London.

Murray, J.W. (1973): Distribution and ecology of living benthic foraminiferids. – Crane/Russak, New York, 274 pp.

Murray, J.W. (1991): Ecology and palaeoecology of benthic foraminifera. – Longman Scientific & Technical, Harlow, 408 pp.

Murray, J.W. (2006): Ecology and Application of Benthic Foraminifera. – Cambridge University Press, Cambridge, 440 pp.

Nanayama, F. & Shigeno, K. (2006): Inflow and outflow facies from the 1993 tsunami in southwest Hokkaido. – In: Sedimentary Geology 187: 139-158.

National Oceanic and Atmospheric Administration (NOAA): NOAA/WDC Tsunami Event Database. – http://www.ngdc.noaa.gov/nndc/struts/form?t=101650&s=70&d=7. (latest access: 12/2011).

Orama Editions (2011): Road and Tourist Map – Cephalonia/Ithaka 1:75.000. – Rafina.

Pakkanen, J., Baika, K., Geraga, M., Evangelistis, D., Fakiris, E., Heath, S., Christodoulou, D., Iatrou, M. & Papatheodorou, G. (2010): Archaeological topographical survey and marine geophysical investigation at ancient and medieval harbor of Kyllini/Glarentza (NW Peloponnese, Greece). – Επιστημονική Επετηρίδα του Τμήματος Γεωλογίας (ΑΠΘ) 39 (1/2): 283-28.

Pallas, D.J. (1960): Anaskaphe en Lechaio. – Praktika: 144-170.

Pallas, D.J. (1970): Über die Datierung eines Kapitells der Basilika von Lechaion (Korinth). – Byzantinische Zeitschrift 63 (1): 69-70.

Pantosti, D., Pucci, S., De Martini, P.M., Smedile, A. (2011): Is the decadence of Leptis Magna (Lybia) the consequence of a destructive earthquake? – In: 2nd INQUA-IGCP-567 International Workshop on Active Tectonics, Earthquake Geology, Archaeology and Engineering, Corinth, Greece: 159-162.

Papadimitriou, P., Kaviris, G. & Makropoulos, K. (2006): The Mw = 6.3 2003 Lefkada earthquake (Greece) and induced stress transfer changes. – Tectonophysics 423: 73-82.

Papadopoulos, G.A. (2003): Tsunami hazard in the eastern Mediterranean: strong earthquakes and tsunamis in the Corinth Gulf, Central Greece. – Natural Hazards 29: 437-464.

Papadopoulos, G.A. & Chalkis, B.J. (1984): Tsunamis observed in Greece and the surrounding area from Antiquity up to the present times. – Marine Geology 56: 309-317.

Papadopoulos, G.A. & Fokaefs, A. (2005): Strong tsunamis in the Mediterranean Sea: a re-evaluation. – ISET Journal of Earthquake Technology 42 (4): 159-170.

Papadopoulos, G.A., Daskalaki, E. & Fokaefs, A. (2007a): Tsunamis generated by coastal and submarine landslides in the Mediterranean Sea. – Advances in Natural and Technological Hazard Research 27: 415-422.

Papadopoulos, G.A., Daskalaki, E., Fokaefs, A. & Giraleas, N. (2007b): Tsunami hazards in the eastern Mediterranean: strong earthquakes and tsunamis in the east Hellenic Arc and Trench system. – Natural Hazards and Earth System Sciences 7: 57-64.

Papathoma, M. & Dominey-Howes, D. (2003): Tsunami vulnerability assessment and its implications for coastal hazard analysis and disaster management planning, Gulf of Corinth. – Natural Hazards and Earth System Science 3 (6): 733-747.

Papazachos, B.C. & Dimitriu, P.P. (1991): Tsunamis in and near Greece and their relation to the earthquake focal mechanism. – Natural Hazards 4: 161-170.

Papazachos, B. & Papazachou, C. (1997): The earthquakes of Greece. – Thessaloniki, 304 pp.

Paris, J. (1915): Contributions à l'étude des ports antiques du monde grec. Notes sur Léchaion. – Bulletin de Correspondance Hellénique 39 (1): 5-16.

Partsch, J. (1890): Kephallenia und Ithaka. Eine geographische Monographie. – Justus Perthes, Gotha, 108 pp.

Paton, W.R. (1922): Polybius. The Histories. Vol. 2. Books 3-4. – Harvard University Press, Cambridge: 576 pp.

Paton, W.R. (1923): Polybius: Histories Vol. 3 (Books 5-8). – William Heinemann Ltd., London, 559 pp.

Philippides, M. (1980): The fall of the Byzantine Empire. A chronicle (1401-1477) by Georgius Sphrantzes. – University of Massachusetts Press, Amherst

Pirazzoli, P.A. (2010): Scientific report on the COST-STSM-ES0701-6735. – http://www.cost-es0701.geoenvi.org/attachments/article/202/Pirazzoli_STSM _2010Report.pdf. (latest access: 10/2012).

Pirazzoli, P.A., Ausseil-Badie, J., Giresse, P., Hadjidaki, E. & Arnold, M. (1992): Historical environmental changes at Phalasarna harbour, West Crete. – Geoarchaeology 7 (4): 371-392.

Pirazzoli, P.A., Stiros, S.C., Arnold, M., Laborel, J., Laborel- Deguen, F. & Papageorgiou, S. (1994): Episodic uplift deduced from Holocene shorelines in the Perachora Peninsula, Corinth area, Greece. – Tectonophysics 229: 201-209.

Pirazzoli, P.A., Laborel, J. & Stiros, S.C. (1996): Earthquake clustering in the Eastern Mediterranean during historical times. Journal of Geophysical Research, 101(B3), 6083-6097.

Poppe, G.T. & Goto, Y. (1991): European seashells. Volume I: Polyplacophora, Caudofoveata, Solenogastra, Gastropoda. – ConchBooks, Wiesbaden, 352 pp.

Poppe, G.T. & Goto, Y. (2000): European seashells. Volume II: Scaphopoda, Bivalvia, Cephalopoda. – Hackenheim, 221 pp.

Poulos, S.E., Collins, M.B., Pattiaratchi, C., Cramp, A., Gull, W., Tsimplis, M. & Papatheodorou, G. (1996): Oceanography and sedimentation in the semi-enclosed, deep-water Gulf of Corinth (Greece). – Marine Geology 134 (3-4): 213-235).

Pucci, S., Pantosti, D., De MArtini, P.M., Smedile, A. Munzi, M., Cirelli, E., Pentiricci, M. & Musso, L. (2011): Environment-human relationships in historical time: The balance between urban development and natural forces at Leptis Magna (Lybia). – Quaternary International 242 (1): 171-184.

Pytharoulis, I., Craig, G.C. & Ballard, S.P. (2000): The hurricane-like Mediterranean cyclone of January 1995. – Meteorological Applications 7: 261-279.

Randsborg, K. (ed., 2002): Kephallénia. Archaeology and History. The Ancient Greek cities. – In: Acta Archaeologica 73 (2). Copenhagen, 308 pp.

Raphael, N. (1973): Late Quaternary Changes in Coastal Elis, Greece. – Geographical Review 63 (1): 73-89.

Reading, H.G. (ed.) (1996): Sedimentary environments: processes, facies and stratigraphy. – Blackwell Science, Oxford, 688 pp.

Reimer, P.J. & McCormac, F.G. (2002): Marine radiocarbon reservoir corrections for the Mediterranean and Aegean Seas. – Radiocarbon 44 (1): 159-166.

Reimer, P.J., Baillie, M.G.L., Bard, E., Bayliss, A., Beck, J.W., Bertrand, C.J.H., Blackwell, P.G., Buck, C.E., Burr, G.S., Cutler, K.B., Damon, P.E., Edwards, R.L., Fairbanks, R.G., Friedrich, M.; Guilderson, T.P., Hogg, A.G., Hughen, K.A., Kromer, B., McCormac, G., Manning, S., Ramsey, C.B., Reimer, R.W., Remmele, S., Southon, J.R., Stuiver, M., Talamo, S., Taylor, F.W., van der Plicht, J. & Weyhenmeyer, C.E. (2004): IntCal04 terrestrial radiocarbon age calibration, 0–26 cal kyr BP. – Radiocarbon 46 (3): 1029-1058.

Reimer, P.J., Baillie, M.G.L., Bard, E., Bayliss, A., Beck, J.W., Blackwell, P.G., Bronk Ramsey, C., Buck, C.E., Burr, G.S., Edwards, R.L., Friedrich, M., Grootes, P.M., Guilderson, T.P., Hajdas, I., Heaton, T.J., Hogg, A.G., Hughen, K.A., Kaiser, K.F., Kromer, B., McCormac, F.G., Manning, S.W., Reimer, R.W., Richards, D.A., Southon, J.R., Talamo, S., Turney, C.S.M., van der Plicht, J., & Weyhenmeyer, C.E. (2009): IntCal09 and Marine09 radiocarbon age calibration curves, 0-50,000 years cal BP. – Radiocarbon 51: 1111-1150.

Reineck, H.-E. & Singh, I.B. (1980): Depositional Sedimentary Environments. – Springer, Berlin: 549 pp.

Reinhardt, E.G., Goodman, B.N., Boyce, J.I., Lopez, G., van Hengstum, P., Rink, W.J., Mart, Y. & Raban, A. (2006): The tsunami of 13 December A.D. 115 and the destruction of Herodot the Great's harbour at Caesarea Maritima, Israel. – Geology 34 (12): 1061-1064.

Reinhardt, E.G., Patterson, R.T. & Schroeder-Adams, C.J. (1994): Geoarchaeology of the ancient harbour site at Caesarea Maritima, Israel: evidence from sedimentology and paleoecology of benthic foraminifera. – Journal of Foraminiferal Research 24: 37-48.

Roberts, G. P., Houghton, S. L., Underwood, C., Papanikolaou, I., Cowie, P. A., van Calsteren, P., Wigley, T., Cooper, F. J. & McArthur, J. M. (2009): Localization of Quaternary slip rates in an active rift in 10^5 years: An example from central Greece constrained by ^{234}U-^{230}Th coral dates from uplifted paleoshorelines. – Journal of Geophysical Research 114 (B10), DOI: 10.1029/2008JB005818.

Röbke, B.R., Schüttrumpf, H., Wöffler, T., Fischer, P., Hadler, H., Ntageretzis, K., Willershäuser, T. & Vött, A. (2013): Tsunami inundation scenarios for the Gulf of Kyparissia (western Peloponnese, Greece) derived from numerical simulations and geoscientific field evidence. - Zeitschrift für Geomorphologie N.F. Suppl. 57 (4): 69-104.

Rolfe, J.C. (1940): Ammianus Marcellinus. The Roman History. – Harvard University Press, Cambridge: 704 pp.

Rothaus, R. (1995): Lechaion, western port of Corinth: a preliminary archaeology and history. – Oxford Journal of Archaeology 14 (3): 293-306.

Sabatiere, P., Dezileau, L., Condomines, M., Briqueu, L., Colin, C., Bouchette, F., Le Duff, M. & Blanchemanche, P. (2008): Reconstruction of palaeostorm events in a coastal Lagoon (Hérault, South of France). – Marine Geology 251: 224-232.

Sabatier, P., Dezileau, L., Briqueu, L., Colin, C., & Siani, G. (2010): Clay minerals and geochemistry record from northwest Mediterranean coastal lagoon sequence: Implications for paleostorm reconstruction. – Sedimentary Geology 228 (3): 205-217.

Sachpazi, M., Clément, C., Laigle, M., Hirn A. & Roussos, N. (2003): Rift structure, evolution, and earthquakes in the Gulf of Corinth, from reflection seismic images. – Earth and Planetary Science Letters 216: 243-257.

Sachpazi, M., Hirn, A., Clément, C., Haslinger, F., Laigle, M., Kissling, E., Charvis, P., Hello, Y., Lépine, J.-C., Sapin, M. & Ansorge, J. (2000): Western Hellenic subduction and Cephalonia Transform: local earthquakes and plate transport and strain. – Tectonophysics 319: 301-319.

Salamon, A., Rockwell, T., Ward, S.T., Guidoboni, E. & Comastri, A. (2007): Tsunami hazard evaluation of the eastern Mediterranean: historical analysis and selected modeling. – Bulletin of the Seismological Society of America 97 (3): 705-724.

Sanders, G.D.R. & Whitebread, I.K. (1990): Central places and major roads in the Peloponnese. – The Annual of the British School at Athens 85: 333-361.

Satake, K., Sawai, Y., Shishikura, M., Okamura, Y., Namegaya, Y. & Yamaki, S. (2007): Tsunami sources of the unusual AD 869 earthquake off Miyagi, Japan, inferred from tsunami deposits and numerical simulation of inundation. – AGU Fall Meeting Abstracts #T31G-03.

Schäfer, A. (2005): Klastische Sedimente. Fazies und Sequenzstratigraphie. – Elsevier, Spektrum Akademischer Verlag, München, 414 pp.

Scheffer, F. & Schachtschabel, P. ([16]2010): Lehrbuch der Bodenkunde. – Spektrum Akademischer Verlag, Heidelberg, 569 pp.

Scheffers, A., Kelletat, D., Vött, A., May, S.M. & Scheffers, S. (2008): Late Holocene tsunami traces on the western and southern coastlines of the Peloponnesus (Greece). – Earth Planetary Science Letters 269: 271-279.

Scicchitano, G., Costa, B., Di Stefano, A., Longhitano, S.G. & Monaco, C. (2010): Tsunami and storm deposits preserbed within a ria-type rocky coastal setting (Siracusa, SE Sicily). – Zeitschrift für Geomorphologie N.F. Suppl. Issue 54 (3): 51-77.

Scicchitano, G., Monaco, C. & Tortorici, L. (2007): Large boulder deposits by tsunami waves along the Ionian coast of south-eastern Sicily (Italy). – Marine Geology 238: 75-91.

Scordilis, E., Karakaisis, G., Panagiotopoulos, D. & Papazachos, B. (1985): Evidence for transform faulting in the Ionian Sea: the Cephalonia Island earthquake sequence of 1983. – Pure and Applied Geophysica 123 (3): 388-397.

Scranton, R.L. (1960): Ancient Corinth. A guide to the excavations. – American School of Classical Studies at Athens, Athens, 98 pp.

Shaw, B., Jackson, J.A., higham, T.f.G., England, O.C. & Thomas, A.L. (2010): Radiometric dates of uplifted marine fauna in Greece: Implications for the interpretation of recent earthquake and tectonic histories using lithophagid dates. – Earth and Planetary Science Letters 297 (3-4): 305-404.

Shaw, J.W. (1969): A foundation in the inner harbour at Lechaeum. – American Journal of Archaeology 73 (3): 370-373.

Smedile, A., De Martini, P.M., Pantosti, D., Bellucci, L., Del Carlo, P., Gasperini, L., Pirrotta, C., Polonia, A. & Boschi, E. (2011): Possible tsunami signatures from an integrated study in the Augusta Bay offshore (Eastern Sicily – Italy). – Marine Geology 281: 1-13.

Soloviev, S. L. (1990): Tsunamigenic zones in the Mediterranean Sea. – Natural Hazards 3: 183-202.

Soloviev, S.L., Solovieva, O.N., Go, C.N., Kim, K.S. & Shchetnikov, N.A. (2000): Tsunamis in the Mediterranean Sea 2000 B.C. – 2000 A.D. – Kluwer Academic Publishers, Dordrecht, 240 pp.

Soter, S. & Katsonopoulou, D. (2011): Submergence and uplift of settlements in the area of Helike, Greece, from Early Bronze Age to late antiquity. – Geoarchaeology 26 (4): 584-610.

Soter, S. (1999): Holocene uplift and subsidence of the Helice Delta, Gulf of Corinth, Greece. – Geological Society London 146: 41-56.

Soukissian, T., Hatzinaki, M., Korres, G., Papadopoulos, A., Kallos, G. & Anadranistakis, E. (2007): Wind and wave atlas of the Hellenic Seas. – Hellenic Center for Marine Research Publications, Athens.

Soukissian, T., Prospathopoulos, A., Hatzinaki, M. & Kabouridou, M. (2008): Assessment of the Wind and Wave Climate of the Hellenic Seas Using 10-Year Hindcast Results. – The Open Engineering Journal 1: 1-12.

Stanley, J.-D. & Bernasconi, M.P. (2006): Holocene depositional patterns and evolution in Alexandria's eastern harbour, Egypt. – Journal of Coastal Research 22 (2): 283-297.

Stefatos, A. Papatheodorou, G., Ferentinos, G., Leeder, M. & Collier, R. (2002): Seismic reflection imaging of active offshore faults in the Gulf of Corinth: their seismotectonic significance. – Basin Research 14 (4): 487-502.

Stefatos, A., Charalambakis, M., Papatheodorou G. & Ferentinos, G. (2006): Tsunamigenic sources in an active European half-graben (Gulf of Corinth, Central Greece). – Marine Geology 232 (1-2): 35-37.

Steinhart, M. & Wirbelauer, E. (2002): Aus der Heimat des Odysseus. Reisende, Grabungen und Funde auf Ithaka und Kephallenia bis zum ausgehenden 19. Jahrhundert. – Verlag Philipp von Zabern, Mainz, 336 pp.

Stiros, S., Pirazzoli, P. Rothaus, R. Papageorgiou, S. Laborel J. & Arnold, M. (1996): On the date of construction of Lechaion, western harbour of Corinth, Greece. – Geoarchaeology 11 (3): 251-263.

Stiros, S.C., Arnold, M., Pirazzoli, P.A., Laborel, J. & Laborel-Deguen, F. (1994): The 1953 earthquake in Cephalonia (western Hellenic arc): Coastal uplift and halotectonic faulting. – Geophysical Journal International 117: 834-849.

Stückelberg, A. (ed., 2006): Claudius Ptolemaeus. Handbuch der Geographie. – Schwabe, Basel: 471 pp.

Sugawara, D. Minoura, K. & Imamura, F. (2002): Tsunamis and Tsunami Sedimentology. – In: Shiki, T., Tsuji, Y., Minoura, K & Yamazaki, T. (eds., 2002): Tsunamiites. Features and Implications. Elsvier, 432 pp.

Taylor, B., Weiss, J.R., Goodliffe, A.M., Sachpazi, M., Laigle, M. & Hirn, A. (2011): The structures, stratigraphy and evolution of the Gulf of Corinth rift, Greece. – Geophysical Journal International 185 (3): 1189-1219.

Tinti, A., Armigliato, A. Bressan, L. Gallazzi, S. Pagnoni, G. Tonini R. & Zaniboni, F. (2007a): Earthquake-generated tsunamis in the western Gulf of Corinth, Greece: single-fault and worst-case scenarios. – Geophysical Research Abstracts 9.

Tinti, A., Zanibani, F., Armigliato, A., Pagnoni, G., Gallazzi, S., Manucci, A., Brizuela Reyes, B., Bressan, L. & Tonini, R. (2007b): Tsunamigenic landslides in the western Corinth Gulf: numerical scenarios. – Advances in Natural and Technological Hazards Research 27: 405-414.

Tinti, S., Maramai, A. & Graziani, L. (2004): The new catalogue of Italian tsunamis. – Natural Hazards 33: 439-465.

Tous, M. & Romero, R. (2012): Meteorological environments associated with medicane development. – International Journal of Climatology. doi: 10.1002/joc.3428

Traquair, R. (1906/07): Mediaeval fortresses of the north-western Peloponnesus. – The Annual of the British School at Athens 13: 268-281.

Tselentis, G.A., Stavrakakis, G. Sokos, E. Gkika F. & Serpetsidaki, A. (2010): Tsunami hazard assessment in the Ionian Sea due to potential tsunamogenic sources – results from numerical simulations. – Natural Hazards and Earth System Sciences 10: 1-10.

Tsimplis, M.N. & Blackmann, D. (1997): Extreme Sea-level Distributions and Return Periods in the Aegean and Ionian Seas. – Estuarine, Coastal and Shelf Science 44 (1): 79-89.

Tsimplis, M.N. & Shaw, A.G.P. (2010): Seasonal sea level extremes in the Mediterranean Sea and at the Atlantic European coasts. – Natural Hazards of Earth System Sciences 10: 1457-1475.

Verdelis, N.M. (1960): Anaskaphe tou diolkou. – Praktika: 136-143.

Vita-Finzi, C. & King, G.C.P. (1985): The seismicity, geomorphology and structural evolution of the Corinth area of Greece. – Philosophical Transactions of the Royal Society of London Series A 314: 379-407.

Vött, A. (2007): Silting up Oiniadai's harbours (Acheloos River delta, NW Greece) – geoarchaeological implications of late Holocene landscape changes. – Géomorphologie: relief, processus, environnement 1: 19-36.

Vött, A. & Brückner, H. (2006): Versunkene Häfen im Mittelmeerraum. Antike Küstenstädte als Archive für die Kultur- und Umweltforschung. – Geographische Rundschau 58 (4): 12-21.

Vött, A., May, S.M., Brückner, H. & Brockmüller, S. (2006): Sedimentary evidence of late Holocene tsunami events near Lefkada Island (NW Greece). – Zeitschrift für Geomorphologie N.F. Suppl. (146): 139-172.

Vött, A., Schriever, A., Handl, M. & Brückner, H. (2007): Holocene palaeogeographies of the central Acheloos River delta (NW Greece) in the vicinity of the ancient seaport Oiniadai. – Geodinamica Acta 20 (4): 241-256.

Vött, A., Brückner, H., Brockmüller, S., Handl, M., May, S.M., Gaki-Papanastassiou, K., Herd, R., Lang, F., Maroukian, H., Nelle, O. & Papanastassiou, D. (2009a): Traces of Holocene tsunamis across the Sound of Lefkada, NW Greece. – Global and Planetary Change 66 (1-2): 112-128.

Vött, A., Brückner, H., May, S.M., Sakellariou, D., Nelle, O., Lang, F., Kapsimalis, V., Jahns, S., Herd, R., Handl, M. & Fountoulis, I. (2009b): The Lake Voulkaria (Akarnania, NW Greece) palaeoenvironmental archive – a sediment trap for multiple tsunami impact since the mid-Holocene. – Zeitschrift für Geomorphologie N.F. Suppl. Issue 53 (1): 1-37.

Vött, A., Bareth, G., Brückner, H., Curdt, C., Fountoulis, I., Grapmeyer, R., Hadler, H., Hoffmeister, D., Klasen, N., Lang, F., Masberg, P., May, S.M., Ntageretzis, K., Sakellariou, D. & Willershäuser, T. (2010): Beachrock-type calcarenitic tsunamites along the shores of the estern Ionian Sea (western Greece) – case studies from Akarnania, the Ionian Islands and the western Peloponnese. – Zeitschrift für Geomorphologie N.F. Suppl. Issue 54 (3): 1-50.

Vött, A., Lang, F., Brückner, H., Gaki-Papanastassiou, K., Maroukian, H., Papanastassiou, D., Giannikos, A., Hadler, H., Handl, M., Ntageretzis, K., Willershäuser, T. & Zander, A. (2011a): Sedimentological and geoarchaeological evidence of multiple tsunamigenic imprint on the Bay of Palairos-Pogonia (Akarnania, NW Greece). – Quaternary International 242 (1): 213-239.

Vött, A., Bareth, G., Brückner, H., Lang, F., Sakellariou, D., Hadler, H., Ntageretzis, K. & Willershäuser, T. (2011b): Olympia's harbour site Pheia (Elis, western Peloponnese, Greece) destroyed by tsunami impact. – Die Erde 142 (3): 259-288.

VÖTT, A., HADLER, H., WILLERSHÄUSER, T., NTAGERETZIS, K., BRÜCKNER, H., WARNECKE, H., GROOTES, P.M., LANG, F., NELLE, O., SAKELLARIOU, D. (2012): Ancient harbours used as tsunami sediment traps – the case study of Krane (Cefalonia Island, Greece). – In: PIRSON, F., LADSTÄTTER, S., SCHMIDTS (Hrsg.): Häfen und Hafenstädte im östlichen Mittelmeerraum von der Antike bis in byzantinische Zeit. Aktuelle Entdeckungen und neue Forschungsansätze. Byzas, Istanbul (in press).

WALTHER, J. (1894): Einleitung in die Geologie als historische Wissenschaft: Beobachtungen über die Bildung der Gesteine und ihrer organischen Einschlüsse. – G. Fischer, Jena, 1055 pp.

WARNECKE, H. (2008): Homers Wilder Westen. Die historisch-geographische Wiedergeburt der Odyssee. – Steiner, Stuttgart, 341 pp.

WERNER, W. (1997): The largest ship trackway in ancient times: the diolkos of the Isthmus of Corinth, Greece, and early attempts to build a canal. – International Journal of Nautical Archaeology 26 (2): 98-119.

WILLERSHÄUSER, T., VÖTT, A., BRÜCKNER, H., BARETH, G., HADLER, H. & NTAGERETZIS, K. (2011): New insights in the Holocene evolution of the Livadi coastal plain, Gulf of Argostoli (Cefalonia, Greece). – Coastline Reports 17: 99-110.

WILLERSHÄUSER, T., VÖTT, A., HADLER, H., HENNING, P. & NTAGERETZIS, K. (2012): Evidence of high energy-impact near Kato Samiko, Gulf of Kyparissia (western Peloponnese), during history. – Bremer Beiträge zur Geographie und Raumplanung 44: 26-36.

WILLERSHÄUSER, T., VÖTT, A., BRÜCKNER, H., BARETH, G., NELLE, O., NADEAU, M.-J., HADLER, H. & NTAGERETZIS, K. (2013): Holocene tsunami landfalls along the shores of the inner Gulf of Argostoli (Cefalonia Island, Greece). – Zeitschrift für Geomorphologie N.F. Suppl. 57 (4): 105-138.

ZELT, J.A. (1986): Tsunamis: The response of harbours with sloping boundaries to long wave excitation. – California Institute of Technology, Pasadena, 334 pp.

ZHU, Y. & WEINDORF, D. (2010): Determination of soil calcium using field portable X-ray fluorescence. – Soil Science 174 (3):151-155.